NASA CR-114463
Boeing Document D6-40381
Available to the Public

PREDICTED FLIGHT CHARACTERISTICS OF THE AUGMENTOR WING JET STOL RESEARCH AIRCRAFT

By
R.E. Spitzer

July 1972

Prepared under Contract No. NAS2-6025 by
THE BOEING COMPANY
Commercial Airplane Division
Renton, Washington

for
NATIONAL AERONAUTICS AND SPACE ADMINISTRATION
Ames Research Center

TABLE OF CONTENTS

TABLE OF CONTENTS (Cont'd)

SUMMARY

An existing deHavilland C-8A "Buffalo" airplane has been modified into an augmentor wing flight test vehicle. Research objectives are to verify the augmentor flap concept and to produce data for STOL airworthiness criteria. The Modified C-8A provides the means for jet-STOL flight research down to a 60 knot approach speed. The airplane has a high thrust-to-weight ratio, high-lift flap system, vectored thrust, powerful flight controls, and lateral-directional stability augmentation system.

Normal performance and handling qualities are expected to be satisfactory. Analysis and piloted simulator results indicate that stability and control characteristics in conventional flight are rated "satisfactory". Handling qualities in the STOL regime are also generally satisfactory, although pilot workload is high about the longitudinal axis.

Program scope has limited the depth of the design data base and the extent of airplane modification. As a result, there are flight control risks associated with "corners" of the flight envelope and with certain remote single failures. In addition, adverse ground effects could result in hard landings. Engine failure in the last few seconds of STOL approach may produce touchdown sink rates in excess of landing gear capability. However, by adhering to a carefully planned test program using experienced test pilots, the Modified C-8A has been considered acceptable for STOL flight research.

1.0 INTRODUCTION

1.1 Background

The technology for short takeoff and landing (STOL) airplanes is rapidly being developed. One STOL powered-lift concept is the augmentor wing jet flap. Early work with this concept was performed by deHavilland of Canada. NASA-Ames joined in the aerodynamic development with a series of large-scale wing tunnel tests beginning in 1965. The ensuing NASA research program, conducted with deHavilland of Canada support, has been traced in Reference 1.

The NASA wind tunnel testing led to configuration studies to convert an existing deHavilland "Buffalo" (U.S. designation C-8A) into an augmentor wing flight test vehicle. A joint Canada-USA program was started in 1970. The Canadian Department of Industry, Trade and Commerce (DITC) has provided the propulsion package through a contract with deHavilland of Canada and Rolls-Royce. The modified airframe has been provided by NASA through Contract NAS2-6025 with The Boeing Company. Boeing design work began in mid-1970. The Modified C-8A is scheduled to fly early in 1972.

Principal airplane modifications have consisted of installation of jet engines, ducting and the augmentor flap high-lift system. Other changes have included redesigned control systems, the addition of a lateral-directional stability augmentation system and modified hydraulic and electrical systems. Stability and control analyses have been made to evaluate flight safety and handling qualities. This document collects and summarizes these analyses of predicted flight characteristics.

1.2 MODIFIED C-8A DESCRIPTION

1.2.1 General

Figures 1-1 and 1-2 show the general arrangement of the Modified C-8A. Pertinent configuration data are listed on Table 1-1. Augmentor-wing jet flaps, blown and flap-drooped ailerons and fixed leading edge slats have been installed on the wing (see Figure 1-2). Wing span has been shortened by cutting the tips off the original Buffalo wing in order to increase wing loading to 50 lb/ft^2 at maximum landing weight (43,000 lb). Two Rolls-Royce Spey 801-SF split flow jet engines have been installed in modified underwing nacelles.

The fan flow from each engine is independently ducted to blow the augmentor flaps and the aileron on the opposite side of the airplane. The ducting systems feature a "duct-within-a-duct" dual nozzle flap blowing arrangement and crossover ducts through the fuselage. With only one engine operating the entire flap span continues to receive blowing air. Engine-out rolling moment compensation is provided by asymmetric blowing to the opposite aileron. Duct routing is through the wing leading and trailing edge areas to preserve the fuel tanks located between the spars. With no diverter valves the flaps are blown at all times, including the flaps-up cruise. As a result the augmentor flap remains open even in the cruise configuration.

Engine primary flow exhausts through vectorable conical nozzles. The pilot can rotate the hot thrust vector from a nearly horizontal acceleration force (engine exhausting aft at 6° below the horizontal) to vertical lift at 90°. The nozzles may be rotated further to crease a combined lifting and retarding (or decelerating)force at 104° orientation. With the conical nozzles occupying the nacelle space, the landing gear is no longer retractable and remain extended for all flight conditions.

The Modified C-8A has two redesigned hydraulic systems which power the lateral and directional flight controls, flaps, brakes, nosewheel steering, lift dump surfaces, and the lateral-directional SAS actuators. Each hydraulic system is powered by two engine-driven pumps, one on each engine. Either system, operating on only one pump, can operate the critical flight controls including flap actuation.

The Modified C-8A is equipped with two normally isolated electrical systems. The left hand and right hand bus systems are each powered by an engine driven AC generator via a constant speed drive unit. A failure of any one of the buses or loss of a generator causes automatic transfer of the loads from the faulty bus to the remaining operative bus. A battery provides power for lighting and communication equipment should both main AC generators fail. Electrical power is not required for operation of engines, flight controls or primary instruments. The airplane can be safely flown to a landing without generated electrical power.

Being a research airplane, the Modified C-8A has permanently installed flight test instrumentation. An instrumented nose boom has been added as part of this system.

Typical operational data for the airplane are listed on Table 1-2. Descriptions of the primary flight controls and lateral-directional SAS follow.

1.2.2 Longitudinal Control System

The Modified C-8A retains the manual elevator spring tab longitudinal control system of the original Buffalo. Figure 1-3 shows the elevator control system schematic. Pilot and co-pilot control solumns are connected by a torque tube. Column movement actuates the elevator spring tab via a single cable run. The pilot moves the spring tab through a relatively stiff outer torque tube while remaining attached to the elevator through a weaker inner torque tube. Stick

force is derived through a combination of spring tab and direct elevator hinge moments. Elevator torque tube and spring tab follow-up ratio have been modified to reduce stick forces for "one-hand" operation. The pilot comes into direct, firm contact with the elevator after the torque tube winds up to a pre-set limit (θ_1 stops in Figure 1-3). Elevator gearing to the column varies with airspeed due to hinge moments, cable stretch, and torque tube wind-up.

The stabilizer on the Modified C-8A has a fixed incidence setting. Hands-off trim is produced by the balancing elevator trim tab as shown in Figure 1-4. A motor and clutch have been added to the original trim tab circuit to provide the pilots with electrical trim control using thumbswitches. A flap-trim interconnect varies the airplane nose down trim authority to prevent the occurrence of an excessive mistrim.

1.2.3 Lateral Control System

The original manual lateral control system has been replaced by a new, powered system on the Modified C-8A. Lateral control is derived from a combination of three aerodynamic surfaces: drooped and blown ailerons, spoilers ahead of the ailerons, and augmentor flap chokes located on the outboard flap panels (see Figure 1-5). Choke surfaces are also provided on the inboard flaps, and along with the outer choke panels, are used for lift dumping on the ground.

The lateral control system schematic is presented in Figure 1-6. Hydraulic actuators and control system components have been adapted from other airplanes to assure airworthiness and high reliability. Pilot control is summed in series with the lateral SAS actuator to produce the input command to the central power actuator via the feel, centering and trim unit. The dual-hydraulic central P.C.U. then actuates the dual cables: one direct to the ailerons and the other commanding inputs to the spoiler actuators (hydraulic system A) and the choke actuators

(hydraulic system B). The aileron is drooped by mechanical input from the flaps. Spoiler and choke programmers are included in the system. In the event of total hydraulic failure, the pilot reverts to direct manual control of the ailerons.

1.2.4 Directional Control System

Directional control is produced by the Buffalo double-hinged, two-piece rudder. The rudder is powered by a dual-tandem hydraulic actuator. Pilot control from the rudder pedals is summed in series with the directional SAS actuator output to produce the input command to the rudder actuator. Pedal forces are provided by the feel, centering and trim unit. The directional control system is sketched in Figure 1-7.

1.2.5 Lateral-Directional SAS

The Modified C-8A has a lateral-directional stability augmentation system to enhance STOL flying qualities below 100 knots (automatic disengage speed). Two basic modes are provided:

1. Normal Stability Augmentation

   The normal mode provides the following:

   (a) roll mode augmentation (roll damping)
   (b) spiral mode augmentation
   (c) turn coordination
   (d) dutch roll damping ($\dot{\beta}$ damper)

   Automatic gain switching with flap position is included to produce more uniform response over the flap operating envelope. Control wheel position is programmed into the lateral SAS channel to improve the linearity of the airplane roll response for small wheel inputs.

2. Variable Stability Augmentation

   The variable stability mode permits selection of a wide range of lateral-directional characteristics by gain and sense control of the following:

(a)	roll rate to lateral control feedback	(C_{l_p})
(b)	yaw rate to lateral control feedback	(C_{l_r})
(c)	sideslip to lateral control feedback	(C_{l_β})
(d)	yaw rate to directional control feedback	(C_{n_r})
(e)	roll rate to directicnal control feedback	(C_{n_p})
(f)	roll attitude to directional control feedback	Turn Coordination
(g)	aileron to directional control crossfeed	Cross-coupling

The stability augmentation system is non-redundant with SAS actuators limited in rate and authority to a safe value. In the "normal mode" isolation is maintained between the lateral and directional SAS circuits. Separate sensors are used to prevent simultaneous failures about both axes. Figure 1-8 shows the SAS schematic with the separate roll axis and yaw axis computers.

All signal computation for the variable stability mode is done in one computer (axis isolation does not exist in this mode). Surface commands from the variable stability computer are fed to their respective "normal" mode augmentation computers in order to use the same SAS servo actuator loops.

The servo actuators are connected in series, so that SAS commands are not reflected at the pilot's controls.

Two control panels are provided for mode and gain control. In addition, disconnect switches are located on the pilot's and co-pilot's wheels for quick SAS disengagement.

To maintain continuous SAS operation in the event of an electrical system failure (perhaps caused by an engine failure), circuitry has been installed to automatically transfer the SAS to the remaining electrical bus.

1.3 Data Base

The aerodynamic data base for the Modified C-8A comes from a deHavilland-built, large-scale augmentor wing model tested for NASA in the Ames 40x80 wind tunnel

and from the original DHC Buffalo itself. Two tests were conducted with the model configured to represent the Modified C-8A: PHASE IV in free air (Reference 2) and PHASE V in the presence of a ground plane. Figure 1-9 shows a 3-view drawing of the Ames model. The data base also extends to earlier developmental testing conducted by deHavilland and NASA (see Reference 3). Empennage aerodynamic characteristics were obtained from data on the original Buffalo.

Working data used in the prediction of Modified C-8A characteristics were interpolated and extrapolated from the wind tunnel data base. Extensive corrections were made for differences in geometry between the actual airplane and the wind tunnel model. Jet flap theory was required to fill in voids in the data. Linear superposition techniques were used in the data build-up. Downwash was computed using a "horse shoe" vortex theoretical model factored to match the limited amount of wind tunnel data.

Lateral-directional static stability derivatives were obtained from wind tunnel data. Considerable scatter exists in the wind tunnel data for C_{ℓ_β} At STOL approach conditions it appears that the Modified C-8A may have no dihedral effect, i.e. $C_{\ell_\beta} \approx 0$. Dynamic stability derivatives for the Modified C-8A have been estimated using theoretical expressions developed by deHavilland for the augmentor jet flap. Vertical and horiziontal tail contributions have been calculated using "force-times-arm" techniques.

Hinge moment data for the elevator and rudder were obtained directly from work done on the original Buffalo. Spoiler hinge moments were estimated using Boeing data on similar spoiler arrangements. Aileron hinge moments were estimated from test data on the large-scale Ames model and from other sources (e.g., Reference 4).

Piloted operation characteristics were evaluated using the simulator. Use was made of the Flight Simulator for Advanced Aircraft (FSAA) facility located at NASA-Ames. The digital simulation included a six degree-of-freedom motion base cab configured to represent the Modified C-8A. A color T.V. display, engine noise and a turbulence model were a part of the simulation. Pilots from NASA, The Boeing Company and deHavilland Aircraft of Canada "flew" the simulation based on a detailed mathematical model of the Modified C-8A (References 5 & 6). The testing provided both design information for new systems (e.g., lateral control and SAS) and preliminary evaluations of operational characteristics. Piloted characteristics reported in this document came from the simulator studies, which are reported in detail in Reference 7.

While not up to commercial aircraft standards, the data base was deemed sufficient for design of an experimental flight test vehicle. It must be kept in mind, however, that a considerable amount of interpolation and extrapolation has been used in predicting the Modified C-8A flight characteristics. The probability that the actual airplane will not fly exactly like the predictions is much higher than for "production" airplane programs with a more extensive data base.

TABLE 1-1

CONFIGURATION DESCRIPTION

I. GEOMETRY

WING

S_W = 865 ft^2 (excluding slats)

b_w = 78.75 ft

$\bar{C}_{W_{REF}}$ = 149 inches {ROOT CHORD}

AR = 7.2

$\Lambda_{.25} \approx 0°$

t/c ≈ 16%

i_w = 2.5°

λ_{eff} = .80

HORIZONTAL TAIL

S_H = 233 ft^2

b_H = 32 ft

$\bar{C}_H$ = 88 inches

AR = 4.4

$\Lambda_{.25}$ = 3°

t/c ≈ 12%

$\bar{V}_{H_{.25}}$ = 1.0

λ = .75

i_T = +1° {ORIGINAL C-8A INCIDENCE RETAINED}

VERTICAL TAIL

S_V = 152 ft^2

b_V = 13.6 ft

$\bar{C}_V$ = 137 inches

AR = 1.22

$\Lambda_{.25}$ = 17°

t/c ≈ 14%

$\bar{V}_{V_{.25}}$ = .097

λ = .57

AUGMENTOR FLAPS

- Avg. Chord = 29% c_w (L.E. Coanda to T.E./ wing chord)
- Span: 12% (SOB) ≤ η ≤ 71%
- 5.6°(Up) ≤ δ_F ≤ 75°

ELEVATOR

- Avg. Chord = 35%

Full-Span

- -25° ≤ δ_e ≤ +15°
- Two 83% Semi-span Tabs (7% Tail chord)
- $S\bar{C}_e$ = 209 ft^3

RUDDER

- Avg. Chord = 40%
- Double-Hinged Rudder (Hinges @ 60% & 80% Chord)
- Full-Span
- -25° ≤ δ_r ≤ +25°
- Aft Rudder Segment deflects an additional 25° at 1:1 gearing
- $S\bar{C}_{r_{total}}$ = 272 ft^3

AUGMENTOR CHOKE

- Avg. Chord = 9% c_w
- Full-Span on all Flap Panels (0% ≤ δ_{CH} ≤ 100%)

BLC AILERON

- Avg. Chord = 22.5% c_w
- Span: 71% ≤ η ≤ 100%
- -16.5° ≤ δa ≤ 64°
- Half-Span Geared Tab (4% wing chord)
- $S\bar{C}_a$ = 46 ft^3/surface

AD 1546D

TABLE I-1

(Cont'd)

SPOILER

- Avg. Chord = 14% c_w
- Hinge Line @ 62% c_w
- $0° \leq \delta_{sp} \leq 50°$
- $S\bar{c}_{sp}$ = 17 ft^3/surface

II. WEIGHT, C.G., INERTIA

	Nominal CG*	Structural Design Limits
Max. Taxi Weight = 45,000 lb	30% Mac	25-34%
Max. Zero Fuel Wt. = 37,000 lb		
Max. Gross Weight = 45,000 lb	30% Mac	
Max. Landing Weight = 43,000 lb		
O.E.W. (NASA Instrumentation) = 31,400 lb	27% Mac	20.5-31.5%

*With fuel added, beyond O.E.W., the nominal CG follows a single linear line between 27% and 30% Mac

At 40,000 lbs

I_{XX} = 260,000 slug-ft^2 (fuel system modified)

I_{YY} = 205,000 " "

I_{ZZ} = 495,000 " "

I_{XZ} = 35,500 " "

III. PROPULSION

At 60 kts, sea level, standard day**

- Maximum gross hot thrust, T_{HOT} ≐ 7150 lb/engine (vectorable)
- Ram Drag = 650 lb/engine
- Maximum isentropic* cold thrust ≐ 3550 lb/engine

*Installation losses, including ducts, included out to nozzles.

**NOTE: Actual typical approach power setting is at 92% RPM with T_{HOT} ≐ 3200 lb/eng and T_{COLD} ≐ 2375 lb/eng.

AD 1546D

TABLE 2-2

OPERATIONAL DATA

I. PLACARDS

DESIGN FLAP SPEEDS

δ_F	$V_f \sim$ KTS
75°	90
50°	100
30°	120
5.6°(Up)	160

FLAPS UP DESIGN SPEEDS

Gust V_B = 140 kts

Maneuvering V_A = 140

Design Cruise $V_C = V_{MO}$ = 160

Design Dive Speed = 180

DESIGN LOADS

Flaps Down $0g \leq n_z \leq 2.0g$

Flaps Up (5.6°) $-.5g \leq n_z \leq 2.25g$

MAXIMUM ALTITUDE

15,000 ft

II. TYPICAL DESIGN FLIGHT CONDITIONS

TAKEOFF

$\delta_F = 30°, \nu = 6°, V_e = 80$ kts, $\gamma = 15°$ (2 eng, takeoff power, 45,000 lb)

CRUISE

δ_F = Up, $\nu = 6°$, V_e = 140 to 160 kts, $\gamma = 0$

LANDING

$\delta_F = 65°, \nu = 90°, V_e = 60$ kts, $\gamma = -7.5°$, $\Delta n_{z_{margin}} = .35g$

ΔV_{margin} = 16 kts

III. TYPICAL PERFORMANCE

Takeoff & Landing Field Lengths: 2200 ft (T.O.)* → 1500 ft (LDG)**

Ferry Range: 350 N. Mi.

Endurance (Landings & Go-arounds Test Work): > 1 Hour

---

* Includes R.T.O. stopping distance; two-engine takeoff requires only 1000ft.

** Actual, unfactored field length. (Brakes do not have anti-skid).

AD 1546D

TYPICAL WING SECTION

ASPECT RATIO	7.2
WING AREA	865.0 ft²
SPAN	78.75 ft
FLAP SEMI-SPAN	23.0 ft

MODIFIED C-8A

MAX. GROSS WT = 45,000 LB
V_{MO} (FLAPS UP) = 160 KT

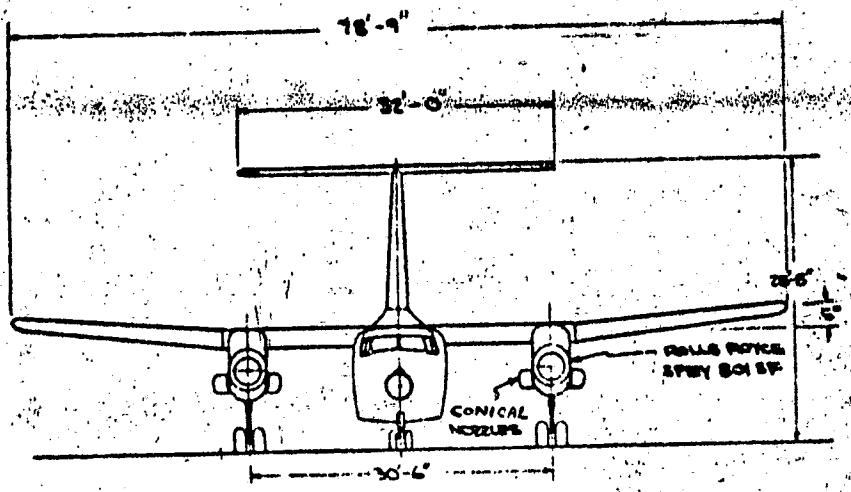

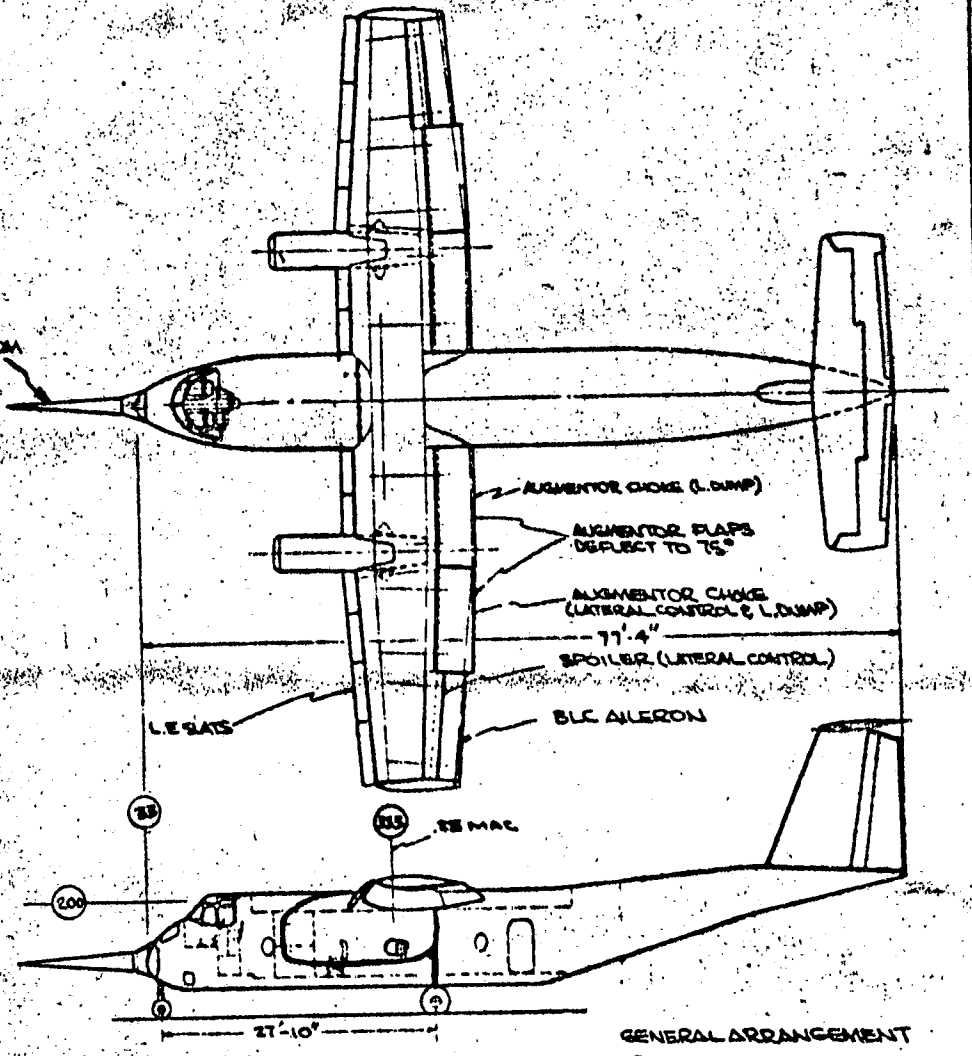

GENERAL ARRANGEMENT
REF: D6-25416

FIG. 1-1

MODIFIED C-8A "BUFFALO"
AUGMENTOR WING STOL RESEARCH AIRPLANE

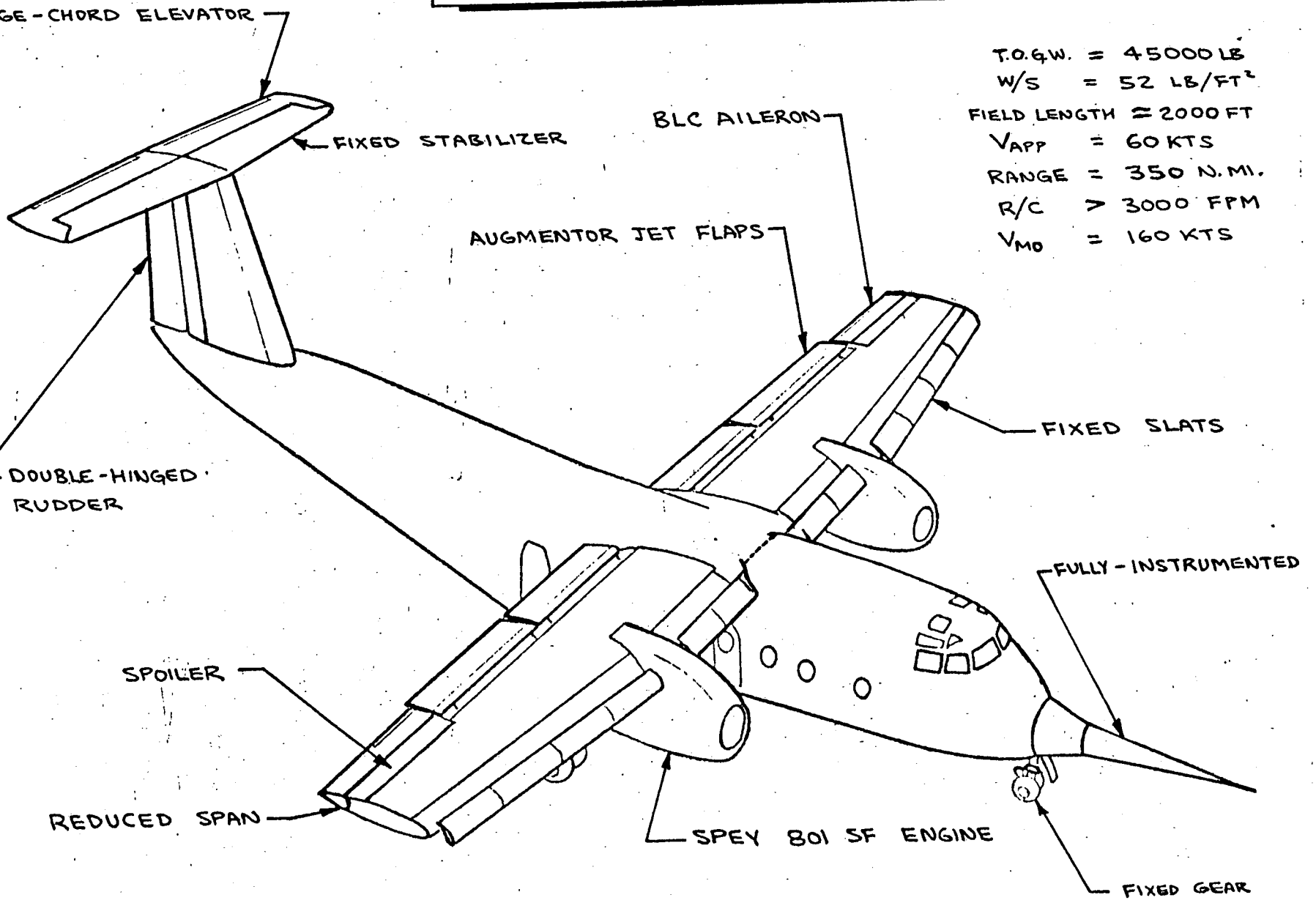

T.O.G.W. = 45000 LB
W/S = 52 LB/FT²
FIELD LENGTH ≃ 2000 FT
V_{APP} = 60 KTS
RANGE = 350 N.MI.
R/C > 3000 FPM
V_{MO} = 160 KTS

FIG 1-2

ELEVATOR CONTROL SYSTEM

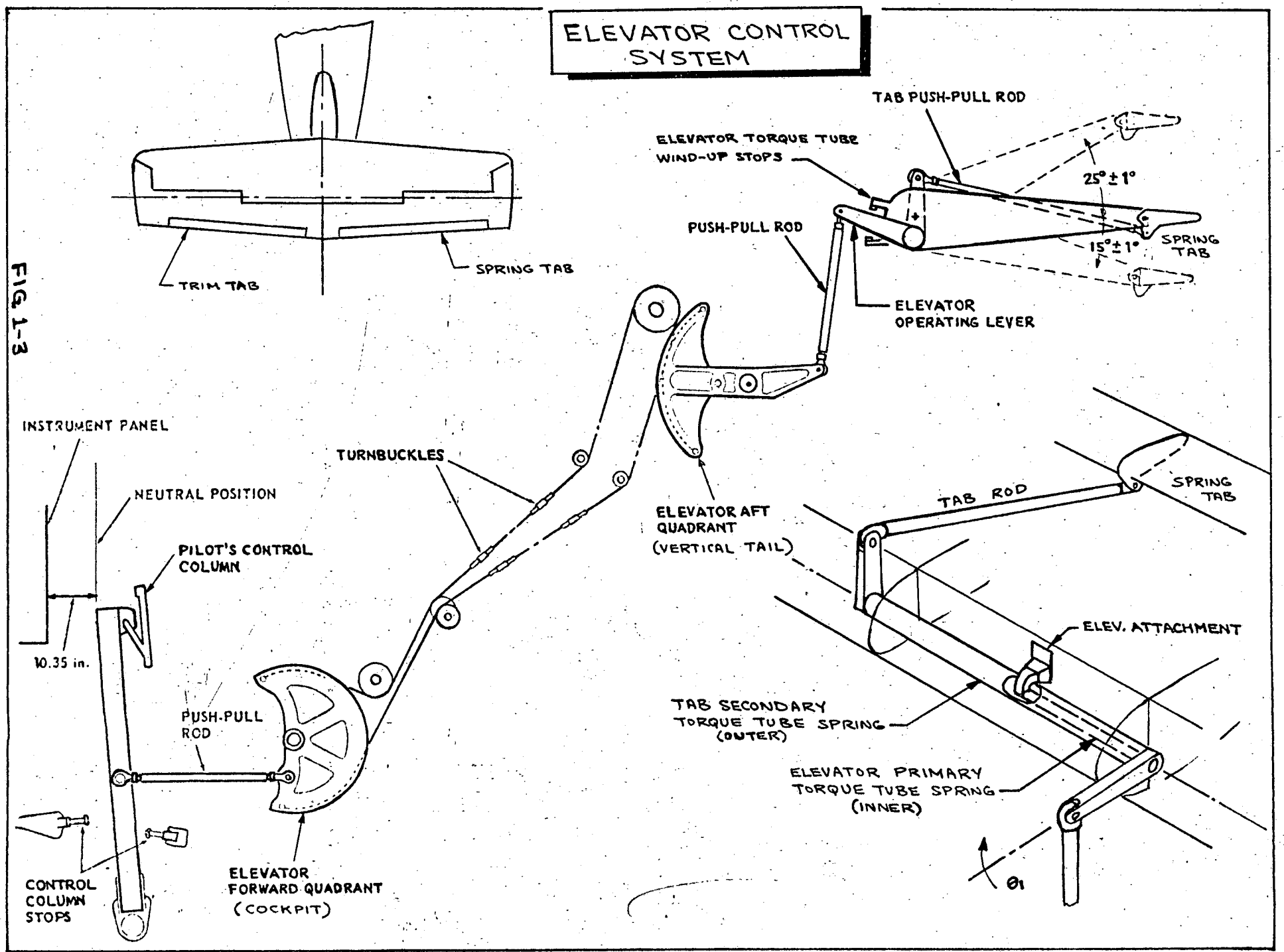

FIG. 1-3

ELEVATOR TRIM TAB SYSTEM

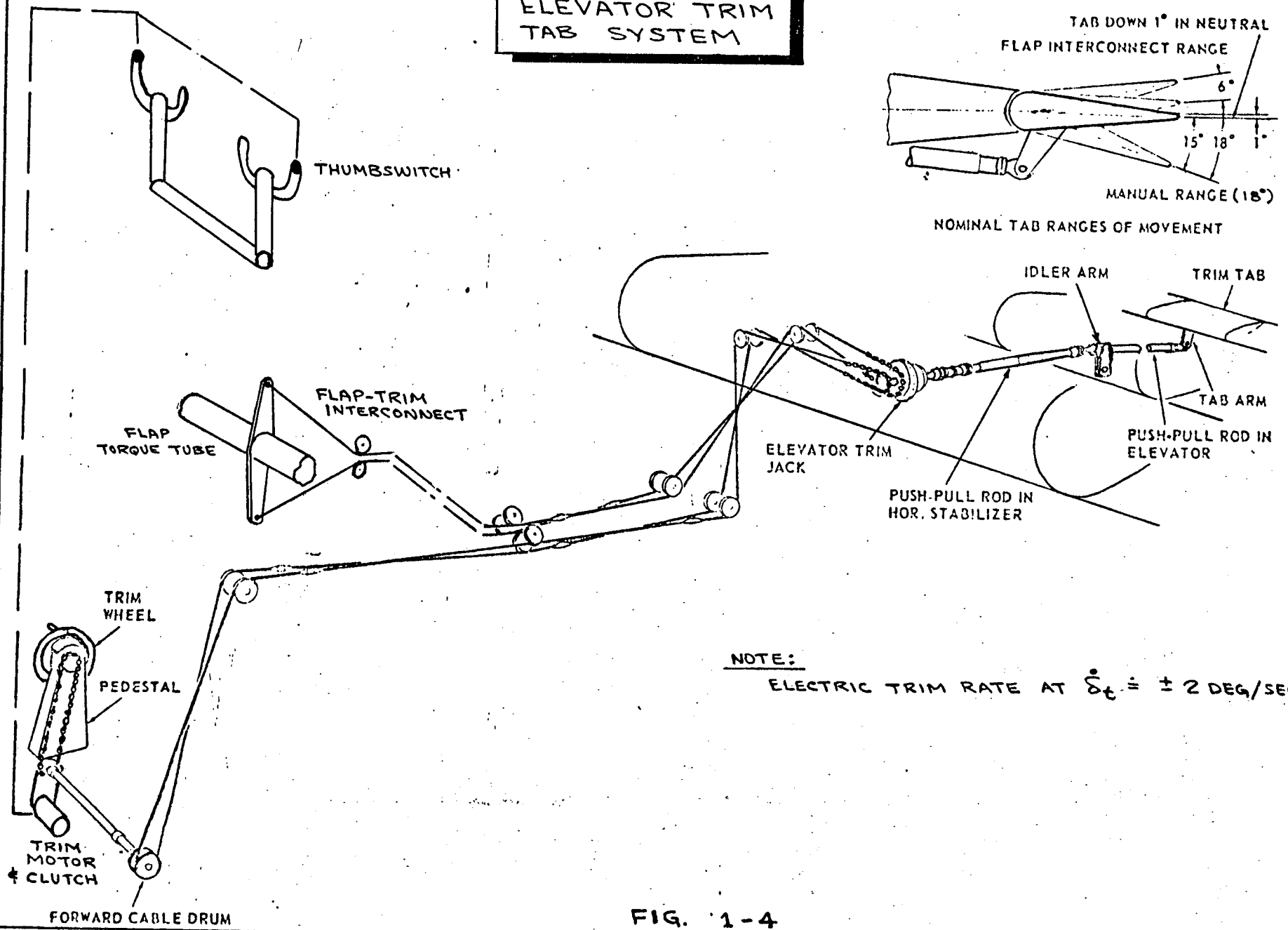

NOTE:

ELECTRIC TRIM RATE AT $\dot{\delta}_t \doteq \pm 2$ DEG/SEC

FIG. 1-4

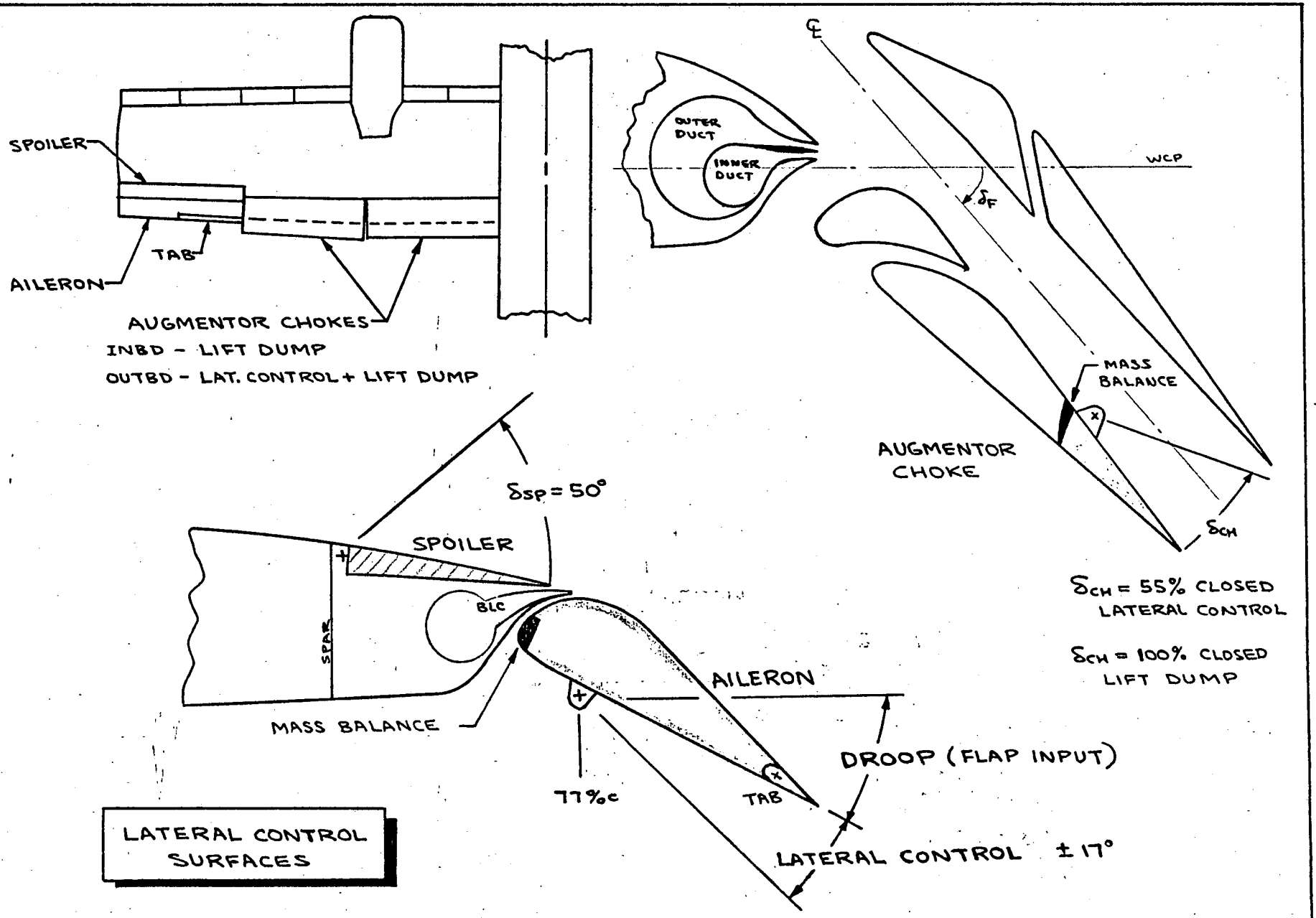

LATERAL CONTROL SURFACES

FIG. 1-5

LATERAL CONTROL SYSTEM

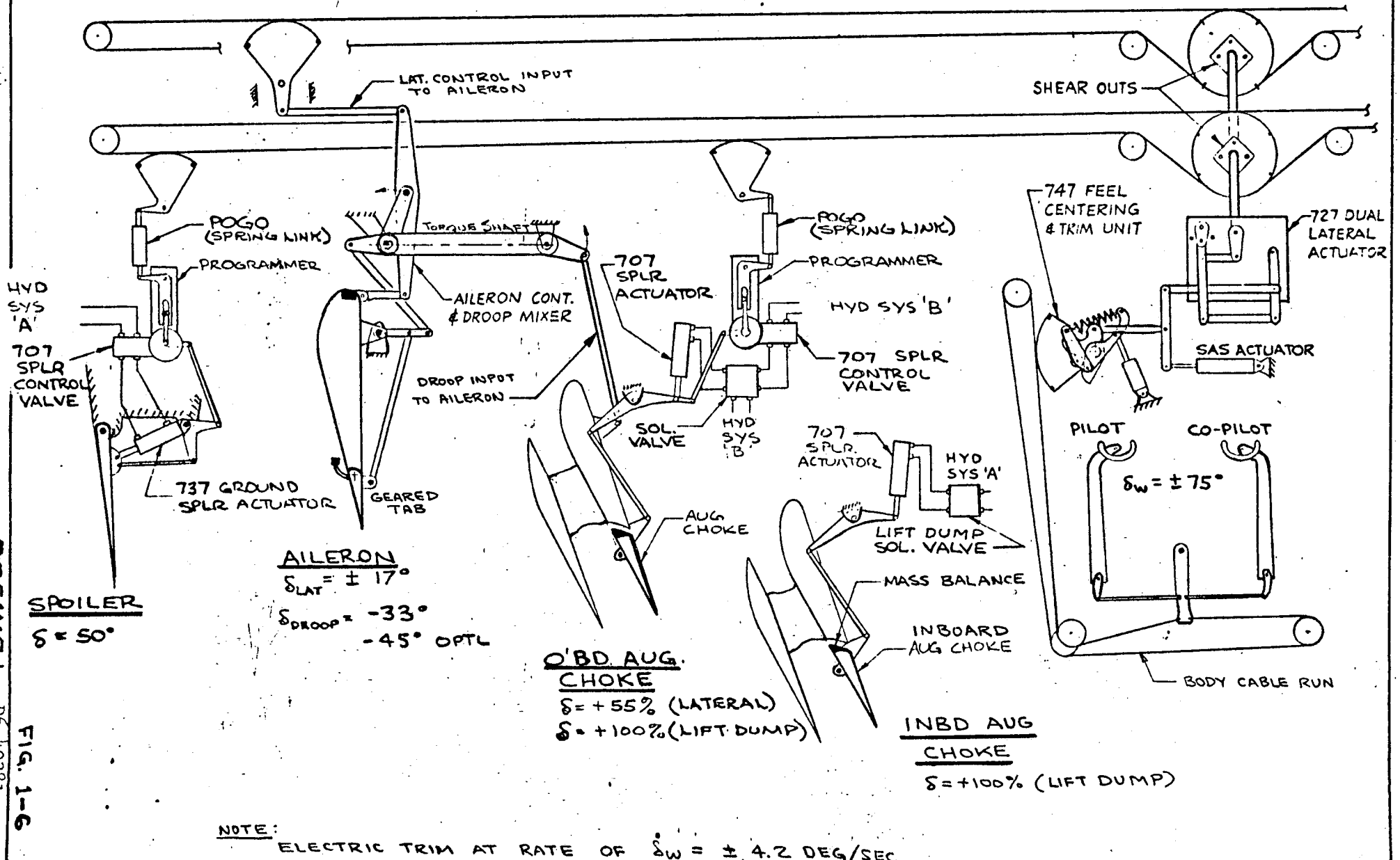

SPOILER

$\delta = 50°$

AILERON

$\delta_{LAT} = \pm 17°$

$\delta_{DROOP} = -33°$
$-45°$ OPTL

O'BD AUG. CHOKE

$\delta = +55\%$ (LATERAL)
$\delta = +100\%$ (LIFT DUMP)

INBD AUG CHOKE

$\delta = +100\%$ (LIFT DUMP)

NOTE:
ELECTRIC TRIM AT RATE OF $\dot{\delta}_w = \pm 4.2$ DEG/SEC

FIG. 1-6

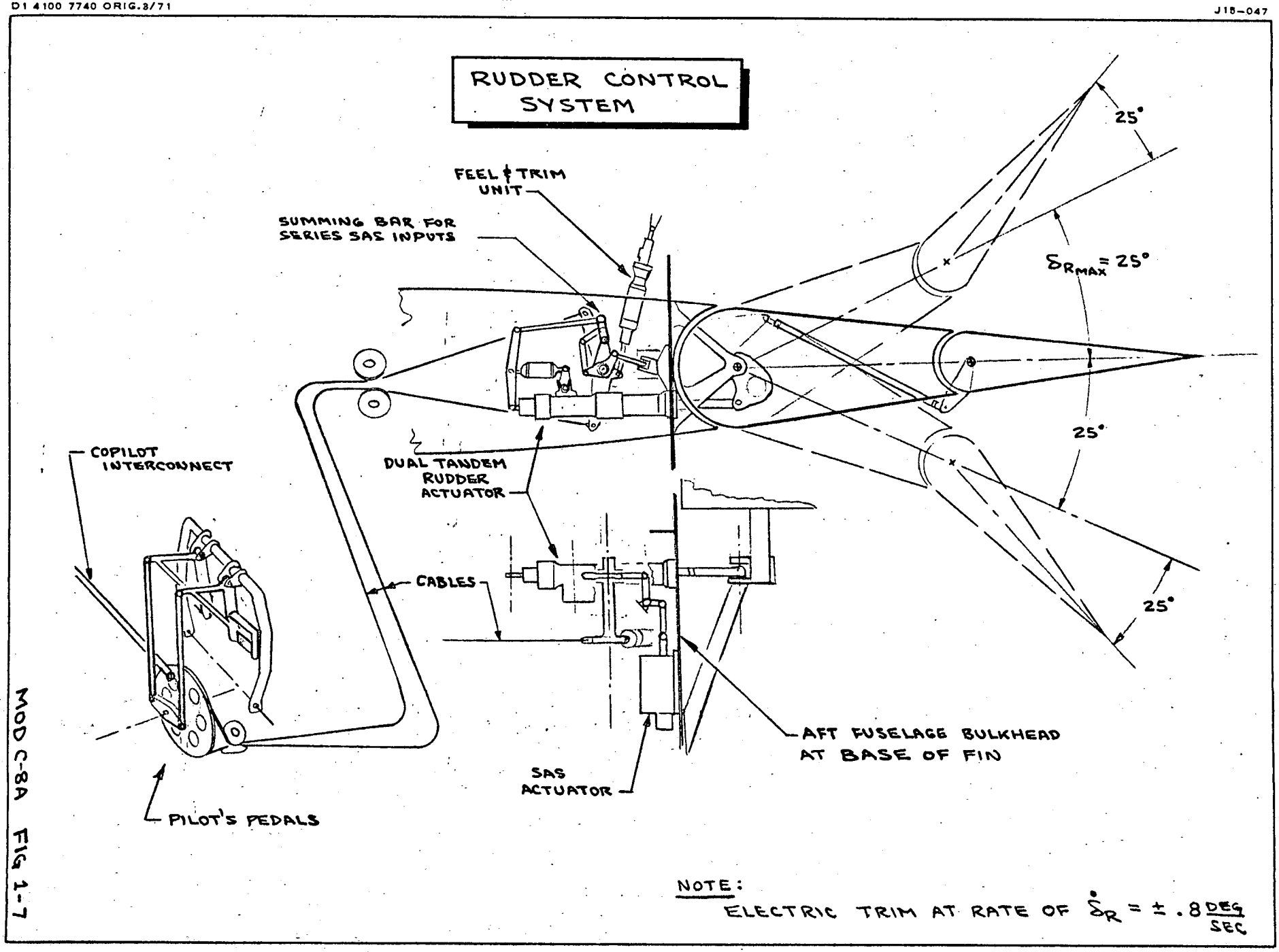

MOD C-8A FIG 1-7

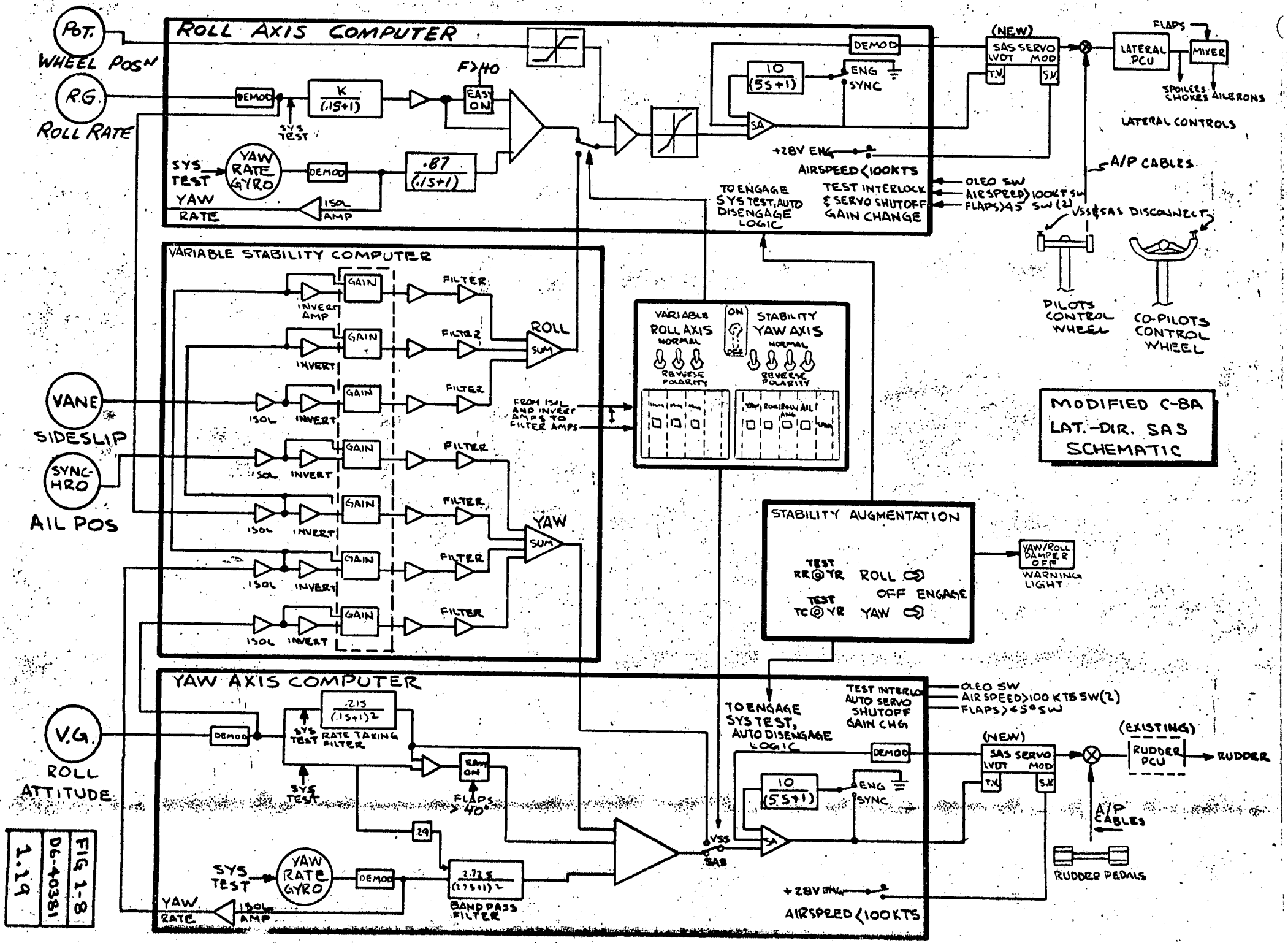
POT. WHEEL POSN
R.G. ROLL RATE
ROLL AXIS COMPUTER
DEMOD
K (.15+1)
SYS TEST
F>40
EAS ON
SYS TEST
YAW RATE GYRO
DEMOD
.87 (.15+1)
ISOL AMP
YAW RATE
10 (5S+1)
ENG SYNC
SA
+28V ENG
AIRSPEED <100KTS
TO ENGAGE SYS TEST, AUTO DISENGAGE LOGIC
TEST INTERLOCK & SERVO SHUTOFF GAIN CHANGE
OLEO SW
AIRSPEED >100KT SW
FLAPS >45 SW (2)
(NEW)
SAS SERVO LVDT MOD
T.V.
S.V.
LATERAL PCU
FLAPS
MIXER
SPOILERS CHORDS AILERONS
LATERAL CONTROLS
A/P CABLES
VSS & SAS DISCONNECT
PILOTS CONTROL WHEEL
CO-PILOTS CONTROL WHEEL
VARIABLE STABILITY COMPUTER
GAIN
INVERT AMP
FILTER
FILTER2
ROLL SUM
INVERT
ISOL
YAW SUM
VANE SIDESLIP
SYNCHRO AIL POS
FROM ISOL AND INVERT AMPS TO FILTER AMPS
VARIABLE ROLL AXIS NORMAL REVERSE POLARITY
ON OFF
STABILITY YAW AXIS NORMAL REVERSE POLARITY
MODIFIED C-8A LAT.-DIR. SAS SCHEMATIC
STABILITY AUGMENTATION
TEST RR @ YR ROLL
OFF ENGAGE
TEST TC @ YR YAW
YAW/ROLL DAMPER OFF WARNING LIGHT
YAW AXIS COMPUTER
V.G. ROLL ATTITUDE
.215 (.15+1)²
SYS TEST
RATE TAKING FILTER
RAM ON
FLAPS >40°
29
SYS TEST
YAW RATE GYRO
DEMOD
2.72 S (.75+1)²
BAND PASS FILTER
YAW RATE
ISOL AMP
TO ENGAGE SYS TEST, AUTO DISENGAGE LOGIC
TEST INTERLOCK AUTO SERVO SHUTOFF GAIN CHG
OLEO SW
AIRSPEED >100 KTS SW (2)
FLAPS >45° SW
VSS
SAS
(NEW)
SAS SERVO LVDT MOD
T.V.
S.V.
(EXISTING)
RUDDER PCU
RUDDER
A/P CABLES
RUDDER PEDALS
+28V ENG
AIRSPEED <100KTS
1.1.9
09-40381
FIG 1-8

NASA AMES AUGMENTOR WING WIND TUNNEL MODEL

All dimensions in feet

WING:

$S = 230$ FT.^{2}

$b = 44.1$ FT.

$\bar{c} = 5.67$ FT. {ROOT CHORD}

$AR = 8.45$

$t/c = .16$

$C_{flap} = .35\, C_{WING}$

$i_w = 0°$

HORIZONTAL:

$S = 63.7$ FT.

$AR = 4.68$

$\bar{V}_H = 1.08$

VERTICAL:

$S = 41.9$ FT

$AR = 1.36$

$\bar{V}_V = .085$

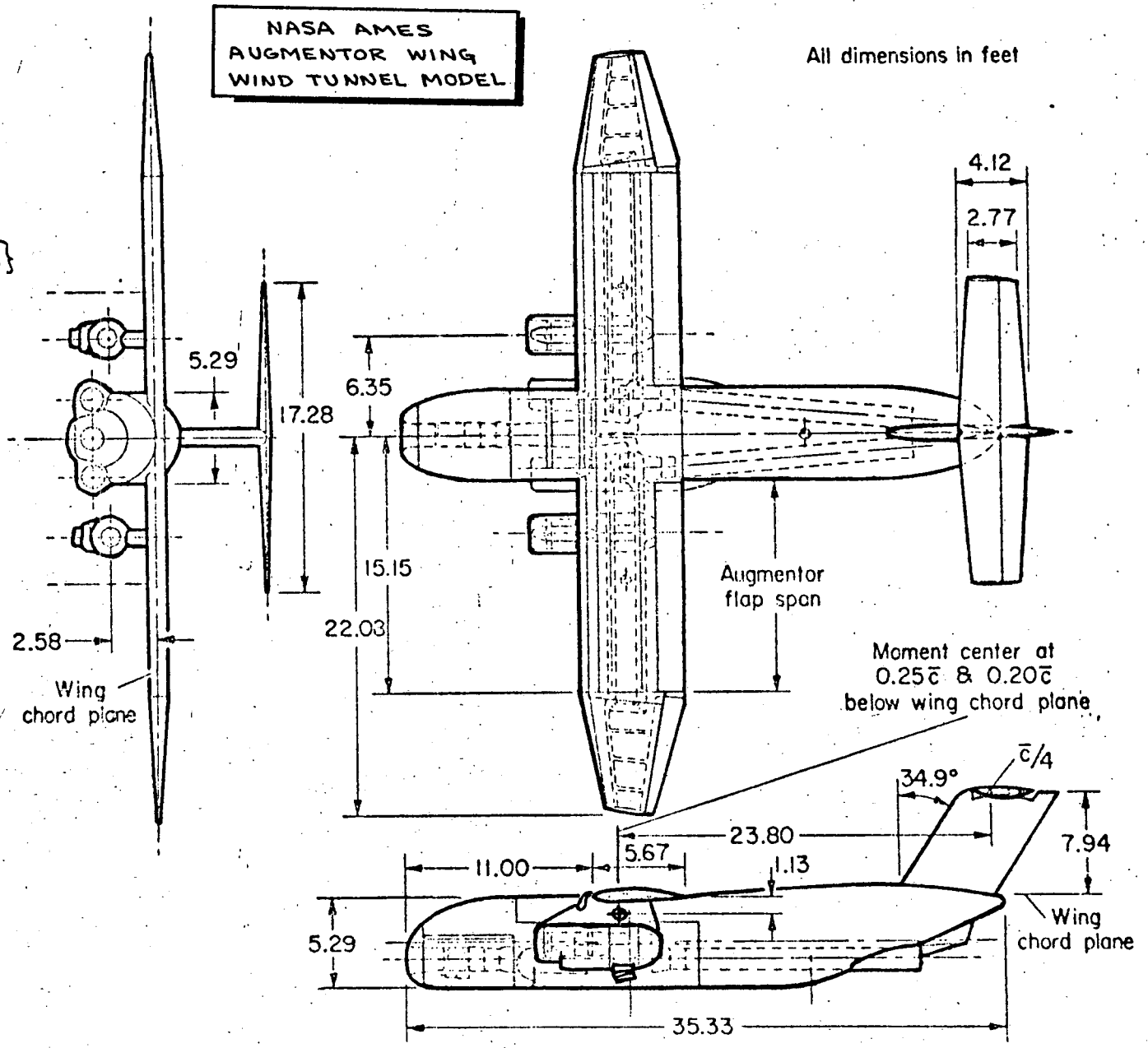

FIG 1-9

2.0 STABILITY AND CONTROL CRITERIA

This section presents a brief listing of criteria affecting the stability and control characteristics of the Modified C-8A.

Stability and control criteria used in the design and analysis of the Modified C-8A are derived from a number of sources:

- NASA design preferences
- Boeing design experience
- Results of NASA/Boeing simulator studies
- Airworthiness regulations (References 8 and 9)
- Published reports on STOL handling qualities (e.g. References 15 and 16)

Every attempt was made, where possible within the contract scope, to satisfy the following criteria.

2.1 General Criteria

These "general" criteria apply to overall airplane characteristics:

1. Flight control characteristics shall permit safe, acceptable STOL operation with a skilled pilot. Adequate control and maneuverability shall be available to enable the pilot to make speed, power and configuration changes, to negotiate moderate levels of turbulence, wind shear and cross wind and to counteract probable failure conditions.

2. Control systems shall be designed to provide satisfactory handling qualities through adequate rate, authority and dynamic characteristics. Generally, full control deflection should be available within 0.5 sec at STOL flight conditions.

3. Under normal operating conditions the airplane shall be dynamically stable about all axes.

4. The airplane shall be controllable for continued safe flight to a landing with any probable single failure, including hydraulic or electrical power failures, or any combination of failures not shown to be extremely remote. This condition excludes jamming.

5. The airplane shall be controllable for continued flight to a safe landing after any single jam in the control system unless shown to be extremely remote. The jam position condition applies only to probable control surface positions.

6. The airplane shall be controllable to a safe landing following loss of both hydraulic systems.

7. The airplane shall be controllable if all engines fail.

2.2 Longitudinal Stability and Control Criteria

1. The existing Buffalo longitudinal control system shall provide adequate control power for trimmed and maneuvering flight within the defined operational flight and CG loading envelopes of the Modified C-8A. Maneuvering requirements shall include, but not be limited to, the following:

AD 1546D

- Load factor capability from $0 \leq n_z \leq 2.0g$.
- Sufficient longitudinal control for flap extension and retraction and for power and thrust vector changes.
- Elevator power to demonstrate the minimum flying speed at each flap position and then recover.
- Sufficient control for takeoff rotation, including realistic takeoff mistrim.
- Elevator control for landing flare.
- Maximum pitch acceleration at 60 kt STOL approach of $\ddot{\theta}_{MAX} \geq .5$ RAD/SEC^2.

2. Pitch control sensitivity (pitch acceleration per unit column deflection) shall have a satisfactory pilot rating, nominally $\ddot{\theta}/X_s \geq .05$ $\frac{\text{RAD/SEC}^2}{\text{INCH}}$ at STOL landing approach.

3. The elevator control system shall produce stick forces compatible with one-hand operation at STOL flight conditions.

4. The elevator control system shall have positive centering.

5. Hands-off trim capability shall be provided for all steady, "1g" flight conditions from STOL reference approach speed to V_{MO}.

6. Longitudinal trim rate shall provide acceptable trimming performance.

7. Control to a safe landing shall be possible with the trim system jammed in normal flight trim positions.

AD 1546D

8. The pilot shall be able to recover from an inadvertent runaway, mistrimmed condition with less than 125 lb of stick force.

9. The Modified C-8A shall have acceptable longitudinal static and maneuvering stability.

10. Flight path or "speed stability" shall be acceptable for normal piloted operation.

11. Longitudinal dynamic stability shall be positively damped.

2.3 Lateral-Directional Stability and Control Criteria

2.3.1 Lateral Control Criteria

1. The Modified C-8A shall have adequate lateral control power for maneuvering, with the following characteristics at 60 kt STOL approach conditions:

   - $\ddot{\phi}_{MAX} \geq .4$ RAD/SEC^2
   - $\dot{\phi}_{MAX} \geq 20$ DEG/SEC
   - $\phi_1 \geq 6$ DEG
   - $t_{30} \leq 2.5$ SEC

2. Lateral control power shall be sufficient to negotiate a 20 kt crosswind or achieve sideslips of $\beta > 15°$ at 60 kt STOL approach conditions using less than 50% maximum available roll control.

3. For emergency landing conditions (at higher approach speeds) the lateral control system shall produce:

   - $\ddot{\phi}_{MAX} \geq .2$ RAD/SEC^2
   - $\dot{\phi}_{MAX} \geq 10$ DEG/SEC
   - $t_{30} \leq 4$ SEC

AD 1346D

4. The Modified C-8A shall have adequate lateral control power to counteract rolling moment due to engine failure with the following constraints:

   - Initial engine-out transient followed by pilot corrective action shall not produce excursions greater than $20°\phi$ or $15°\beta$.
   - At 60 kt STOL approach and emergency power setting on remaining engine, required lateral control must be less than 60% of available roll control.
   - Remaining roll control power must be sufficient to effect recovery from the takeoff or landing approach engine failure conditions.

5. Lateral control power shall be sufficient to counteract failures in the lateral-directional SAS.

6. Lateral control power shall be sufficient to counteract fuel unbalance conditions.

7. Control power and design of the lateral control system shall provide capability to counteract:

   - Jammed surfaces in normal position
   - Cable breaks in the wing
   - Hydraulic system failures
   - Air ducting system failures

8. Lateral control sensitivity (roll acceleration per unit wheel displacement) shall have a satisfactory pilot rating, nominally $\ddot{\phi}/\delta_w \geq .10 \frac{\text{RAD/SEC}^2}{\text{INCH}}$ at STOL landing approach.

AD 1546D

9. Rolling moment shall be linear with wheel up to 40% $\delta_{W_{MAX}}$. Any non-linearities between 40% $< \delta_W <$ 100% $\delta_{W_{MAX}}$ must produce only a "convex" rolling moment characteristic.

10. Lateral control interactions in lift and yawing moment shall be minimized.

11. Wheel force shall be compatible with one-hand operation (less than 20 lb maximum).

12. The lateral control system shall have positive centering.

13. Lateral trim capability shall be provided for all probable lateral mistrim conditions.

14. For emergency operation, in manual reversion, acceptable roll control shall be achieved using a maximum wheel force of $F_{W_{MAX}} \approx 65$ LB.

2.3.2 Directional Control Criteria

1. The Modified C-8A directional control system shall provide adequate control power for maneuvering, with the following characteristics at 60 kt STOL approach:

   - $\ddot{\psi}_{MAX} \geq .15$ RAD/SEC^2
   - $t_{15} \leq 2.2$ SEC

2. Directional control power shall be sufficient to negotiate a 20 kt cross-wind or achieve sideslips of $\beta > 15^\circ$ at 60 kt STOL approach using less than 75% $\delta_{R_{MAX}}$.

3. The Modified C-8A shall have adequate directional control capability to counteract yawing moment due to engine failure such that $V_{MC} < 60$ KTS.

AD 1546D

4. Rudder control power shall be sufficient to counteract failures in the lateral-directional SAS.

5. Directional control sensitivity shall be acceptable. Yawing moment shall increase continuously with pedal deflection producing increasing sideslip angle.

6. Pedal force shall be greater than 50 lb maximum (nominally 100 lb maximum for satisfactory operation).

7. Directional control shall have positive system centering.

8. Directional trim capability shall be provided for all long-term directional trim conditions.

2.3.3 Lateral-Directional Stability Criteria

The following criteria apply to the Modified C-8A with lateral-directional SAS operative.

1. Dutch roll period shall be less than 12 sec, and damping ratio shall be positive.

2. Spiral mode time to double amplitude shall at least be greater than 20 sec; preferably the spiral mode should be slightly stable.

3. Roll mode time constant shall at least be $\tau_R < 2$ sec and preferably be $\tau_R < 1$ sec.

4. Turn entry using only lateral control shall be accomplished with minimum lateral-directional cross-coupling and heading lag. Specifically, induced peak sideslip to peak bank angle should be $\frac{\Delta\beta}{\Delta\phi} \leq .3$. Lag in heading should be less than $t_\psi \leq 2$ sec.

AD 1846D

5. The Modified C-8A shall possess static directional stability (recover from yawed conditions with rudder returned to neutral) and static lateral stability (recover bank angle from a sideslip condition with wheel returned to neutral).

NOTE: With lateral-directional SAS inoperative, the airplane shall be flown in a configuration to assure continued flight to a safe landing.

AD 1546D

3.0 LONGITUDINAL CHARACTERISTICS

3.1 Control Features

Longitudinal characteristics of the Modified C-8A are influenced by two features not found on conventional airplanes: aerodynamics dependent on jet flap blowing and vectored hot thrust. Figure 3-1 illustrates typical wing-body aerodynamic characteristics. Lift, drag and pitching moment are dependent on blowing level (isentropic thrust coefficient, C_j) as well as angle of attack and flap angle. Downwash at the tail, which is related to wing lift and jet strength, is also a function of C_j as shown in Figure 3-2.

Horizontal tail aerodynamic characteristics are presented in Figure 3-3. The tail has a relatively high aspect ratio, inverted camber, and a large-chord elevator. A very effective elevator is important because tail incidence is fixed. The elevator is actuated manually by the pilot via the spring-tab system. Stick force gradient with elevator deflection increases with airspeed. Modifications to the spring tab follow-up ratio and to elevator torque tube stiffness have produced lowered stick forces compatible with one-hand operation. Stick force characteristics are shown in Figure 3-4. At STOL approach maximum stick force is slightly above 30 lbs compared to 55 lbs with the original system. (With the low force gradient system centering could be a problem even with low friction levels). At the torque tube wind-up limit the pilot reacts against elevator hinge moment directly with no more assistance from the tab. Stick force gradient becomes very steep. Normal flight maneuvering does not require elevator deflections into this region.

Elevator-to-column gearing varies with airspeed due to the spring-tab feature as shown in Figure 3-5. The large gearing ratio at the 60 kt STOL condition is advantageous for good pitch response. Elevator dynamic response characteristics to a step column input have been estimated. At 60 kt STOL conditions natural frequency is $\omega_e \approx 10$ rad/sec and damping ratio is $\zeta_e \approx .2$. Frequency and damping both increase with airspeed. Flutter analyses have cleared the spring-tab configuration, and dynamic problems are unlikely.

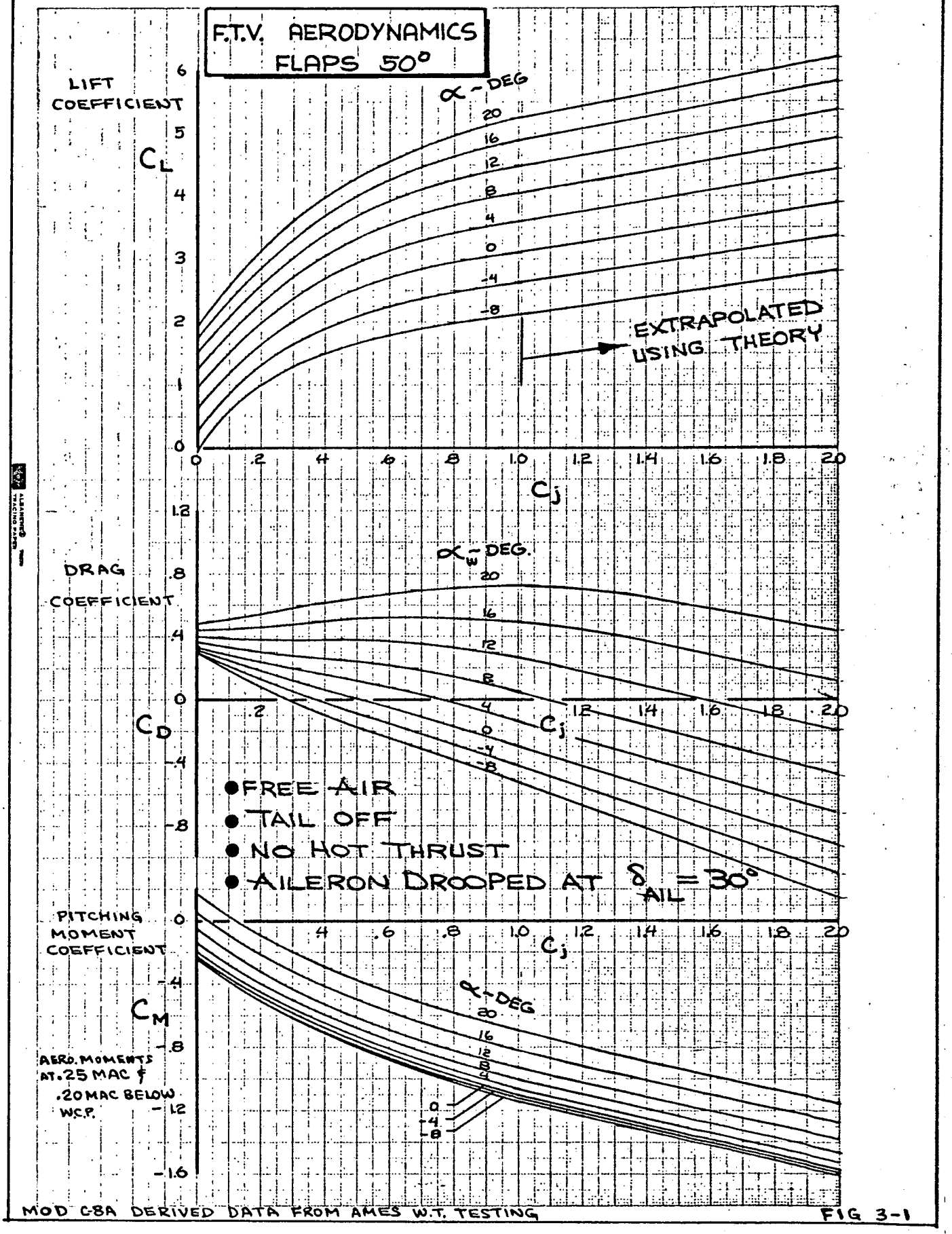

MOD C-8A DERIVED DATA FROM AMES W.T. TESTING

FIG 3-1

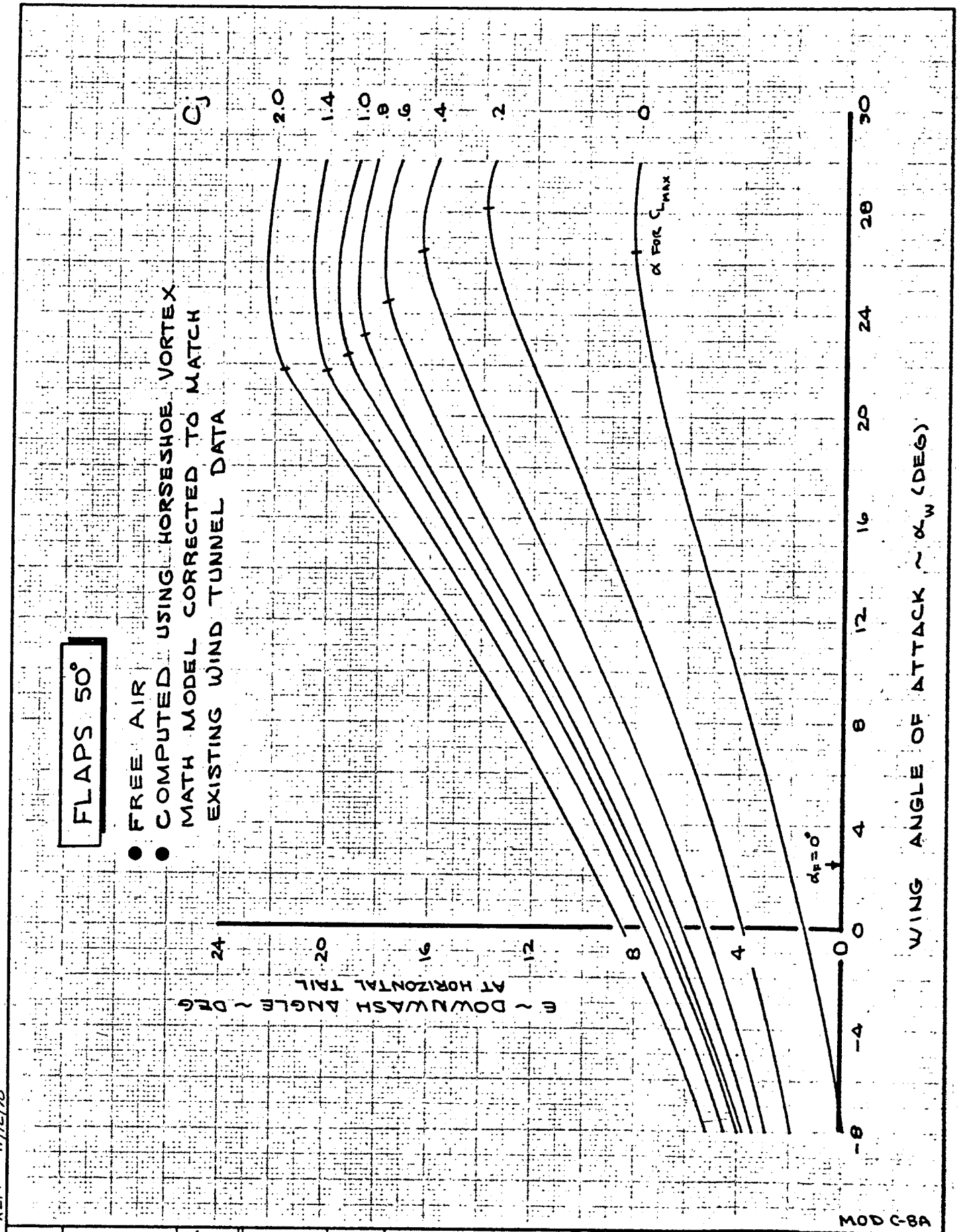

MOD C-8A

REF: 11/12/70

CALC	LDO	11/13/70	REVISED	DATE
CHECK	SPITZER	2-7-72		
APR				
APR				

TYPICAL DOWNWASH ANGLE AT THE HORIZONTAL TAIL

FIG 3-2

D6-40381

THE BOEING COMPANY

PAGE 3.4

CALC	SPITZER	2-8-71	REVISED	DATE	HORIZONTAL TAIL LIFT CHARACTERISTICS	FIG 3-3
CHECK						D6-40381
APR					THE BOEING COMPANY	PAGE 3.5
APR						

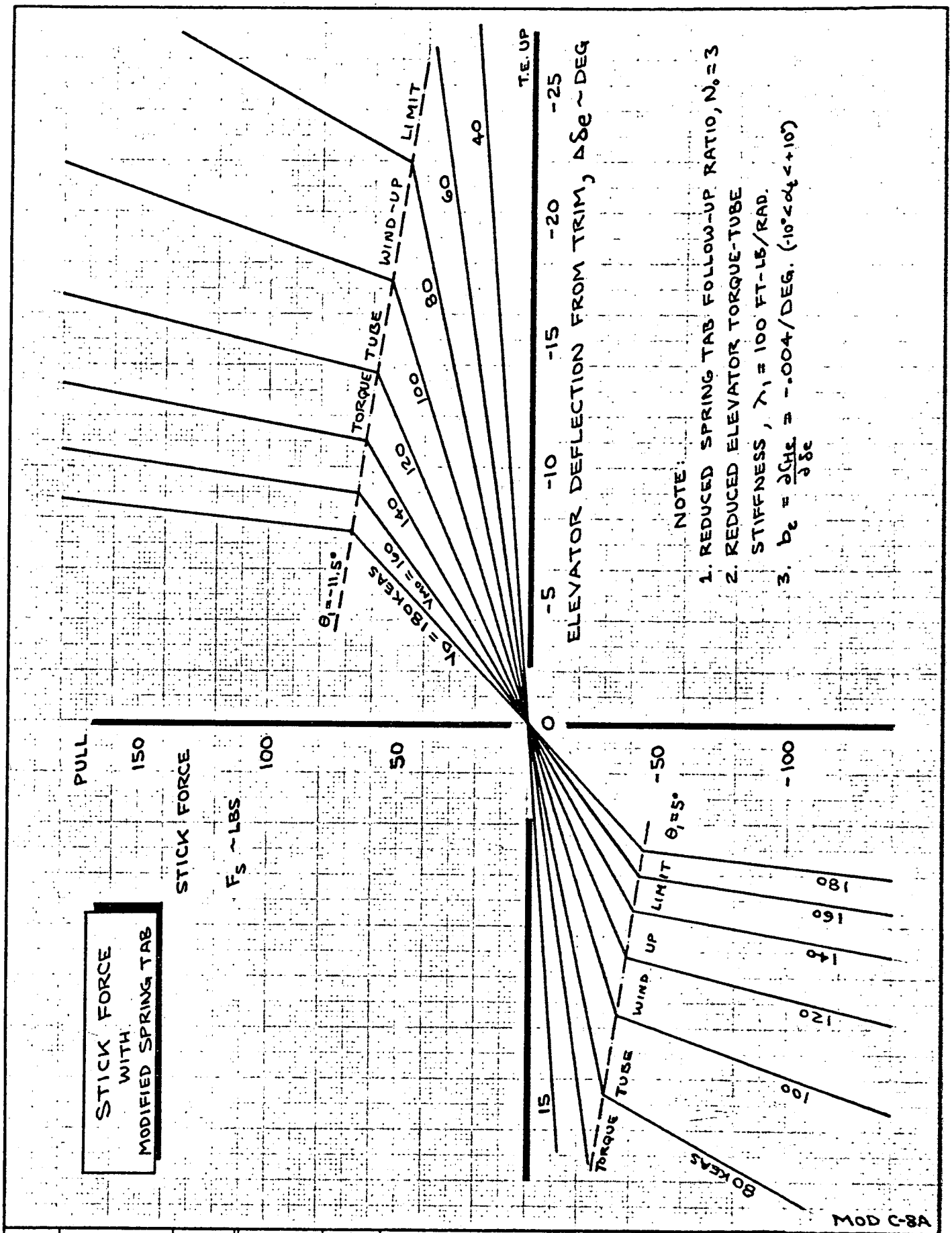

CALC	SPITZER	12-15-71	REVISED	DATE	STICK FORCE	FIG 3-4
CHECK						D6-40381
APR					THE BOEING COMPANY	PAGE 3.6
APR						

DI 4100 3240

K·E ALBANENE 1951

ELEVATOR-TO-COLUMN GEARING

- REDUCED STICK FORCE MODIFICATION
- TORQUE TUBE ROTATION: $\theta_1 < \theta_{1_{LIMIT}}$
- X_s POSITIVE FOR AFT COLUMN
- CABLE STRETCH INCLUDED
- -4.3 INCH $< X_s <$ 7.7 INCHES (AFT)

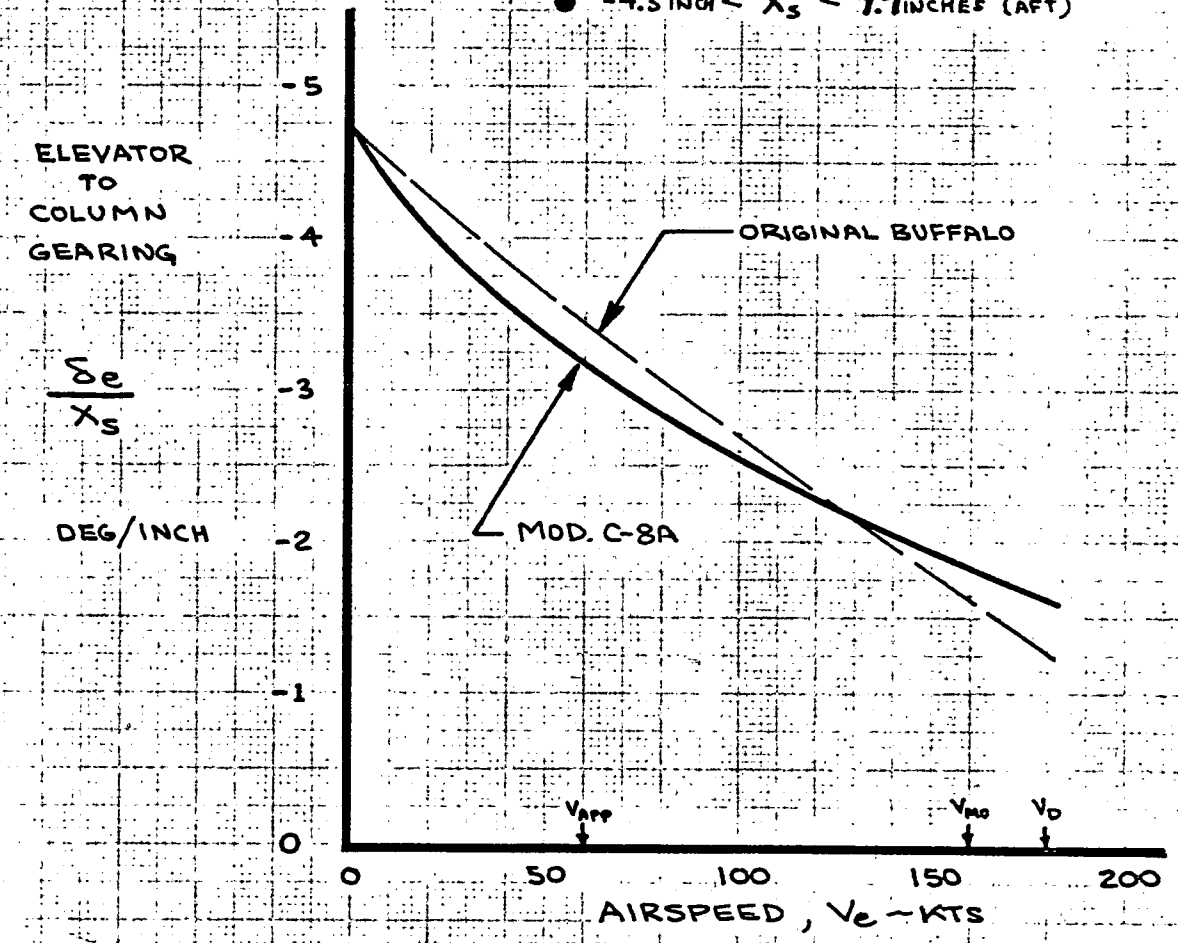

MOD C-8A

CALC	SPITZER	12-15-71	REVISED	DATE	ELEVATOR - TO - COLUMN GEARING	FIG 3-5
CHECK						D6-40381
APR					THE BOEING COMPANY	PAGE 3.7
APR						

3.2 Static Stability and Control

The Modified C-8A has an installed thrust-to-weight ratio approaching $T/W \approx .5$. The very effective high-lift system generates a design approach lift coefficient of $\frac{W}{qs} \approx 4.0$ or roughly twice that of "conventional" high-lift systems. Maximum performance in terms of low operating speeds, short field length and wide variation in flight path angle is impressive. Typical flight path capability for reasonable variation in power setting is shown on Figure 3-6. Climb and descent angles are considerably steeper than found with conventional transports. Body attitude also varies over a large range as shown in Figure 3-7. Takeoff attitude is quite high. Attitude changes significantly with speed in such a way that attitude becomes an indicator of flight condition.

Stall speed (1g at $C_{L_{max}}$) varies over a considerable range as well. Figure 3-8 shows typical minimum airspeed variation with flap and power setting at 40,000 lb. Power effect is quite pronounced. At landing flaps ($\delta_F = 65°$) minimum airspeed varies more than 40 kts. Mose operational flight speeds at takeoff and landing ($V_2 \approx 76$ kts, $V_{app} \approx 60$ kts) occur below power-off stall. The Modified C-8A truly operates in the "powered-lift" STOL regime.

The Modified C-8A has a limited fore and aft center of gravity range shown in Figure 3-9. With fixed equipment installation (basically flight test instrumentation) and no provision for passengers, the need for loadability range is not great. Structural design CG limits have been further restricted by aerodynamic considerations resulting from fixed tail incidence. The instrumentation rack in the cabin has beendesigned for fore-and-aft movement. Minor CG adjustment (+.6% aft at OEW) is possible by this means.

Elevator deflection is used for both '1g' trim and maneuvering. Elevator required to hold steady, '1g' flight has been computed for all combinations of weight, speed, flap deflection, power setting and hot thrust nozzle angle at nominal CG locations along the fuel loading line. Figure 3-10 presents the envelope of these conditions for the existing stabilizer incidence setting of $i_T = +1°$. Typical trim requirements for normal operation at 40,000 lb are also shown on the figure. For most flight conditions elevator angle will lie within a few degrees of neutral. This fortuitous situation occurs because pitching moment produced by flap deflection is almost entirely counteracted by tail lift induced by changes in downwash angle. Large elevator deflections are needed for stall maneuvers and full power application at landing flaps, vectors down.

The trimmed 1g flight conditions at nominal CG produce tail lift requirements shown in Figure 3-11. Tail lift and angle of attack required to trim extreme flight conditions may bring the tail close to stall. These conditions are flaps up stall and high power at landing flaps with nozzles down. Tail stalling produces non-linear elevator hinge moment characteristics with possible stick force lightening. The airplane may exhibit nose down "tuck" in the flaps down critical condition. Flight corners must be approached cautiously.

"Hands-off" trim (Fs = 0) is provided by using the trim tab to balance elevator hinge moment. The trim tab deflection limits are shifted with flap angle by a series interconnect with the flap system. The purpose of the flap interconnect is to prevent running the trim tab to excessive airplane nose-down elevator angles. Diving flight beyond operational placard speeds may result with large stick force required for recovery. Hands off elevator trim limits are shown for the flap-speed envelope on Figure 3-12.

Trim at the structural CG limits requires additional elevator deflection and tail lift shown in Figure 3-13. In order to keep the elevator angle near neutral for normal conditions, the stabilizer incidence angle should be shifted instead. Maneuvering capability is degraded somewhat as the CG moves forward of nominal. At aft CG static longitudinal stability degenerates, particularly in the STOL regime

Classical static longitudinal stability is characterized by the amount of stick force (elevator deflection) required to slow down (pull) or speed up (push) away from a trimmed flight condition. Standard practice dictates a stick force slope of 1 lb/6 kts; however, proper direction of force application is more important than force gradient level. Moreover, STOL flight at very high lift levels generates high induced drag. Many STOL conditions end up on the "backside" of the power-required characteristics. In this situation both power and elevator modulation is required to maintain the trim condition.

Figure 3-14 presents static longitudinal stability characteristics at nominal takeoff condition. The airplane is on the "front side" of the power curve as indicated by the flight path angle variation with speed. The stick force gradient is stable down to about 14 kts below trim speed. Below 67 kts the airplane tends to be self-stalling and requires close pilot attention.

The cruise condition shown in Figure 3-15 is stable and well-behaved. The airplane has adequate longitudinal stability at "conventional" approach condition (Figure 3-16). Mild powered lift effects are evidenced by the change in required trim angle of attack (constant speed) when power setting is used to vary glide slope. The 90 kt approach was found a suitable alternate landing condition.

Powered lift effects become very pronounced at the design STOL landing approach ($\gamma = -7.5°$ at 60 kts). Flight path may be controlled in two ways: by power changes or by thrust vector (nozzle) modulation. Figure 3-17 illustrates the wide

variation in glide slope attained by either method. The design approach condition (δ_F = 65°, γ = 90°, 92% RPM) was selected to assure the following margins with hot thrust perpendicular to flight path: $\Delta n_z \geq .35g$, $V_{APP} \geq 10$ kts from V_{MIN} and $\alpha_F \leq 5°$ (15° from stall). It can be seen that power changes vary the margins. At 60 kts, advancing throttles to takeoff setting produces $\Delta n_z \approx .65g$ and $\Delta V \approx 22$ kts. Reducing power setting on the other hand lower margins. This characteristic is due to the "lift coupling" with the throttle. In fact, advancing throttles on approach generates a net instantaneous force on the airplane oriented almost directly perpendicular to the flight path. Significant changes in angle of attack must take place to maintain trim speed. The upper curves on Figure 3-17 show that margins and trim angle of attack remain relatively constant when hot thrust vectoring is used to set glide slope. Nozzle modulation about the γ = 90° trim point produces instantaneous axial forces on the airplane analogous to power setting on conventional airplanes.

Figure 3-18 illustrates the effect the two control techniques on airplane attitude and trim. Extending the approach, i.e. raising the flight path angle, by rotating the nozzles aft produces a conventional nose-up change in attitude. Increased power also reduces glide slope but the airplane pitches nose down, which is unconventional. Airplane attitude variation with change in airspeed at γ = -7.5° is quite pronounced but conventional in direction. Trim elevator change is small in all cases. In the simulator studies, the pilots considered the reversed attitude change with power as "unstable". For STOL approach the pilots concluded that nozzle modulation provided the best means of flight path control.

Figure 3-19 presents typical static longitudinal stability characteristics at STOL landing approach. The rate of change of glide slope with speed is $\frac{\partial \gamma}{\partial V}$ = .2 deg/kt (unstable), which is over three times greater than that permitted by MIL-F-8785 (Reference 11) for conventional airplane operation. Using thrust

vector modulation, the pilots were able to track the approach path with acceptable results. Static stability exists for speed increase above 60 kts, but the slope and magnitude of pull force below 60 kts is very low. The pilots had to devote considerable attention to the task of maintaining control at STOL approach.

Reduced stability with lowering flight speed is brought on by several effects. First, reduced airspeed increases blowing coefficient, Cj, thereby producing an inherent degradation in aerodynamic stability. This degradation is caused primarily by change in wing lift curve slope and downwash flow field at the tail. The second contributor to reduced stability is the nose-up hot thrust moment. The hot thrust nozzles are located below and ahead of the center of gravity. Tail lift is required to trim the thrust moment. If, for example, speed is reduced, the hot thrust nose-up moment remains constant while the aerodynamic pitching moment is reduced ("q" effect). The net result is a virtual destabilizing pitch-up due to thrust. Figure 3-20 presents the "equivalent" (includes thrust effects) static aerodynamic stability characteristic of the Modified C-8A at landing approach. Even though a stable slope $\left(\frac{\partial C_m}{\partial C_L} < 0\right)$ exists at constant speed, the effects of Cj and hot thrust produce a de-stabilizing trend as speed is reduced at "1g".

Hot thrust effects are even more pronounced in the two-engine go-around condition. Figure 3-21 presents static longitudinal stability characteristics for the "wave-off" condition. Elevator-to-trim actually reverses slope markedly as speed is reduced below the 65 kt nominal wave-off trim speed.

STOL, powered-lift flight produces a number of undesirable pitch-axis characteristics. Powered flight controls, longitudinal SAS, and automatic airspeed control have been investigated and found beneficial (Reference 10). Program scope precluded their addition to the Modified C-8A. Actual flight testing will reveal just what improvements are needed for satisfactory pilot ratings.

FLIGHT PATH ANGLE CAPABILITY AT 40000 LBS

- TWO ENGINES OPERATING
- SEA LEVEL, STANDARD DAY

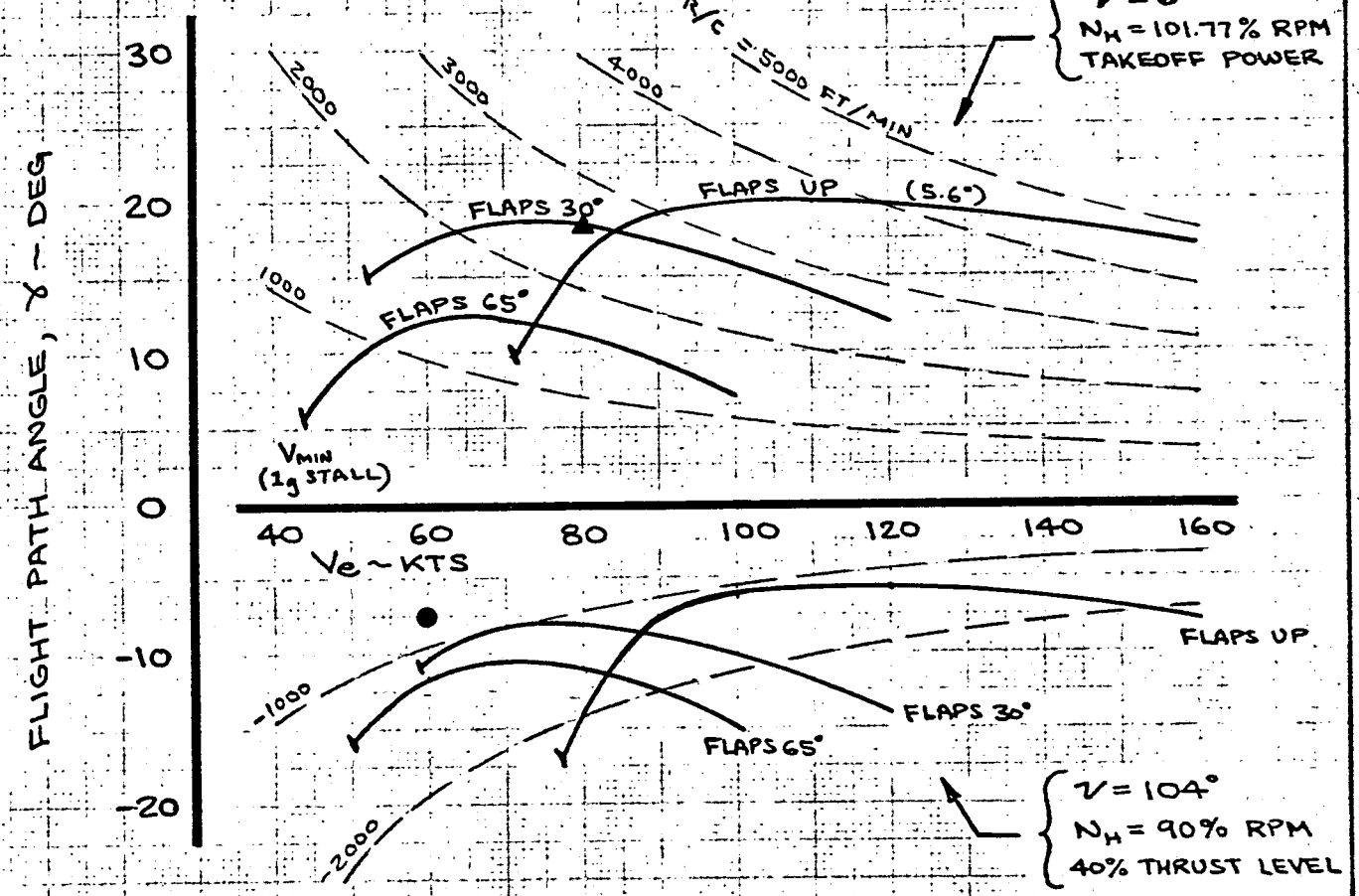

NOTE:
10% THRUST LEVEL AT 82% RPM

MOD C-8A

53, 55, 56

CALC	SPITZER	12-10-71	REVISED	DATE	TYPICAL FLIGHT PATH AND RATE OF CLIMB ENVELOPE
CHECK					
APR					
APR					
					THE BOEING COMPANY

FIG 3-6

D6-40381

PAGE 3.13

FUSELAGE ATTITUDE CAPABILITY AT 40000 LBS.

- TWO ENGINES OPERATING
- SEA LEVEL, STANDARD DAY

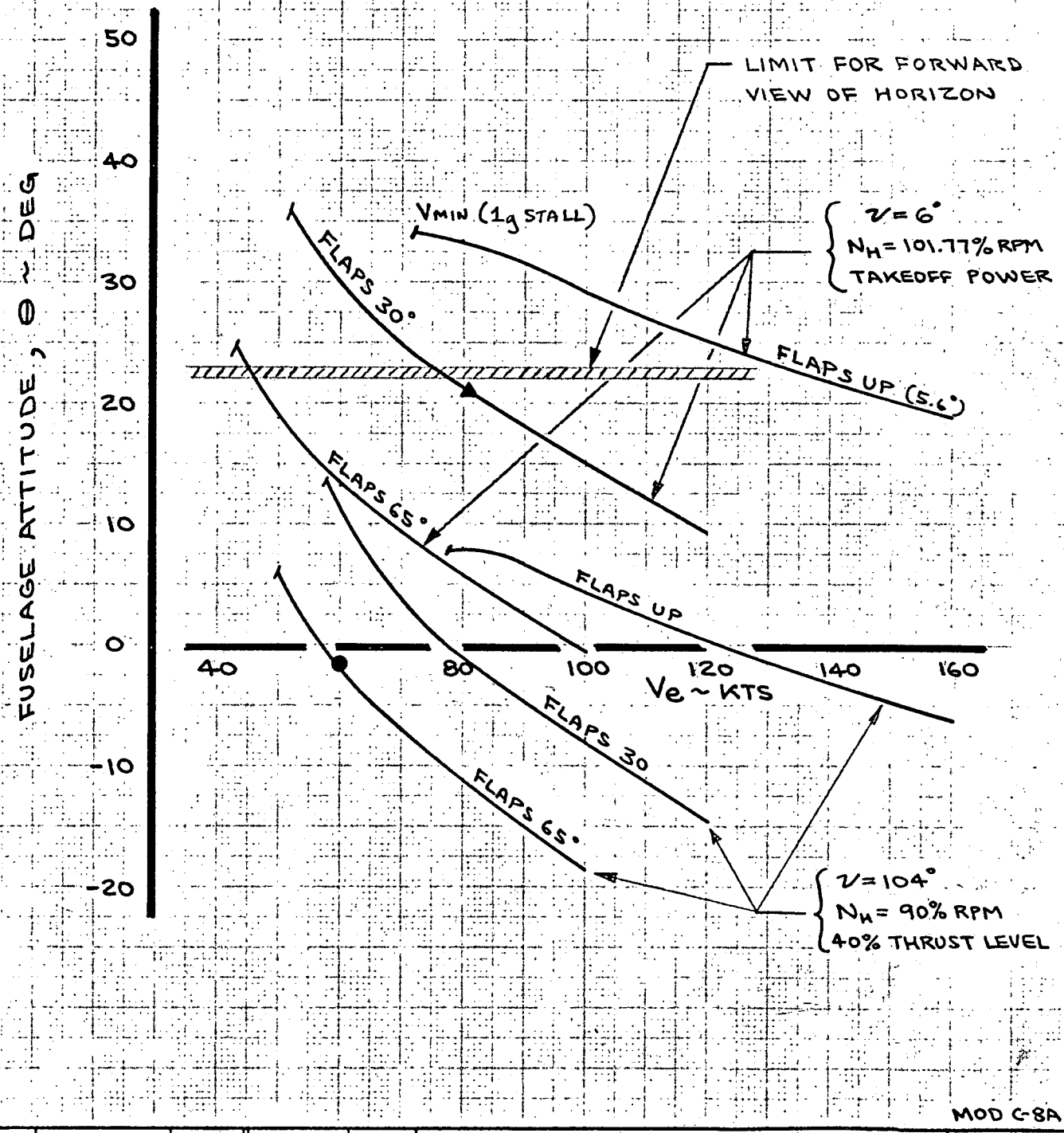

MOD C-8A

53, 55, 56

CALC	SPITZER	12-10-71	REVISED	DATE	TYPICAL BODY ATTITUDE ENVELOPE	FIG 3-7
CHECK						D6-40381
APR					THE BOEING COMPANY	PAGE 3.14
APR						

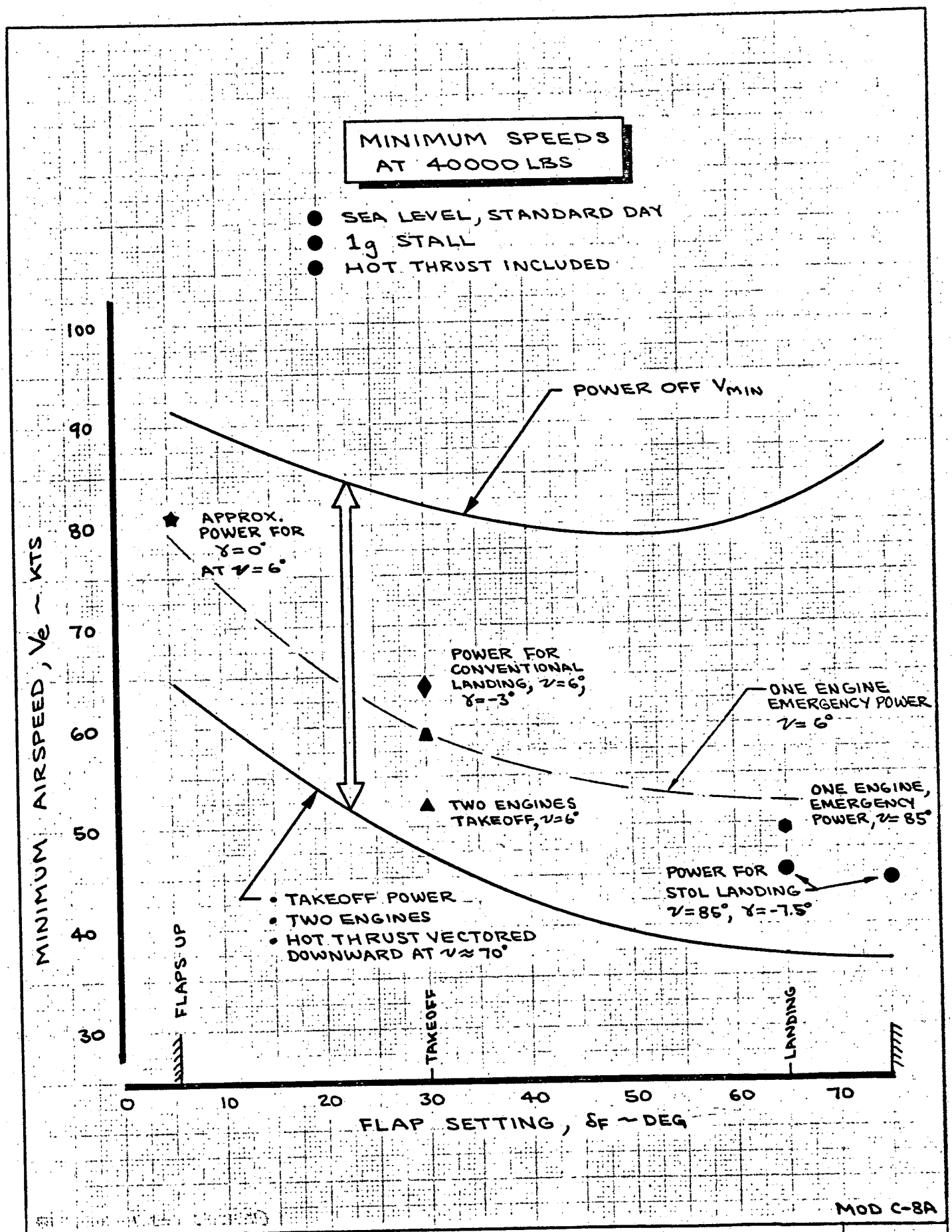

CALC	SPITZER	12-10-71	REVISED	DATE
CHECK				
APR				
APR				

TYPICAL MINIMUM AIRSPEED VARIATION WITH FLAPS & POWER

FIG 3-8

D6-40381

THE BOEING COMPANY

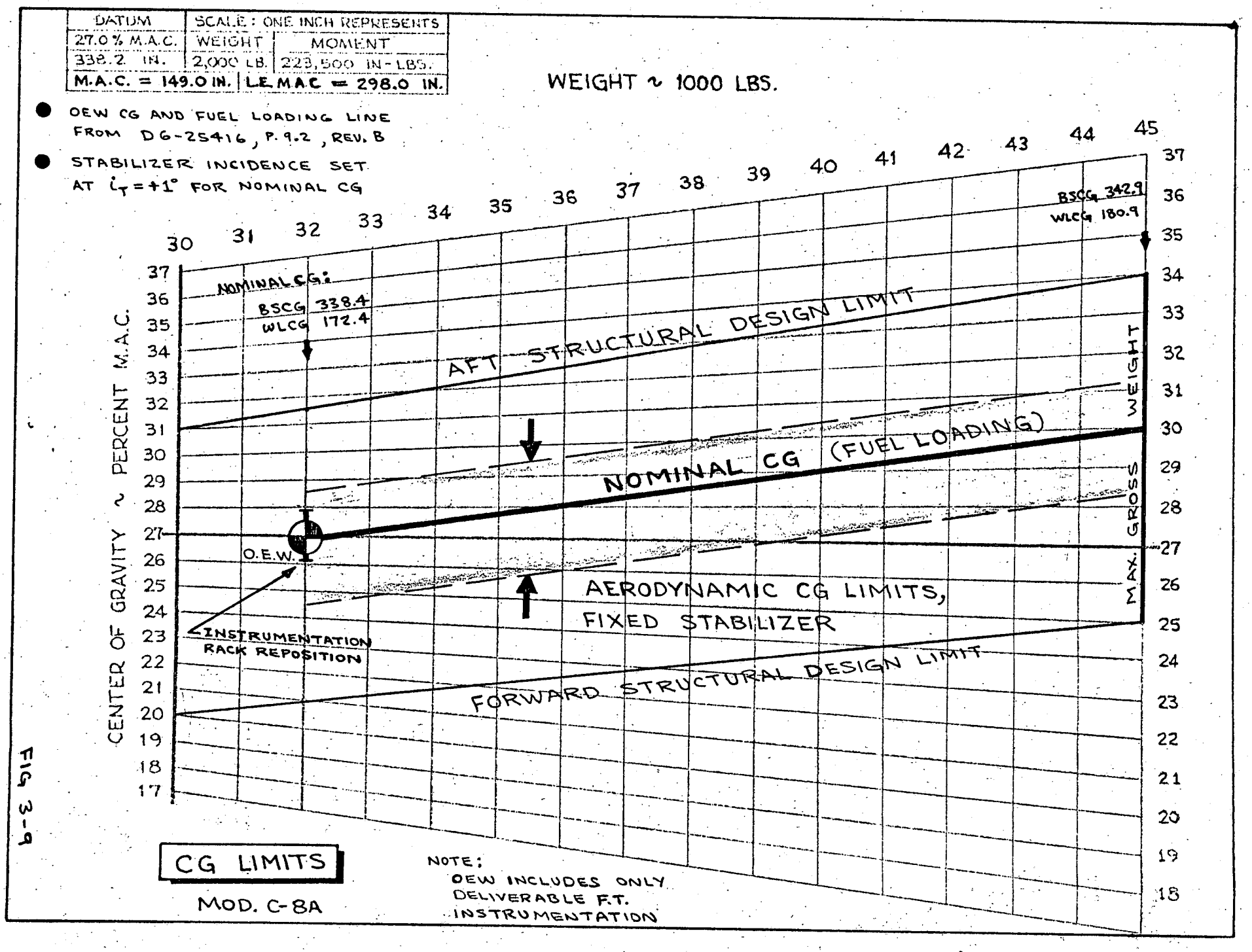
DATUM
27.0 % M.A.C.
338.2 IN.
M.A.C. = 149.0 IN.
SCALE : ONE INCH REPRESENTS
WEIGHT
2,000 LB.
MOMENT
223,500 IN-LBS.
L.E.M.A.C = 298.0 IN.
WEIGHT ~ 1000 LBS.
OEW CG AND FUEL LOADING LINE FROM D6-25416, P. 9-2, REV. B
STABILIZER INCIDENCE SET AT $i_T = +1°$ FOR NOMINAL CG
CENTER OF GRAVITY ~ PERCENT M.A.C.
NOMINAL C.G.:
BSCG 338.4
WLCG 172.4
BSCG 342.9
WLCG 180.9
AFT STRUCTURAL DESIGN LIMIT
NOMINAL CG (FUEL LOADING)
O.E.W.
INSTRUMENTATION RACK REPOSITION
AERODYNAMIC CG LIMITS, FIXED STABILIZER
FORWARD STRUCTURAL DESIGN LIMIT
MAX. GROSS WEIGHT
CG LIMITS
MOD. C-8A
NOTE:
OEW INCLUDES ONLY DELIVERABLE F.T. INSTRUMENTATION

FIG 3-9

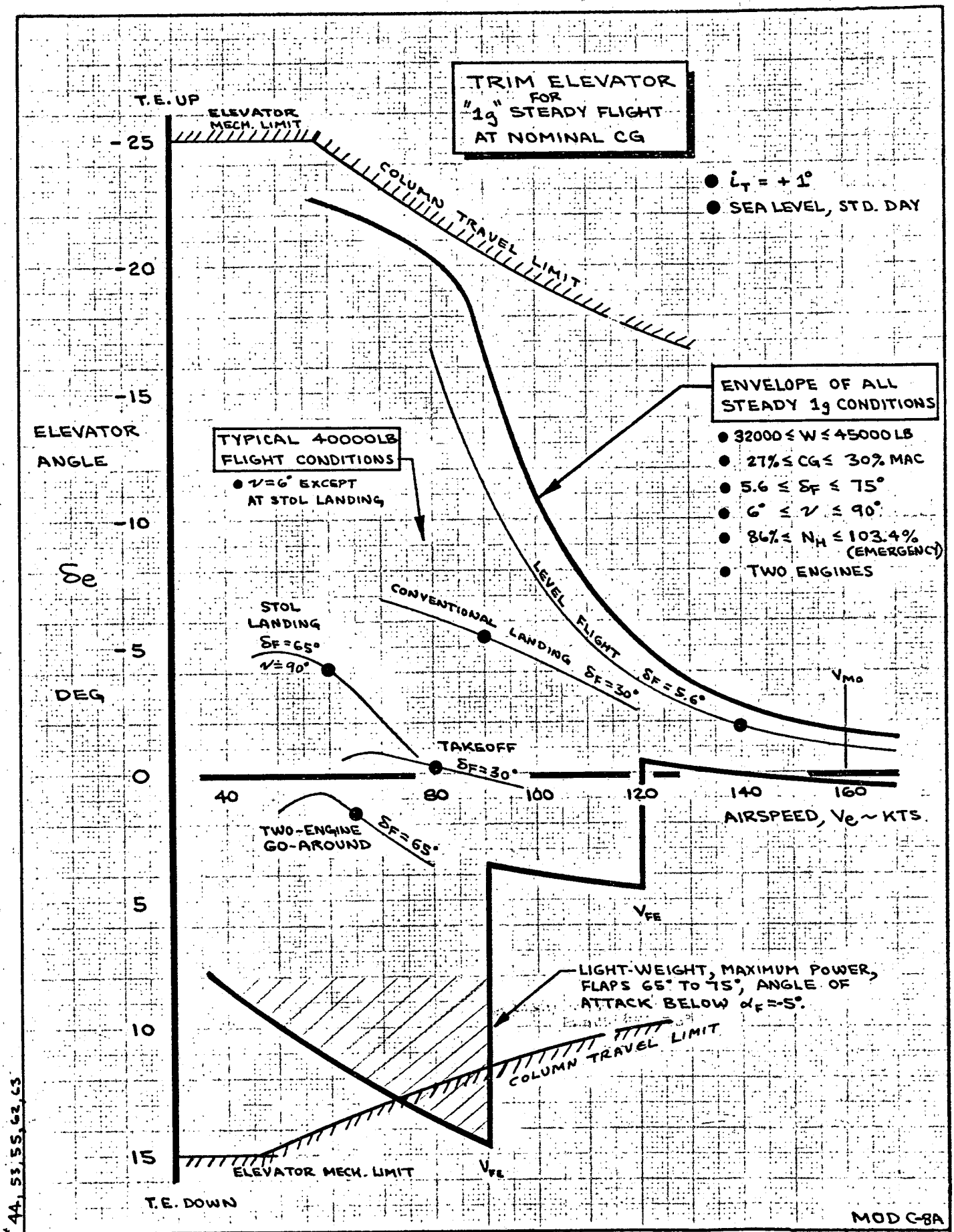

44, 53, 55, 62, 63

CALC	SPITZER	2-9-72	REVISED	DATE
CHECK				
APR				
APR				

ELEVATOR-TO-TRIM ENVELOPE

FIG 3-10

D6-40381

THE BOEING COMPANY

PAGE 3.17

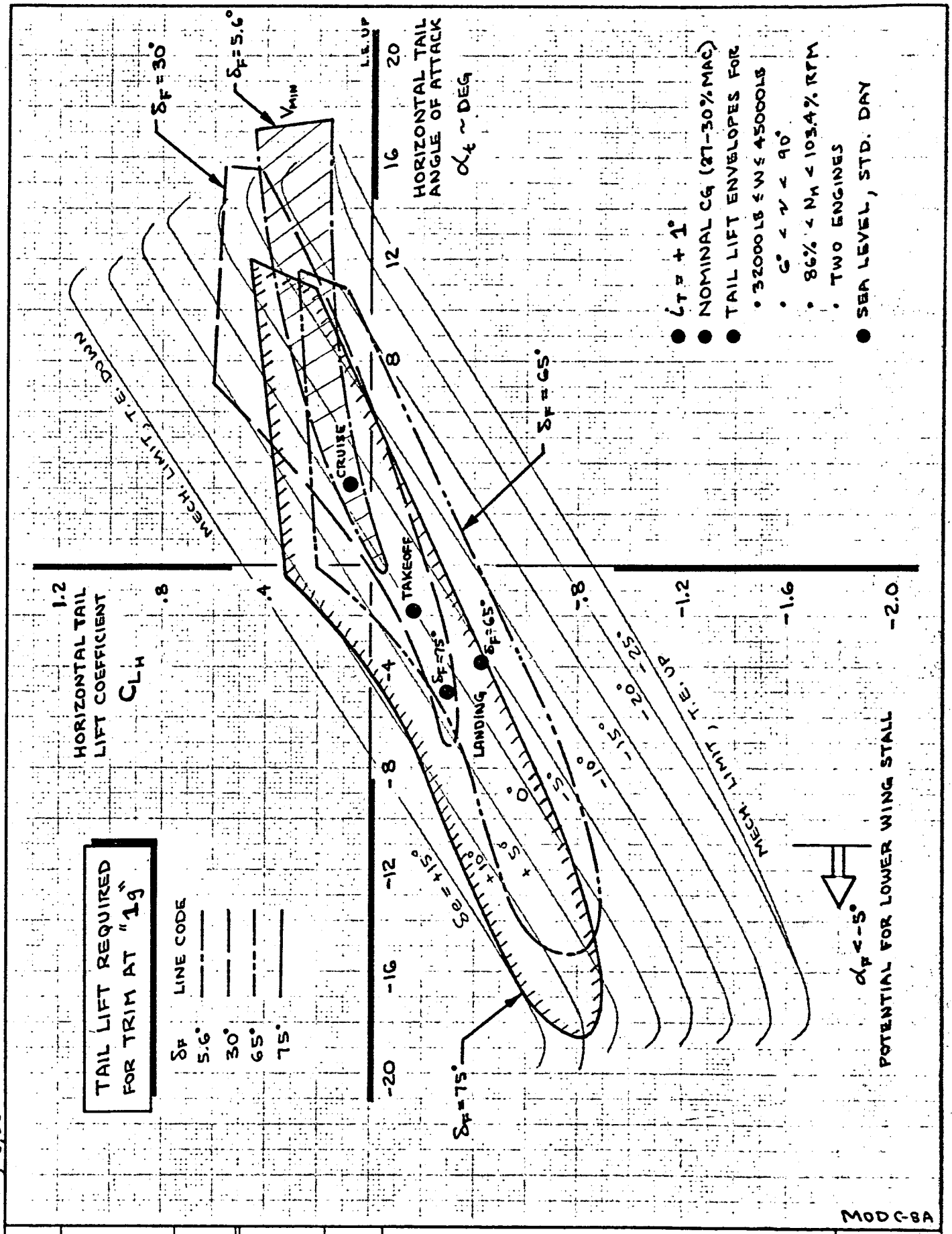

CALC	SPITZER	2-9-72	REVISED	DATE
CHECK				
APR				
APR				

TAIL LIFT REQUIREMENTS FOR "1g" FLIGHT

THE BOEING COMPANY

FIG 3-11

D6-40381

PAGE 3.18

*44, 52, 55

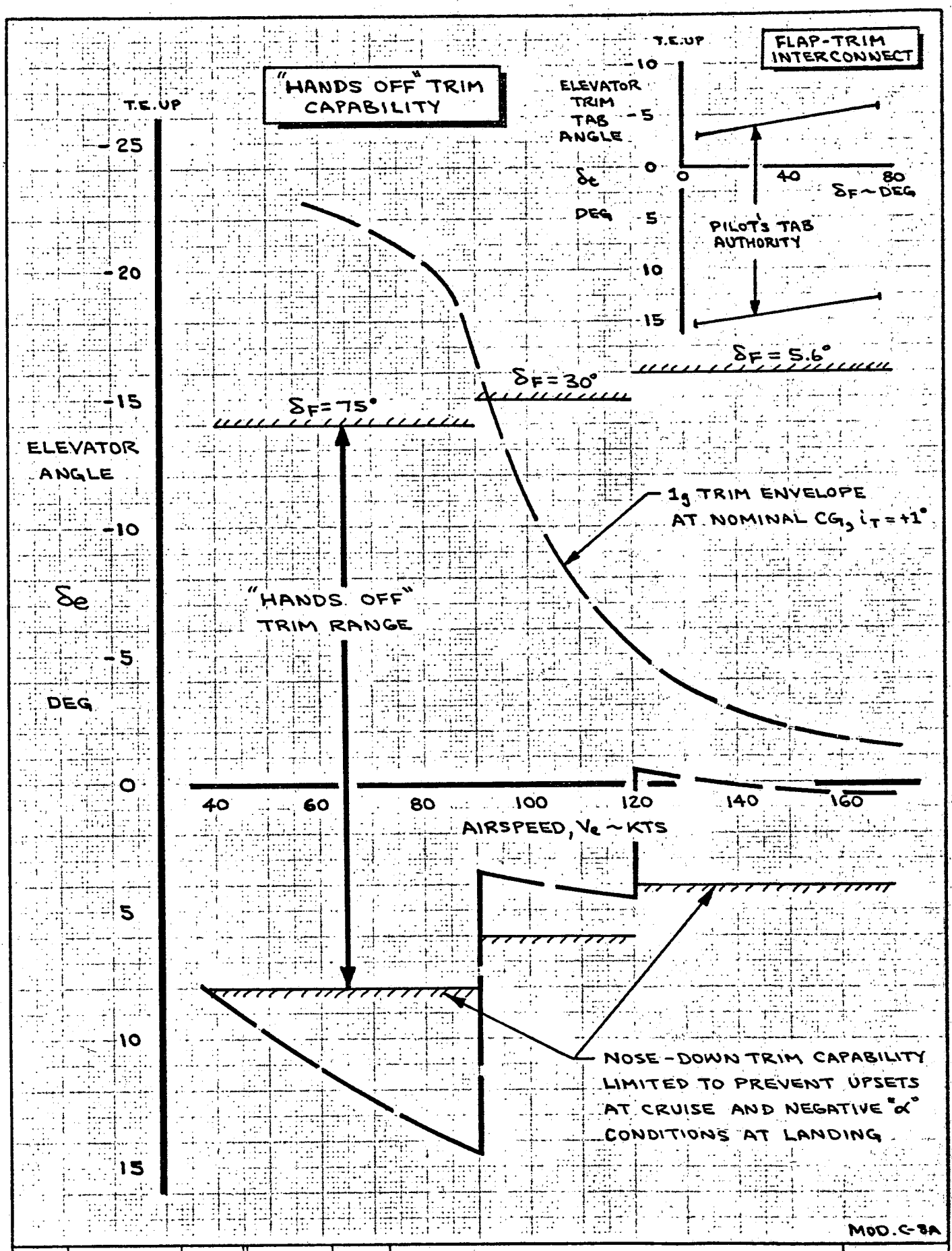

CALC	SPITZER	4-6-71	REVISED	DATE	TRIM CAPABILITY
CHECK			SPITZER	2-9-72	
APR					
APR					THE BOEING COMPANY

FIG 3-12
D6-40381
PAGE 3.19

TRIM CHANGE FOR CG SHIFT TO STRUCTURAL CG LIMITS

● REVERSE SIGN ON $\Delta\delta e$ AND ΔC_{L_H} FOR FORWARD CG SHIFT

$$\Delta\delta e = -\frac{\left(\frac{W}{qS}\right)}{Cm_{\delta e}} \Delta CG$$

$$\Delta i_T = .6\ \Delta\delta e$$

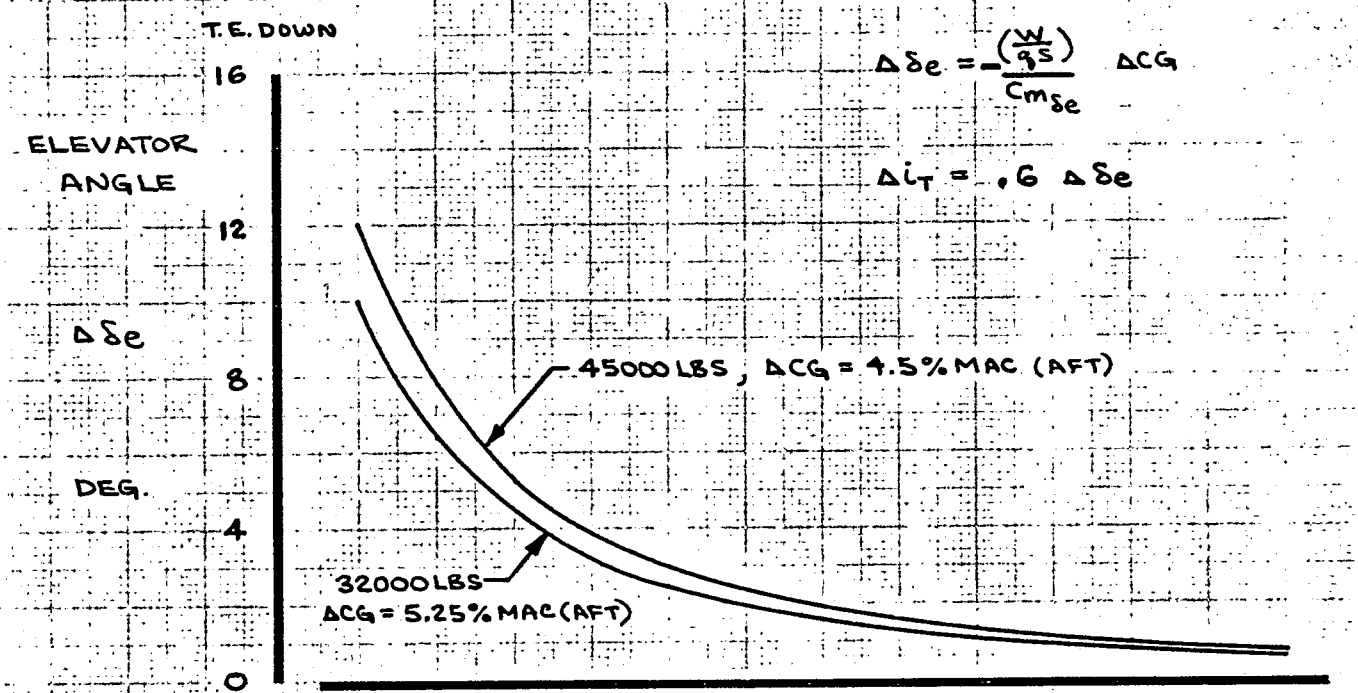

$$\Delta C_{L_H} = \frac{\left(\frac{W}{qS}\right)}{V_H} \Delta CG$$

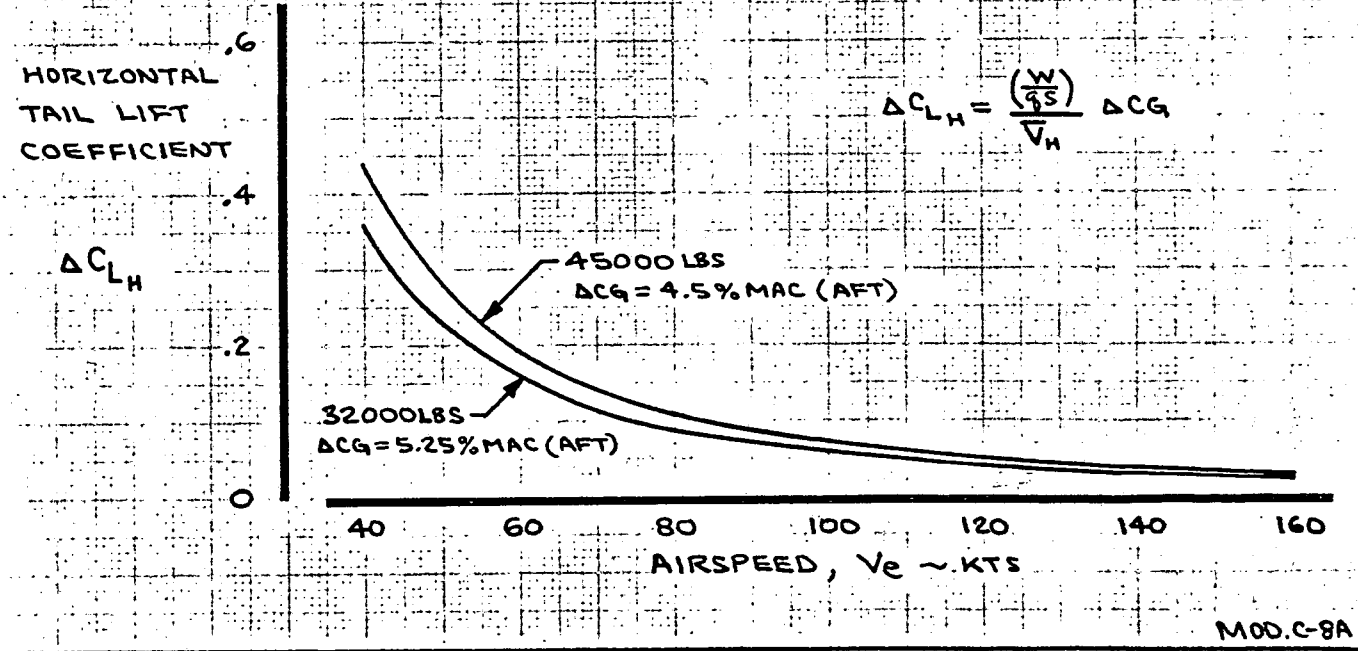

MOD. C-8A

CALC	SPITZER	2-9-72	REVISED	DATE	INCREMENTAL TRIM CHANGE FOR CG SHIFT FROM "NOMINAL" TO STRUCTURAL LIMITS	FIG 3-13
CHECK						D6-40381
APR					THE BOEING COMPANY	PAGE 3.20
APR						

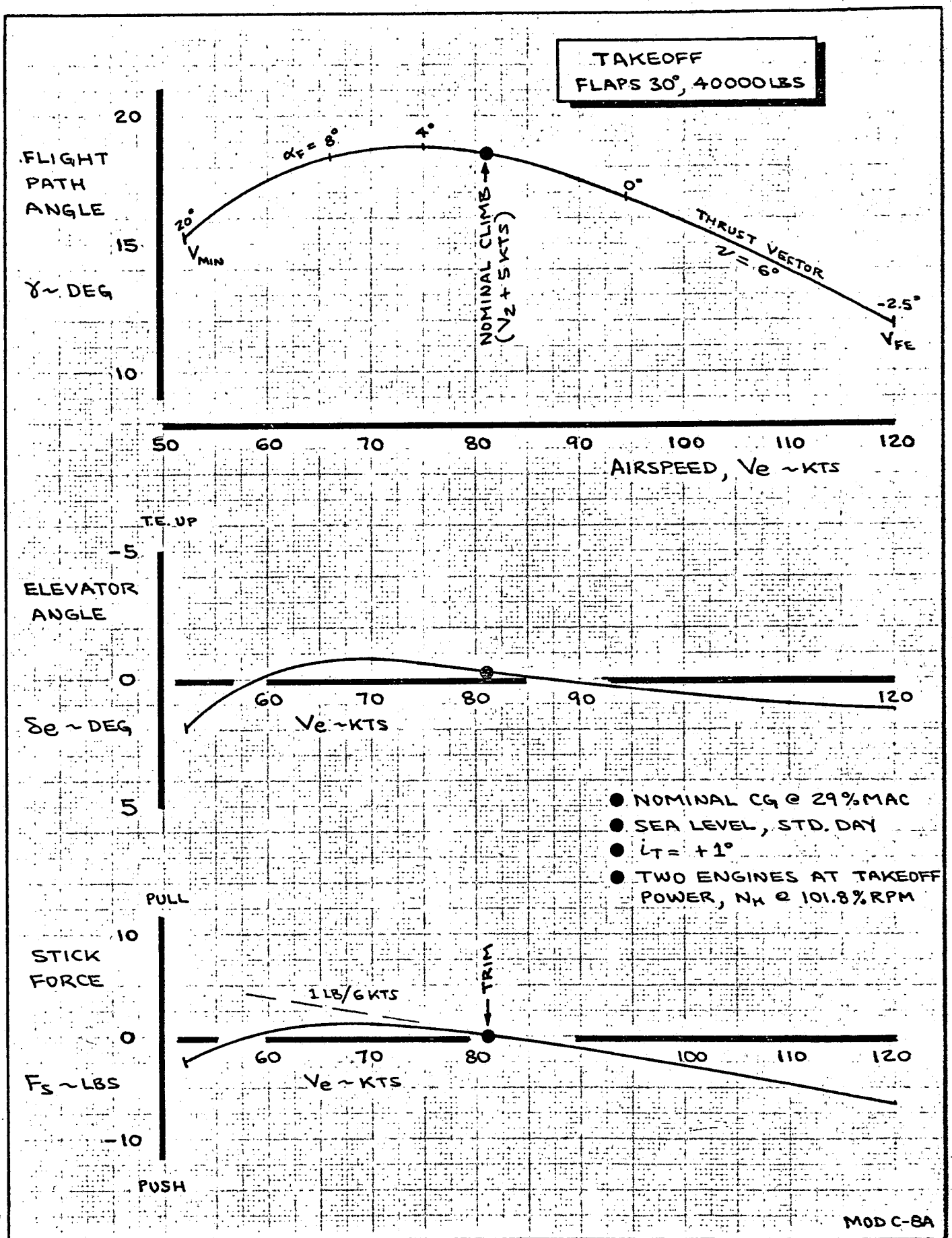

CALC	SPITZER	1-7-72	REVISED	DATE	STATIC LONGITUDINAL STABILITY AT FLAPS 30° TAKEOFF	FIG 3-14
CHECK						D6-40381
APR					THE BOEING COMPANY	PAGE 3.21
APR						

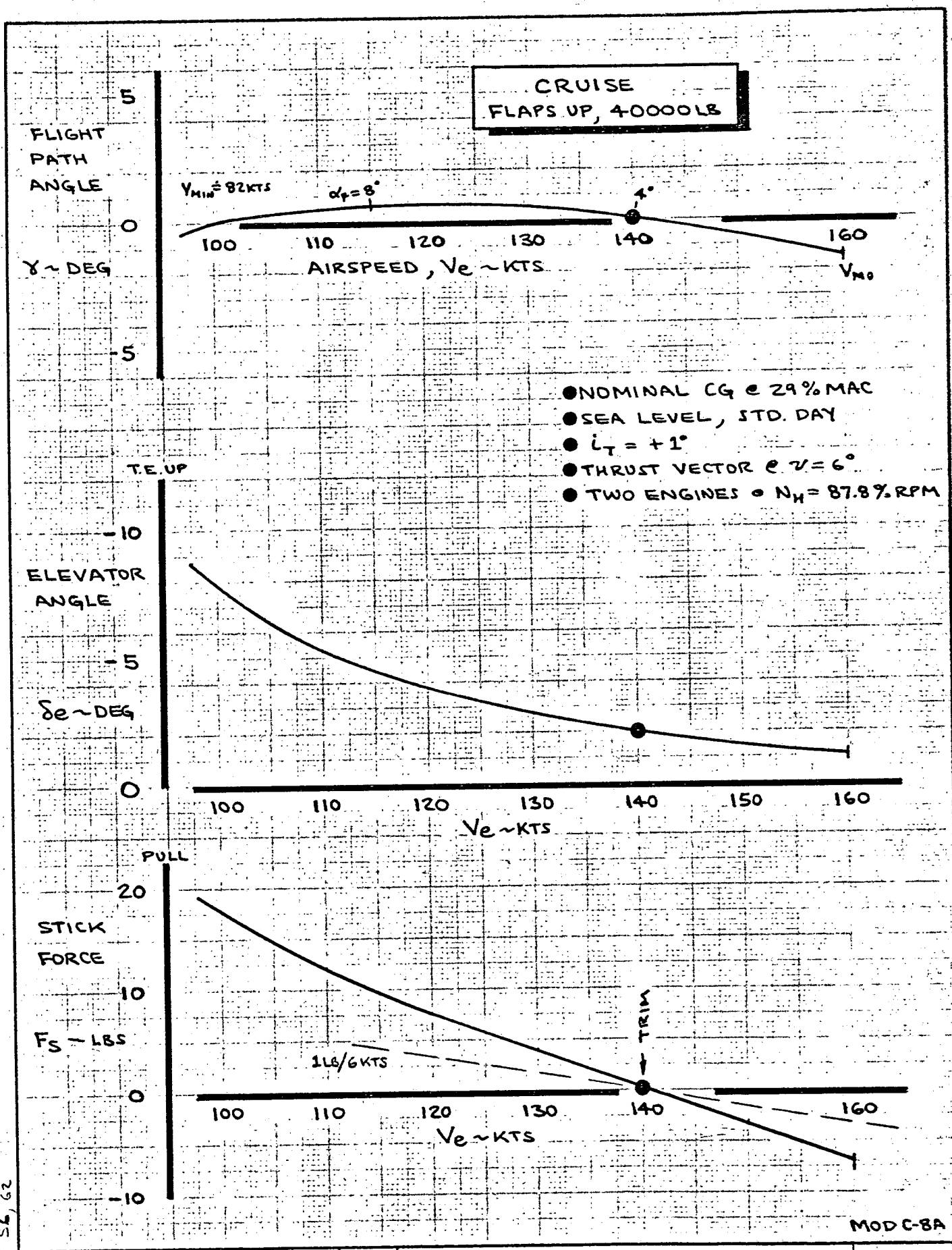

CALC	SPITZER	1-19-72	REVISED	DATE	STATIC LONGITUDINAL STABILITY AT TYPICAL FLAPS UP CRUISE	FIG 3-15
CHECK						D6-40381
APR					THE BOEING COMPANY	PAGE 3.22
APR						

AD 461 C-R6

K·E ALBANENE 1964 3.5 C-2000

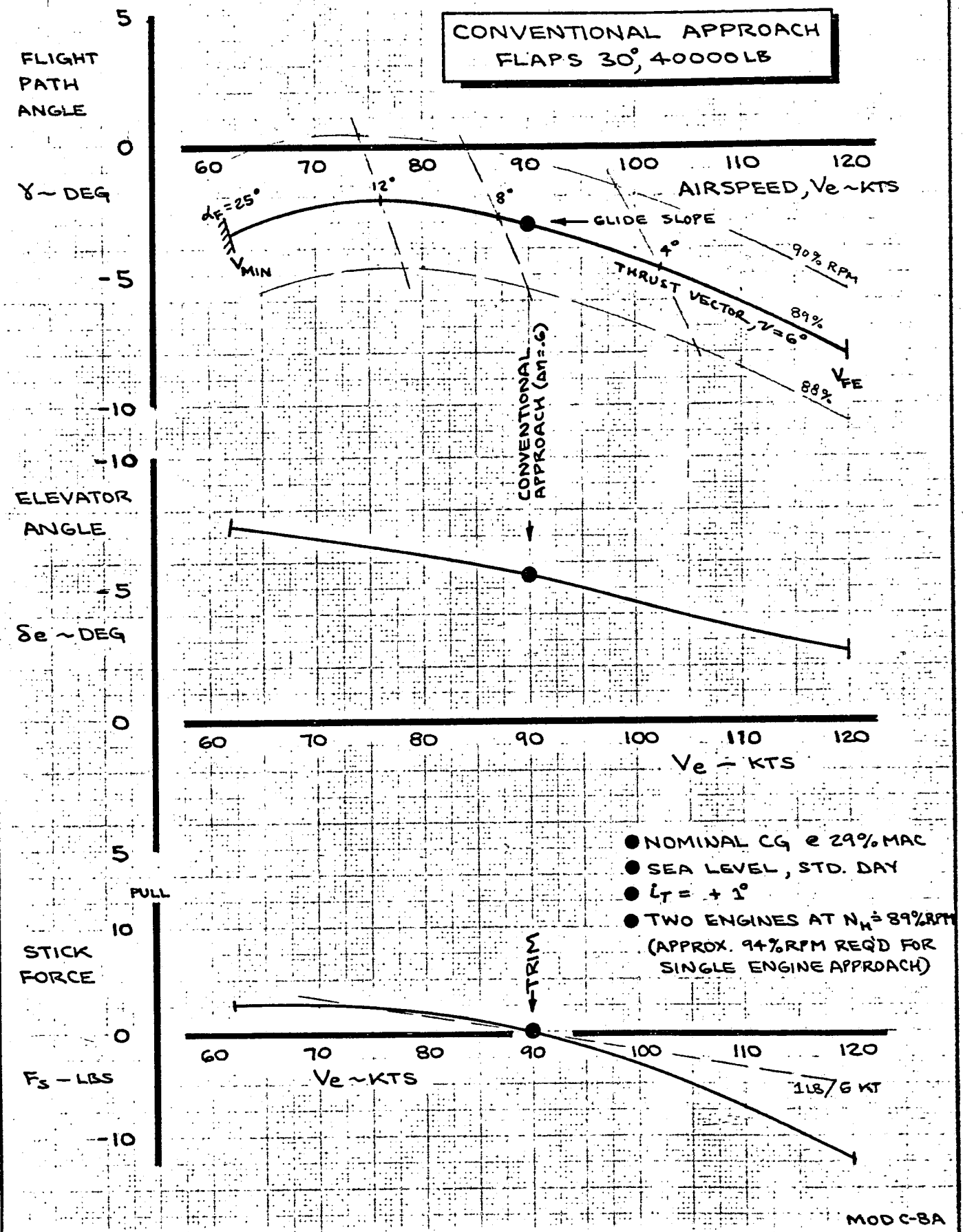

CALC	SPITZER	1-17-72	REVISED	DATE	STATIC LONGITUDINAL STABILITY AT FLAPS 30° CONVENTIONAL APPROACH	FIG 3-16
CHECK						D6-40381
APR					THE BOEING COMPANY	PAGE 3.23
APR						

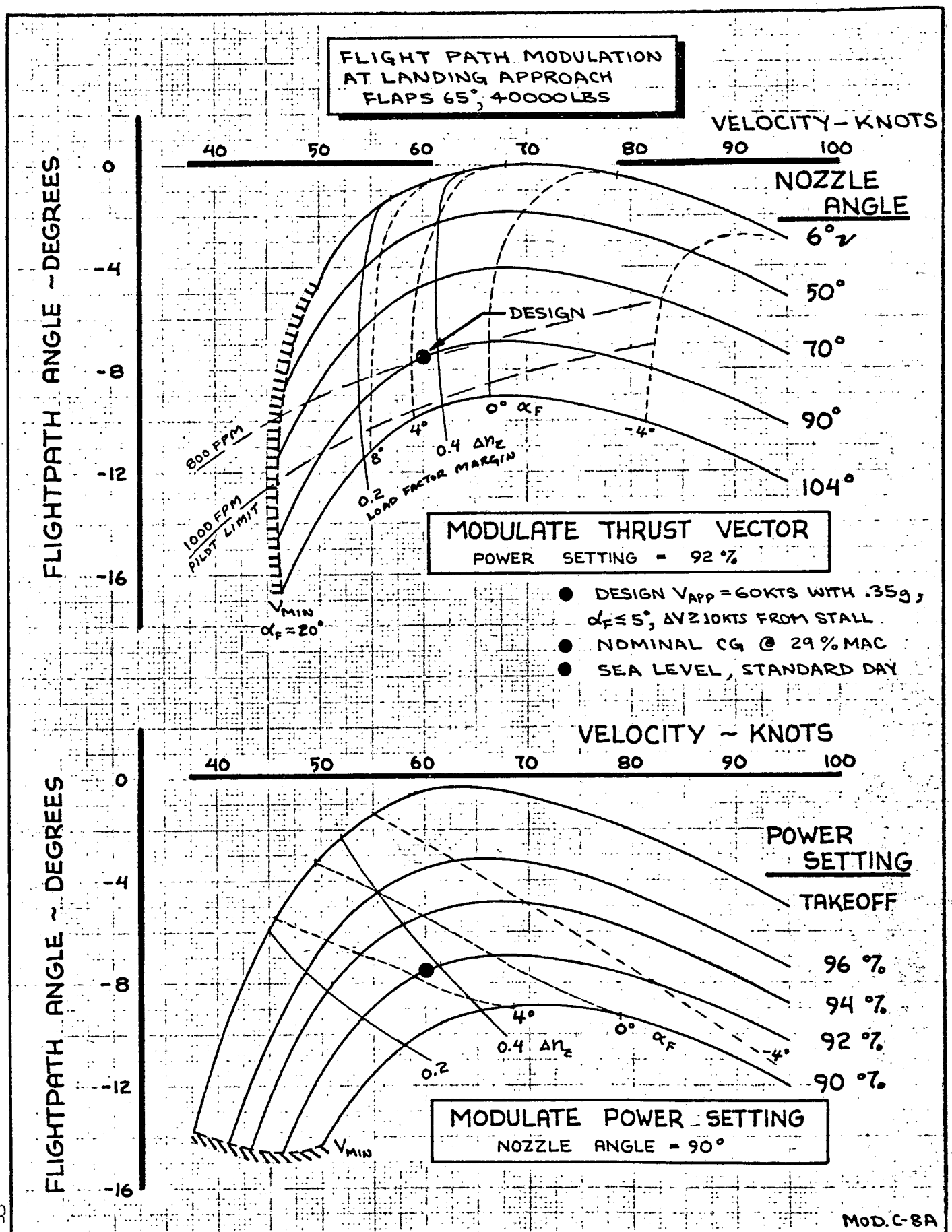

CALC	DHP	10-29-71	REVISED	DATE	TWO FLIGHT PATH CONTROL TECHNIQUES AT STOL APPROACH
CHECK			SPITZER	2-10-72	
APR					
APR					

FIG 3-17

D6-40381

THE BOEING COMPANY

PAGE 3.24

#55

AD 461 C-R6

K-E ALBANENE 1961 8.5 G-8000

24

ATTITUDE & TRIM CHANGES AWAY FROM STOL APPROACH

- FLAPS 65°, 40000LBS
- SEA LEVEL, STD. DAY
- NOMINAL CG AT 29% MAC
- TRIM AT 60KTS, γ = -7.5 DEG, ν = 90°, N_H = 92% RPM

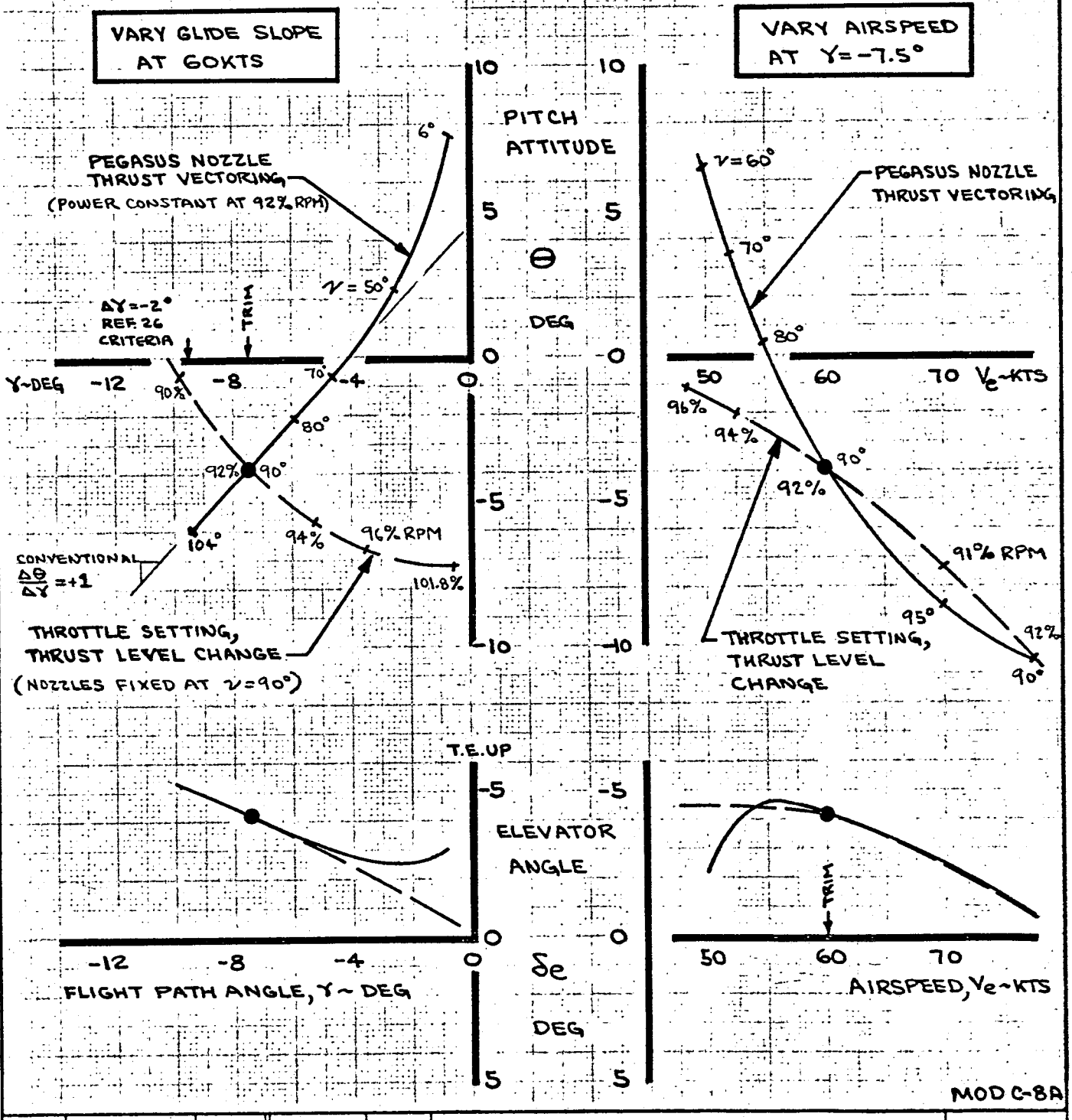

MOD C-8A

#55,70

CALC	SPITZER	1-6-72	REVISED	DATE	EFFECT OF TWO FLIGHT PATH CONTROL TECHNIQUES ON PITCH ATTITUDE AND TRIM AT STOL APPROACH
CHECK			SPITZER	2-25-72	
APR					
APR					
					THE BOEING COMPANY

FIG 3-18

D6-40381

PAGE 3.25

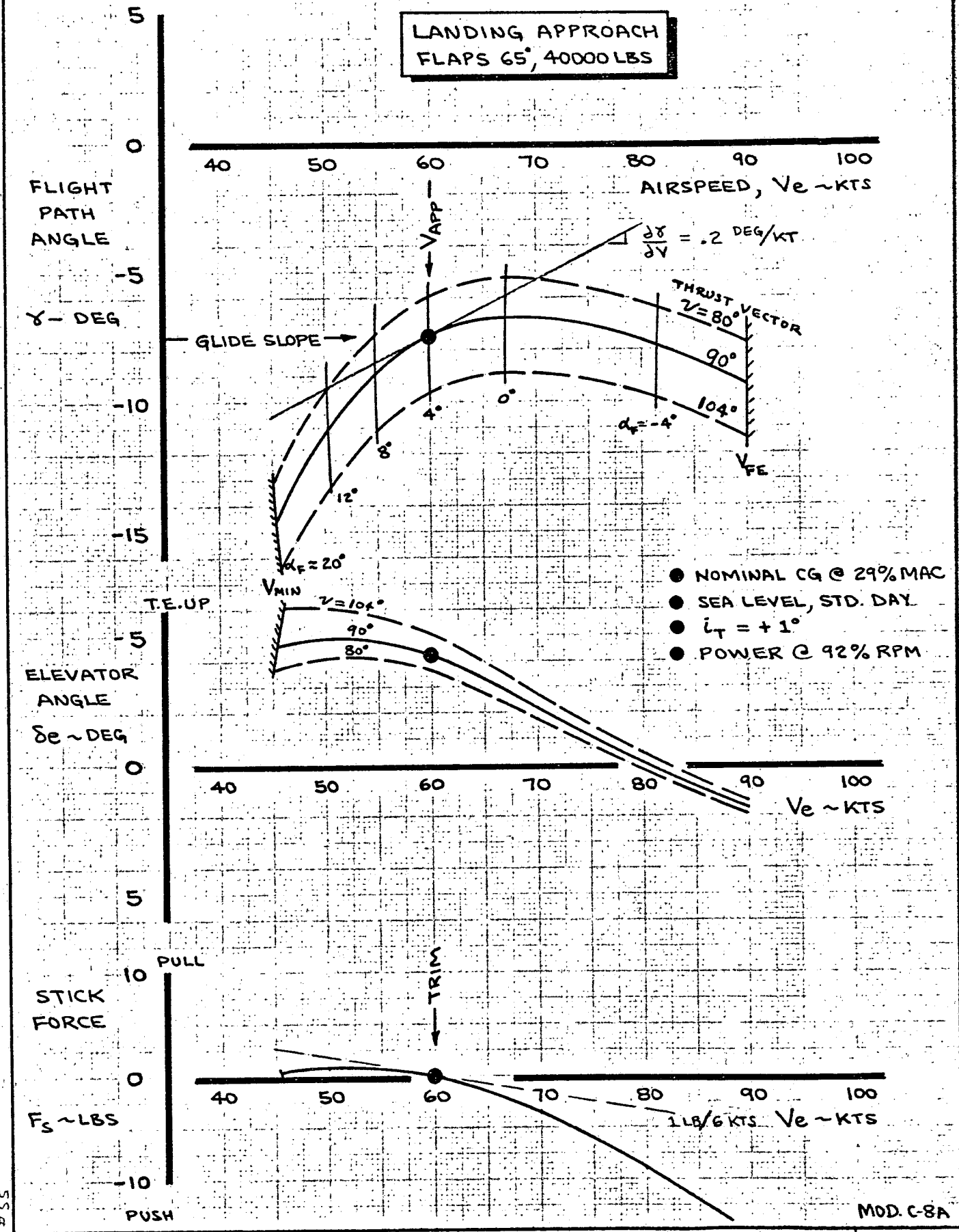

CALC	SPITZER	1-7-72	REVISED	DATE	STATIC LONGITUDINAL STABILITY AT FLAPS 65°, STOL LANDING APPROACH	FIG 3-19
CHECK						D6-40381
APR					THE BOEING COMPANY	PAGE 3.26
APR						

STATIC LONGITUDINAL STABILITY "EQUIVALENT" AERODYNAMIC CHARACTERISTIC INCLUDING THRUST EFFECTS AT FLAPS 65°, 40000LB

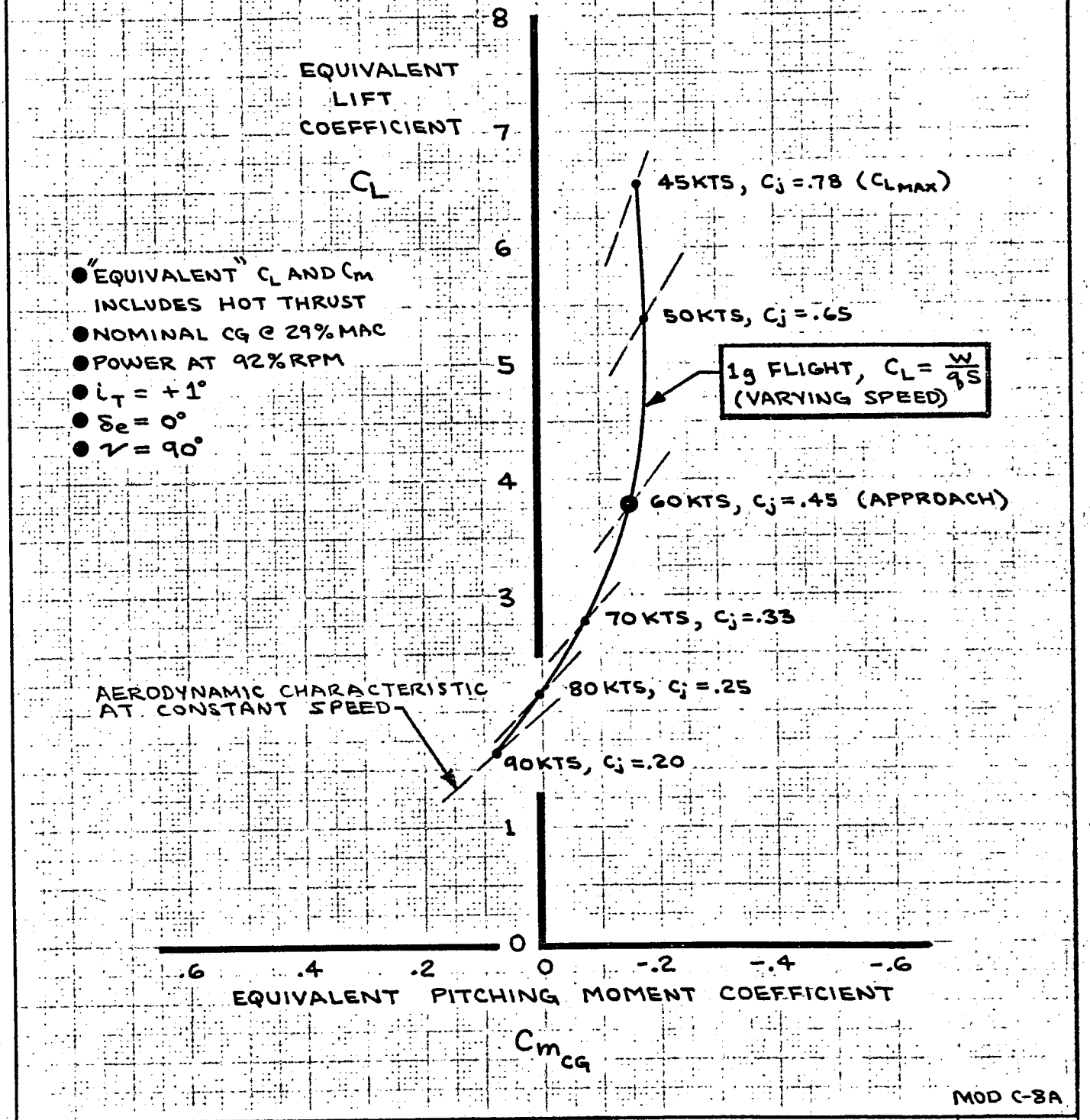

MOD C-8A

CALC	SPITZER	1-24-72	REVISED	DATE
CHECK				
APR				
APR				

EQUIVALENT LONGITUDINAL STABILITY CHARACTERISTIC AT FLAPS 65°, $\nu = 90°$

FIG 3-20

D6-40381

THE BOEING COMPANY

PAGE 3.27

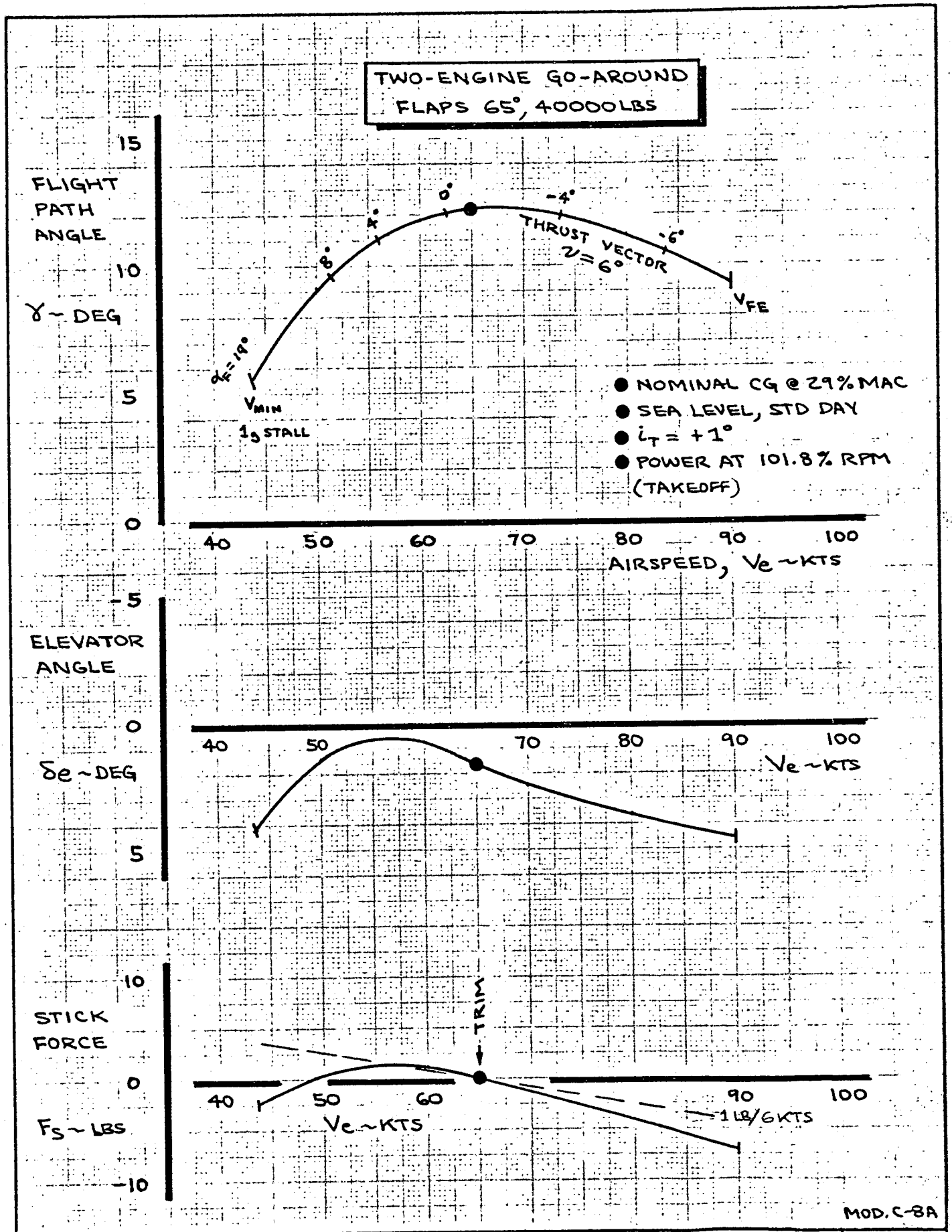

CALC	SPITZER	1-21-72	REVISED	DATE	STATIC LONGITUDINAL STABILITY AT TWO-ENGINE GO-AROUND, FLAPS 65°	FIG 3-21
CHECK						D6-40381
APR					THE BOEING COMPANY	PAGE 3.28
APR						

C.2.

7.8

3.3 Maneuvering Stability and Control

Typical flight maneuvers affecting longitudinal control consist of takeoff rotation, pulling load factor, flap and power changes, reaching minimum airspeed (stall), flight path tracking, and landing flare. The following shows that the Modified C-8A has adequate longitudinal maneuvering control capability.

Takeoff Rotation

Short takeoff field lengths imply high lift capability, rapid acceleration and low operating speeds. There must be sufficient elevator power to begin rotation at a low enough speed such that takeoff attitude is reached on or below the design liftoff speed. Takeoff rotation speeds have been determined in Reference 7 between $58 \leq V_R \leq 72$ kts for standard day takeoff at Flaps 30°. Figure 3-22 presents the elevator angle required for nose wheel liftoff at the beginning of rotation. Minimum nosewheel liftoff speed using maximum elevator is on the order of $50 \leq V_e \leq 57$ kts depending on airplane gross weight. Takeoff rotation can be initiated at V_R using approximately $\delta_e \approx -10°$ and a stick force of $F_s \approx 15$ lbs. The airplane speed is increasing quite rapidly making continued rotation easy.

Load Factor Capability

The Modified C-8A has acceptable load factor capability for pull-ups and turns. Figure 3-23 presents a summary of elevator-per-g, stick-force-per-g, and maneuver point. It happens that the rearward shift in CG along the fuel loading line (Figure 3-9) offsets the increased gross weight effect in

establishing δ_e/g. For all practical purposes δ_e/g has only a single value at a given flight speed. With the modified spring tab system, stick-force-per-g is now satisfactory at $Fs/g \approx 35$ to 45 lb/g. Original Fs/g was about twice the current level. Maneuver point (CG where $\delta e/g = 0$) is well aft of the nominal CG. Note that the destabilizing effect of Cj does cause the maneuver point to move forward at low speed, flaps down conditions.

Sufficient elevator authority exists to maneuver to limit load factor at cruise. Stick force gradient is low up to elevator torque tube wind-up limit (θ_1) as previously shown in Figure 3-4. Beyond this point there is a tenfold increase in force gradient which effectively limits further elevator rotation. Figure 3-24 shows airplane load factor capability at elevator θ_1 limit. Capability is slightly in excess of design limit load factor at maximum gross weight. Stick force at the θ_1 limit is on the order of $F_s \approx 60$ lbs at cruise speeds. At low speeds and flaps down conditions, load factor is limited by wing lift and not elevator deflection.

One important maneuvering flight condition is recovery from overspeed condition at V_D = 180 kts. Figure 3-24 shows that there is plenty of capability at V_D when maneuvering from a 1g trimmed (Fs = 0) flight condition. An electrical trim system has been installed on the Modified C-8A which actuates the trim tab via thumbswitches. A failure in this single-channel system could conceivably produce a trim runaway which would tend to dive the airplane if the pilot released the control column. Safety is provided by three design features:

(1) The pilot can override the trim motor and re-trim with the manual trim wheel using less than 10 lb of force,

(2) A disconnect switch is provided to shutoff the trim motor, and

(3) The flap-trim interconnect mechanism limits airplane nose-down trim authority to a safe level (see Figure 3-12).

Recovery capability from a full nose-down mistrim is shown in Figure 3-25. The pilot can maintain 1g flight by pulling approximately 40 lbs on the column. At the Θ_1 limit the pilot can generate $n_z \approx 1.5$ g using about 70 lbs of stick force. Without the flap-trim interconnect the pilot would not be able to hold 1 g at the Θ_1 limit.

Flap Transitions

Elevator control power is adequate to trim the effects of power, thrust vector and flap setting as shown in Figure 3-10. It is important that transitions from cruise to landing and go-arounds from landing can be made with "one-hand" stick forces. The reduced stick force modification plus small elevator requirements make this possible. Typical trim changes for a flap transition from cruise to landing are shown in Figure 3-26. Elevator required to trim at Flaps Up, V_e = 120 kts is almost unchanged by the time landing approach configuration is reached (δ_F = 65°, V_e = 60 kts). Starting from trim (F_s = 0) at 120 kts the stick force required without re-trimming is less than 7 lbs (pull). Most of the stick force is caused by the flap-trim interconnect which moves the elevator position where F_s = 0. Power must be increased from 87% RPM (level flight at δ_F = 5.6, 120 kts) to 90% RPM (level flight at δ_F = 30°) to 92% RPM on approach.

The most stringent flap retraction condition is at go-around on two engines when power and thrust vector changes are included. Figure 3-27 shows the trim changes for this maneuver. Most of the stick force required to maintain trim away from the approach condition comes from power and thrust vector change at $\delta_F = 65°$. For the go-around (and takeoff transition as well) the flap-trim interconnect programming actually helps to reduce force change. Maximum stick force for this condition is well within the "one-hand" category at $F_s = -16$ lbs (push).

Transitions from cruise-to-landing and landing-to-cruise were evaluated on the piloted simulator. Figure 3-28 shows a typical flap extension maneuver. The technique shown was used most often in setting up the approach from cruise. First, the pilot rotated the nozzles downward which effectively reduced forward thrust permitting speed bleedoff. Thrust was increased to maintain lift and rate of climb. Power setting was then left at the "approach" level and was not subsequently modulated. This insures adequate lift margins and reduces workload. The flaps were then extended to $\delta F = 65°$ and the speed reduced to $V_{APP} = 60$ kts at about the desired rate of descent. Two things may be noted: (1) elevator deflection required to accomplish this transition is small and (2) selection of $\delta F = 30°$ in one step may be too abrupt since rate of climb "ballooned" at that point. Transition to STOL approach was considered satisfactory by the pilots.

A flap retraction maneuver from the simulator is presented in Figure 3-29. Beginning at the 60 kt approach condition the pilot's first step was to rotate

nozzles aft. Note the momentary increase in sink rate as direct thrust lifting force was rotated out from under the airplane. Speed increased almost immediately and the airplane approached level flight. The pilot elected to partially retract flaps and maintain level flight (the altitude was over 1000 ft). Thrust setting had to be reduced to keep airspeed from increasing. Further flap retraction was accomplished in level flight. With reduced power the elevator deflection to trim actually went a few degrees trailing edge up in contrast to the full power go-around of Figure 3-27. It appears that the flaps up speed at the end of transition was somewhat low at 100 kts ($\alpha_F \approx 10°$), although the pilot was able to maneuver well.

Stall Characteristics

The Modified C-8A has sufficient elevator authority to reach minimum airspeed ($C_{L_{MAX}}$, 1 g stall) and recover. Elevator to stall is shown in the static longitudinal stability data (Figures 3-14, 16, 19, and 21). The stability degenerates at low speeds due to effects of jet flap blowing and direct hot thrust moments (Figure 3-20). In many instances V_{MIN} is reached holding "down" elevator. Pilots noted this effect in the simulator. By staying alert to these "self-stalling" tendencies the pilots rated the airplane acceptable as a research test vehicle.

The Modified C-8A can achieve very low stall speeds (Figure 3-8). Nose-up attitude may be very high for power-on stalls (Figure 3-7). In other cases rate of sink may be large at stall (Figure 3-6). All of these characteristics may preclude actually reaching many "1 g stall" minimum speed conditions.

Characteristics at or beyond $C_{L_{MAX}}$ are inferred by analyzing the existing augmentor wing wind tunnel data. Figure 3-30 presents lift and pitching moment data from the Ames Phase IV wind tunnel test (References 2 and 3). Lift loss beyond $C_{L_{MAX}}$ is gentle as expected with leading edge slats. Sharp rolloff or wing drop is not expected. Pitching moment breaks nose down at

stall with only some "flattening" in stability at $C_{L_{MAX}}$. Pitch up at stall is not envisioned, keeping in mind the low stability levels prior to reaching $C_{L_{MAX}}$.

Tuft flows and pitching moment characteristics on the Ames model have been analyzed by deHavilland. . . . . Wing stalling begins at the root and spreads outward. Body blowing was incorporated into the model to smooth out spanwise lift distribution. Maximum lift, $C_{L_{MAX}}$, increased and stall characteristics improved. Body BLC has been installed on the Modified C-8A.

Data on flaps up ($\delta_F = 5.6°$) stall are virtually non-existent, although they are thought to be similar to flaps down characteristics. One thing is apparent: the flaps up Modified C-8A reaches $C_{L_{MAX}}$ at a much higher angle of attack (and attitude, power-on) than the original Buffalo. This characteristic does mean that the tail is at high angle of attack and near its own stall point at flaps up V_{MIN} (see Figure 3-11). Elevator hinge moments shift at tail stall causing an elevator upfloat tendency which is exhibited to the pilot as force lightening. "T-tail" stall characteristics are not completely known for the Modified C-8A configuration. It is deemed prudent to approach flaps up stalls with caution when determining characteristics in flight.

Pitch Control Sensitivity

Tight pitch attitude control is important, especially when tracking glide slope on landing approach. The pitch attitude time constant is proportional to $L_\alpha = \frac{g}{V}\left\{C_{L_\alpha} \Big/ \frac{W}{qS}\right\}$. At 60 kt approach Modified C-8A pitch time constant is

good with L_{α} = .48 1/sec. This value is the same as the average L_{α} for conventional jet transports operating at twice the approach speed. Modified C-8A wing loading at about half that for conventional jets offsets the effect of reduced approach speed. Pitch response is also dependent on elevator effectiveness. Pilot opinion of pitch control effectiveness is related to pitch sensitivity (pitch acceleration produced by unit control column displacement).

Figure 3-31 shows the effect of pitch sensitivity on pilot rating from earlier NASA/Boeing studies. Modified C-8A pitch sensitivity level at 60 kt STOL approach is shown with the pilot rating obtained in the simulator study. The Modified C-8A pitch sensitivity is about twice the average for conventional jet transports at landing approach. The lower dynamic pressure at 60 kts is offset by effective, large-chord elevator and very low pitch inertia. Pitch sensitivity at higher speeds was high enough to draw an occasional pilot comment in the simulator studies.

Maximum pitch acceleration with full aft column at the STOL approach condition is $\ddot{\Theta}_{max} \geq .4$ RAD/SEC^2. While less than the original design objective (which is attainable with elevator trimmed at $\delta e = 0°$), pitch acceleration capability actually exceeds that of most conventional jet transports.

At this point, it should be mentioned that pilot induced oscillations (PIO) were experienced in the simulator studies. All pilots experienced it at various times during the two simulator test periods. Improvements were made to the simulator T.V. display, motion system and

elevator system which reduced the tendency for PIO. However, PIO continued to occur on occasion. Rapid pitching moment input or change in flight condition could set it off. The PIO period was approximately 3 seconds and the amplitude was often nearly constant. These pitch oscillations could not be induced without the pilot in the loop. A mild PIO is evident in the flap retraction maneuver shown in Figure 3-29. Pitch rate oscillates for over 30 seconds duration due to elevator cycling. It is thought that PIO is unlikely to occur in the actual airplane; however, pilots are advised to be alert to any tendency to PIO.

Landing Flare

The landing flare maneuver is more difficult from STOL approach than conventional for three fundamental reasons: steeper glide slope angle, lower airspeed, and stronger ground effect.

The STOL landing design condition for the Modified C-8A calls for V_{APP} = 60 kts at γ = -7.5° compared to $V_{APP} \geq$ 120 kts and γ = -3° for conventional jet transports. Design rate of descent is 800 fpm (13.3 ft/sec), which is about one-third higher than conventional. Sink rate must be arrested in the flare because the landing gear touchdown limit is 12 ft/sec. The steep approach path results in nose-down body attitudes in contrast with most jet transports which approach slightly nose up. Rotation in the flare is mandatory to prevent hitting the nose gear first. The requirement to arrest sink rate and rotate calls for load factor to bring flight path nearly tangent to the runway at touchdown. (A 3 to 4 ft/sec touchdown sink rate is considered reasonable.) Flare initiation altitude increases with steepening glide slope for a given load

factor flare. Using a typical flare at $n_z = 1.07g$ ($\Delta n_{z_{flare}} = .07g$) the Modified C-8A must commence flaring at 40 to 50 ft altitude, roughly double that of conventional transports.

The second factor, low airspeed, detracts from the ability to generate load factor by increasing angle of attack. Conventional flaring is done by pitching up with elevator to increase lift. Angle of attack increase required to achieve a given load factor is inversely proportional to $n_{z_\alpha} = \frac{C_{L\alpha}}{W/_S}$. Conventional transports average $n_{z_\alpha} = 3.5$ g/rad at approach compared to $n_{z_\alpha} \leq 1.5$ g/rad for the Modified C-8A at 60 kts. The Modified C-8A must increase angle of attack by over twice that of conventional jets to flare at the same load factor.

Finally, adverse ground effects hinder the flare even further. Near the ground it becomes increasingly difficult to generate high lift coefficients because the presence of the ground restricts the upwash flow field to the wing. Additional lift degradation is produced if the jet sheet from the flap and/or direct hot thrust flow impinges on the ground. At the same time the downwash flow field at the tail can no longer "flow downward" due to the ground. The relative angle of attack of the horizontal tail changes producing a nose down pitching moment shift on the airplane, requiring up elevator control input. In contrast, conventional jet transports approaching at moderate lift coefficients experience little, if any, ground effect in the flare.

The only ground effect data for the augmentor wing configuration comes from the NASA Ames wind tunnel testing. [illegible]. Figure 3-32 presents the effect of proximity to the ground on basic aerodynamics for the landing configuration tested. The lowest height tested was h/c = 1.3 which corresponds

to Modified C-8A h_{gear} = 4 ft. Data show a reduction in lift-curve-slope resulting in 10% lift loss relative to free air at $\alpha \approx 10°$. The lift loss is of the same magnitude as flare load factor. Maximum lift capability is also restricted. At constant lift coefficient drag is increased due to increased angle of attack. Pitching moment shifts as wing lift and downwash are affected. Airplane stability in ground effect is increased because downwash angle no longer changes with angle of attack. The magnitude of the pitching moment change is about the same as that for an elevator control input of $\Delta\delta_e = 20°$.

Existing wind tunnel data also show the following trends:

1. Ground effect is negligible at h/c = 2.1g corresponding to h_{gear} = 16 ft on the Modified C-8A.

2. Ground effect becomes less severe with decreased blowing coefficient, Cj (i.e. reduced lift level).

3. Ground effect is much reduced with hot thrust nozzles rotated aft.

4. Ground effect on lift was virtually non-existent by rotating the flaps back to $\delta_F = 50°$ indicating reduced jet sheet effect.

5. Ground effect on pitching moment was evident in all data, but about halved at $\delta_F = 50°$.

Considerable speculation abounds about actual Modified C-8A ground effect severity. There are valid arguments that the wind tunnel data are pessimistic due to the effects of wind tunnel boundary layer and relatively low hot thrust

nozzle location on the model. Nevertheless, the trends seen in the data have been seen before (e.g. see Reference 12). It is expected that at least the qualitative features of ground effect will be seen on the Modified C-8A.

Elevator to flare using the standard technique (pull back on column) has been estimated. Figure 3-33 presents elevator requirements for STOL and conventional landings. Considerable elevator deflection from approach trim is necessary for the STOL landing. Conventional landing flare should present no problem. With the spring tab modification, stick force at flare is well within "one-hand" capability. While Figure 3-33 shows sufficient elevator capability, actual STOL landing flare may be hampered by limitations on maximum lift and body attitude.

STOL landing flares were studied using the simulator. The pilots had difficulty with the simulator visual display which adversely influenced their capacity to judge flare initiation altitude. For the sake of simplicity, a single set of ground effect characteristics, representing the most severe wind tunnel data, were used for all landings. At actual approach flight condition the simulated ground effect influence on wing lift was roughly 50% over the corresponding wind tunnel increment. Even with these shortcomings, the simulator provided insight into the landing flare maneuver.

In general, simulator flaring was begun between 35 and 55 ft altitude. Nose-up rotation achieved attitudes between $3° < \Theta < 6°$ at touchdown at angle of attack between $10° < \alpha_F < 14°$. Lift gained by rotation merely offset lift loss in ground effect. Flight path angle was still about $\gamma = -7°$ at touchdown. Very little load factor was generated in the flare. Airspeed bleed-off was about 3 to 5 knots in the flare. Touchdown sink rate using full "simulator" ground effect averaged 8.8 ft/sec for 45 landings.

Upon recognizing the severity of the landing flare maneuver, reductions were made in the simulated ground effect. Drag and wing-body pitching moment effects were put to zero since previous investigation had shown these terms to have little effect. Lift loss was reduced by 50% (to below wind tunnel levels). The downwash changes at the tail were left at full value. Figure 3-34 shows a typical elevator flare into this level of ground effect. Full elevator was used to generate the desired change in attitude and angle of attack. The load factor was still small ($n_{z_{max}} \approx 1.05$ g) and touchdown sink rate was high. With further trials, the average touchdown sink rate with modified ground effect came out near 5 ft/sec. All lift loss in ground effect was removed from the simulation, and the average touchdown sink rate remained near 5 ft/sec. Even with mild ground effect on lift, Modified C-8A STOL landings are apt to be "firm" even using full elevator.

Landing flare characteristics are one of the research objectives for the Modified C-8A. A number of flare techniques using thrust and nozzle rotation were practiced on the simulator. Advancing throttles in the flare increases lift directly by increased jet flap blowing and by direct hot thrust since the nozzles are at $\nu = 90°$. (Throttles should never be retarded in the flare in the powered-lift mode). The pilots took advantage of this feature. Figure 3-35 shows a landing using this technique which reduces elevator required to flare and allows flare to be initiated at lower, more conventional, altitude. Touchdown sink was quite low using this technique. Using power to flare requires careful timing and precise control coordination.. With the proper aids or systems the powered flare has good potential.

A step-by-step approach to full STOL landing is recommended. Conventional landings at $\delta_F = 30°$, $\nu = 6°$, $V_{APP} = 90$ kts, $\gamma = -3°$ pose no problem. Testing should proceed carefully to lower speeds, higher flap settings, and steeper approaches. Hot thrust vector angle should be lowered by increments. In this way landing flare and ground effect can be assessed safely.

TAKEOFF ROTATION
FLAPS 50°
δf = 50°

Reproduced from best available copy.

① TAKEOFF THRUST
② SEA LEVEL, STD. DAY
③ NOMINAL C.G.
④ i_T = +1°
⑤ GROUND EFFECT INCLUDED

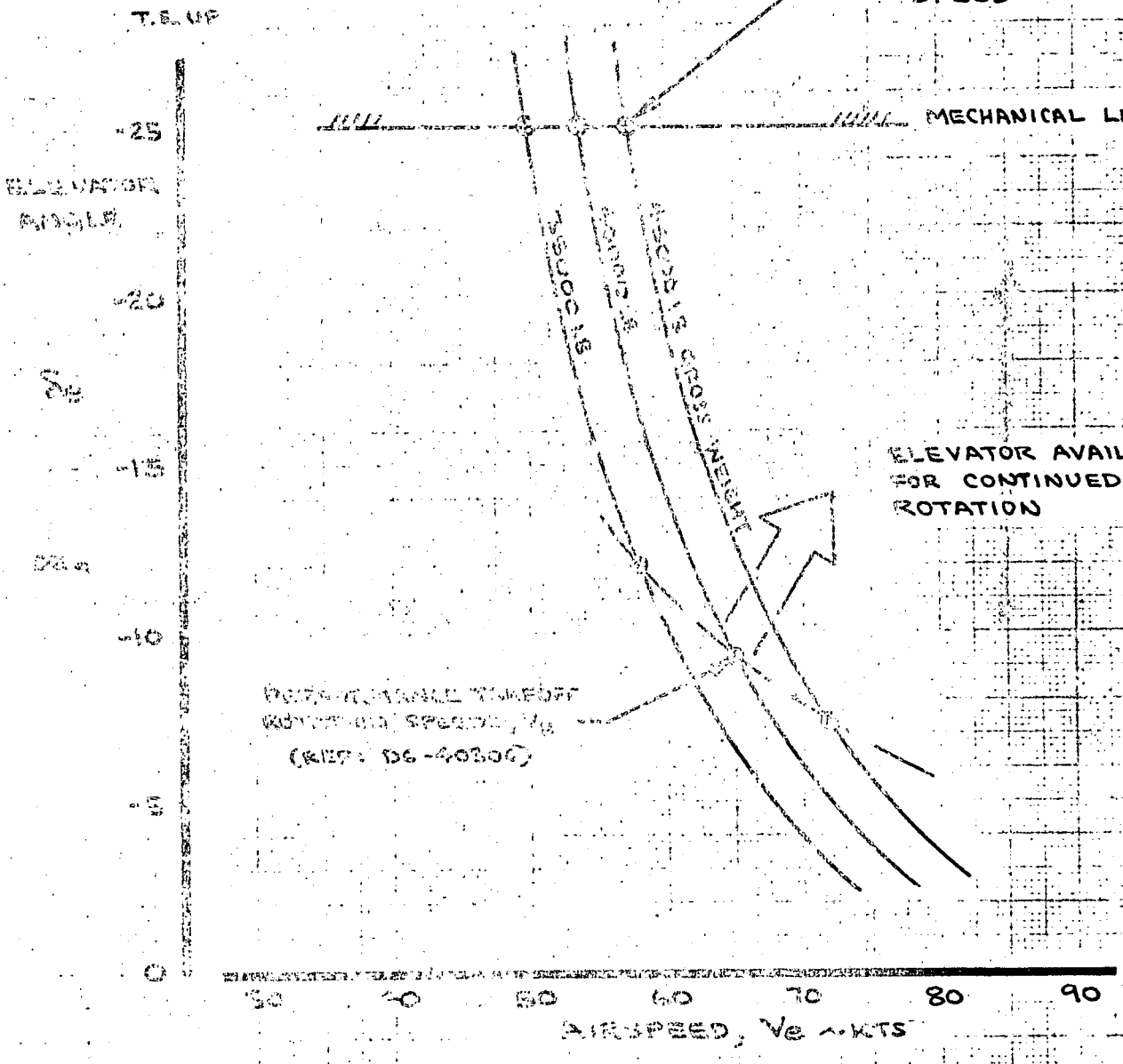

MOD C-8A

CHK		FIG 3-22
CHECK	ELEVATOR ANGLE FOR NOSE WHEEL LIFT OFF	
APP		D6-40381
ENG	THE BOEING COMPANY	PAGE 3.42

At STOL approach the hot thrust vector is perpendicular to the flight path ($\gamma \doteq 90°$). Thrust vectoring effects on flight path and body attitude have been shown in Figures 3-17 and 3-18. Transient response to nozzle rotation with pilot controlling elevator is shown in Figure 3-41. Nozzle rotation initially causes the airplane to settle as direct lifting force is removed. Subsequent airspeed and angle of attack changes result in stabilized climbing and descending conditions. Attitude change is "correct". Pitching moment due to thrust orientation (nozzles are below and ahead of the CG) must be counteracted by the pilot to prevent stalling. Smaller changes in nozzle angle were used in the simulator for glide slope tracking. Transient effects in speed and elevator were then smaller. The pilots found that nozzle rotation took the place of "throttles" at STOL landing approach.

Gross changes in flight path are possible by rotating nozzles fully aft and increasing power setting. The transition to a two-engine go-around from STOL approach is shown in Figure 3-42. The transient characteristics shown in Figure 3-40 and 3-41 are seen to combine in Figure 3-42. The airplane pitched nose up, increased speed, pulled load factor and climbed away - all conventional characteristics. The pilot, however, had to use considerable down elevator to maintain trim. Positive climb gradient was achieved within 5 seconds of initial control input using about 80 ft altitude. Subsequent modifications to throttle and nozzle control handles allow simultaneous control inputs using one hand. Two engine go-around can be effected with very little altitude loss and with more-or-less conventional transient response.

MANEUVERING STABILITY

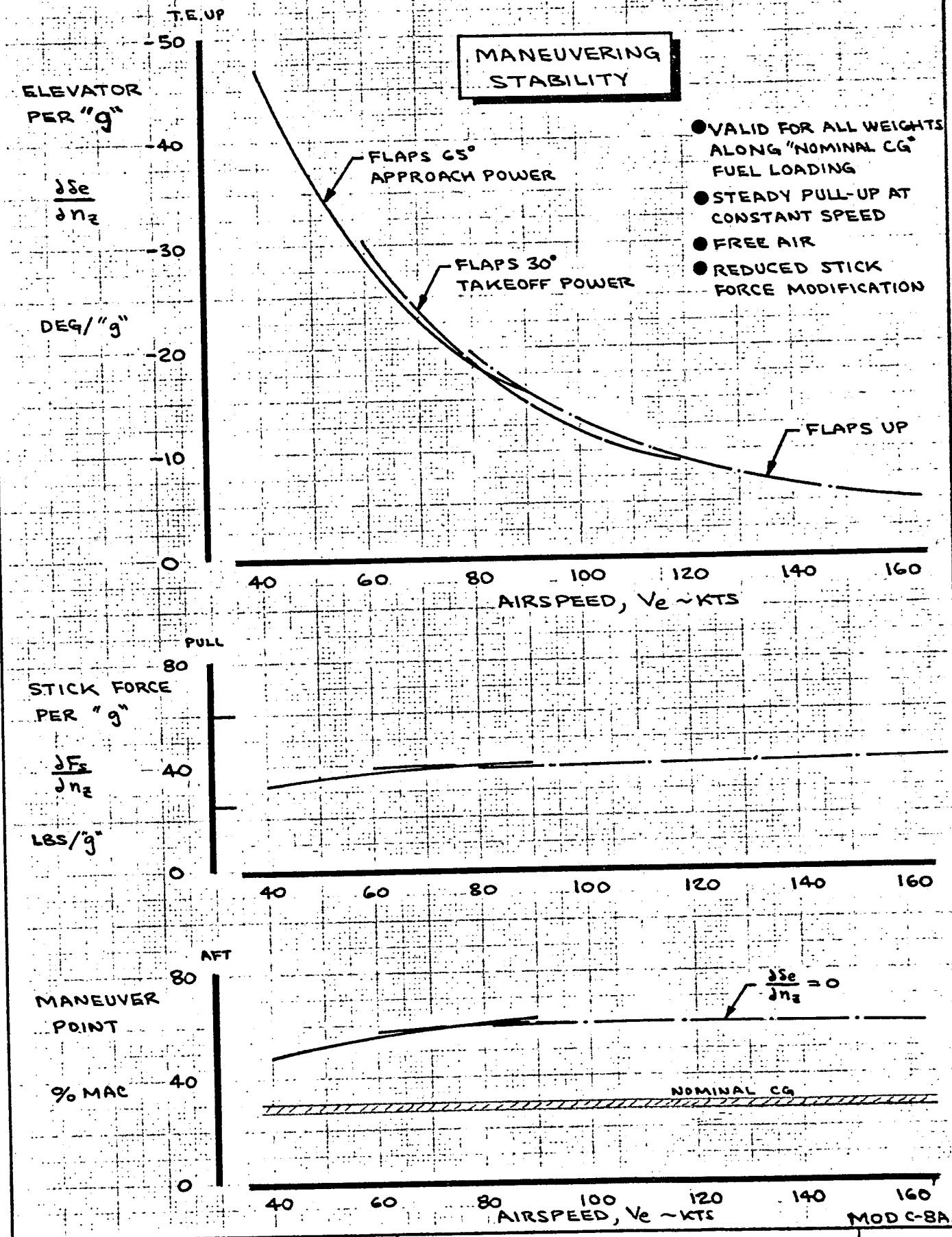

MOD C-8A

CALC	SPITZER	4-6-71	REVISED	DATE	ELEVATOR - PER - "g" MANEUVERING STABILITY
CHECK			SPITZER	2-9-72	FIG 3-23
APR					D6-40381
APR					THE BOEING COMPANY
					PAGE 3.43

LOAD FACTOR CAPABILITY

- 45000 LB
- FLAPS UP
- NOMINAL CG

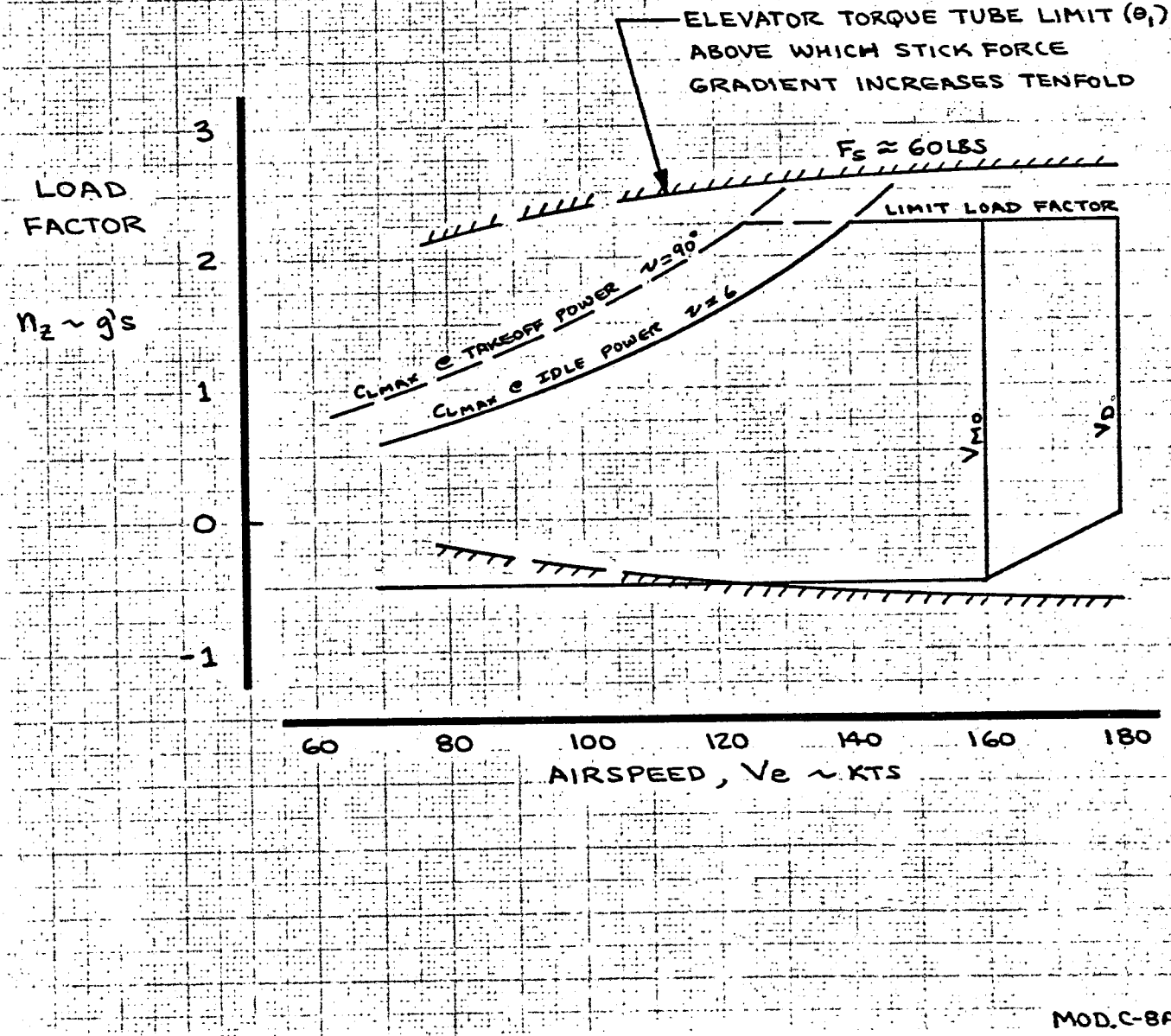

MOD. C-8A

CALC	SPITZER	1-19-72	REVISED	DATE	LOAD FACTOR CAPABILITY	FIG 3-24
CHECK						D6-40381
APR					THE BOEING COMPANY	PAGE 3.44
APR						

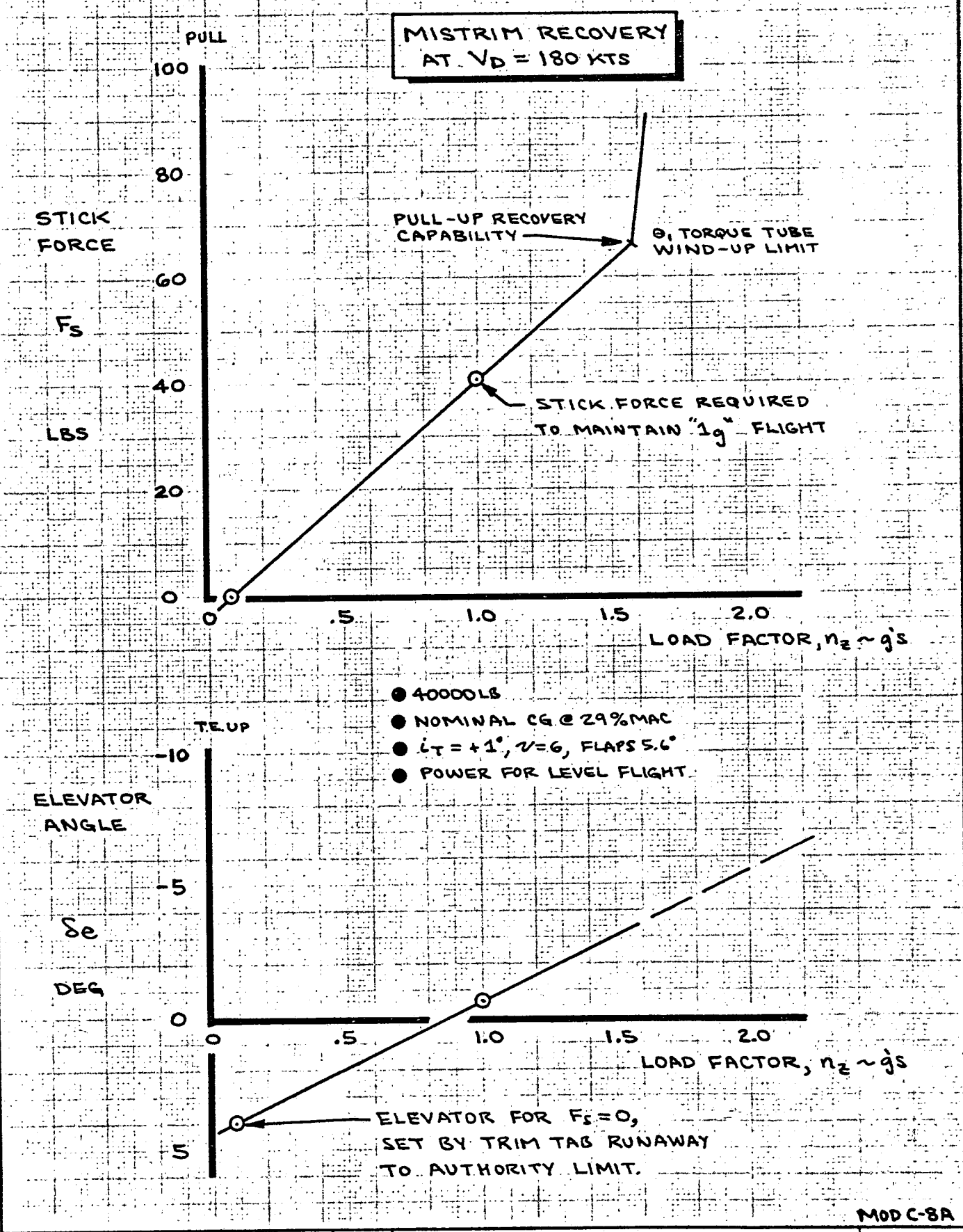

MOD C-8A

CALC	SPITZER	2-2-72	REVISED	DATE
CHECK				
APR				
APR				

RECOVERY FROM FULL NOSE-DOWN MISTRIM AT DIVE SPEED

FIG 3-25

D6-40381

THE BOEING COMPANY

FLAP EXTENSION

- 40000 LBS
- NOMINAL CG
- SEA LEVEL, STD. DAY
- FLAP-TRIM INTERCONNECT
- STEADY TRIM POINTS @ 1g

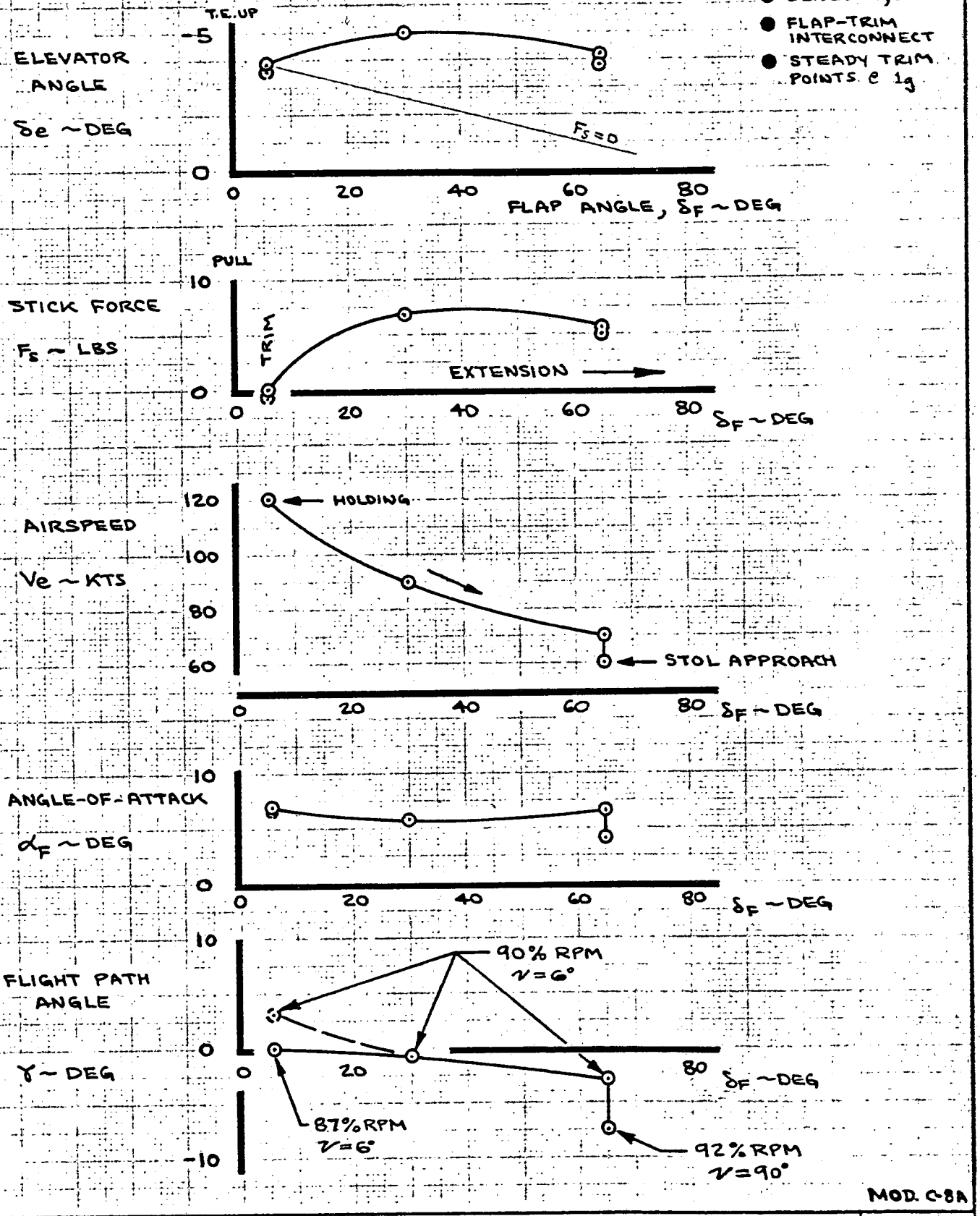

MOD. C-8A

CALC	SPITZER	2-2-72	REVISED	DATE
CHECK				
APR				
APR				

TRIM CHANGE FOR TRANSITION FROM CRUISE TO LANDING APPROACH

FIG 3-26

D6-40381

THE BOEING COMPANY

PAGE 3.46

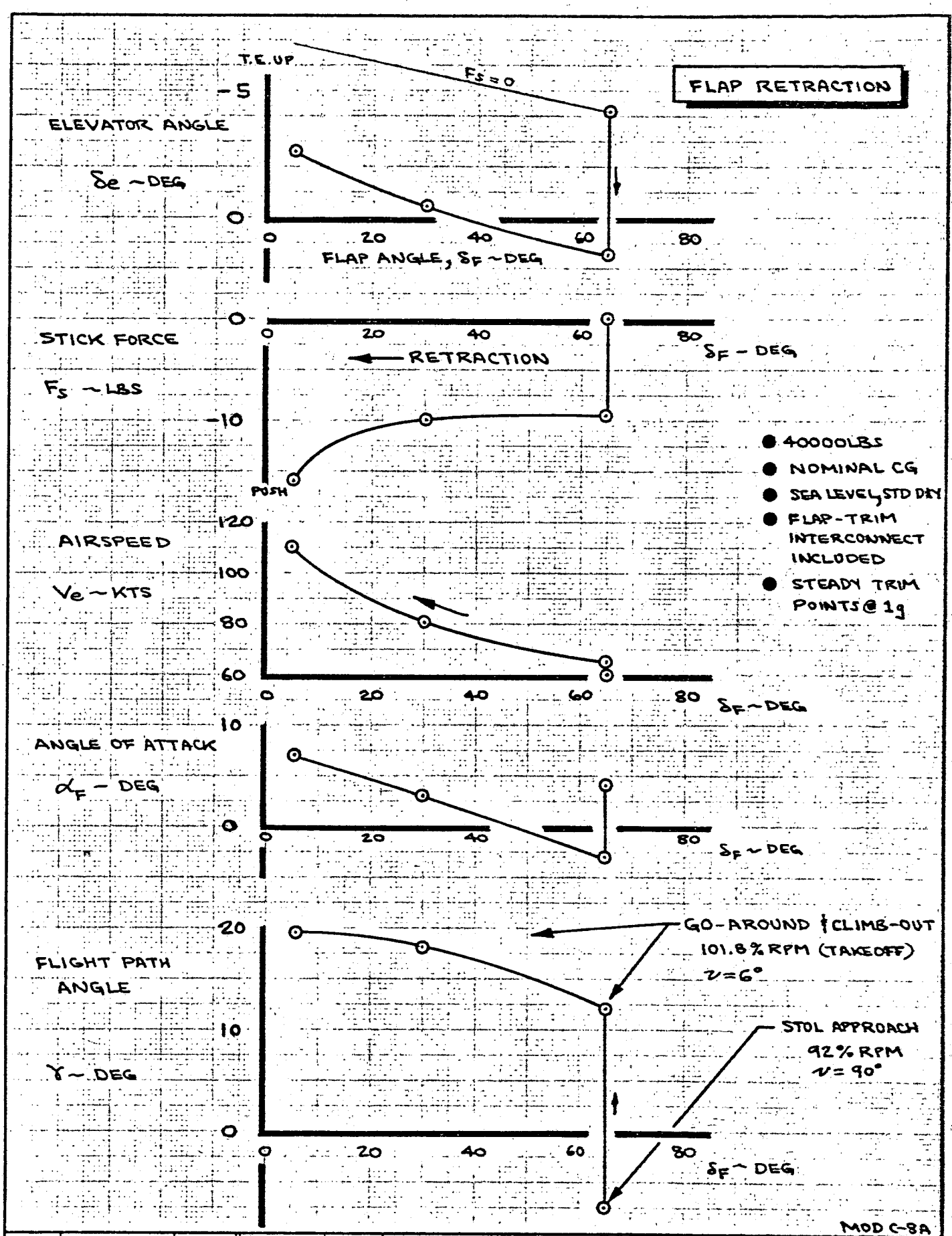

MOD C-8A

CALC	SPITZER	2-2-72	REVISED	DATE	TRIM CHANGE FOR TRANSITION FROM LANDING TO FLAPS UP CLIMB
CHECK					
APR					
APR					

FIG 3-27

D6-40381

THE BOEING COMPANY

PAGE 3.47

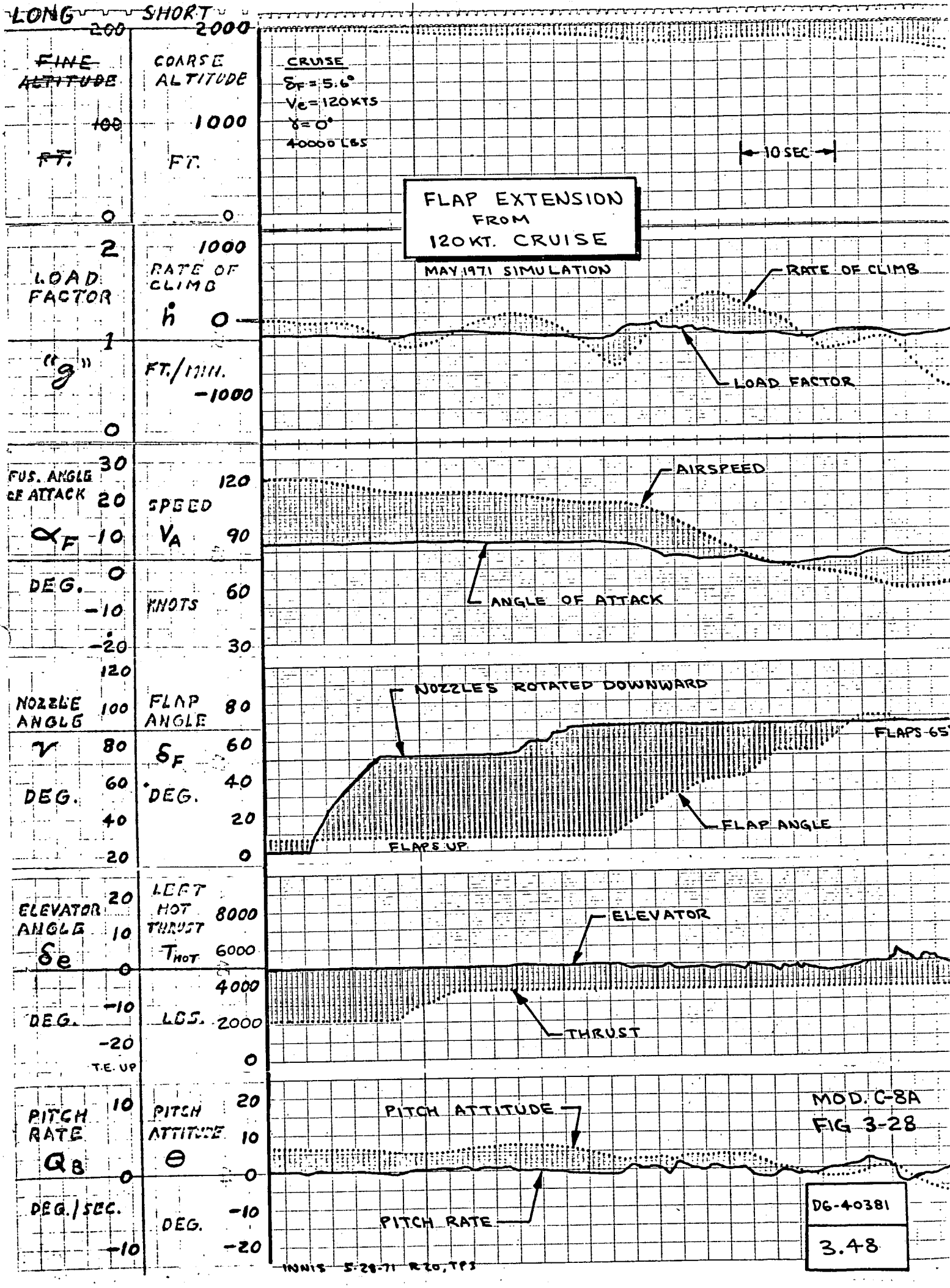
LONG
SHORT
200
2000
~~FINE~~
~~ALTITUDE~~
~~100~~
~~FT.~~
0
COARSE
ALTITUDE
1000
FT.
0
CRUISE
$\delta_F = 5.6°$
$V_c = 120$ KTS
$\gamma = 0°$
40000 LBS
10 SEC
FLAP EXTENSION
FROM
120 KT. CRUISE
MAY 1971 SIMULATION
2
1
LOAD
FACTOR
"g"
1000
RATE OF
CLIMB
$\dot{h}$
0
FT./MIN.
-1000
RATE OF CLIMB
LOAD FACTOR
30
20
10
0
FUS. ANGLE
OF ATTACK
α_F
DEG.
120
90
60
30
0
SPEED
V_A
KNOTS
AIRSPEED
ANGLE OF ATTACK
120
100
80
60
40
20
0
NOZZLE
ANGLE
ν
DEG.
80
60
40
20
0
FLAP
ANGLE
δ_F
DEG.
NOZZLES ROTATED DOWNWARD
FLAPS 65
FLAP ANGLE
FLAPS UP
20
10
0
-10
-20
T.E. UP
ELEVATOR
ANGLE
δ_e
DEG.
8000
6000
4000
2000
0
LEFT
HOT
THRUST
T_{HOT}
LBS.
ELEVATOR
THRUST
10
0
-10
-20
PITCH
RATE
Q_B
DEG./SEC.
20
10
0
-10
-20
PITCH
ATTITUDE
θ
DEG.
PITCH ATTITUDE
PITCH RATE
MOD. C-8A
FIG 3-28
DG-40381
3.48
INNIS 5-28-71 R20, TPS

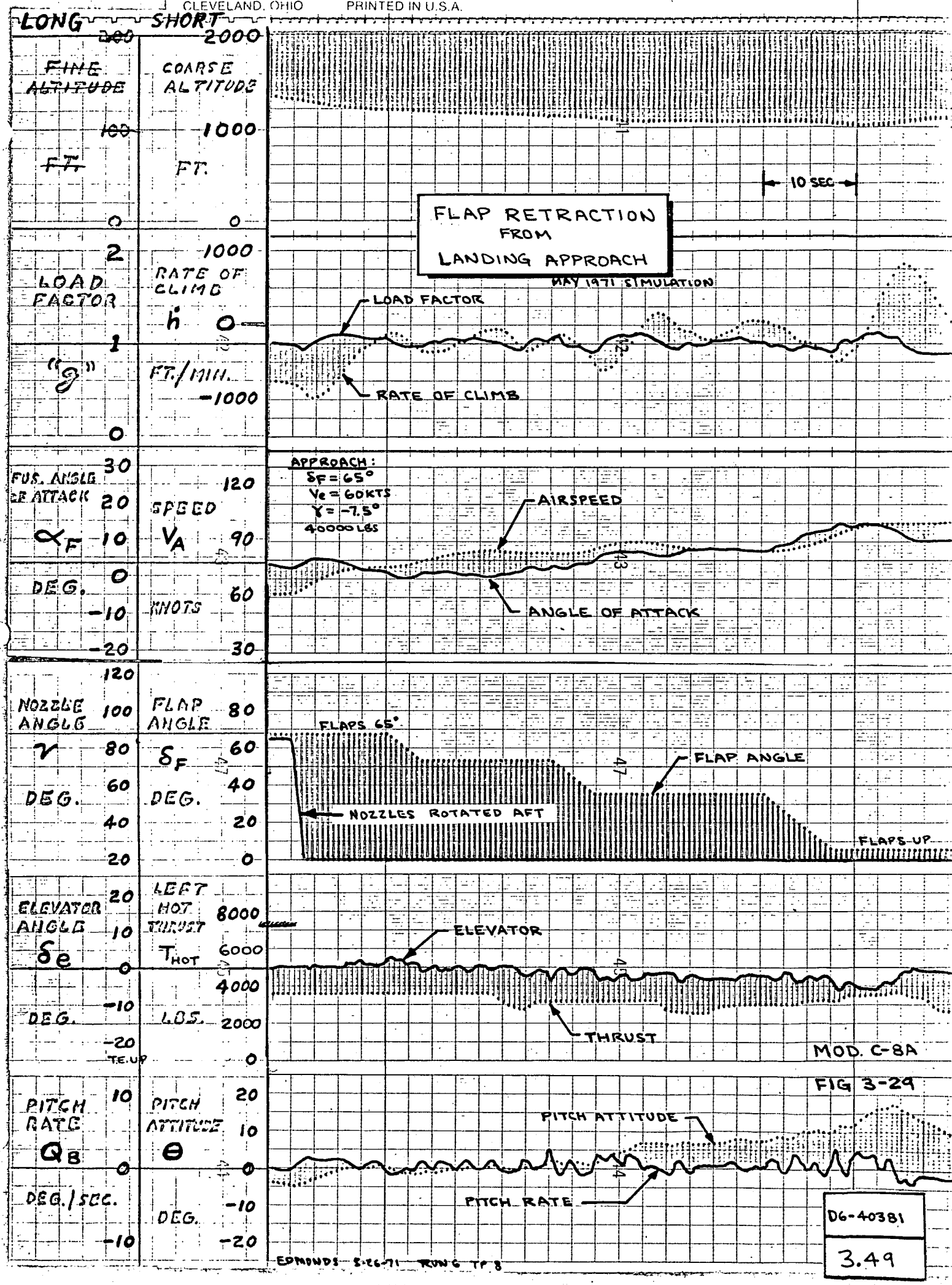
LONG
SHORT
FINE ALTITUDE
100
FT.
0
2000
COARSE ALTITUDE
1000
FT.
0
2
LOAD FACTOR
"g"
1
0
1000
RATE OF CLIMB
ḣ
FT./MIN.
-1000
0
41
10 SEC
FLAP RETRACTION FROM LANDING APPROACH
MAY 1971 SIMULATION
LOAD FACTOR
RATE OF CLIMB
42
30
FUS. ANGLE OF ATTACK
20
10
α_F
DEG.
0
-10
-20
120
SPEED
V_A
90
60
KNOTS
30
APPROACH:
$\delta_F = 65°$
$V_e = 60$ KTS
$\gamma = -7.5°$
40000 LBS
AIRSPEED
43
ANGLE OF ATTACK
120
NOZZLE ANGLE
100
80
FLAP ANGLE
ν
δ_F
60
40
20
0
FLAPS 65°
47
FLAP ANGLE
NOZZLES ROTATED AFT
FLAPS UP
20
ELEVATOR ANGLE
δe
10
0
-10
-20
TE UP
LEFT HOT THRUST
T_{HOT}
8000
6000
4000
2000
LBS.
ELEVATOR
45
THRUST
MOD. C-8A
FIG 3-29
10
PITCH RATE
Q_B
PITCH ATTITUDE
θ
20
DEG./SEC.
-10
-20
44
PITCH ATTITUDE
PITCH RATE
EDMONDS 5-26-71 RUN 6 TP 8
D6-40381
3.49

LIFT AND PITCHING MOMENT WIND TUNNEL DATA THROUGH STALL

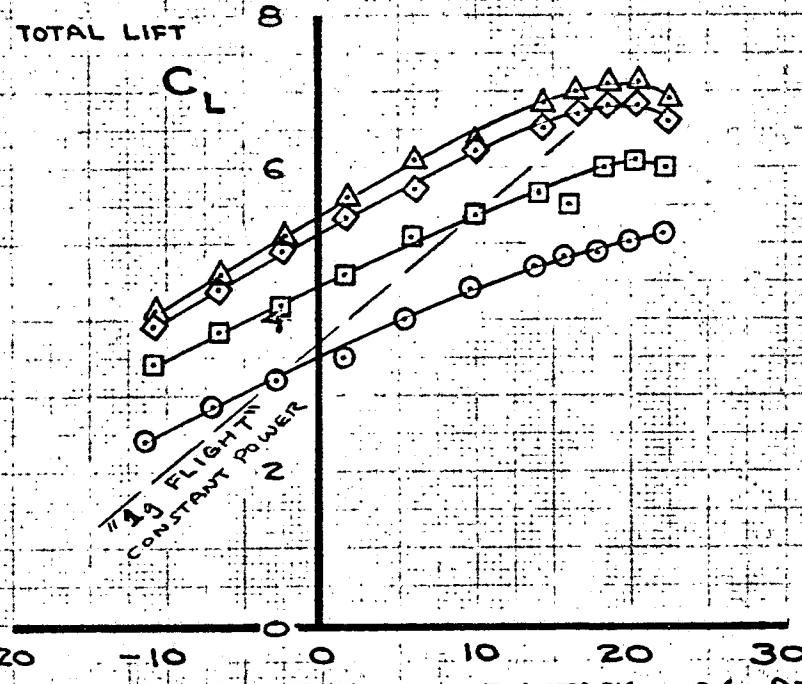

$\delta_F = 75°$

$\gamma = 85°$

$C_T = .81$ { CONSTANT HOT THRUST

$i_T = -4°$

$\delta_e = 0°$

$\delta_{AIL} = 45°/45°$

$i_w = 0°$

SYM	C_J
○	.35
□	.63
◇	.87
△	1.07

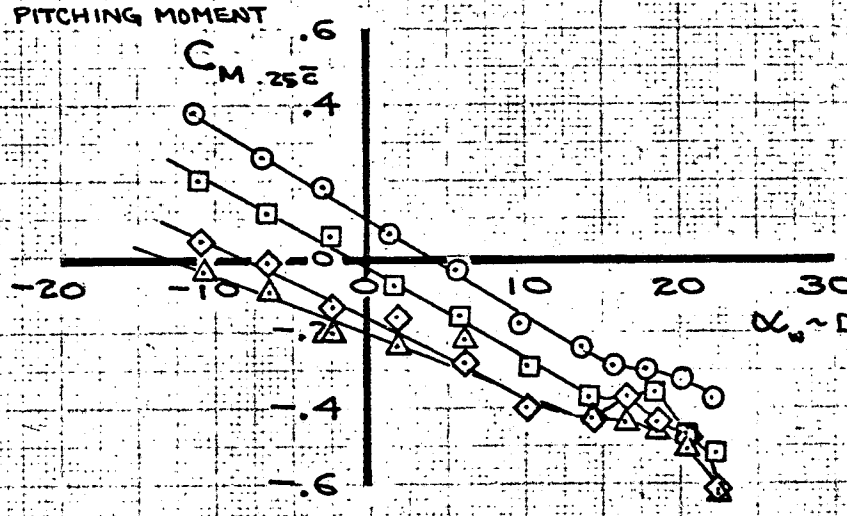

PHASE IV WIND TUNNEL DATA (NASA AMES 40×80).

MOD. C-8A

CALC	V. PAGE	2-7-72	REVISED	DATE	WIND TUNNEL DATA UP TO WING STALL	FIG 3-30
CHECK						D6-40381
APR						
APR					THE BOEING COMPANY	PAGE 3.50

PITCH CONTROL SENSITIVITY AT LANDING APPROACH

- $L_{x_s} = \frac{g}{V} \cdot \frac{C_{L\delta e}}{W/qS} \cdot \frac{\delta e}{x_s} \sim \frac{\text{RAD/SEC}}{\text{INCH}}$
- $\frac{\ddot{\theta}}{x_s} = M_{x_s} = \frac{C_{m\delta e}}{I_{yy}/qS\bar{c}} \cdot \frac{\delta e}{x_s} \sim \frac{\text{RAD/SEC}^2}{\text{INCH}}$
- PILOT RATINGS FROM NASA CR-635

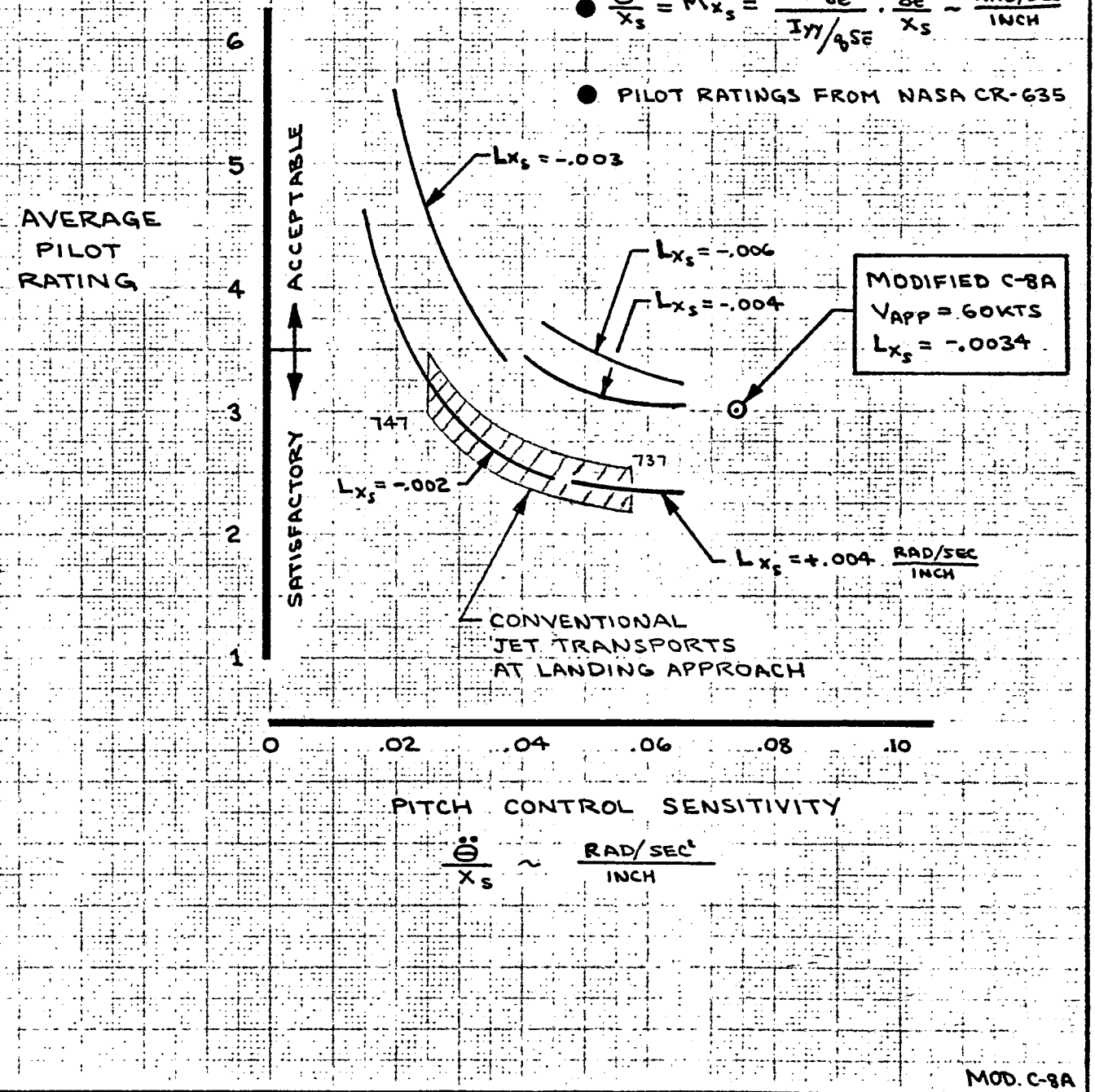

MOD. C-8A

CALC	FOSTER	6-29-71	REVISED	DATE	PITCH CONTROL SENSITIVITY COMPARISON	FIG 3-31
CHECK			SPITZER	2-9-72		D6-40381
APR						
APR					THE BOEING COMPANY	PAGE 3.51

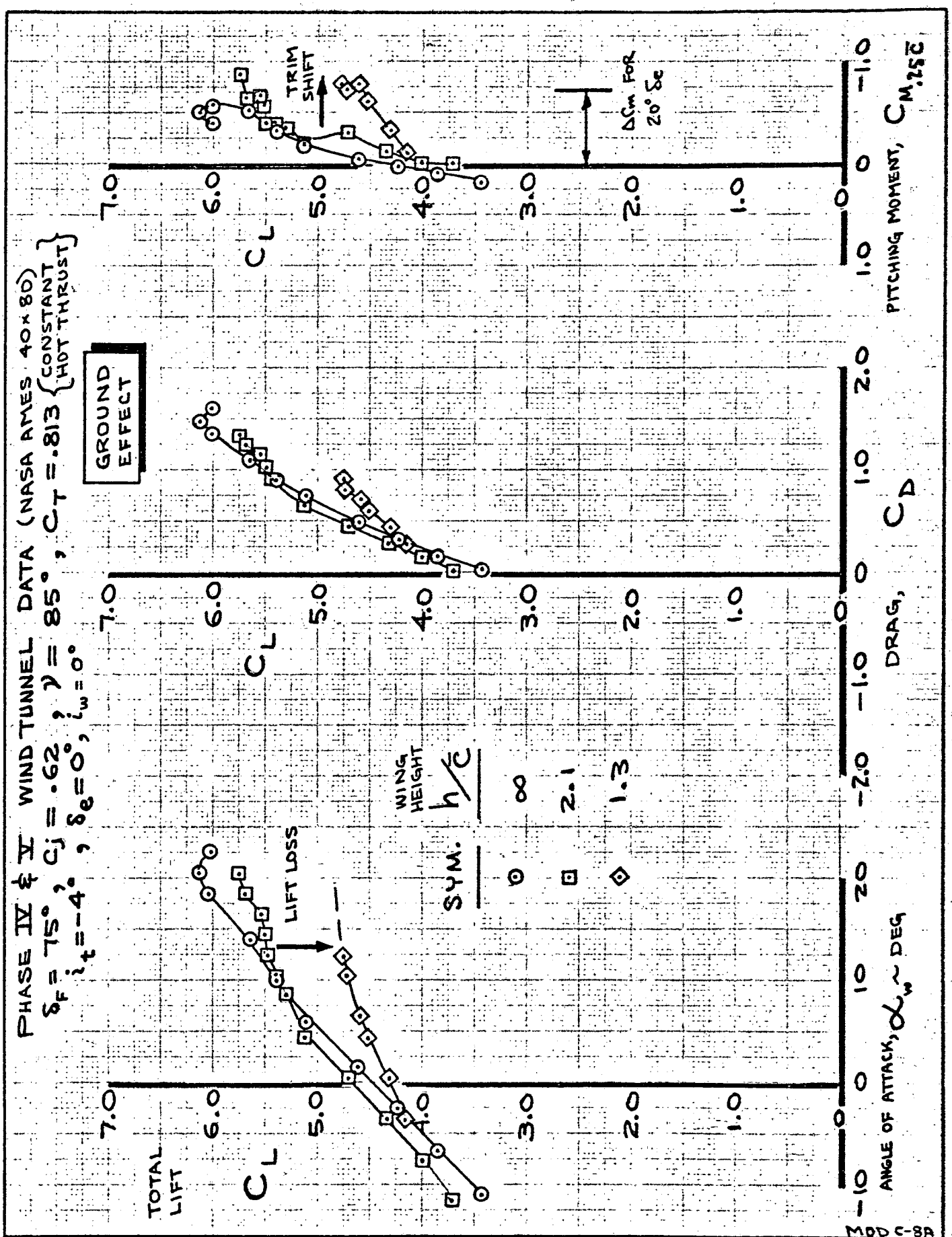

MDD C-8A

CALC	PAGE	2-2-72	REVISED	DATE	WIND TUNNEL GROUND EFFECT DATA	FIG 3-32
CHECK						D6-40381
APR						
APR					THE BOEING COMPANY	PAGE 3.52

ELEVATOR TO FLARE

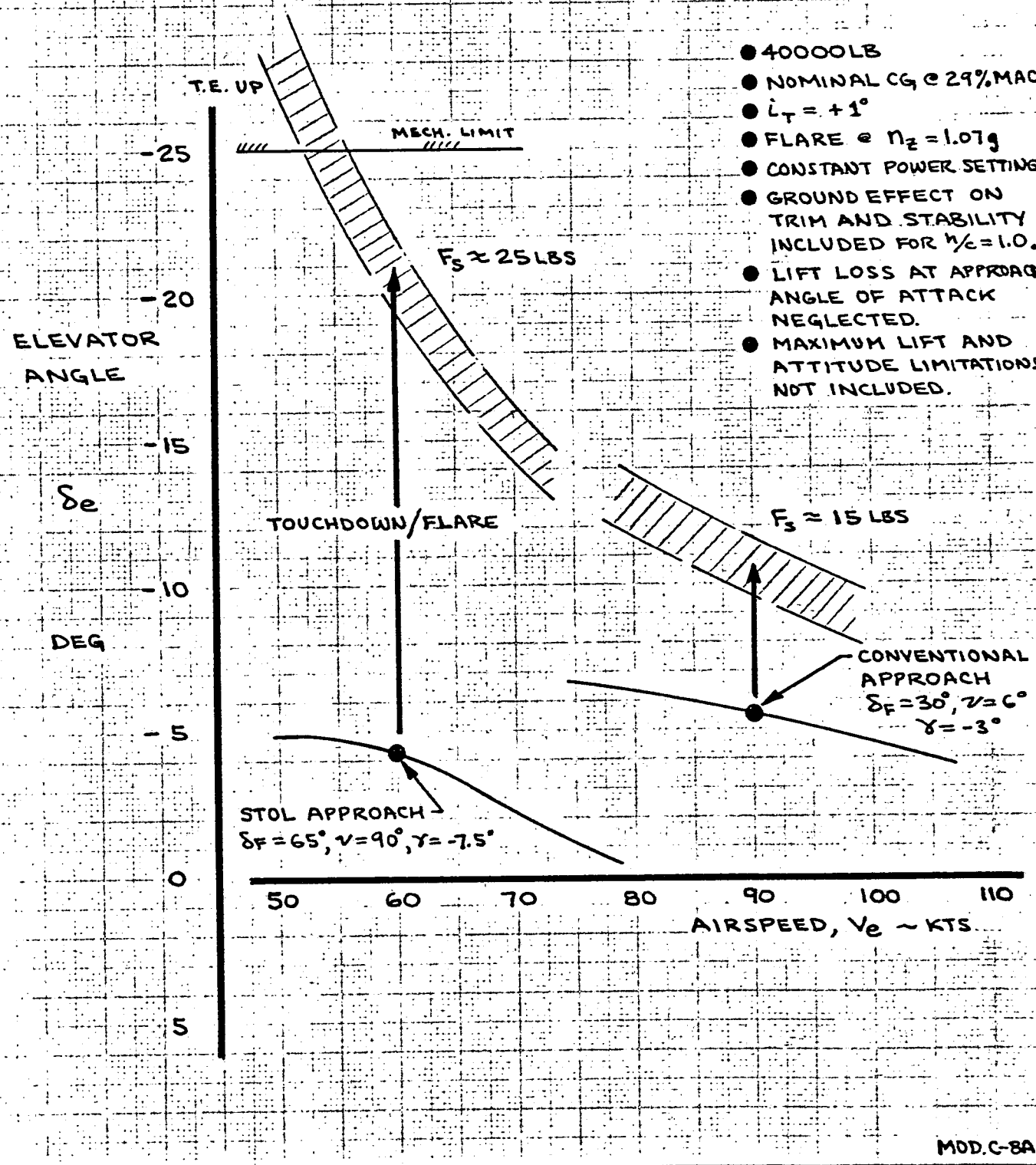

- 40000 LB
- NOMINAL CG @ 29% MAC
- $i_T = +1°$
- FLARE @ $n_z = 1.07g$
- CONSTANT POWER SETTING
- GROUND EFFECT ON TRIM AND STABILITY INCLUDED FOR $h/c = 1.0$.
- LIFT LOSS AT APPROACH ANGLE OF ATTACK NEGLECTED.
- MAXIMUM LIFT AND ATTITUDE LIMITATIONS NOT INCLUDED.

MOD. C-8A

CALC	SPITZER	2-1-72	REVISED	DATE	ESTIMATED ELEVATOR REQUIRED TO FLARE	FIG 3-33
CHECK						D6-40381
APR					THE BOEING COMPANY	PAGE 3.53
APR						

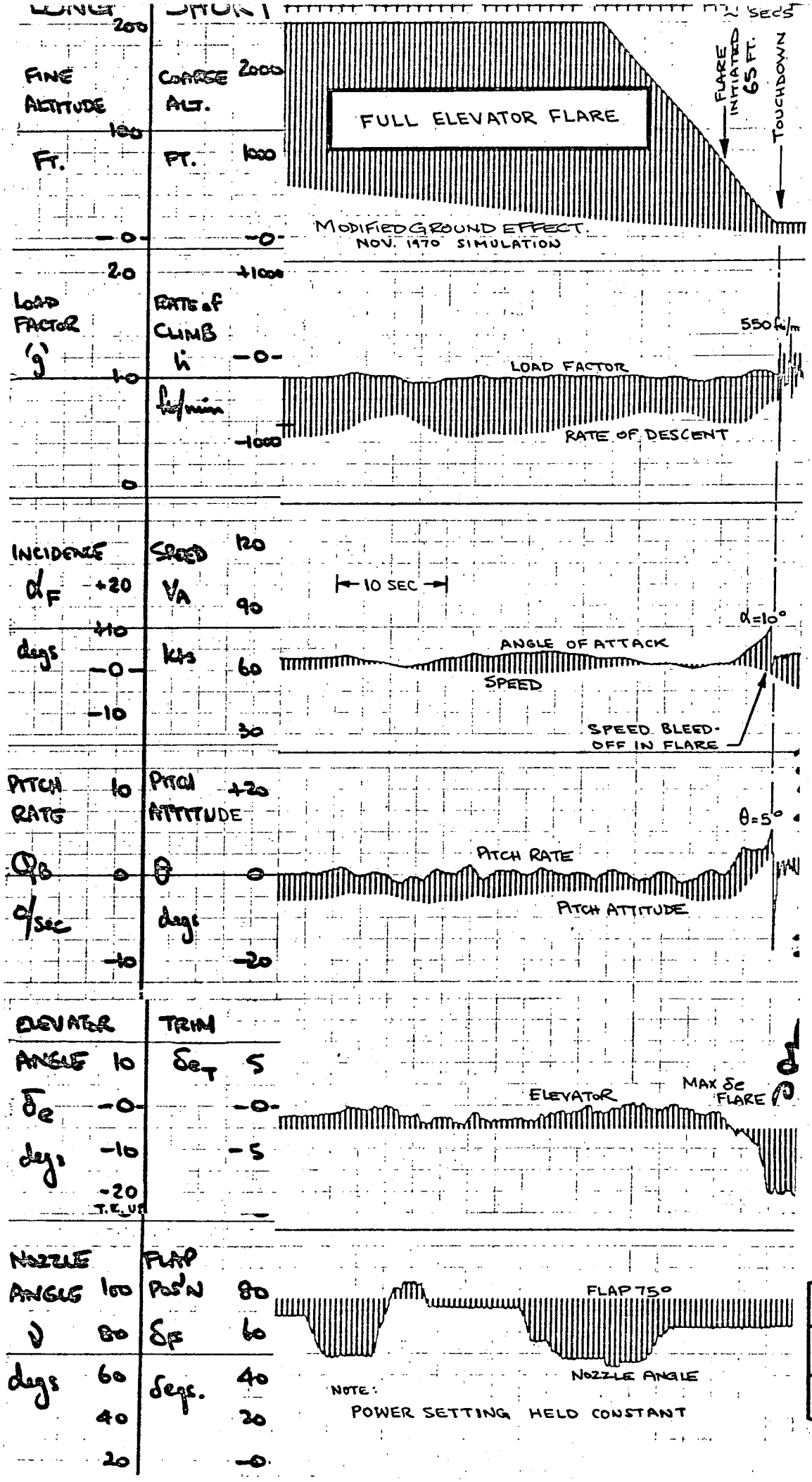

NOTE:
POWER SETTING HELD CONSTANT

MOD. C-8A

FIG. 3-34
DL-40381
3.54

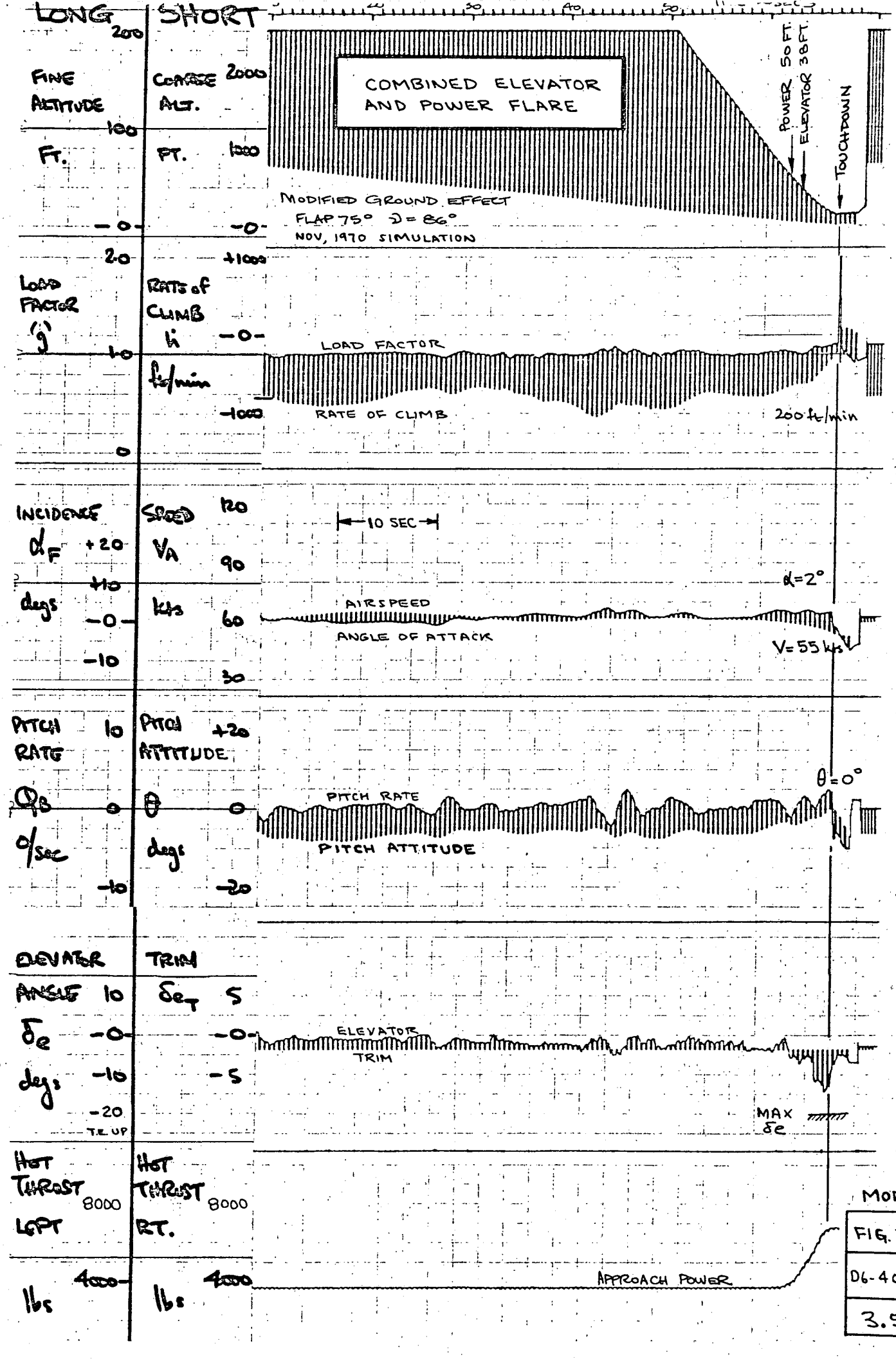

MOD. C-8A

FIG. 3-35

D6-40381

3.55

3.4 Dynamic Stability and Control

The dynamic longitudinal stability characteristics of the Modified C-8A vary from "conventional" at cruise to highly "unconventional" at STOL approach. Low airspeed fundamentally affects frequency and damping: short period is no longer "short" and phygoid period is no longer "long". Aerodynamic characteristics are dependent on speed and power setting through the jet flap. Direct hot thrust effects are strongly felt at STOL speeds. The propulsion system produces normal force as well as axial force. Vectorable thrust adds a new dimension to transient response. High induced drag effect produces considerable speed change if angle of attack is changed. The simulator, with its non-linear data base, provided the most meaningful insight into dynamic response.

The most conventional flight mode is "cruise" where flaps are up and power effects are minimum. Figure 3-36 shows the response to step column input at 155 kt, flaps-up cruise. The short period has about a 3 second period and damping ratio of $\zeta = .5$. Phugoid has a 40 second period with $\zeta \approx .05$. The separation between short period (attitude) and phugoid (speed) permits conventional short term control of attitude and flight path using only elevator. Airspeed changes little for the first 5-6 seconds and n_z crossover takes 11 seconds.

A step increase in throttle at 155 kt cruise is depicted in Figure 3-37. With no pilot input to elevator, the airplane pitches up into a climb (thrust line below CG) and slows down approximately 10 kts. If the pilot holds the nose down (push force), the airplane would accelerate in speed. Thrust changes with nozzles aft produce conventional response for long term control of flight path and/or airspeed.

Nozzle rotation downward from the aft position acts essentially like a decrease in power setting at cruise. The flap extension maneuver shown previously in Figure 3-48 illustrates how the pilot may rotate nozzles to bleed off speed.

Transient response at the other end of the flight envelope, 60 kt approach, is considerably different than cruise. Figure 3-38 shows airplane response to a trailing edge down elevator step at 60 kts. The "short period" is highly damped ($P \doteq .8$ sec, $\zeta = .8$). Airspeed change is immediate. Actual response seen by the pilot is a sluggish combination of classical short period and phugoid modes. Figure 3-39 shows airplane response to pulse and step trailing edge up elevator inputs. Again speed changes are immediate. Initial response is in the correct direction, but an increase in rate of climb turns into a decrease as speed changes. This is typical of "backside" flying. Low static stability (see Figure 3-19) is evident in that only a small trailing edge up elevator step ($\Delta\delta_e = -2°$) is required to stall the airplane. The airplane can no longer be flown conventionally, using elevator alone for modulation of flight path at constant speed.

Response to thrust change is no longer conventional. Figure 3-40 shows a step power increase at STOL approach from the first simulation period. With flaps and nozzles down, thrust increase produces normal force (lift) instead of axial force. The airplane heaves upward pulling load factor. Angle of attack reduced by about $\Delta\alpha = -9°$, and the airplane went into its phugoid (no pilot input to elevator). Average speed was actually less than the original trim value. Attitude was more nose down. Unconventional attitude change (see also Figure 3-18) was regarded as "unstable" by the pilots.

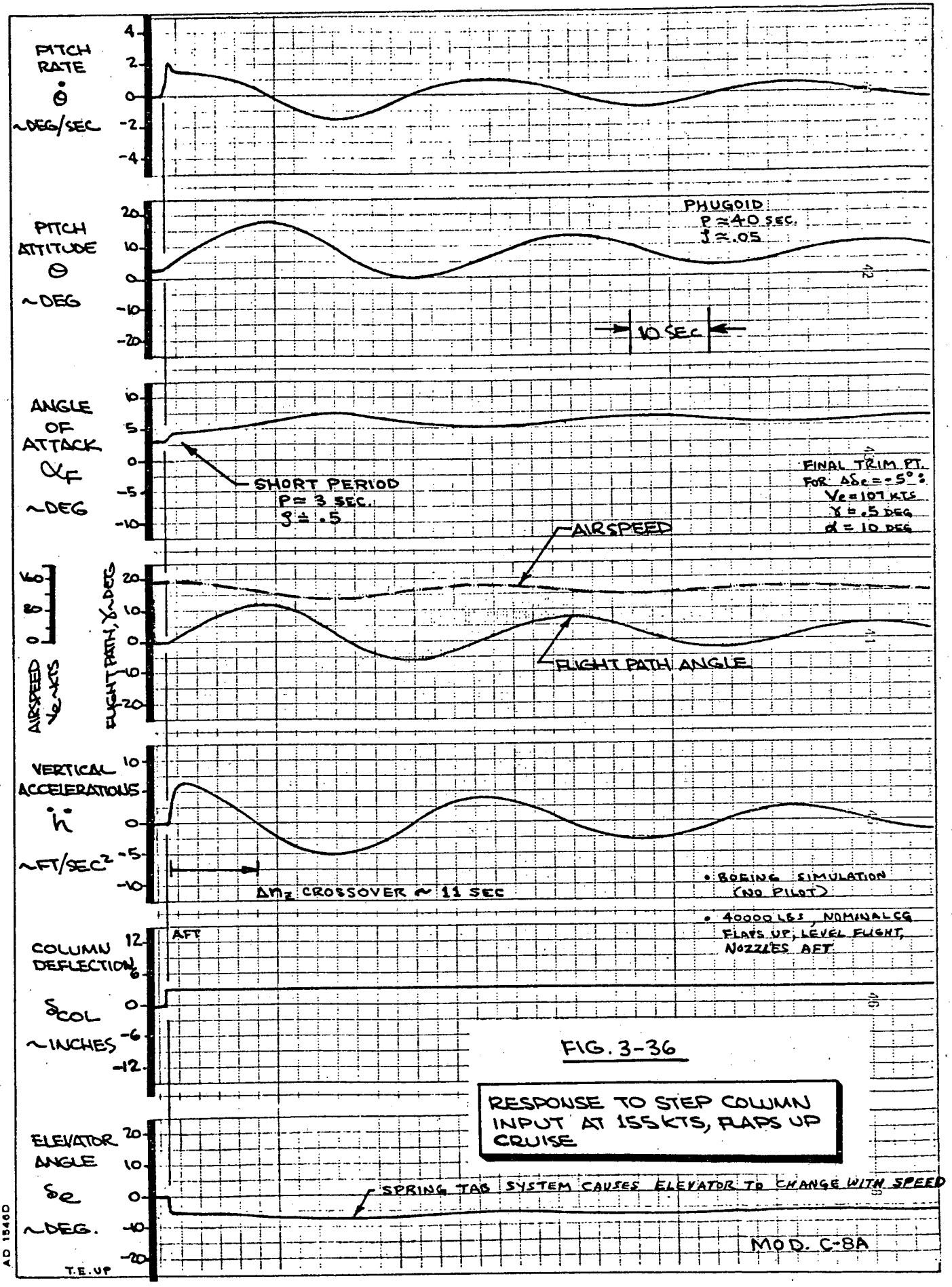

FIG. 3-36

RESPONSE TO STEP COLUMN INPUT AT 155 KTS, FLAPS UP CRUISE

MOD. C-8A

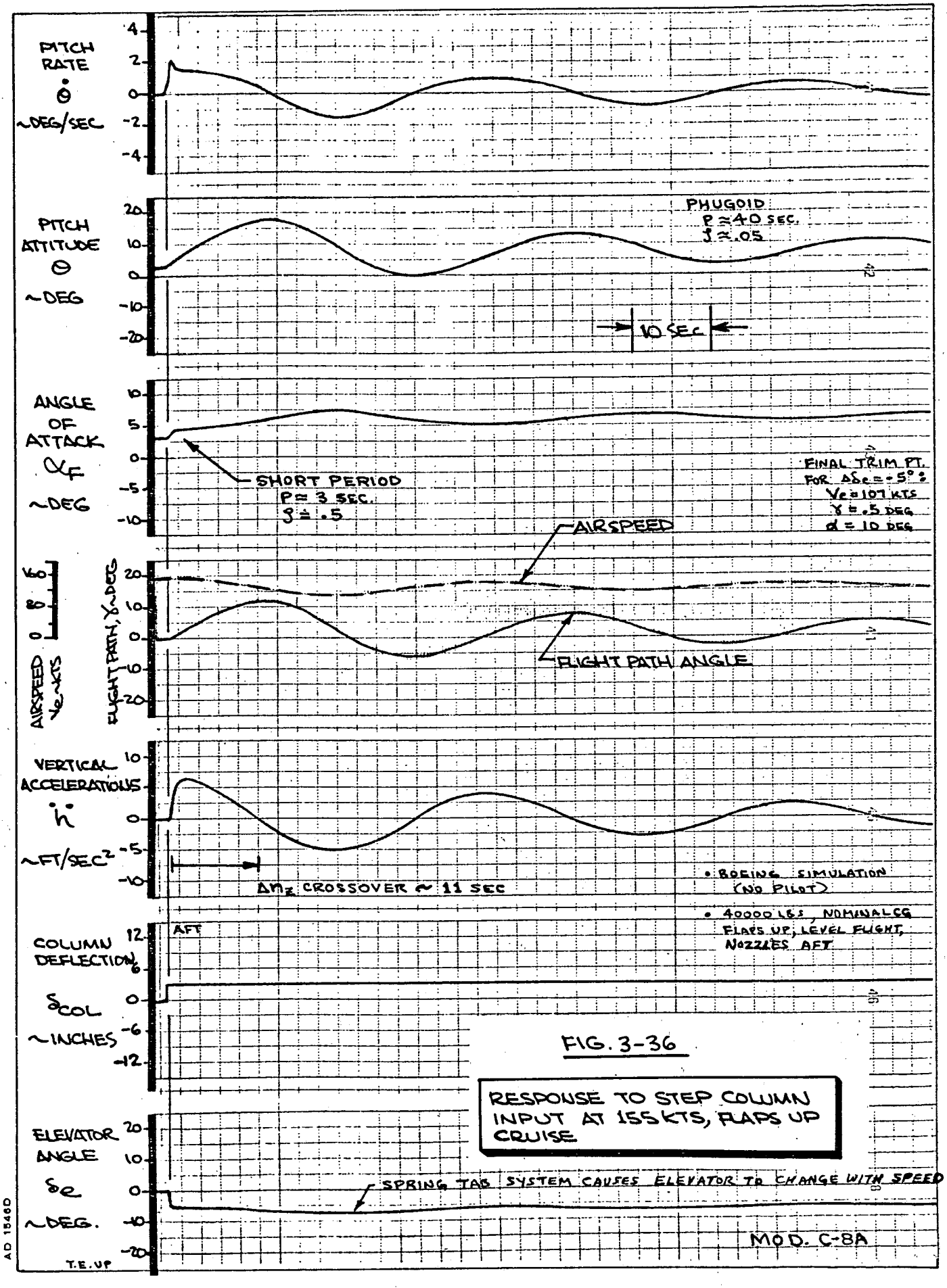

FIG. 3-36

RESPONSE TO STEP COLUMN INPUT AT 155 KTS, FLAPS UP CRUISE

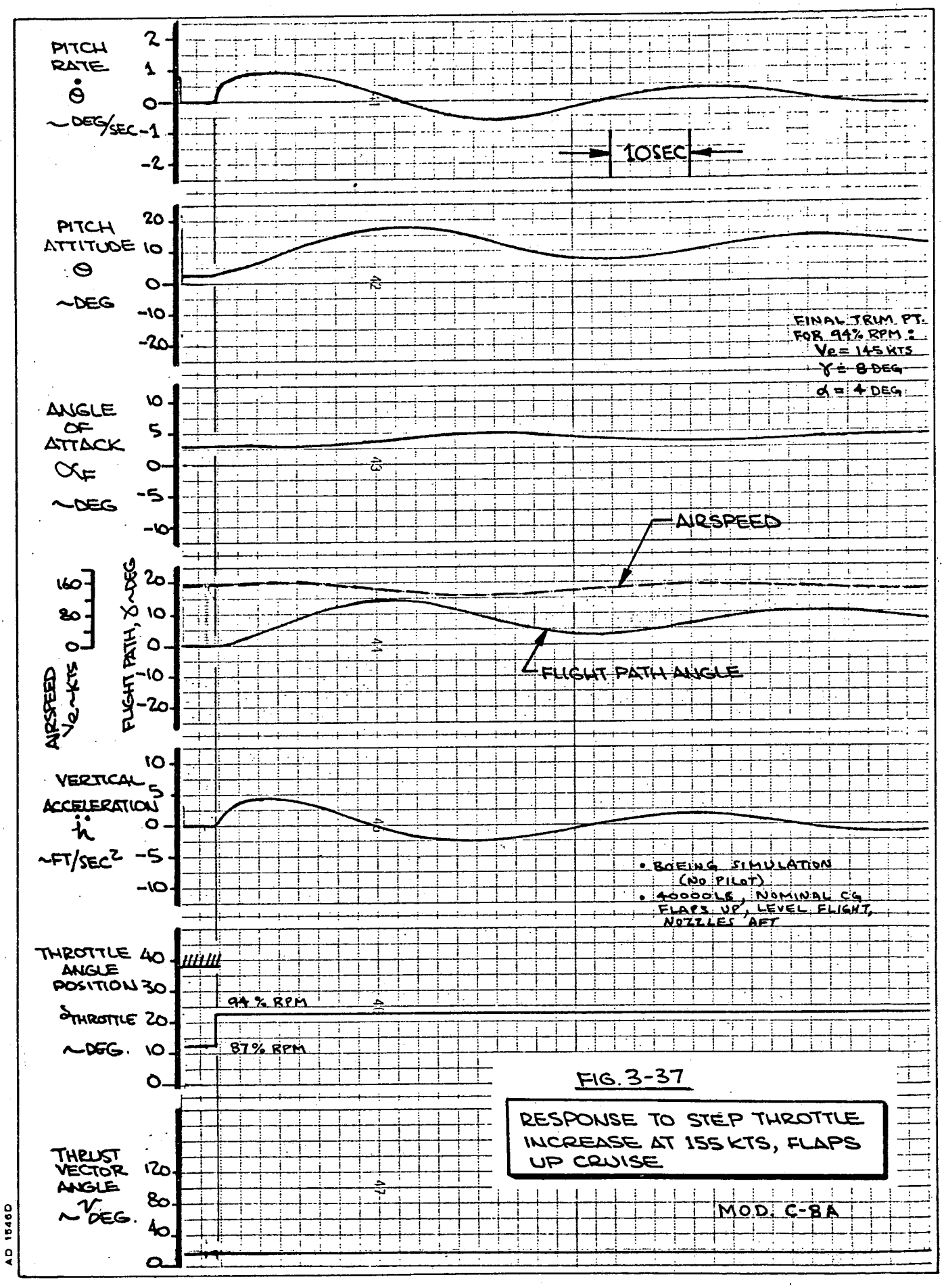

FIG. 3-37

RESPONSE TO STEP THROTTLE INCREASE AT 155 KTS, FLAPS UP CRUISE

M.O.D. C-8A

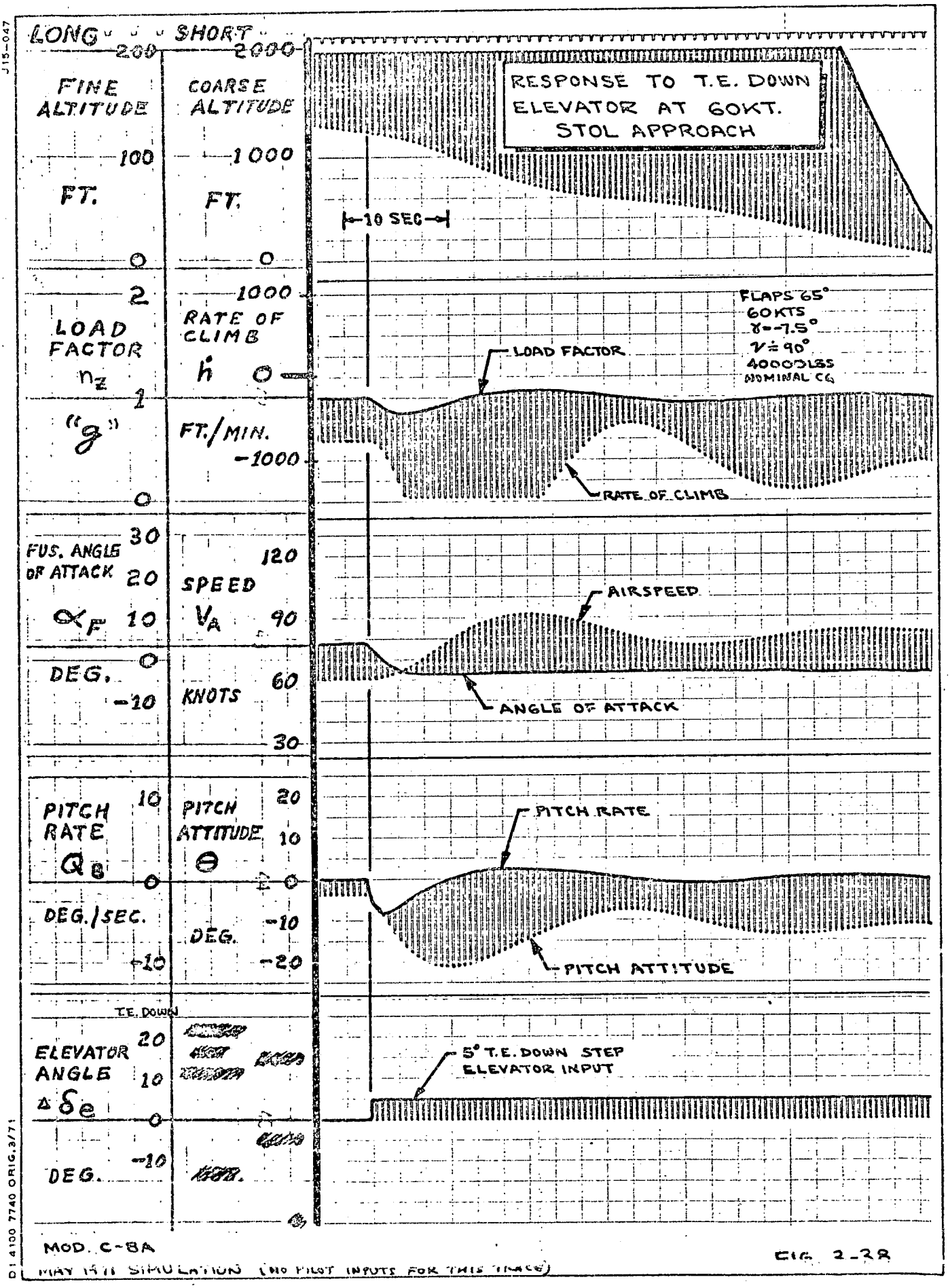

FIG. 2-28

D14100 7740 ORIG. 3/71

J15-047

REV SYM

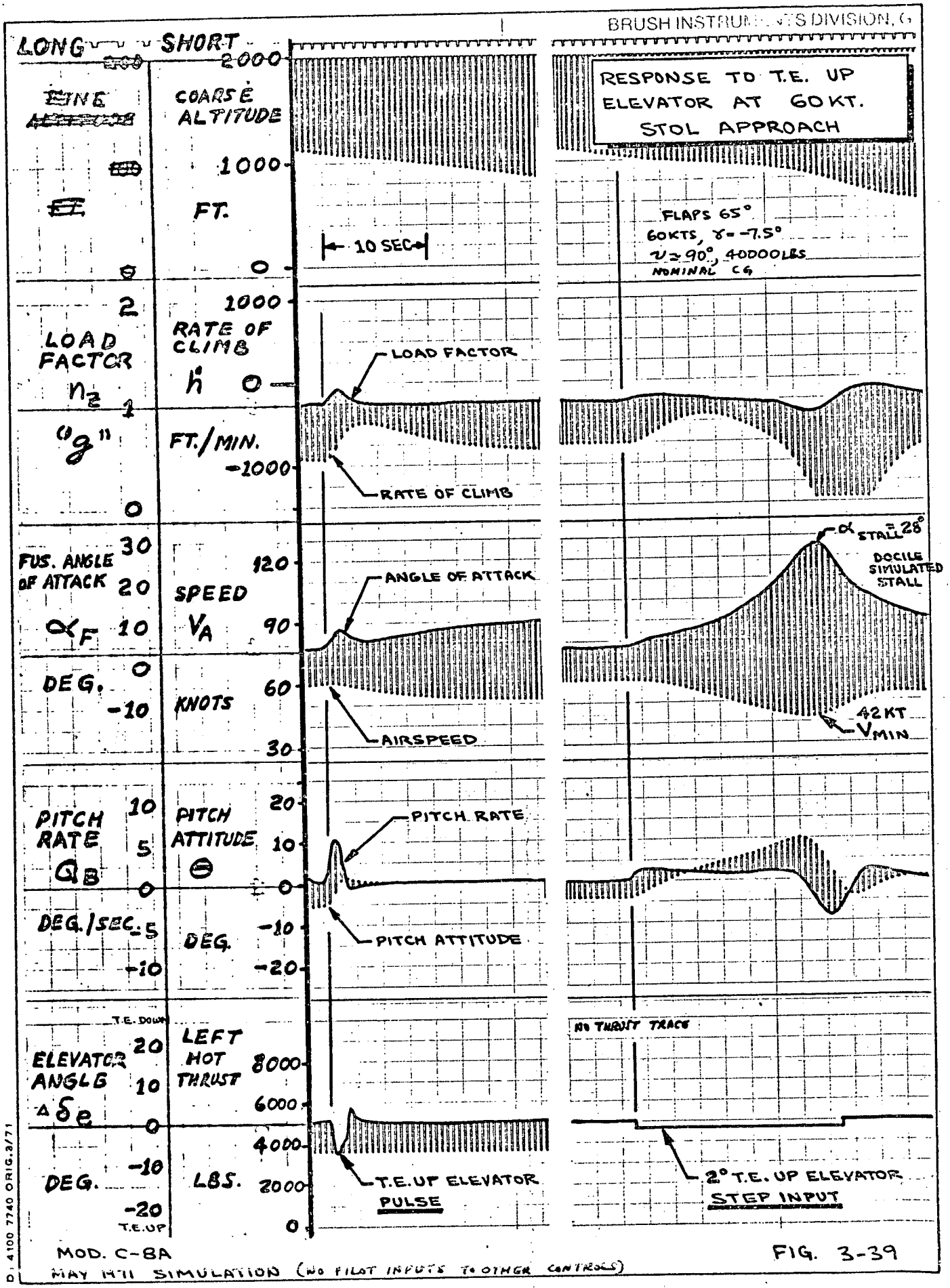

MOD. C-8A
MAY 1971 SIMULATION (NO PILOT INPUTS TO OTHER CONTROLS)

FIG. 3-39

J15-047

D 4100 7740 ORIG. 3/71

REV SYM

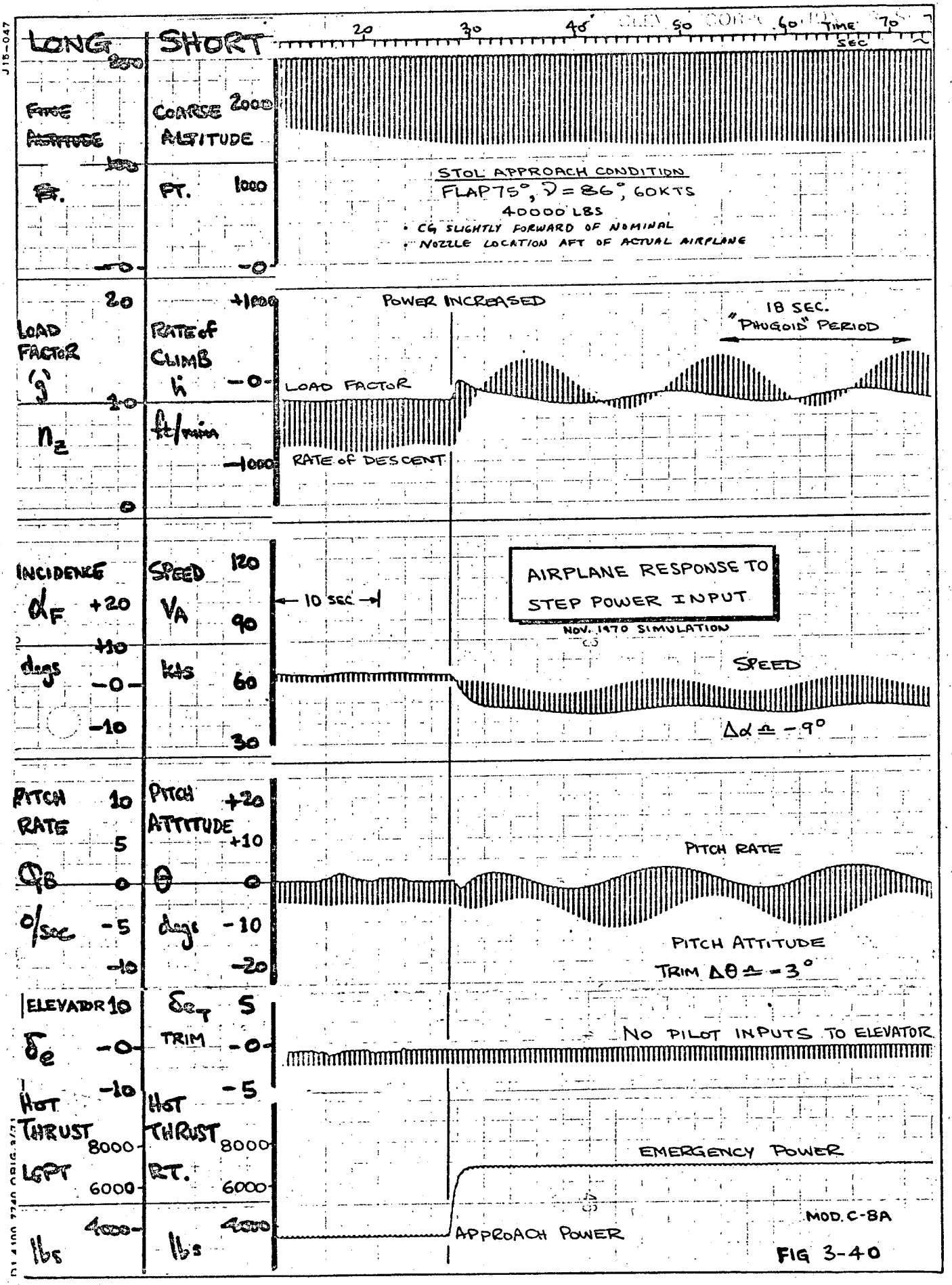
LONG
SHORT
20
30
40
50
60
70
TIME
SEC
FINE ALTITUDE
COARSE ALTITUDE
FT.
STOL APPROACH CONDITION
FLAP 75°, δ = 86°, 60KTS
40000 LBS
• CG SLIGHTLY FORWARD OF NOMINAL
• NOZZLE LOCATION AFT OF ACTUAL AIRPLANE
LOAD FACTOR
RATE of CLIMB
POWER INCREASED
18 SEC.
"PHUGOID" PERIOD
LOAD FACTOR
RATE of DESCENT
INCIDENCE
SPEED
10 SEC
AIRPLANE RESPONSE TO STEP POWER INPUT
NOV. 1970 SIMULATION
SPEED
PITCH RATE
PITCH ATTITUDE
PITCH ATTITUDE
TRIM Δθ ≙ -3°
ELEVATOR
TRIM
NO PILOT INPUTS TO ELEVATOR
HOT THRUST
LEFT
RT.
EMERGENCY POWER
APPROACH POWER
lbs
MOD. C-8A
FIG 3-40

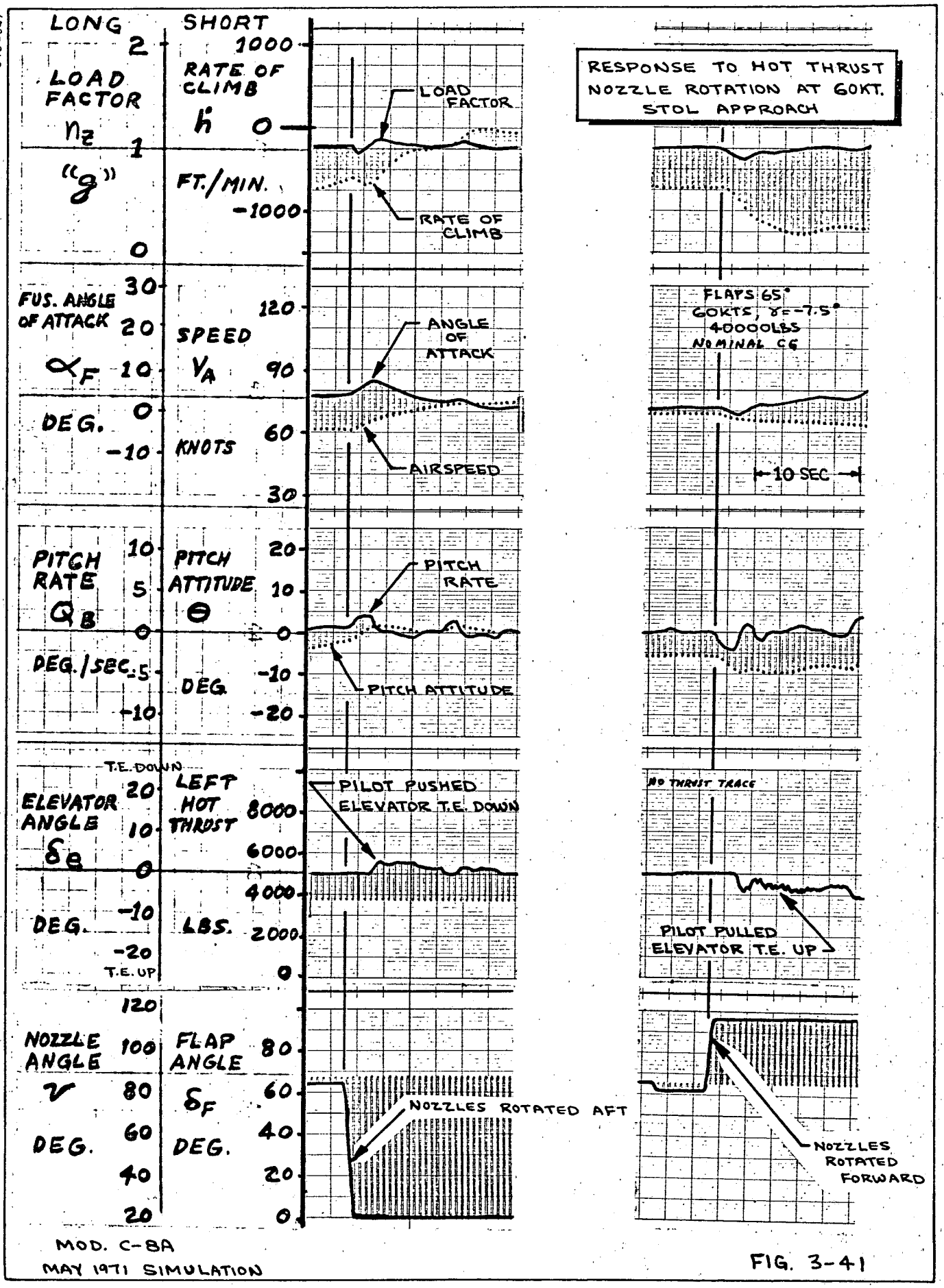

MOD. C-8A
MAY 1971 SIMULATION

FIG. 3-41

J15-047

D1 4100 7740 ORIG. 3/71

REV SYM

64

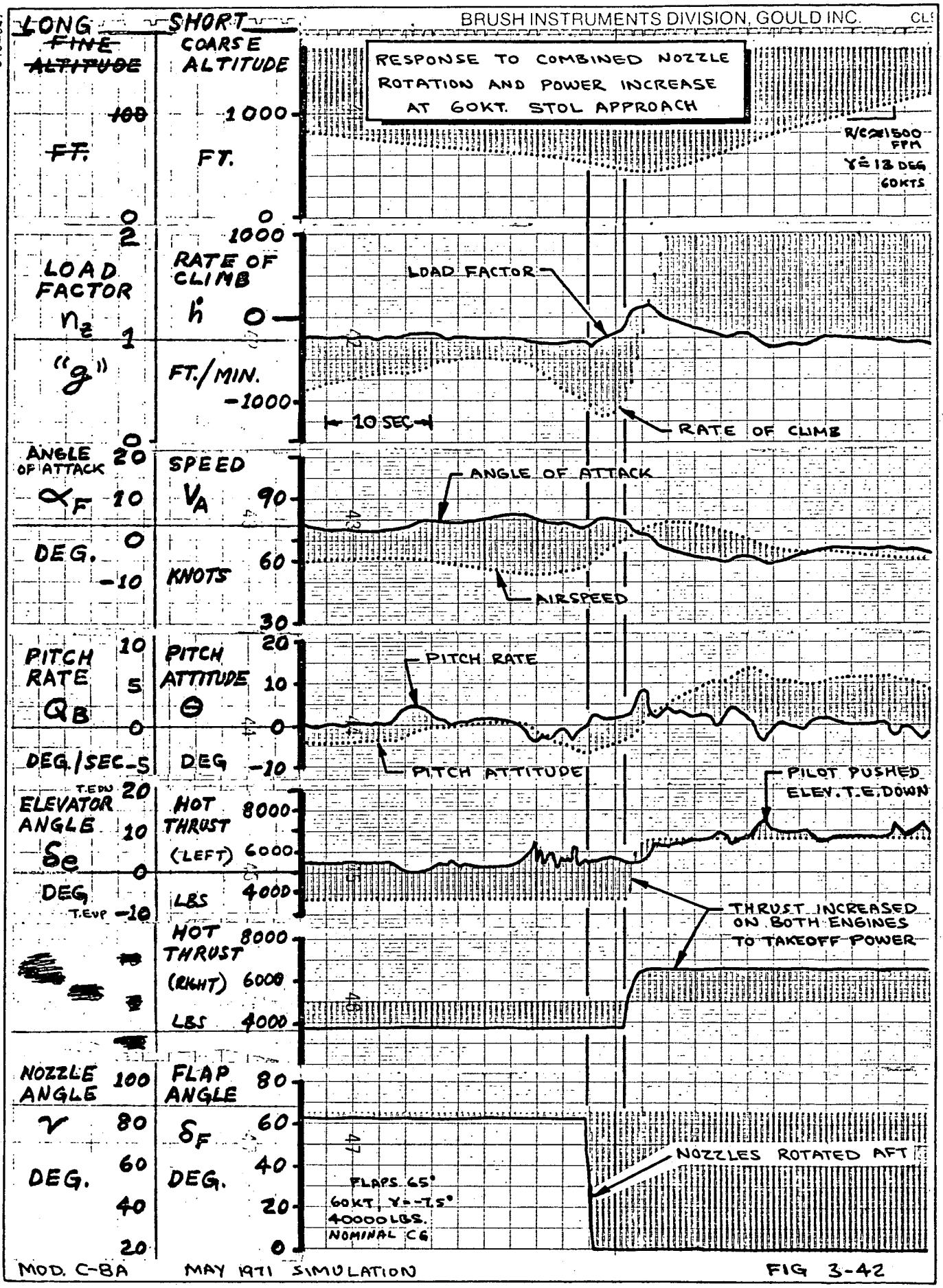

MOD. C-8A MAY 1971 SIMULATION FIG 3-42

D1 4100 7740 ORIG. 3/71

The ailerons droop with flap deflection to improve lift and drag. Figure 4-5 presents the aileron droop schedule. Optional capability for increased droop angle is available as shown. Control surface programming with pilot's wheel is shown in Figure 4-6. Aileron programming has been made nearly linear. $\delta_{w_{max}} = 75°$ to maintain good mechanical advantage in manual reversion. Tight spoiler programming is provided to minimize aerodynamic deadzone and achieve full control input with less than full wheel for better roll sensitivity. Augmentor choke deflection is delayed with wheel deflection to maintain clean flap geometry and minimize lift loss for small control input. Wheel position is fed forward electrically through the SAS to double the system gain for the first $3° \delta w$. This system feature was added to offset any mechanical and/or aerodynamic deadzone which may exist in the system.

Boost-on lateral control feel and centering forces are shown on Figure 4-7. One-hand control is easily possible. Full surface travel is possible within 1/2 second, and control wheel rates up to 200 deg/sec will not cause the valve to bottom in the central power control unit. Lateral trim authority is quite adequate (see Figure 4-7) and trim rate exceeds $\dot{\delta}w > 4$ deg/sec (per pilot requests).

The Modified C-8A lateral control system is quite effective aerodynamically. Figure 4-8 shows that rolling moment coefficient at landing approach is 60% larger than the 737 at its approach condition. Note the "convex" shape to the rolling moment curve and the steep slope about $\delta w = 0°$. These features were purposely designed into the system to satisfy design criteria deemed essential for STOL flight. Yawing moment due to lateral control is very small at the

4.0 LATERAL-DIRECTIONAL CHARACTERISTICS

4.1 Control Features

Estimated lateral-directional aerodynamic data for the Modified C-8A were derived from wind tunnel testing, basic Buffalo characteristics and theoretical methods (dynamic derivatives). Wind tunnel testing of the augmentor wing model indicates that basic sideslip characteristics are well behaved with the exception of C_{l_β}. NASA wind tunnel testing (References 2 and 3) revealed that there may be no dihedral effect at STOL landing conditions, i.e., $C_{l_\beta} = 0$. While this adverse characteristic may not exist in flight, wind tunnel testing of a jet flap model (References 12 and 13) and a BLC model (Reference 14) have revealed the same trend. It seems likely that dihedral effect and related dynamic problems will indeed occur. At the same time high lift coefficient results in a large amount of rolling moment due to yaw rate (C_{l_r}), and spiral stability degenerates. Other dynamic cross-coupling effects become more pronounced at STOL conditions. Lateral-directional handling qualities are poor producing the requirement for powerful flight controls and a stability augmentation system.

Lateral control is provided by a combination of ailerons, spoilers and augmentor chokes. Typical rolling moment data for each surface are shown in Figures 4-1, 4-2 and 4-3. It is immediately evident that lateral control power is dependent on blowing level as well as surface deflection. Even aileron hinge moment is a function of blowing level as shown in Figure 4-4. (High hinge moment slope dictated the geared tab feature to make manual reversion feasible). Lateral control requirements influenced flap and aileron blowing distribution across the wing span to assure adequate control at STOL conditions.

design landing approach condition; however, both favorable and adverse yawing characteristics are found at other conditions. In all cases $\left|\frac{\Delta C_n}{\Delta C_l}\right| < .2$. Lift loss due to lateral control is proportionately less than many airplanes due to outboard spoiler location. At the design approach condition $\Delta C_L \approx -.4$ (10% of $\frac{W}{qS}$) at full wheel with most lift loss coming from the augmentor choke. Effective center of rotation lies within the width of the fuselage. Optional surface programming capability is available and hydraulic power to surface pairs may be shutoff. Rolling moment with wheel may be varied for lateral control testing as shown in Figure 4-9.

The Modified C-8A also has a powerful rudder for crosswind and engine-out control. Fin lift produced by rudder deflection (Figure 4-10) is about 60% greater than the conventional rudder on the 737.

Pedal force from the feel-and-centering unit is shown in Figure 4-11. The pilot has rudder trim for 1/4 pedal travel ($\delta_R \approx 6^\circ$) which is barely adequate. Rudder authority is limited at speeds greater than 100 knots by hydraulic boost hinge moment limitation (blow down). Enough rudder authority exists, even on one hydraulic system, to trim an engine-out condition. With both hydraulic systems operating, the rudder has capability to generate excessive sideslip angles and fin loads at speeds above 100 knots. The pilot is warned not to use too much rudder at cruise conditions.

	CALC	CHECK	APR	APR
SPITZER	12-11-70			
SPITZER	2-8-72			

DATE	REVISED

THE BOEING COMPANY

AILERON EFFECTIVENESS

FIG 4-1

D6-40381

PAGE 4.4

MODC-8A

AERODYNAMIC DATA REVIEW — AILERON EFFECTIVENESS

$$C_{\ell}{}_{AILERON} = f(\delta_a, C_{j_a})$$

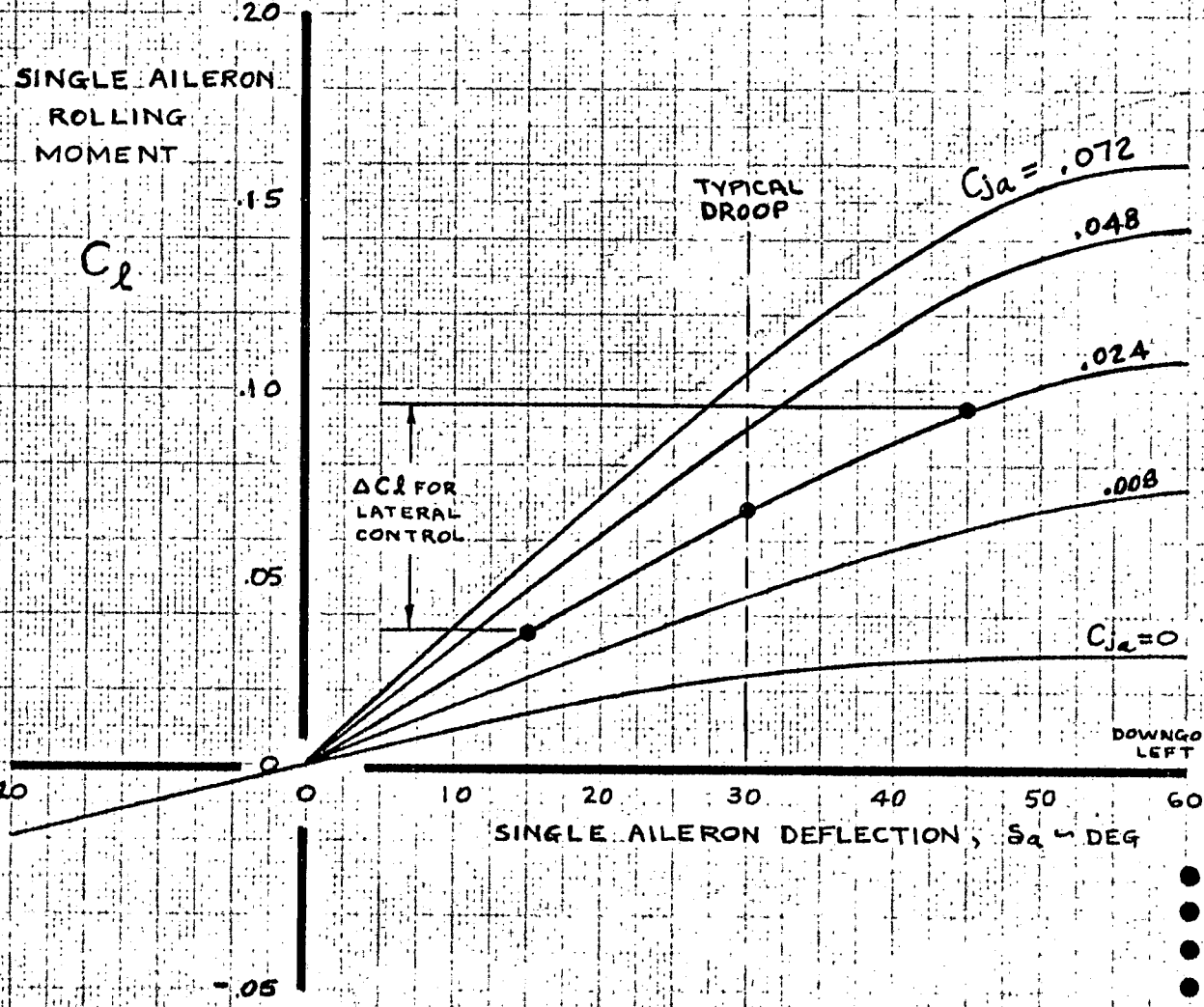

AD 461 C-R6

	CALC	SPITZER	12-11-70	REVISED	DATE
APR	CHECK				
APR					

AERODYNAMIC DATA REVIEW — SPOILER EFFECTIVENESS

$$C_{\ell_{SPOILER}} = f(\delta_{SP}, \delta_a, \alpha, C_{j_a})$$

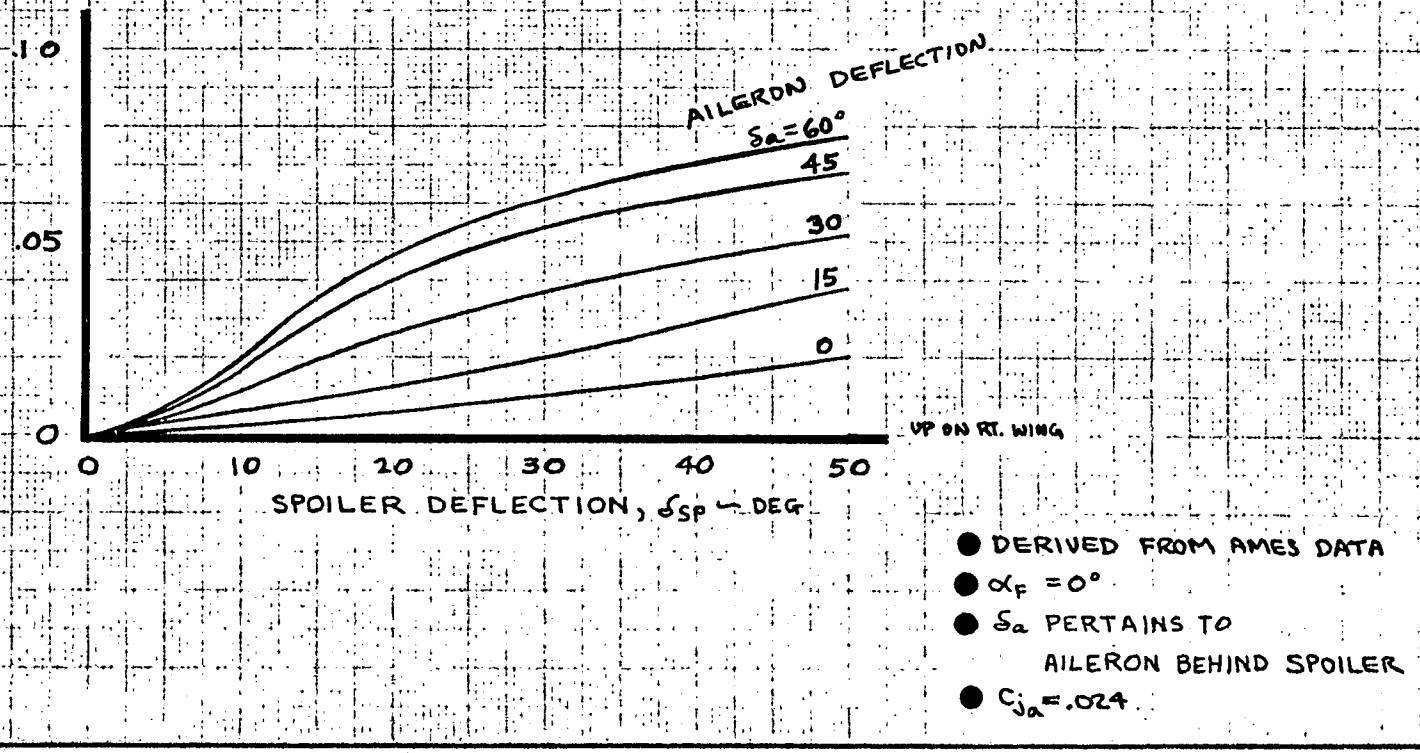

- DERIVED FROM AMES DATA
- $\alpha_F = 0°$
- δ_a PERTAINS TO AILERON BEHIND SPOILER
- C_{j_a}=.024

MOD C-8A

SPOILER EFFECTIVENESS

THE BOEING COMPANY

FIG 4-2	D6-40381	PAGE 4.5

K-E ALBUQUERQUE 1951 8.5 G-8000

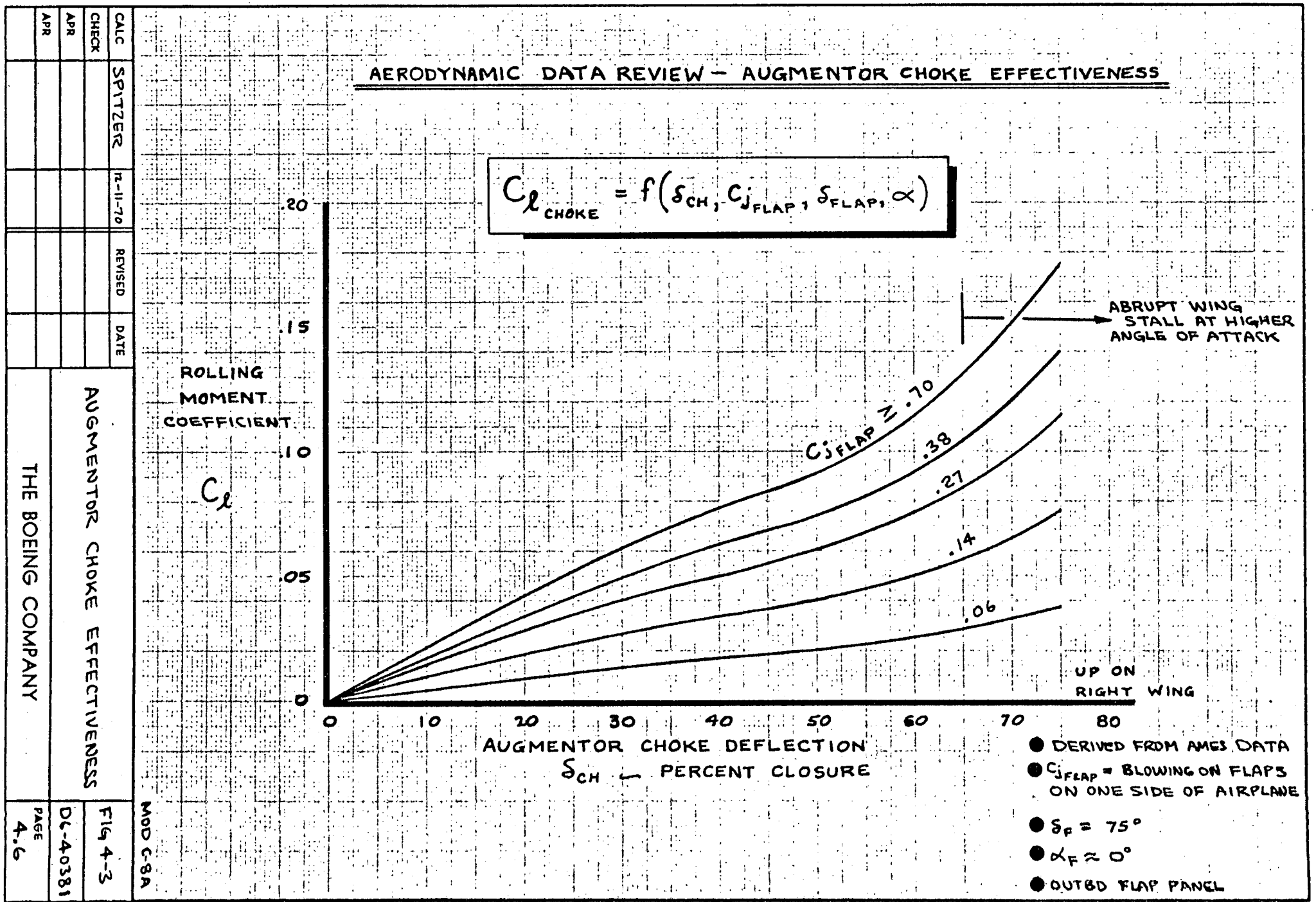
AERODYNAMIC DATA REVIEW – AUGMENTOR CHOKE EFFECTIVENESS
$C_{\ell_{CHOKE}} = f(\delta_{CH}, C_{j_{FLAP}}, \delta_{FLAP}, \alpha)$
ROLLING MOMENT COEFFICIENT
C_ℓ
.20
.15
.10
.05
0
$C_{j_{FLAP}} \geq .70$
.38
.27
.14
.06
ABRUPT WING STALL AT HIGHER ANGLE OF ATTACK
UP ON RIGHT WING
0
10
20
30
40
50
60
70
80
AUGMENTOR CHOKE DEFLECTION
δ_{CH} – PERCENT CLOSURE
● DERIVED FROM AMES DATA
● $C_{j_{FLAP}}$ = BLOWING ON FLAPS ON ONE SIDE OF AIRPLANE
● $\delta_F = 75°$
● $\alpha_F \approx 0°$
● OUTBD FLAP PANEL
CALC SPITZER 12-11-70
CHECK APR
APR
REVISED DATE
AUGMENTOR CHOKE EFFECTIVENESS
THE BOEING COMPANY
MOD C-8A
Fig 4-3
D6-40381
PAGE 4.6
K&E

MODIFIED IC-8A
ESTIMATED AILERON HINGE MOMENTS

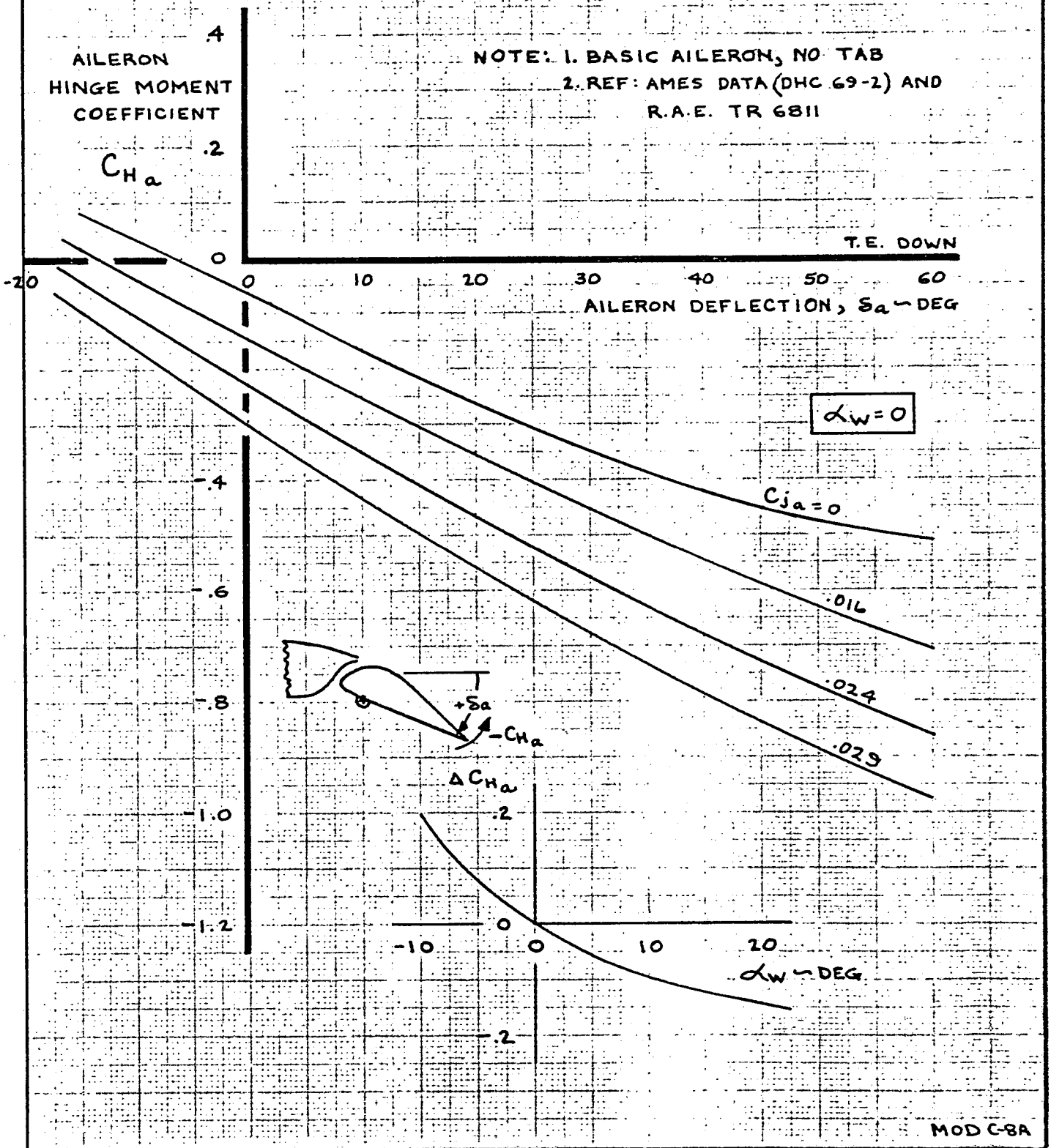

CALC	SPITZER	12-11-70	REVISED	DATE	AILERON HINGE MOMENTS	FIG 4-4
CHECK						D6-40381
APR					THE BOEING COMPANY	PAGE 4.7
APR						

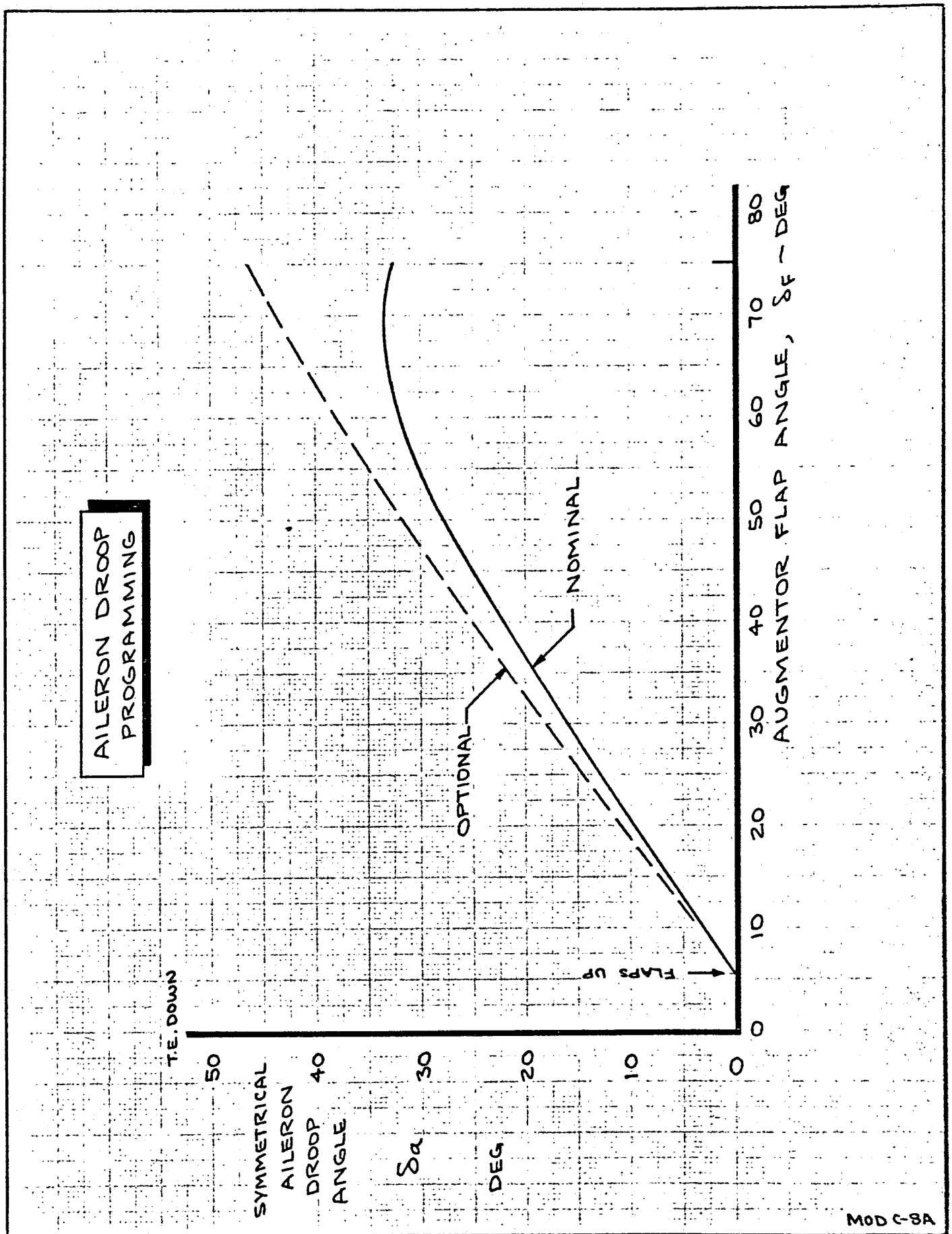

CALC	SPITZER	3-16-71	REVISED	DATE	AILERON DROOP	FIG 4-5
CHECK						D6-40381
APR						
APR					THE BOEING COMPANY	PAGE 4.8

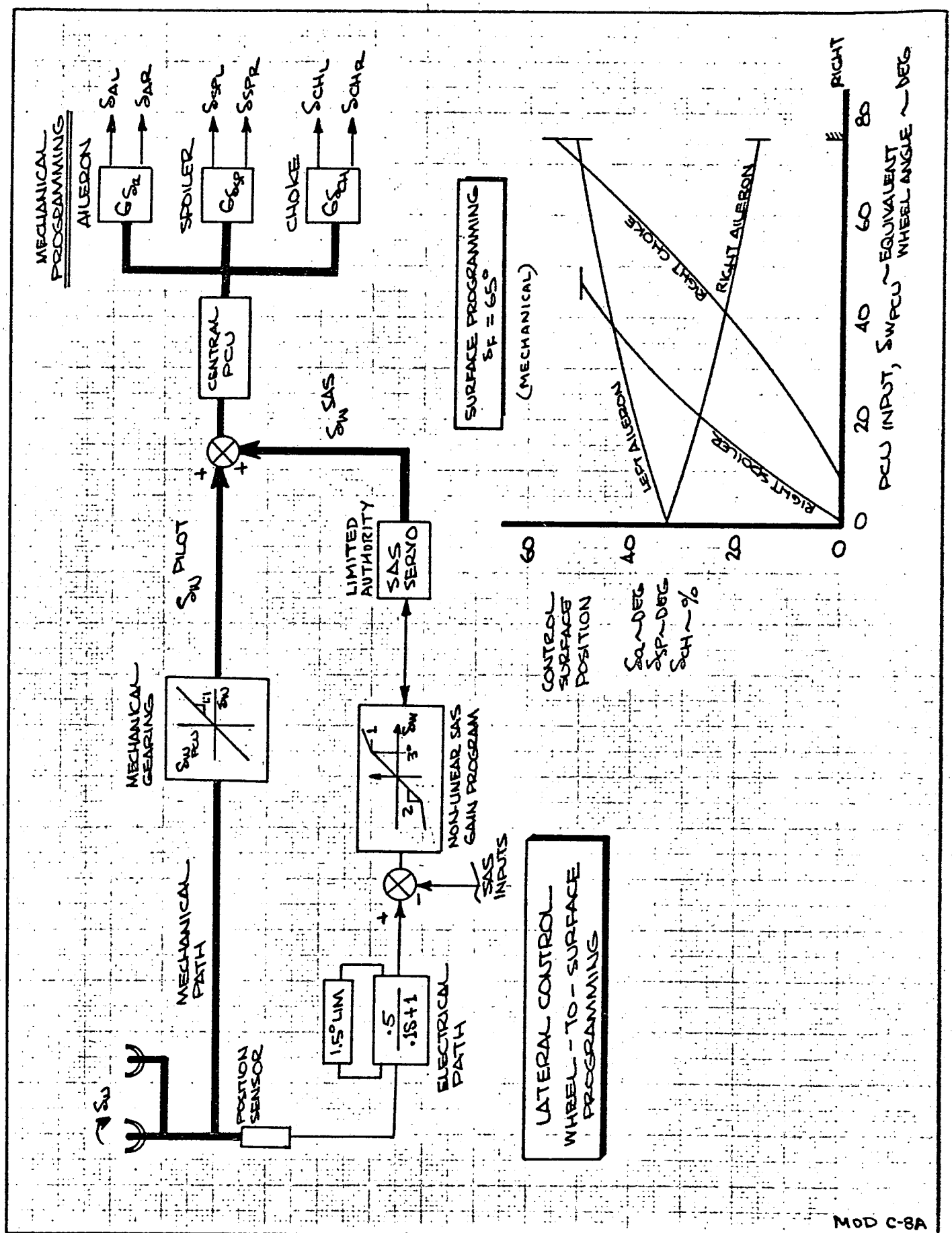

MOD C-8A

CALC	SPITZER	6-15-71	REVISED	DATE	WHEEL-TO-SURFACE PROGRAMMING WITH ELECTRICAL COMPENSATION
CHECK					
APR					
APR					
					THE BOEING COMPANY

FIG 4-6

D6-40381

PAGE 4.9

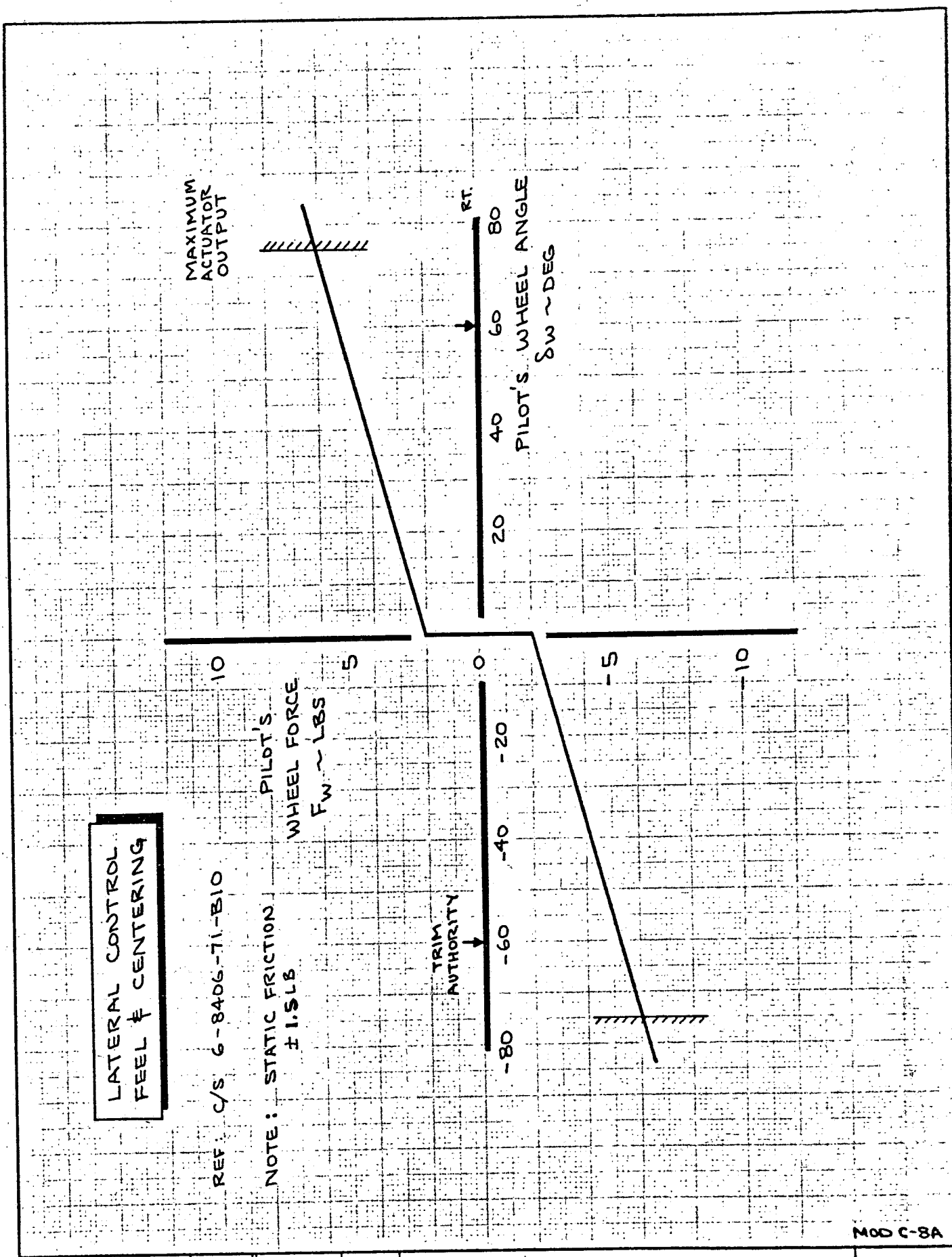

CALC	CWK	1-26-71	REVISED	DATE
CHECK			SPITZER	3-16-71
APR				
APR				

BOOST-ON LATERAL FEEL & CENTERING FORCES

THE BOEING COMPANY

FIG 4-7

D6-40381

PAGE 4.10

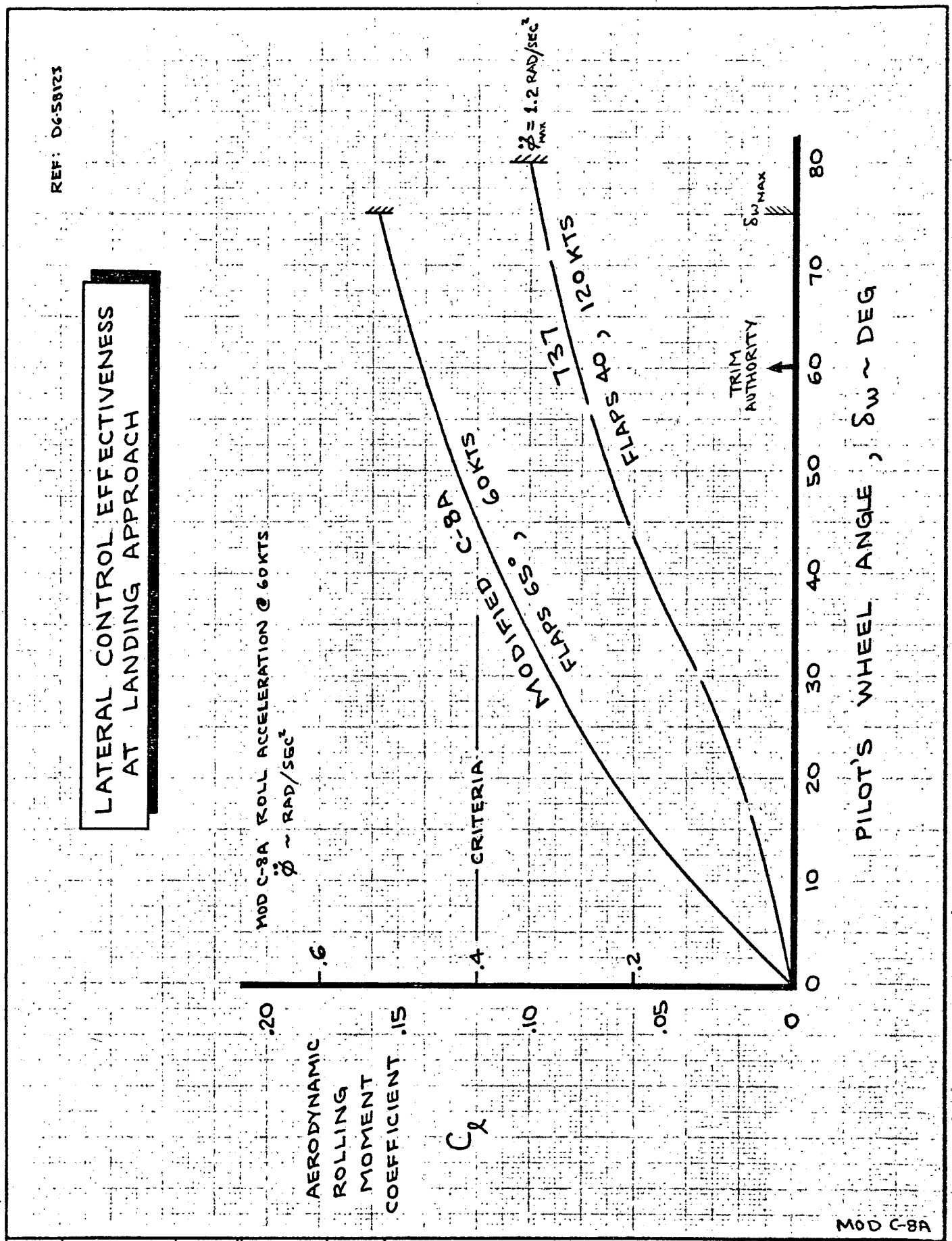

CALC	SPITZER	10/29/71	REVISED	DATE	LATERAL CONTROL AT LANDING APPROACH	FIG 4-8
CHECK						D6-40381
APR					THE BOEING COMPANY	PAGE 4.11
APR						

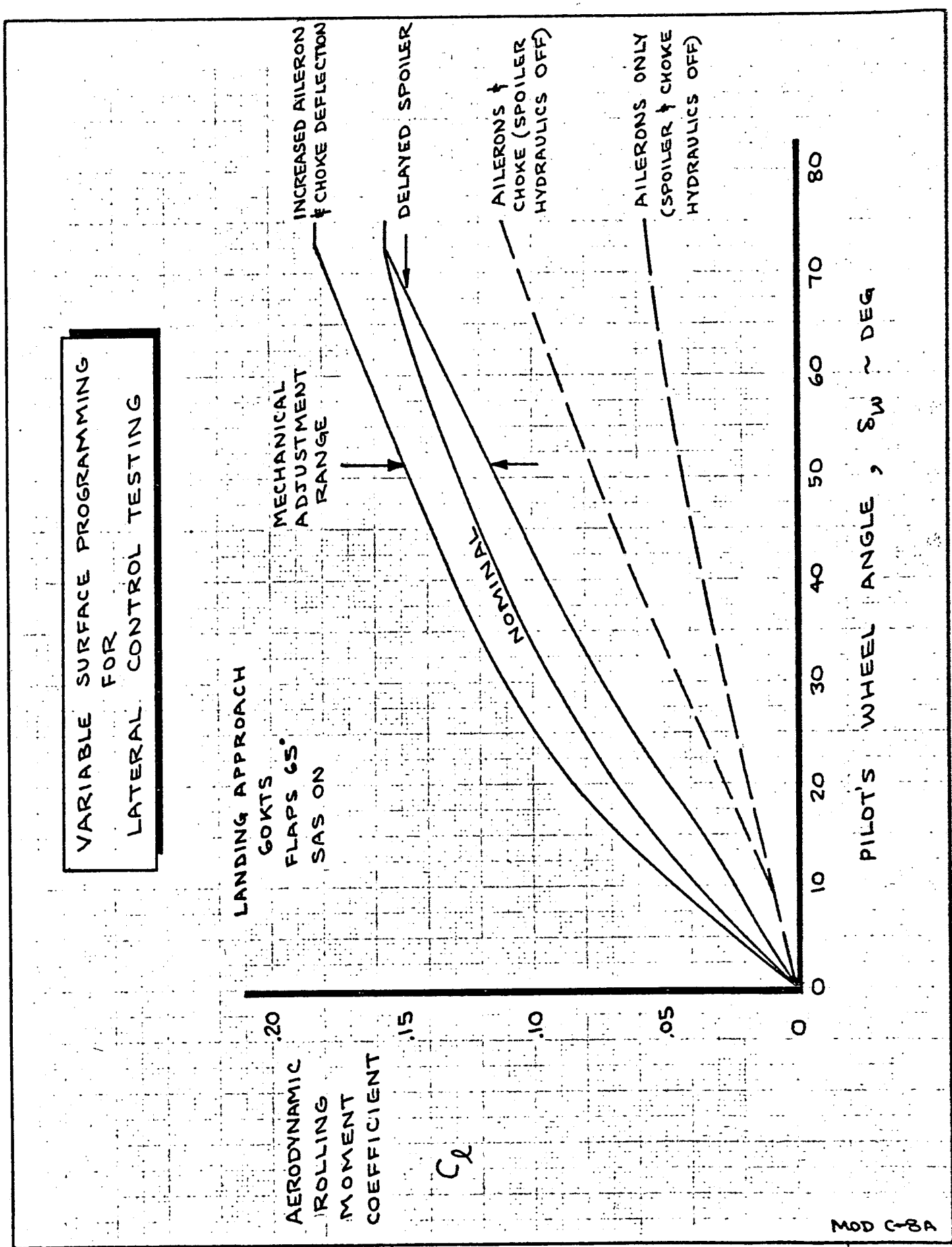

CALC	SPITZER	10/29/71	REVISED	DATE
CHECK				
APR				
APR				

LATERAL CONTROL EFFECTIVENESS WITH VARIABLE SURFACE PROGRAMMING — FIG 4-9

D6-40381

THE BOEING COMPANY

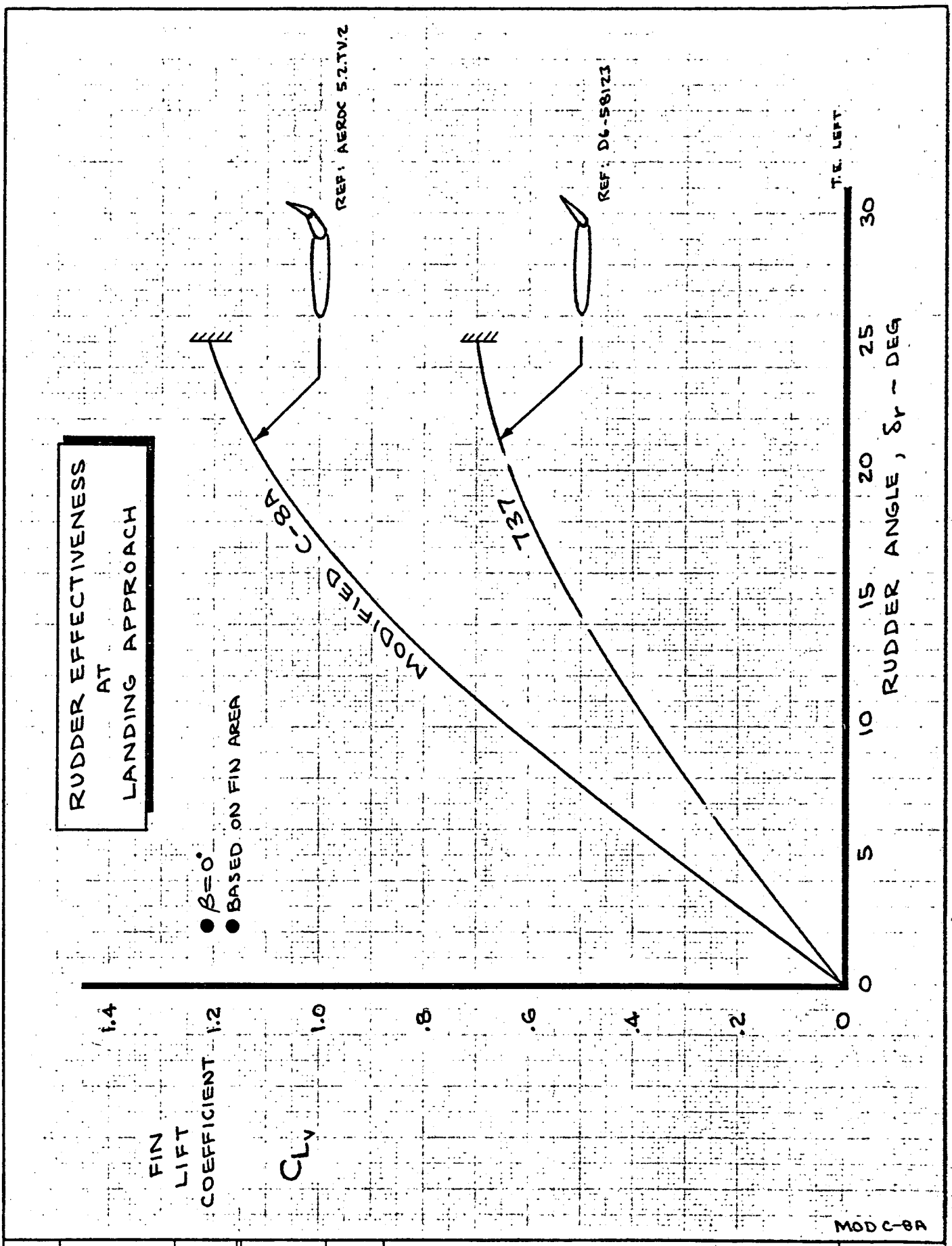

CALC	SPITZER	11-1-71	REVISED	DATE	RUDDER EFFECTIVENESS COMPARISON (LANDING APPROACH)
CHECK					
APR					
APR					
					THE BOEING COMPANY

FIG 4-10

D6-40381

PAGE 4.13

RUDDER - PEDAL CHARACTERISTICS

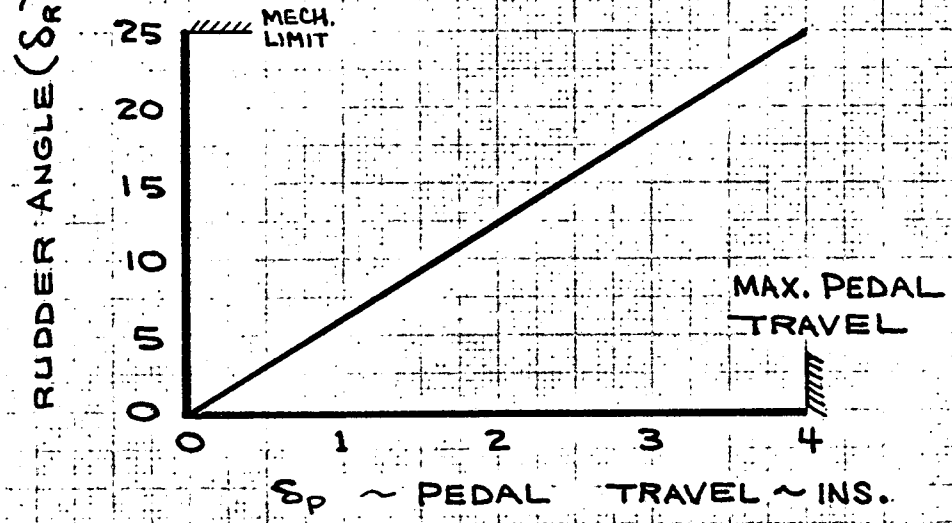

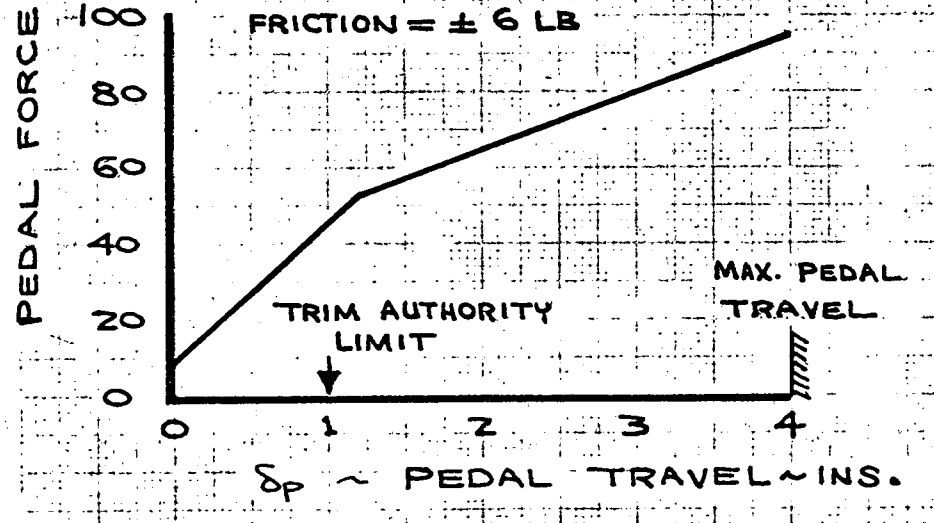

MOD C-8A

CALC-	SPITZER		REVISED	DATE	RUDDER GEARING AND PEDAL FORCE	FIG 4-11
CHECK						D6-40381
APR						
APR					THE BOEING COMPANY	PAGE 4.14
DWN	V. PAGE	2/7/72				

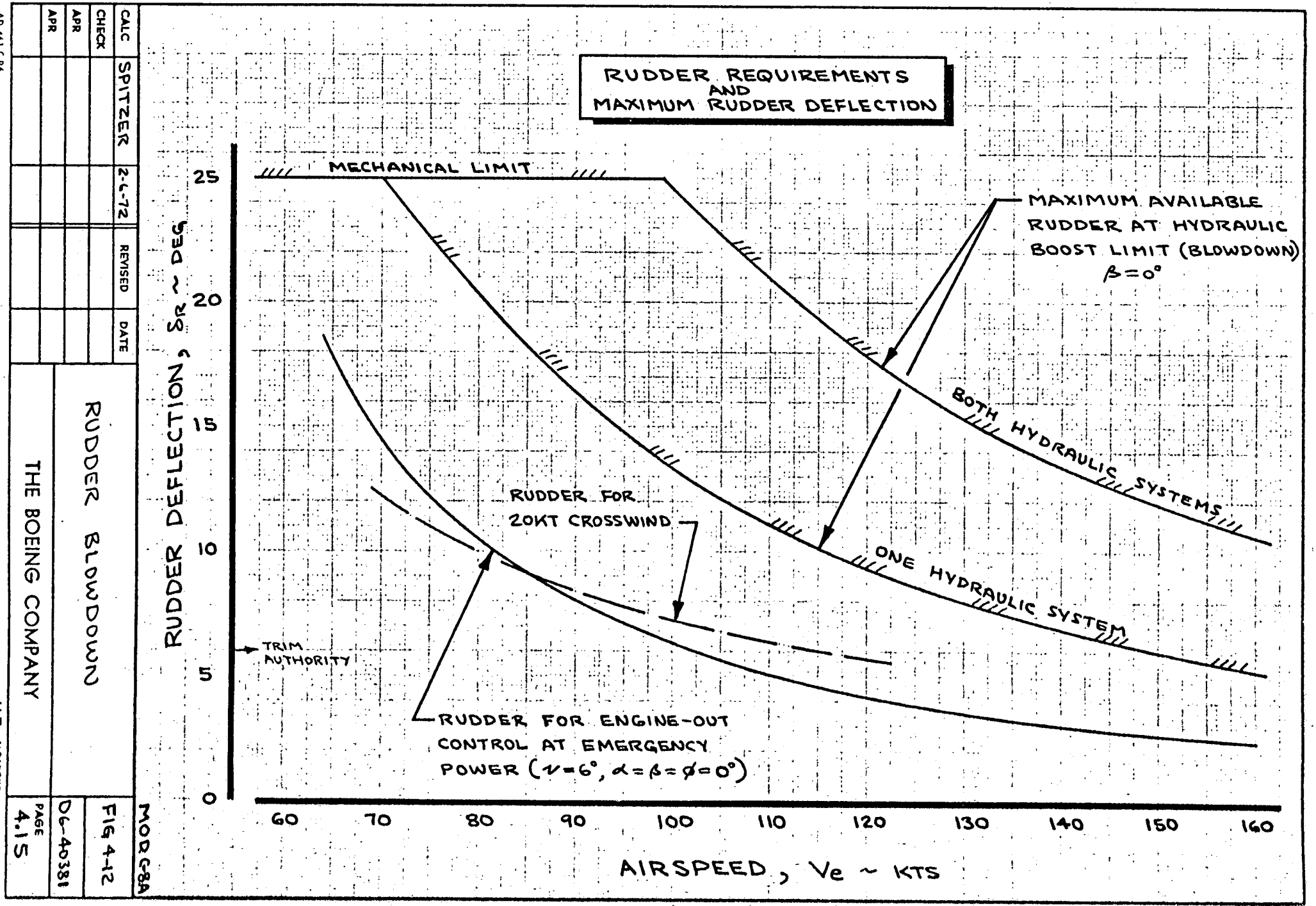
RUDDER REQUIREMENTS AND MAXIMUM RUDDER DEFLECTION
MECHANICAL LIMIT
MAXIMUM AVAILABLE RUDDER AT HYDRAULIC BOOST LIMIT (BLOWDOWN) β=0°
BOTH HYDRAULIC SYSTEMS
RUDDER FOR 20KT CROSSWIND
ONE HYDRAULIC SYSTEM
TRIM AUTHORITY
RUDDER FOR ENGINE-OUT CONTROL AT EMERGENCY POWER (ν=6°, α=β=φ=0°)
RUDDER DEFLECTION, δR ~ DEG
0
5
10
15
20
25
60
70
80
90
100
110
120
130
140
150
160
AIRSPEED, Ve ~ KTS
CALC SPITZER 2-6-72
CHECK
APR
APR
REVISED
DATE
RUDDER BLOWDOWN
THE BOEING COMPANY
PAGE 4.15
D6-40381
FIG 4-12
MODEL

4.2 Static Stability and Control

With its powerful rudder the Modified C-8A has capability of achieving large sideslip angles. Figure 4-12 presents sideslip-to-rudder characteristics at the critical STOL approach condition. Maximum rudder yields $\beta > 25°$ based on extrapolated data. Such angles appear feasible since U.S. Army flight tests on the original Buffalo (Reference 14) showed capability at $\beta > 20°$ from 65 to 109 kts. The wheel deflection shown in Figure 4-13 corresponds to two anticipated extremes in the value of C_{l_β}. Data at landing flaps indicate that $C_{l_\beta} = 0$ while theoretical estimates would show $C_{l_\beta} = -.004$/deg. A "statically stable" airplane requires right wheel for left pedal in a sideslip. With $C_{l_\beta} = 0$ an "unstable" left wheel input is required to offset rolling moment due to fin lift. In fact, the airplane will appear neutrally stable at $C_{l_\beta} = -.0015$/deg. At 60 kts aerodynamic sideforce is relatively small compared to airplane weight, thus only small bank angle is required to maintain straight flight path.

Crosswind requirements and airplane capability are shown in Figure 4-14. The Modified C-8A can handle a 20 kt crosswind at 60 kts using less than full rudder and much less than full lateral control. It should be noted however that the basic Buffalo exhibited some undesirable T-tail flow separation characteristics at high sideslip angles. Vortex generators were added to the fin and horizontal tail to remedy the situation. Until the Modified C-8A is fully tested, a 10 kt crosswind limit appears prudent for STOL operation.

Lateral control power is needed for two other static conditions: engine-out trim and fuel unbalance due to pump system failure. Engine-out control is given special consideration in Section 5.0. Sufficient lateral control exists to trim the worst likely fuel unbalance condition (Figure 4-15).

STEADY SIDESLIP AT LANDING APPROACH

$V_{APP} = 60$ KTS
$\delta_F = 65°$
$C_J = .5$

CURVES SYMMETRICAL FOR OPPOSITE RUDDER

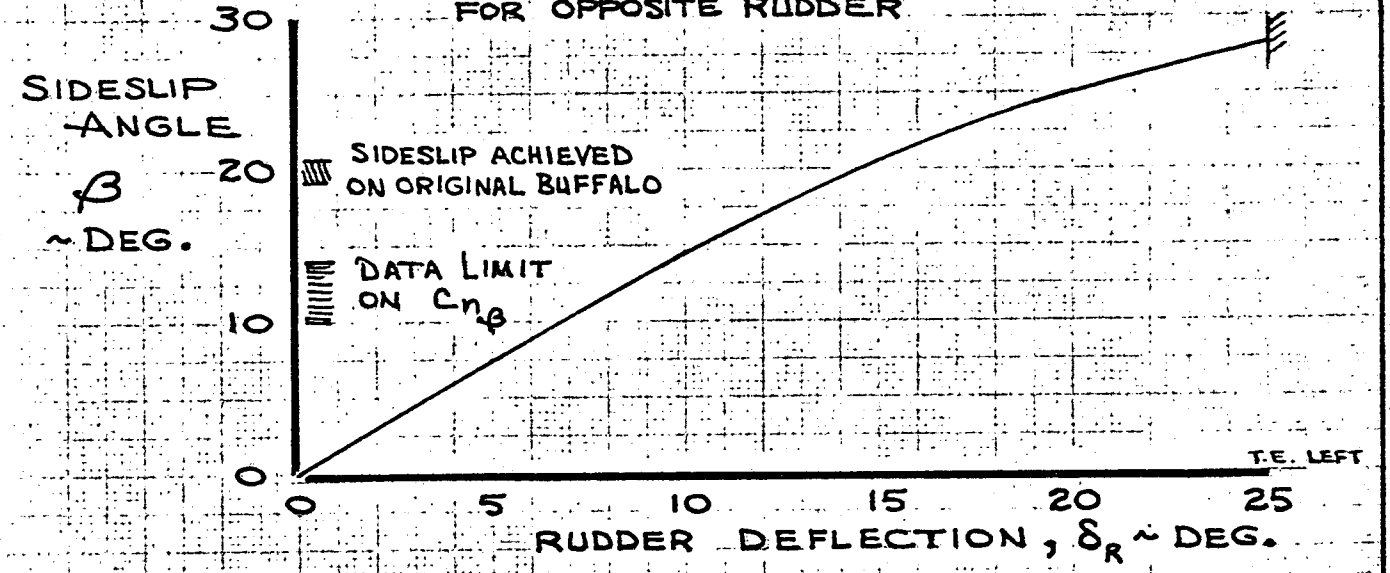

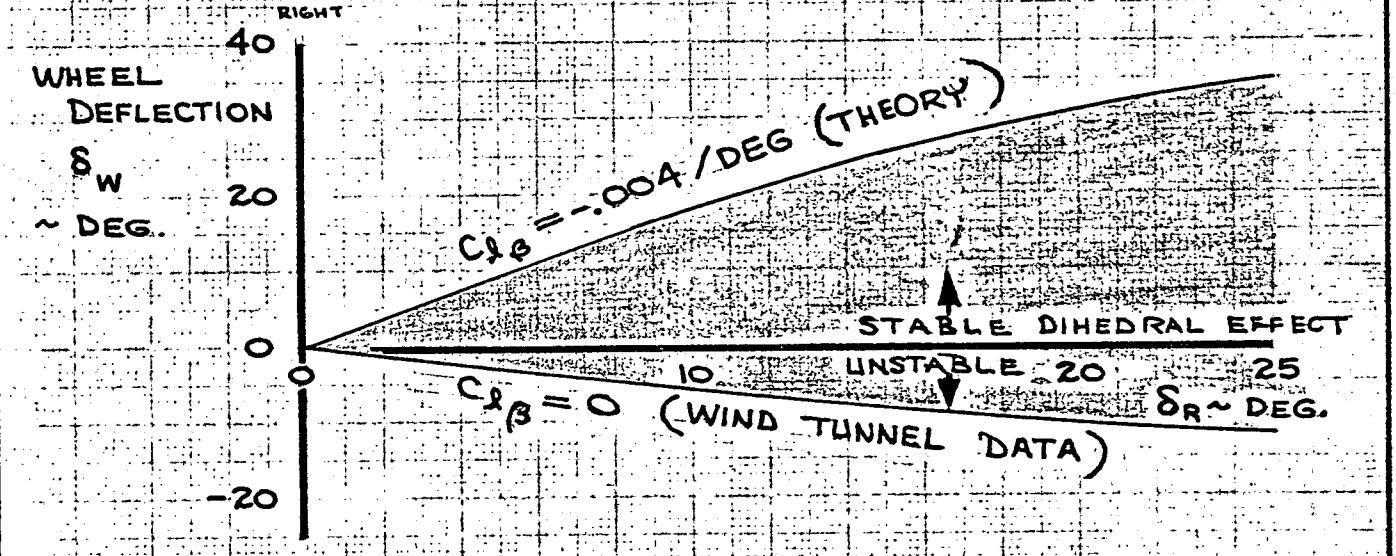

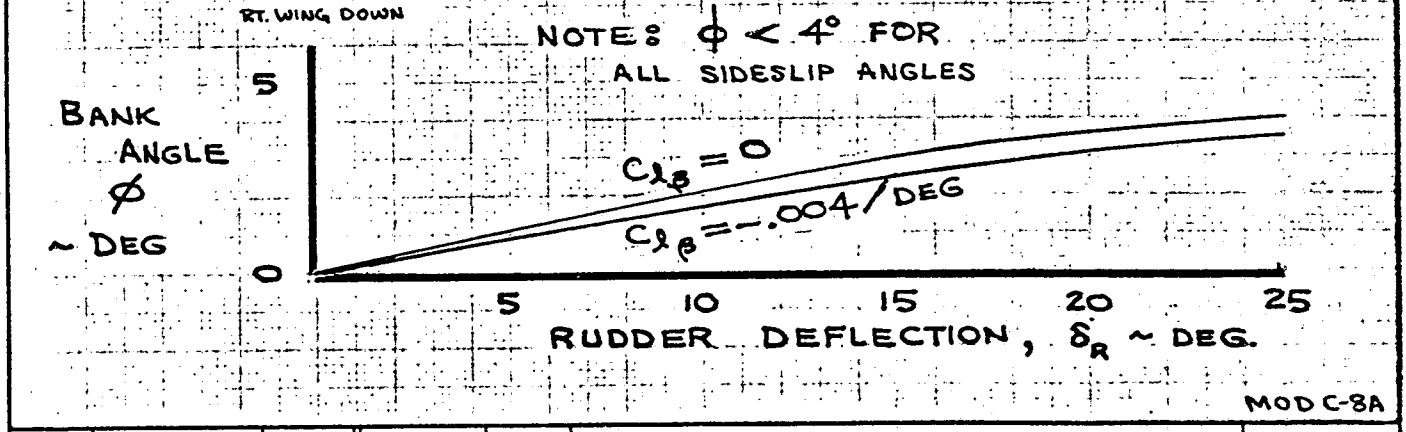

MOD C-8A

CALC	SPITZER	11-3-70	REVISED	DATE	STATIC LATERAL-DIRECTIONAL STABILITY AT LANDING APPROACH	FIG 4-13
CHECK						D6-40381
APR						
APR					THE BOEING COMPANY	PAGE 4.17
DWN	V. PAGE	2-7-72				

MAXIMUM SIDESLIP CAPABILITY AND CROSSWIND REQUIREMENT

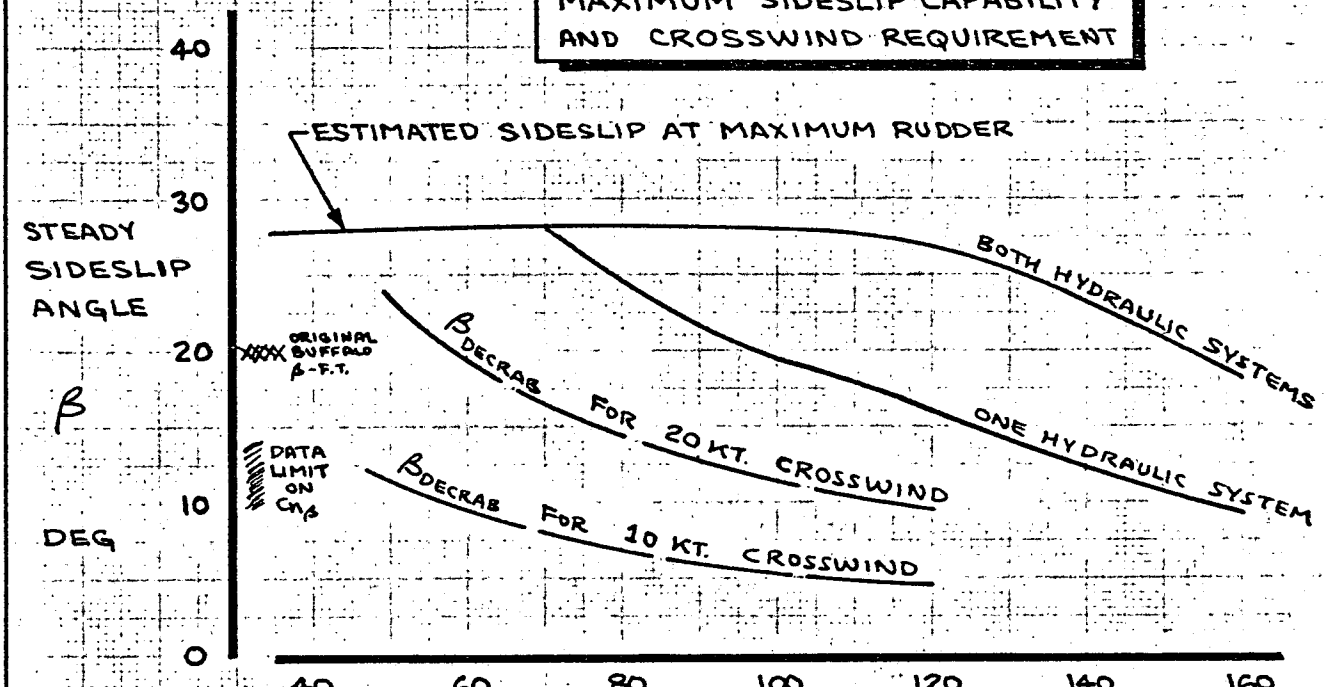

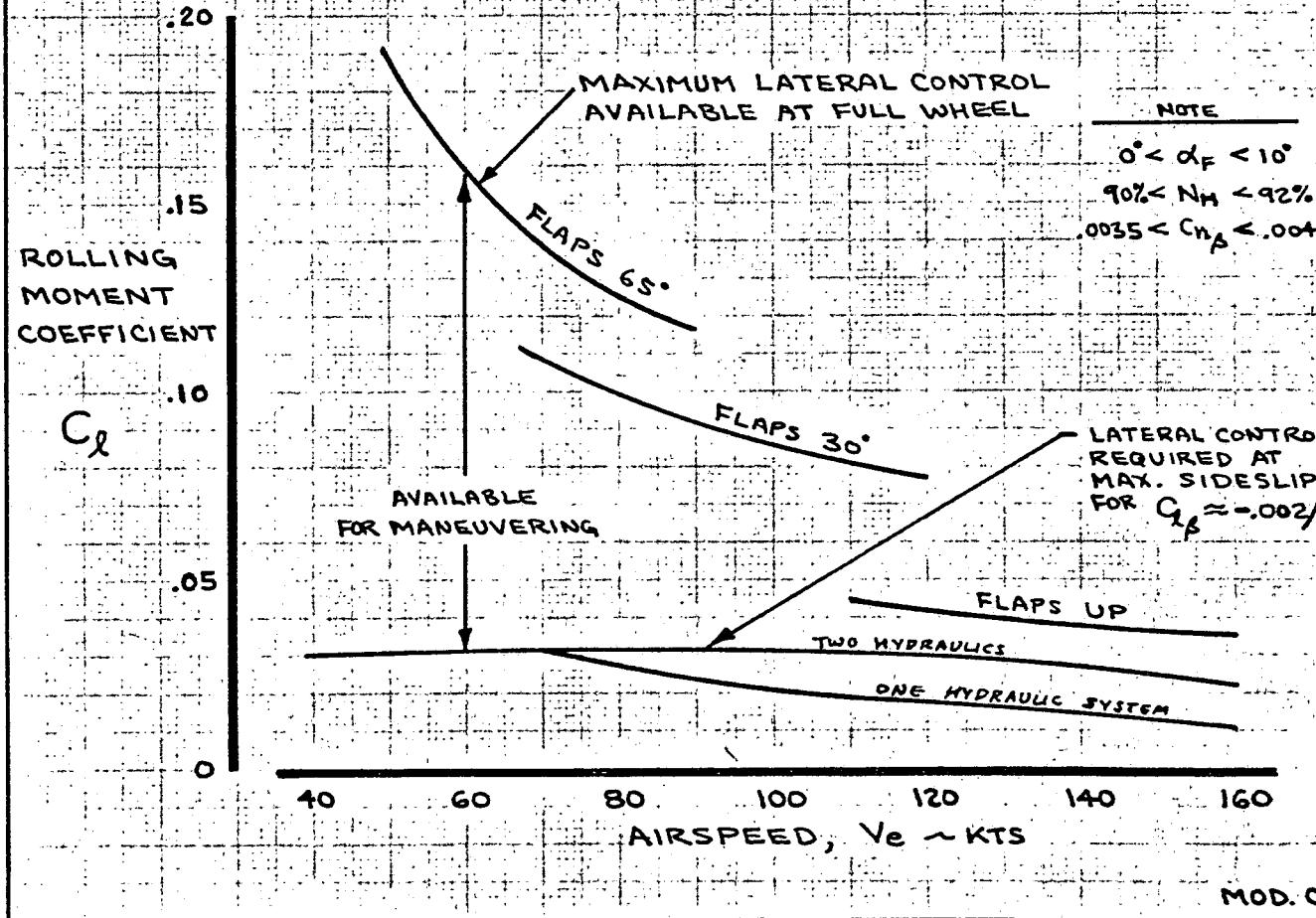

MOD. C-8A

CALC	SPITZER	2-3-72	REVISED	DATE	SIDESLIP CAPABILITY	FIG 4-14
CHECK						D6-40381
APR						
APR					THE BOEING COMPANY	PAGE 4.18

LATERAL CONTROL FOR FUEL UNBALANCE

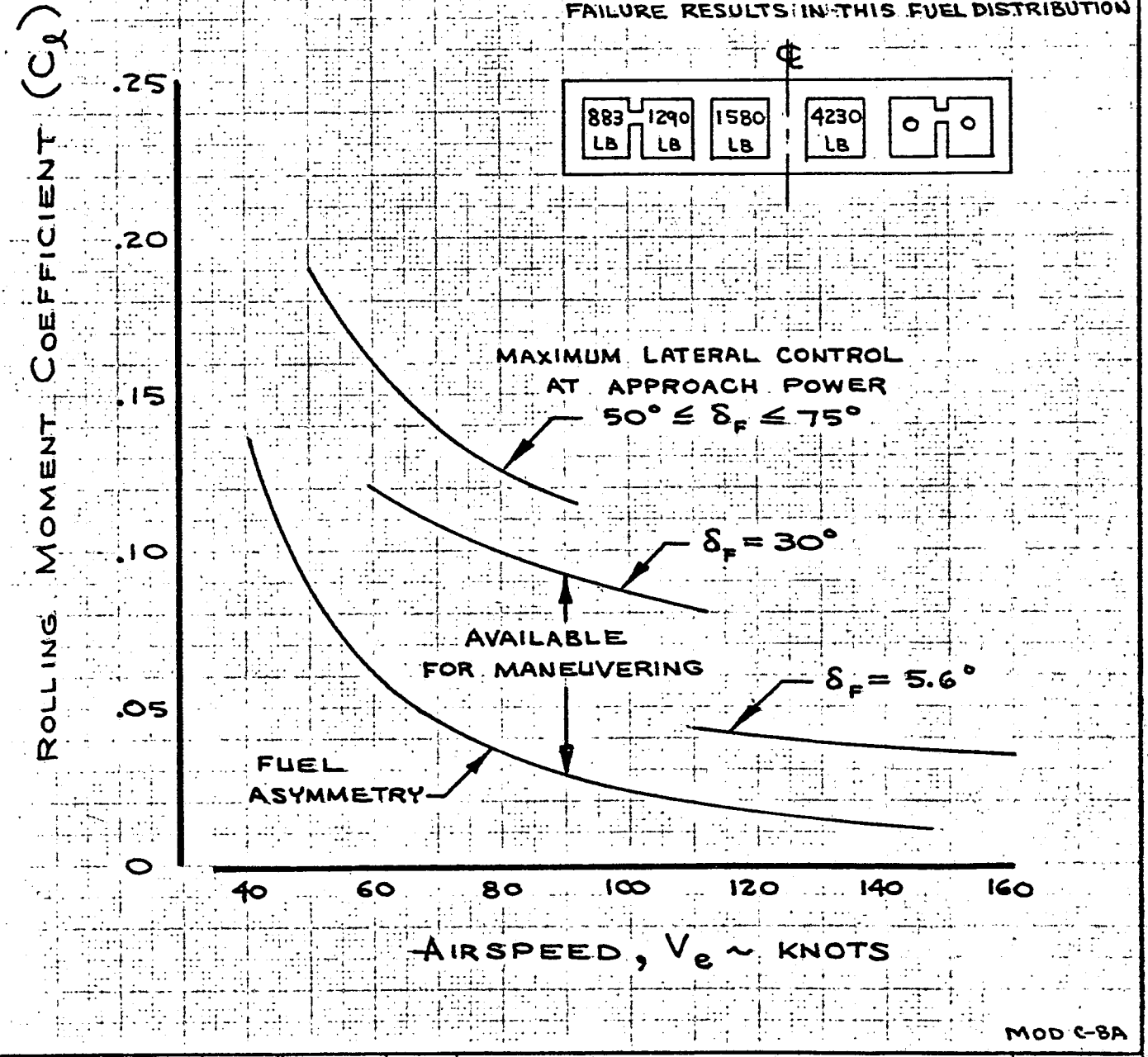

MOD C-8A

CALC	SPITZER	12-11-70	REVISED	DATE	FUEL UNBALANCE	FIG 4-15
CHECK			SPITZER	2-7-72		
APR						D6-40381
APR						
DWN	V. PAGEL	2-7-72			THE BOEING COMPANY	PAGE 4.19

4.3 Maneuvering Stability and Control

The Modified C-8A has satisfactory lateral and directional control power for maneuvering on the critical STOL landing approach. Control power was evaluated on the simulator using "S-turns" on landing approach with moderate turbulance levels. Figure 4-16 presents maximum rolling moment capability ($C_{\ell_{max}}$) for variations in speed, flap angle and power setting. Since surface effectiveness is related to blowing coefficient, $C_{\ell_{max}}$ changes significantly with speed and power. Superimposed on the figure are lines of constant roll acceleration at reduced roll inertia (Figure 4-17). Time required to achieve a $\phi = 30°$ bank angle is less than 2.5 sec with SAS-improved roll time constant. Bank angle in the first second will exceed $\phi_1 = 6°$ with SAS. Steady-state roll rate is in excess of 20 deg/sec even with some control power used by the SAS for roll damping. The Modified C-8A meets its lateral control design criteria.

Good lateral control sensitivity, $\ddot{\phi}/\delta_\omega$, was deemed most important by the pilots who flew the simulator. A number of changes were made in the course of the design cycle to improve the lateral control system. Figure 4-18 shows the progression. The trend to increase aerodynamic rolling moment for small wheel deflections was complemented by reductions in roll inertia (Figure 4-17). Pilot rating of lateral control sensitivity is shown in Figure 4-19. The current Modified C-8A design level is noted by the arrow. Lateral control sensitivity is now rated as satisfactory. (Evaluation of sensitivity levels is possible in flight test by the features noted in Figure 4-9).

Rudder control power is high. Figure 4-20 presents instantaneous yawing acceleration due to full rudder and heading angle change in 2.2 sec. The heading change maneuver was calculated including the effect of yaw damping from the SAS. At 60 kt approach the Modified C-8A meets the design criteria and has more than adequate control power for decrab on the crosswind landing.

Beyond normal maneuvering requirements the lateral and directional control systems must have sufficient capability to handle certain failure modes.

Hydraulic System Failures

The lateral control system is powered by two hydraulic systems. Part of the control capability is lost following a single hydraulic system failure. Figure 4-21 shows this control degradation. The condition of spoiler hydraulics failed was evaluated in the NASA-Ames piloted simulation and found acceptable. If both hydraulic systems fail, the system reverts to direct manual control over the ailerons. In this instance the pilot must also overcome aerodynamic hinge moments on the ailerons through the unpowered central power control unit. Figure 4-22 shows the control power available from the ailerons at a wheel force of F_w = 65 lbs. Lateral acceleration and roll rate capability exceeds the criteria for emergency levels at 85 to 100 knots. Manual reversion (elevator and aileron control) was tested in the simulator and found flyable although some rudder control, which is unavailable, was considered desirable. The wheel force/aileron gearing with control wheel deflection is also illustrated in Figure 4-22. High friction levels and deadspaces produced by the central power control unit valve travel result in non-uniform control characteristics and poor centering. A similar system exists on the 737 and has been accepted for double hydraulic failure conditions.

Lateral Control System Cable Jams

The lateral control system is designed with pogo springs, shear-out points and dual control cables in the wing. FAR.XX.671 requires control over jams for control surfaces in a "normal" position. Potential jams of this sort would result in one spoiler jammed down ($\delta sp = 0°$) or one choke jammed down ($\delta CH = 0\%$) or both ailerons jammed in their drooped position ($\delta a = \delta a_{DROOP}$). Because the

AD 1540D

lateral control system is composed of multiple surfaces, a jam at neutral poses no significant problem. In fact, in most cases, a single surface can be jammed all the way up to its maximum deflection without running out of counteracting control power. (All flight controls have a number of single-load-path elements, which could cause loss of the airplane upon failure. Original Buffalo components, i.e., single cable runs, are simple and straight forward in design. The remote chance of such failures has made the risk acceptable).

Flap Asymmetry

Failures in the flap system which could produce asymmetric flap conditions are generally remote. The flap system is rotated by two hydraulic actuators on each panel. Hydraulic power is supplied by both systems alternately to each actuator so that each flap panel has dual power source. Position control is through a single valve in the body (dual hydraulic). Outboard and inboard flap panels are mechanically tied together, and a large torque tube extends through the fuselage to interconnect the flaps across the airplane. In normal operation the flaps and aileron droop move uniformly with the structural interconnections evening out any differences in airloads. It is conceivable that the flap interconnect between inboard and outboard panels could break. Position feedback to the flap control valve comes from the inboard flap. Thus, the outboard flap may not hold exact position, due to uneven airloads, even though the actuators hold the same pressure as those of the inboard flap. The extent of the variation in flap loads (perhaps caused by sideslip, rolling maneuvers, spanwise location, etc.) is unknown but not expected to produce differences in deflection greater than $\delta_F \approx 5°$ to $10°$. Rolling moment due to asymmetric outboard flap and adjacent aileron have been estimated (Figure 4-23). The most critical condition exists

at flaps up where lateral control power is lower. As shown in the figure, sufficient lateral control does exist to counteract the asymmetry.

Duct Burst

Failures in the air ducting system can have significant effects on lift distribution across the wing. Rolling moment is produced which must be overcome by lateral control. Figure 4-24 shows the effect of a complete failure in the air duct running straight back from the engine to the flap. Engine blowing on the remaining fuselage crossover duct has been assumed unchanged. This burst duct condition can be controlled.

Figure 4-25 shows a corresponding burst in the crossover duct as it passes through the body. Full lateral control is required to balance the rolling moment with nothing left over for maneuvering. This condition was simulated in the NASA-Ames study and found unacceptable. The pilot was able to dive and increase speed to gain control; however, considerable altitude was lost in the maneuver. Figure 4-26 shows that increasing the emergency power to the engine feeding the good duct tends to balance out the condition shown in Figure 4-25. Shutting off the engine connected to the failed duct also alleviates the problem. Because a burst duct is a marginal control situation, a warning system based on duct pressure indication has been installed on the airplane. The pilot will have indication of loss in duct integrity and will be able to shut down the appropriate engine. In addition, the materials used in duct fabrication have been chosen for safe fatigue and crack growth properties. Duct burst is considered a remote situation.

SAS System Failures

The "single channel" stability augmentation system is subject to hardover and oscillatory failures which actuate the flight controls. SAS authority limits are set high enough for satisfactory system operation yet low enough for effective recovery in the event of failures. Current design limits are $19°\delta_w$ and $5°\delta_r$. Pilots were subjected to SAS failures in the simulator (Reference 21) at $25°\delta_w$ and $12.5°\delta_r$ authority. Recovery from single axis hardover failures, either lateral or directional, was no problem at the approach (60 kts) flight condition, with a successful landing made in all cases. (The airplane was flyable to a safe landing with total SAS failure.) Comparable results were found with hardovers during takeoff. Oscillatory failures also posed no recovery problem. A simultaneous hardover in the lateral and directional axes during the approach (possible with variable stability mode) was felt to be the most difficult failure, but still considered acceptable. Bank angle and sideslip upset transients did not exceed 12.5°. Based on the severity of rudder hardovers at higher speeds, the current SAS system automatically switches off above 100 kts. Lateral and directional control power are adequate for overriding the SAS.

With all of the listed failure conditions, flying qualities are degraded, particularly in the STOL regime. If possible, it is best not to enter the STOL flight regime after a system failure. It is deemed prudent that following any first system malfunction the pilot elect to return to base for a conventional landing. The best all-round compromise condition is FLAPS 30° and V_{APP} = 90 kts. At this condition longitudinal characteristics are stable and

well-behaved (Section 3.2) and approach lift coefficient is no higher than conventional transports. Lateral-directional handling qualities should be adequate. The 90 kt landing speed is still low enough to pose no problem to brakes and gear. Thus, flight safety is enhanced if this procedure is followed.

MAXIMUM ROLLING MOMENT CAPABILITY

- MAX. WHEEL INPUT @ $\delta_W = 75°$
- BOTH ENGINES AND HYDRAULIC SYSTEMS OPERATING
- $-5° < \alpha_F < 10°$
- $\ddot{\phi}$ CALC. AT $\dot{\phi} = 0$
- $I_{XX} = 260000$ SLUG-FT^2 (40000LB)

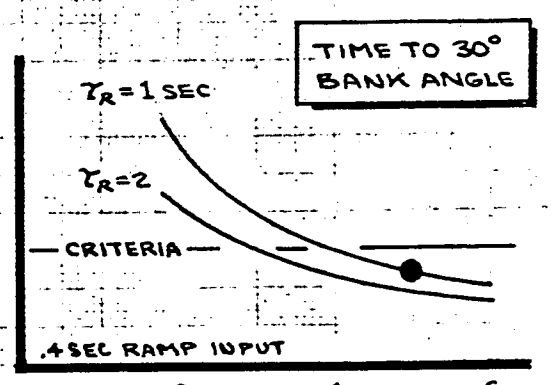

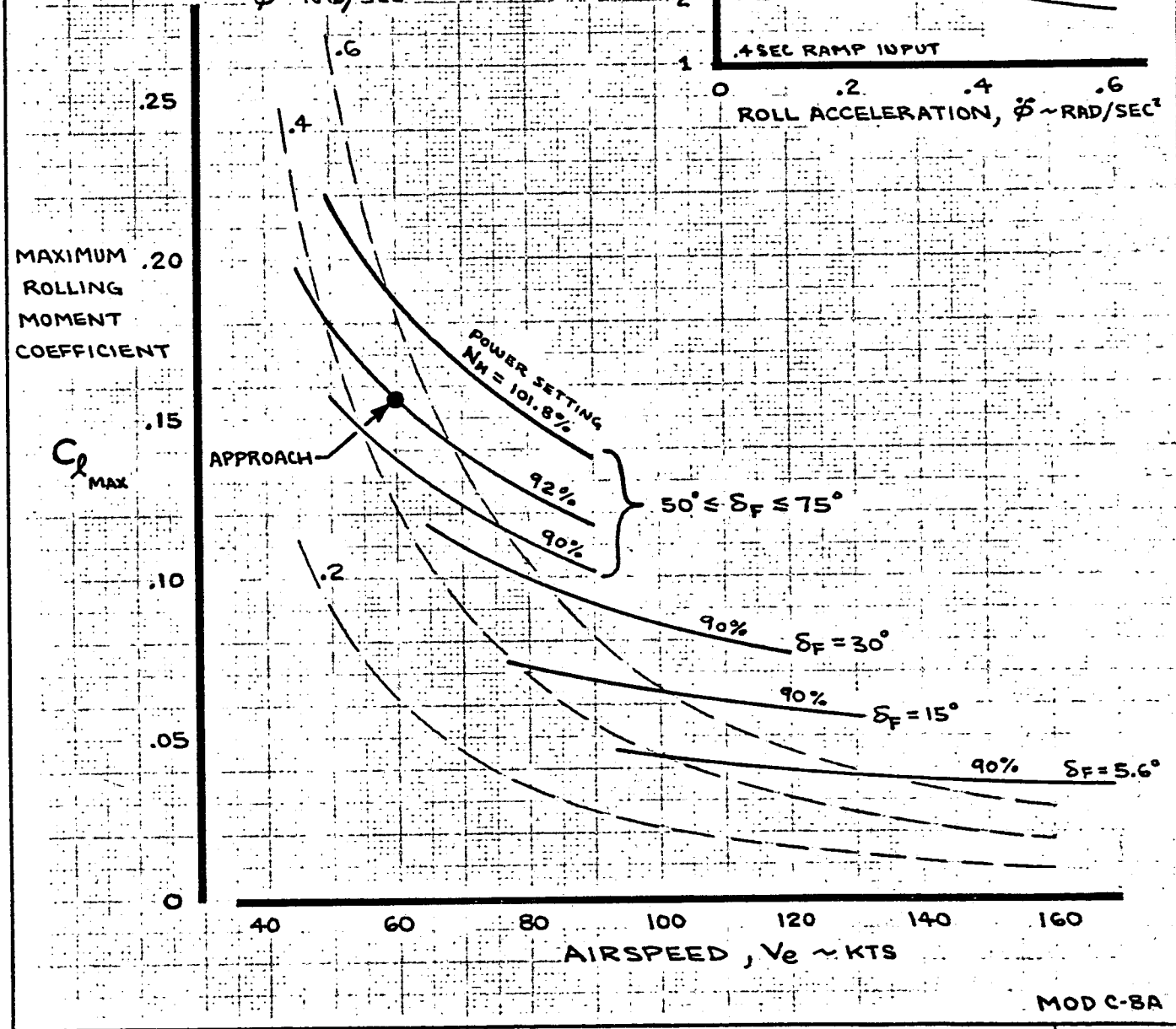

MOD C-8A

CALC	SPITZER	9-29-70	REVISED	DATE	MAXIMUM ROLLING MOMENT LATERAL MANEUVERING CAPABILITY
CHECK			SPITZER	2-8-72	
APR					
APR					
					THE BOEING COMPANY

FIG 4-16
D6-40381
PAGE 4.26

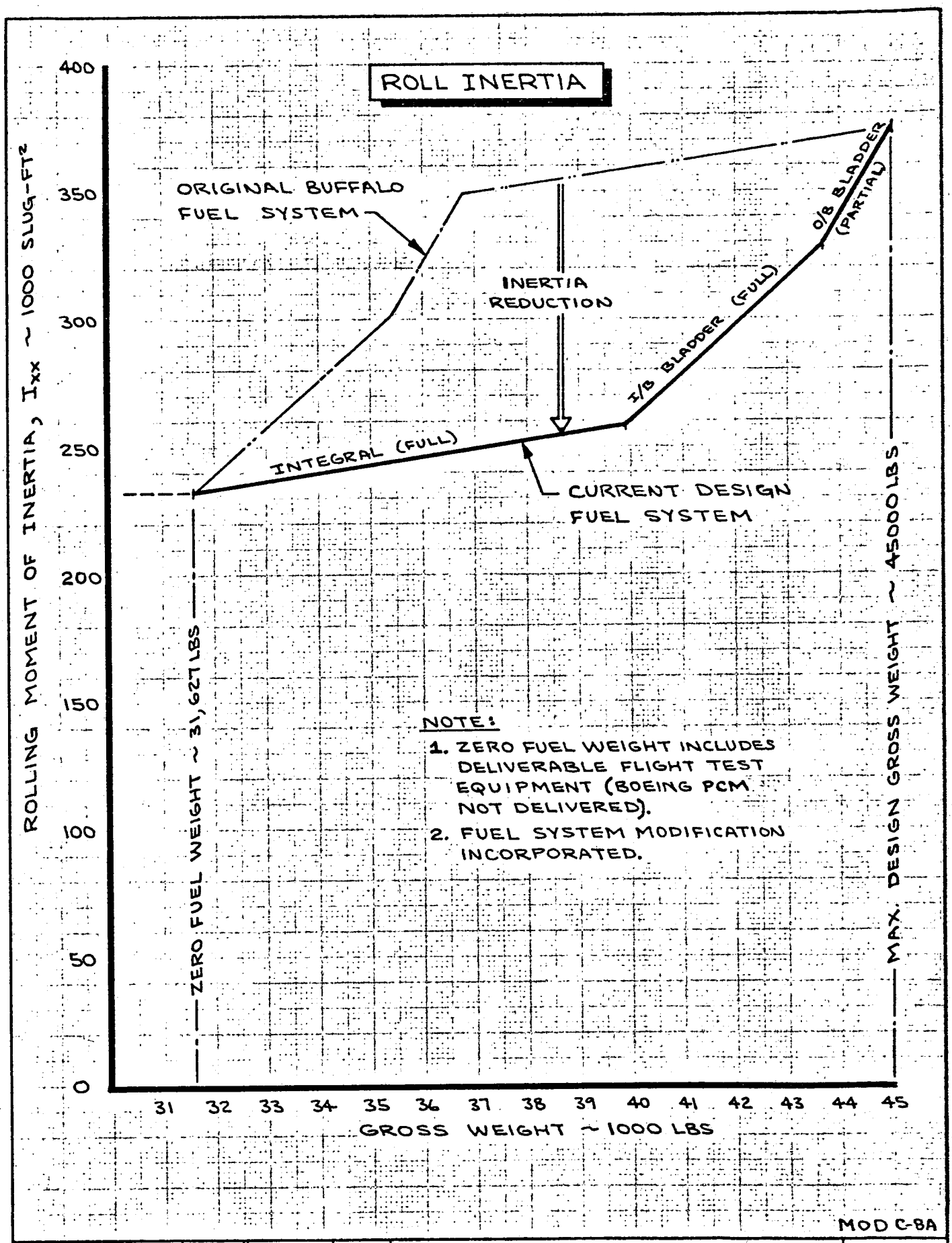

MOD C-8A

CALC	SPITZER	4-1-71	REVISED	DATE	REDUCED ROLL INERTIA WITH FUEL SYSTEM MODIFICATION	FIG 4-17
CHECK	GRIFFITHS	4-1-71	SPITZER	1-15-72		D6-40381
APR						
APR					THE BOEING COMPANY	PAGE 4.27

MOD. C-8A

CALC	SPITZER	4-6-71	REVISED	DATE	LANDING APPROACH ROLLING MOMENT COMPARISON
CHECK			SPITZER	2-7-72	
APR					
APR					

FIG 4-18

D6-40381

THE BOEING COMPANY

	CALC	CHECK	APR
	SPITZER	12-11-70	APR

REVISED	DATE

THE BOEING COMPANY

LATERAL CONTROL SENSITIVITY AT LANDING APPROACH

FIG 4-19

D6-40381

PAGE 4.29

MOD C-8A

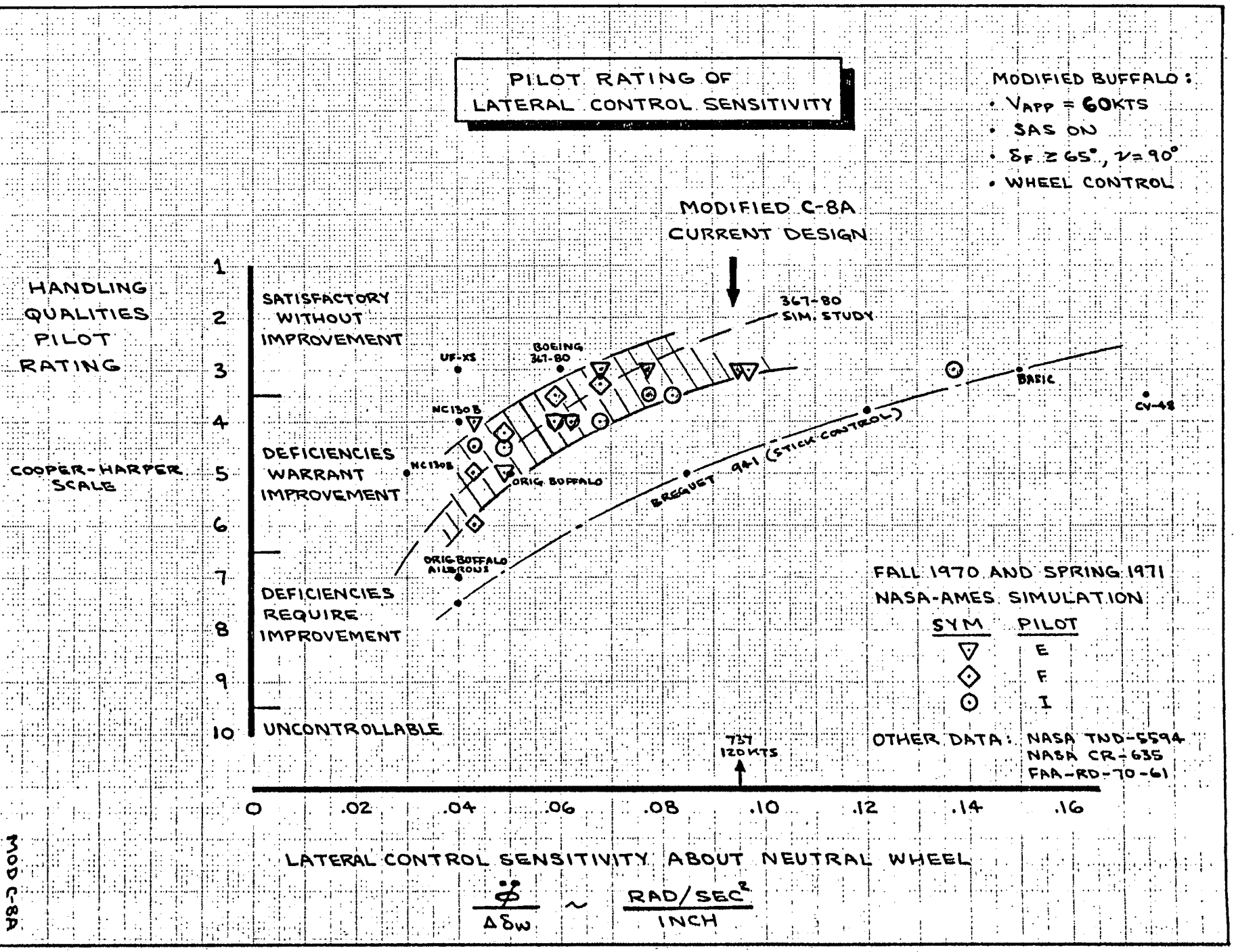

RUDDER EFFECTIVENESS AT LANDING APPROACH

- FLAPS 65
- 40000 LBS
- $\phi = 0°$
- $\dot{\phi} = 0$ (FOR $\ddot{\psi}$)
- SAS ON

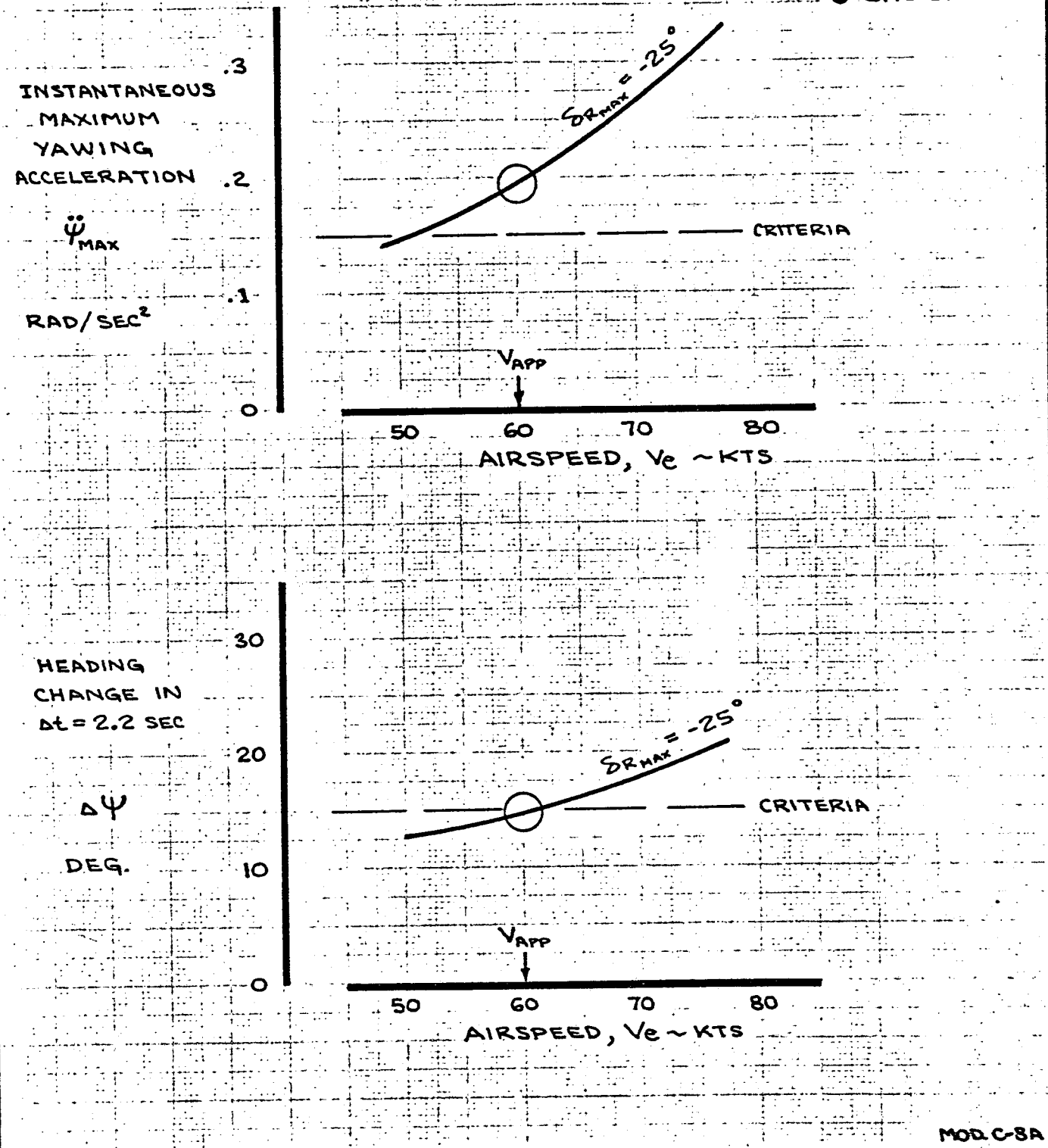

MOD C-8A

CALC	SPITZER	1-31-72	REVISED	DATE	YAWING MANEUVER CAPABILITY
CHECK					
APR					
APR					
					THE BOEING COMPANY

FIG 4-20

D6-40381

PAGE 4.30

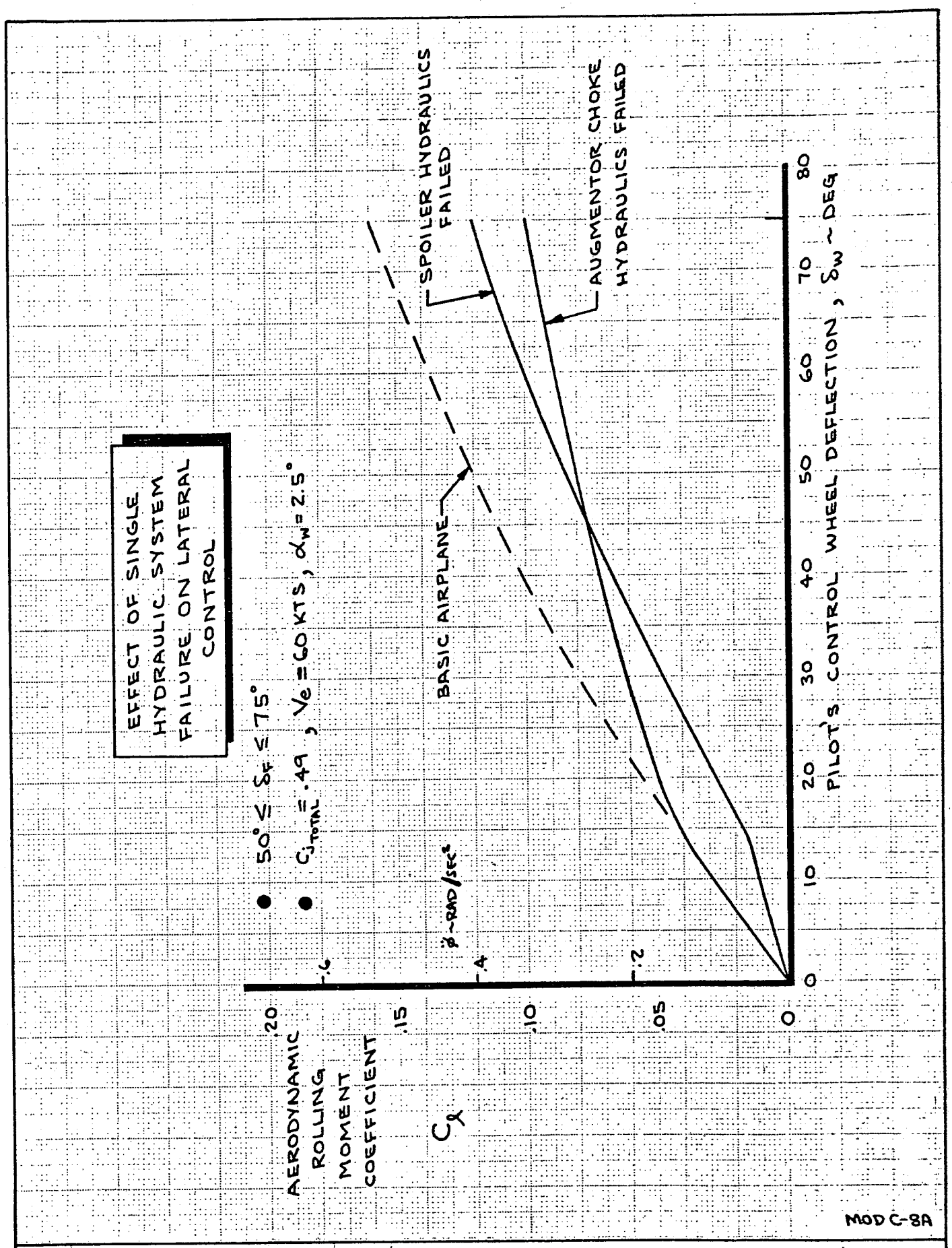

CALC	SPITZER	12-12-70	REVISED	DATE	LATERAL CONTROL CHARACTERISTICS AFTER SINGLE HYDRAULIC FAILURE
CHECK					
APR					
APR					
					THE BOEING COMPANY

FIG 4-21

D6-40381

PAGE 4.31

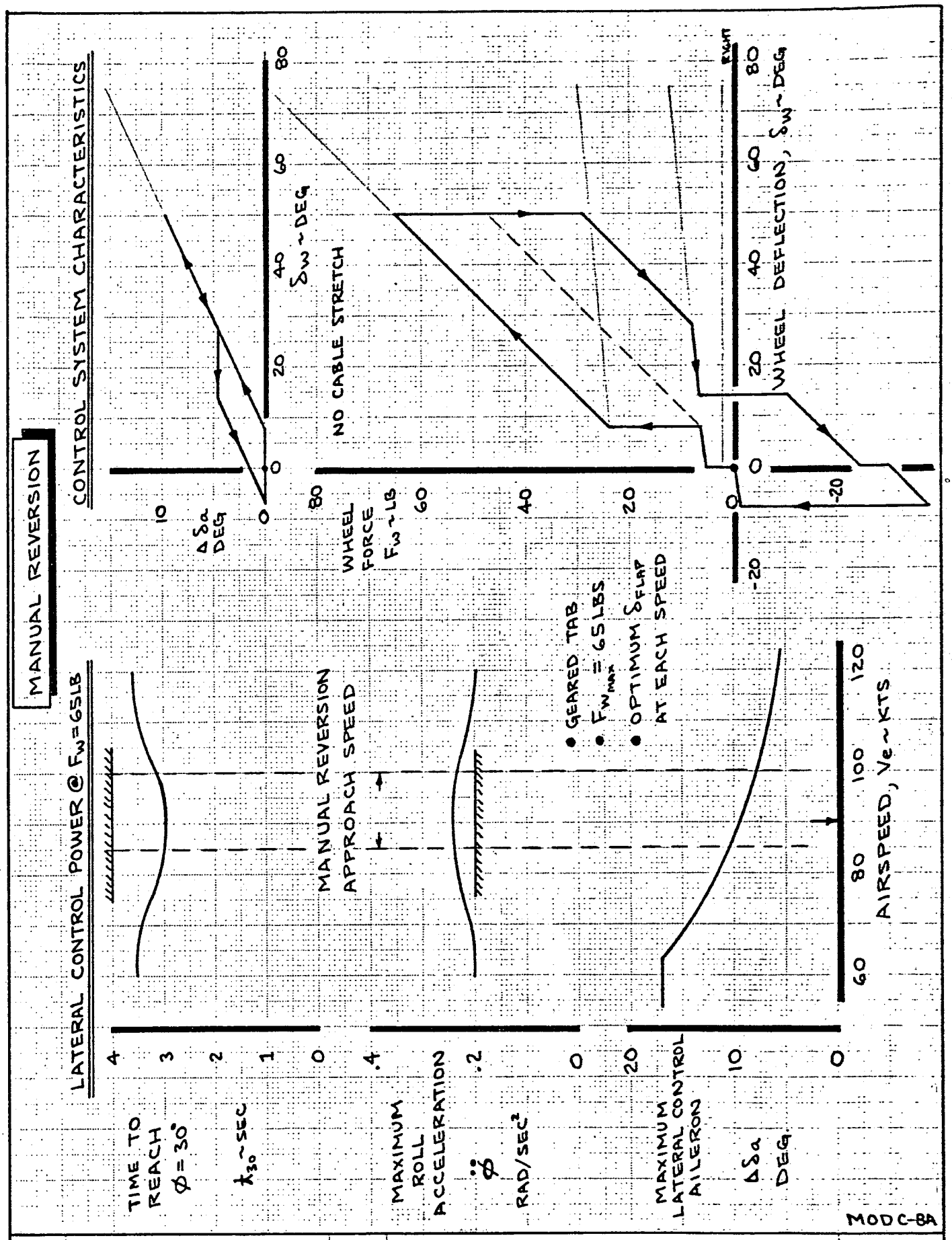

CALC	SPITZER	12-12-70	REVISED	DATE	LATERAL CONTROL CHARACTERISTICS AFTER TWO HYDRAULIC FAILURES	FIG 4-22
CHECK						D6-40381
APR					THE BOEING COMPANY	PAGE 4.32
APR						

ROLLING MOMENT DUE TO ASYMMETRIC FLAPS

- OUTBOARD ASYMMETRIC FLAP INCLUDES ASYMMETRIC DROOP OF ADJACENT AILERON. COMPUTED FOR $0° \leq \delta_F \leq 50°$ AT TAKEOFF POWER BLOWING COEFFICIENTS.
- AVAILABLE LATERAL CONTROL AT APPROACH POWER SETTING

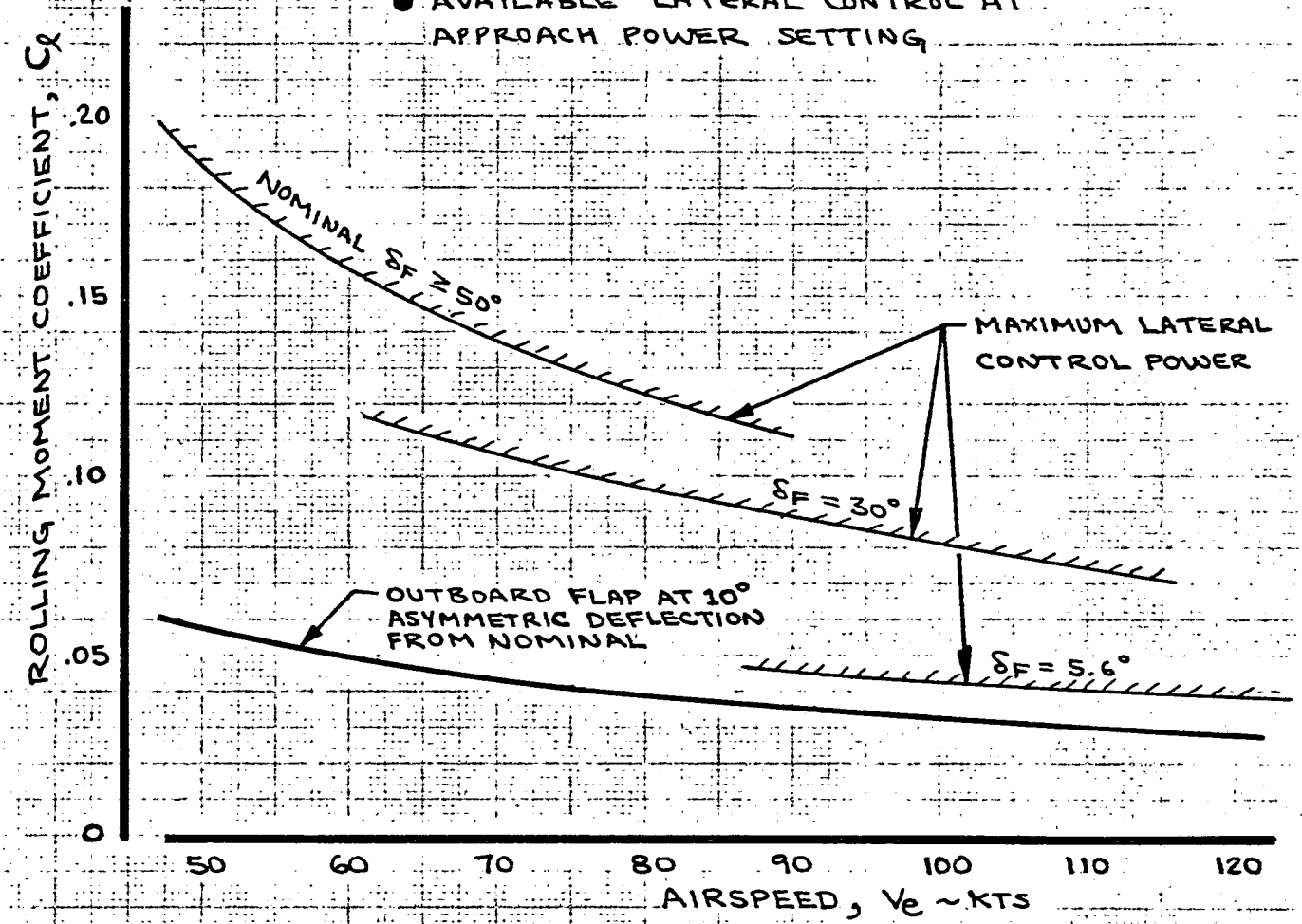

MOD. C-8A

CALC	SPITZER	1-13-72	REVISED	DATE	ROLLING MOMENT DUE TO OUTBOARD FLAP ASYMMETRY	FIG 4-23
CHECK						D6-40381
APR					THE BOEING COMPANY	PAGE 4.33
APR						

ROLLING MOMENT DUE TO FAILURE IN "40%" STRAIGHT-BACK AIR DUCT BOTH ENGINES AT APPROACH POWER

T_{HOT} = 3500 LB/ENG
T_{COLD} = 2600 LB/ENG
N_H = 11500 RPM

$50° \leq \delta_F \leq 75°$
$\delta_{\alpha\ DROOP} = 30°$
$\alpha_W = 6°$

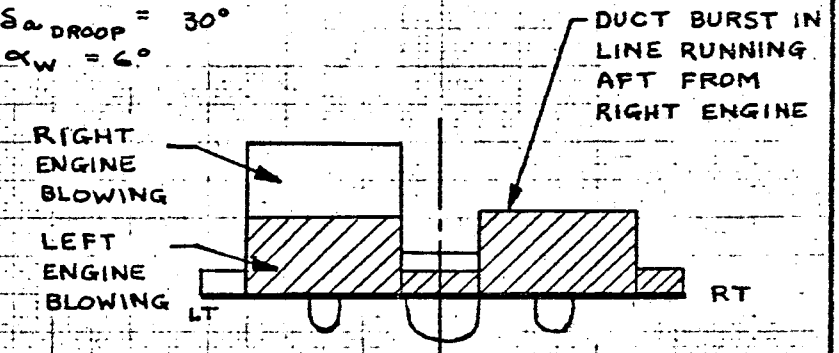

MOD. C-8A

CALC	SPITZER	12-11-70	REVISED	DATE	ROLLING MOMENT DUE TO FAILURE IN "STRAIGHT BACK" DUCT AT APPROACH POWER SETTING	FIG 4-24
CHECK						D6-40381
APR					THE BOEING COMPANY	PAGE 4.34
APR						

ROLLING MOMENT DUE TO FAILURE IN "60%" CROSSOVER AIR DUCT BOTH ENGINES AT APPROACH POWER

$50° \leq \delta_F \leq 75°$

$\delta_{a_{DROOP}} = 30°$

$\alpha_W = 6°$

$T_{HOT} = 3500$ LB/ENG

$T_{COLD} = 2600$ LB/ENG

$N_H \approx 11500$ RPM

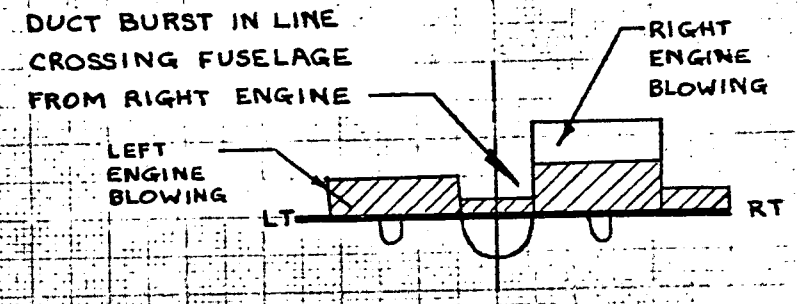

MOD. C-8A

CALC	SPITZER	12-11-70	REVISED	DATE	ROLLING MOMENT DUE TO FAILURE IN "CROSSOVER" DUCT AT APPROACH POWER SETTING	FIG 4-25
CHECK						D6-40381
APR					THE BOEING COMPANY	PAGE 4.35
APR						

ROLLING MOMENT DUE TO FAILURE IN "60%" CROSSOVER AIR DUCT COMBINED WITH ASYMMETRIC ENGINE POWER

$50° \leq \delta_F \leq 75°$

$\delta_{a_{DROOP}} = 30°$

$\alpha_W = 6°$

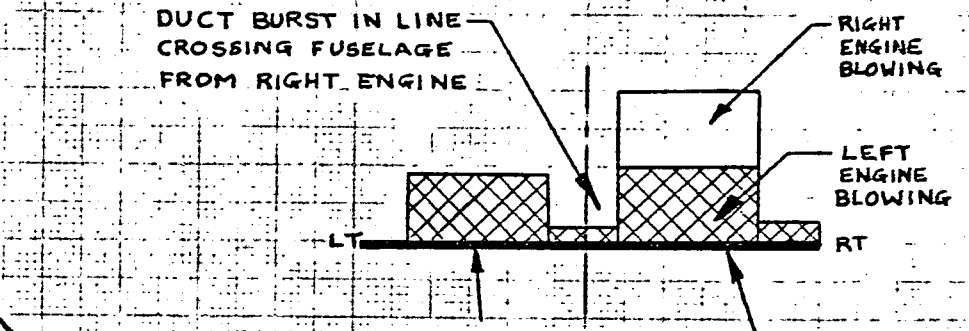

T_{HOT} = 7000 LB EMERENCY @ 12500 RPM

T_{HOT} = 3500 LB APPROACH @ 11500 RPM

ROLLING MOMENT COEFFICIENT C_l

.30 .25 .20 .15 .10 .05 0

MAXIMUM ROLL CONTROL AVAIL. TO COUNTERACT BURST DUCT

AVAILABLE FOR MANEUVERING

NET ROLLING MOMENT FROM ASYMMETRIC LIFT DUE TO BURST DUCT & ASYMMETRIC POWER SETTINGS

30 40 50 60 70 80 90

AIRSPEED, V_e ~ KTS

MOD. C-8A

CALC	SPITZER	12-11-70	REVISED	DATE	ROLLING MOMENT DUE TO FAILED "CROSSOVER" DUCT COMBINED WITH ASYMMETRIC POWER SETTING
CHECK					
APR					
APR					
					THE BOEING COMPANY

FIG 4-26

D6-40381

PAGE 4.36

4.4 Dynamic Stability and Control

Lateral-directional dynamic stability characteristics of the Modified C-8A degenerate in the powered-lift STOL regime. By virtue of low flight speed small bank angles generate large turning rates. Reduced flight speed also reduces the aerodynamic "spring" and "damping" terms relative to mass and inertia. Hence frequency of oscillation becomes lower, and the airplane tends to wander in heading due to reduced directional "stiffness". Damping ratio would perhaps increase if it were not for cross-coupling effects. High lift levels on the wing produce large, adverse levels of "rolling moment due to yaw rate" and "yawing moment due to roll rate". Roll damping itself degenerates and roll mode time constant increases. Lack of dihedral effect produces degraded spiral stability causing the airplane to "roll off" in a very few seconds.

Unaugmented Airplane

Figure 4-27 presents unaugmented airplane dynamic characteristics at STOL and conventional flight points. Cruise flight is not anticipated to be a problem area. Dutch roll damping and period are acceptable, spiral stability is neutral, and roll mode time constant is satisfactory. Piloted operation at speeds above 100 knots, without SAS, was rated acceptable in the simulator. Basic airplane dynamics at conventional landing approach (Flaps 30°, 90 kts) is seen to be acceptable as well.

STOL operation, both takeoff and landing, is characterized by long dutch roll period and long roll mode time constant, making precise flight path control difficult. If $C_{l_\beta} = 0$, as expected, dutch roll damping ratio will be acceptable, however, spiral time-to-double at T_2 = 3 to 4 seconds is very short.

Continuous and excessive pilot attention is required to keep the airplane from rolling off. At the other extreme, if C_{l_β} = -.004/deg, spiral stability becomes tolerable but dutch roll damping degenerates. Characteristic period and damping is only part of the problem; typical flight maneuvering, such as turn entry, becomes a severe problem. Figure 4-28 shows the airplane response to a step wheel input without SAS and with C_{l_β} = -.004/deg. The aerodynamic cross coupling induces large sideslip angles in the turn entry making coordination almost impossible (typically, $\Delta\beta/\Delta\phi$ =.65). The heading response lag is over 4 seconds, an unacceptable situation. With C_{l_β} = 0 the spiral mode is so unstable that airplane response to this type of step input is a complete rollover. Keeping the wings level requires almost 100% lateral control, particularly in moderate turbulence. In the simulator the pilots were able to fly the airplane to a STOL landing without SAS. Pilot rating ranged from 6.0 to 9.0 on the Cooper-Harper scale. Clearly, SAS-off flight in the STOL regime is for emergencies only.

Augmented Airplane

Early in the program it was decided that a lateral-directional stability augmentation system was mandatory for good handling qualities. The two mode SAS resulted: "Normal Mode" for handling qualities improvement and "Variable Stability Mode" for research. Performance objectives used in the control law development were as follows:

- Improve spiral stability to time to double or half amplitude greater than 20 sec.

- Maintain well-damped dutch roll mode with frequency greater than 0.5 rad/sec (Period < 12.5 sec).

AD 1546D

- Reduce the roll mode time constant to $\tau_R < 1.0$ sec.
- Provide turn coordination with ratio of peak sideslip to bank angle developed during rapid turn entry at $\frac{\Delta\beta}{\Delta\phi} < .3$ and heading delay less than 2 sec.

Figure 4-29 shows the lateral axis stability augmentation system. With flaps down, roll rate and yaw rate feedback to the lateral controls are used to modify the free airplane roll and spiral mode. Two discrete gains are provided for the roll rate feedback which are automatically selected as a function of flap position. Gain programming with flaps is provided for a more uniform roll response at all flaps-down flight conditions. Spiral mode augmentation uses a fixed gain, as no set variation with flight condition was noted. Lateral axis stability augmentation is not necessary at cruise flight conditions. The system is therefore locked out for speeds (V_e) greater than 100 knots.

Directional axis stability augmentation system is shown in Figure 4-30. For flaps down, the directional augmentation system provides turn coordination and dutch roll damping.

For flap settings greater than 40°, roll rate and roll angle feedback to the rudder improve turn coordination by minimizing peak and steady-state sideslip angles during turns. To avoid excessive proverse yaw at higher airspeeds, the gains are automatically reduced for flap settings less than 40°.

A derived sideslip rate signal is used to increase the dutch roll damping. A fixed roll attitude gain in the sideslip rate derivation is satisfactory since steady-state signals are washed out by the bandpass filter. With flaps up, a yaw rate damper was considered desirable, although not mandatory. However,

simulator results showed rudder SAS hardovers induced unacceptably large transients at cruise. The directional system is therefore automatically disengaged for $V_e > 100$ knots.

The lateral-directional dynamics at STOL landing approach have been improved to satisfactory levels by the SAS. Figure 4-31 presents a comparison of response to a small wheel pulse with and without SAS. The augmented airplane is well-behaved at 60 knot STOL approach with stable dutch roll and spiral modes. Dutch roll damping is $\zeta \approx .5$ with lengthened period at $P \approx 12$ sec. Spiral mode is stable with time-to-half-amplitude at $T_{1/2} \doteq 10$ sec. Rapid turn entries conducted during the piloted simulator study are shown on Figure 4-32. Turn coordination characteristics satisfy the SAS design goals with acceptable sideslip and short heading lag. The augmented lateral-directional handling qualities were rated as satisfactory (pilot ratings of 3.5).

For handling qualities research the SAS has the variable stability mode of operation permitting a wide range of lateral-directional characteristics. Destabilizing feedback is possible. Figure 4-33 tabulates the range of feedback gains built into the system. The primary controlled parameter in most cases can be varied to generate very unstable characteristics. All combinations of feedback gains have not been analyzed to determine gain settings for neutral stability. Extreme caution is deemed prudent when using the variable stability mode.

AD 1546D

Flaps	V_e kts	α_F Deg	$\frac{W}{qs}$	C_j	C_{l_β} per deg	Dutch Roll Mode: ζ_{DR}	Dutch Roll Mode: ω_N cps	Dutch Roll Mode: $C_{1/2}$	Dutch Roll Mode: Damped Period P-sec	Dutch Roll Mode: Roll-to-Yaw Amplitude $\left\|\frac{\phi}{\beta}\right\|_{D.R.}$ Approx.	Spiral Mode: T_2 sec (Time-to-Double Amplitude)	Roll Mode: τ_R sec
Landing:												
65°	60 kts	0°	3.8	.50	0	.25	.14	.45	7.2	.6	3	1.65
65°	60 kts	0°	3.8	.50	-.004	.05	.14	2.2	7.2	2.0	13	1.25
Takeoff:												
30°	80 kts	2°	2.1	.38	0	.25	.15	.45	6.6	.7	4	1.40
30°	80 kts	2°	2.1	.38	-.004	.05	.15	2.2	6.6	2.0	10	1.10
Approach:												
30°	90 kts	7°	1.7	.13	-.0026	.15	.16	.73	6.0	2.0	17	.95
Cruise:												
Up	150 kts	3.6	.6	.04	-.0026	.15	.21	.73	4.8	2.0	Neutral	.77
Up	110 kts	10	1.1	.07	-.0026	.20	.17	.55	5.7	2.0	20	.83

MODIFIED C-8A UNAUGMENTED LATERAL-DIRECTIONAL DYNAMICS

(SAS OFF)

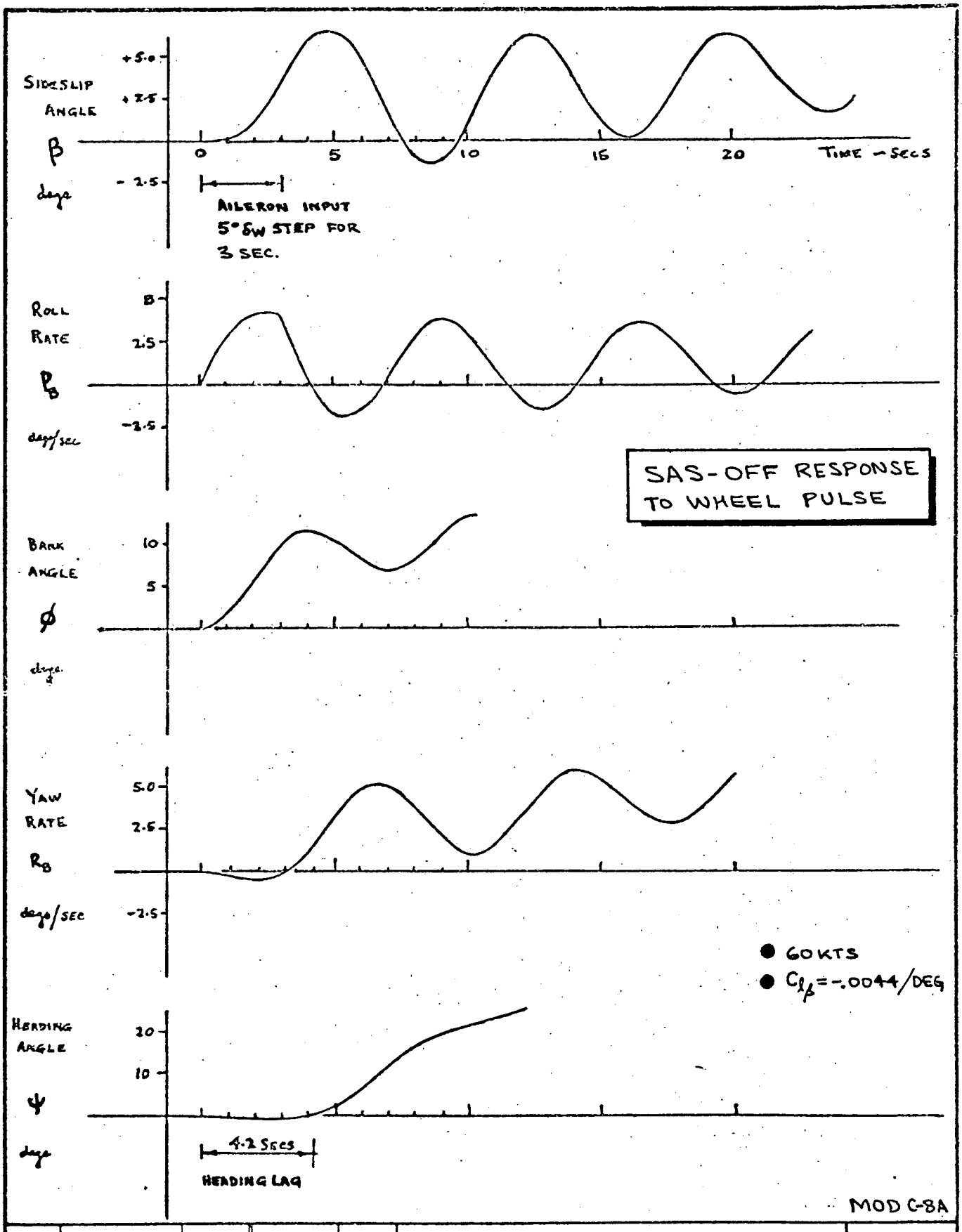

MOD C-8A

CALC	RUMSEY	1-11-71	REVISED	DATE	RESPONSE TO 5° WHEEL STEP FOR 3 SECS	FIG 4-28
CHECK			SPITZER	2-8-72	SAS OFF ~ C_{l_β} = -.0044/DEG	D6-40381
APPD	NARK	1-11-71			STOL LANDING CONFIGURATION	
APPD					THE BOEING COMPANY RENTON WASHINGTON	PAGE 4.42

TD 073 D-83

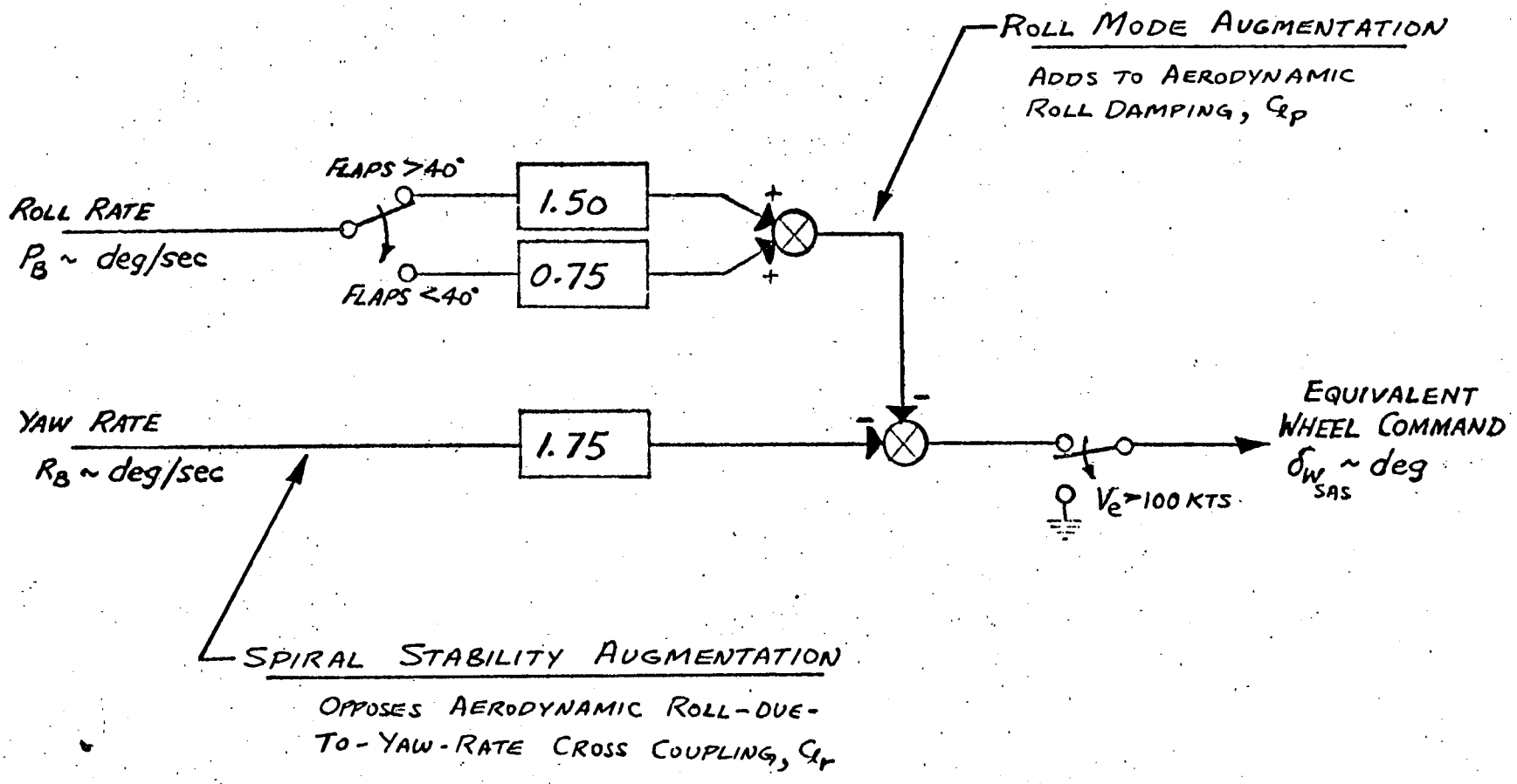

FIG 4-29

LATERAL AXIS STABILITY AUGMENTATION

"NORMAL MODE" MOD. C-8A

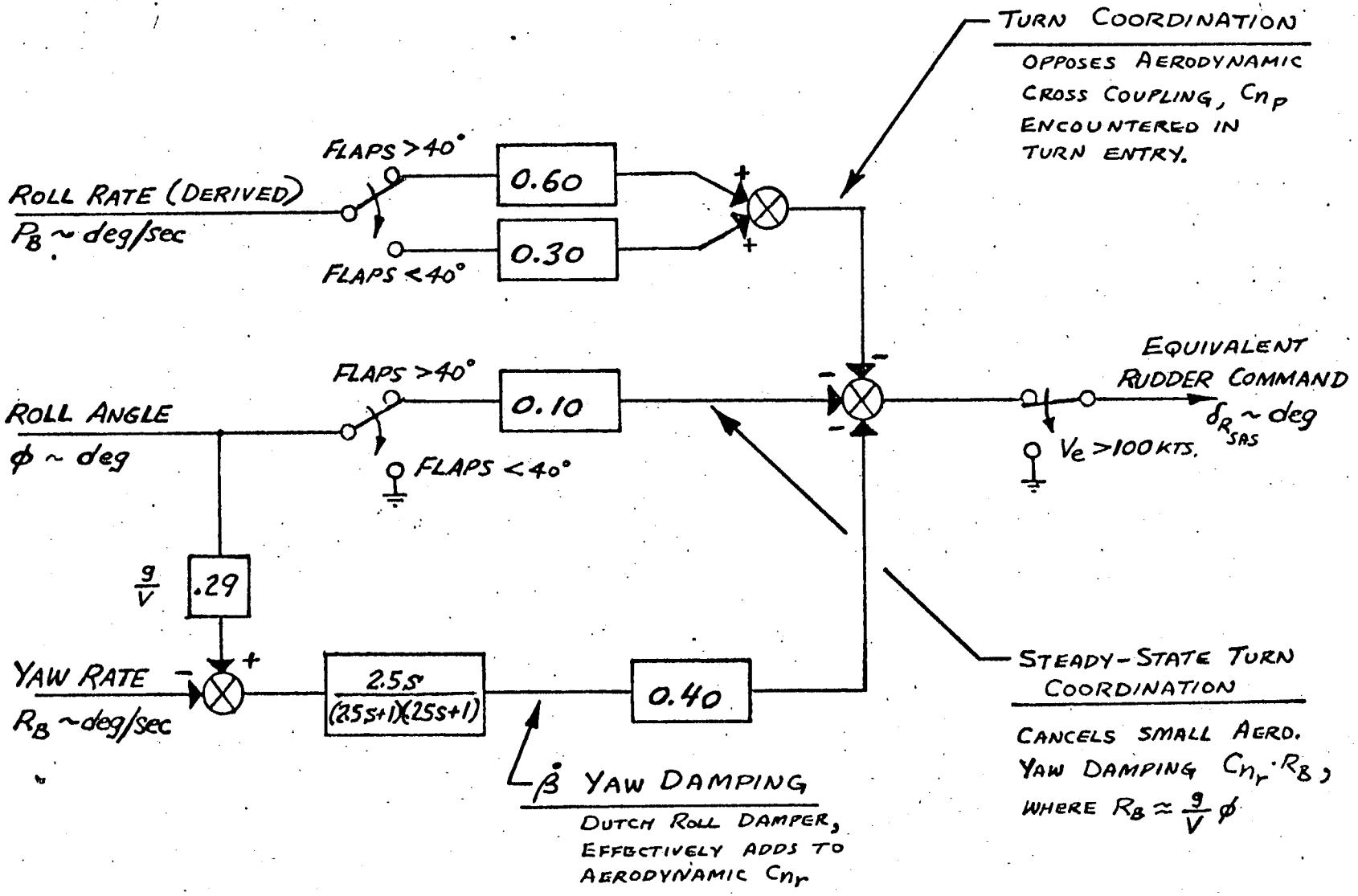

FIG 4-30

DIRECTIONAL AXIS STABILITY AUGMENTATION

"NORMAL MODE" MOD. C-8A

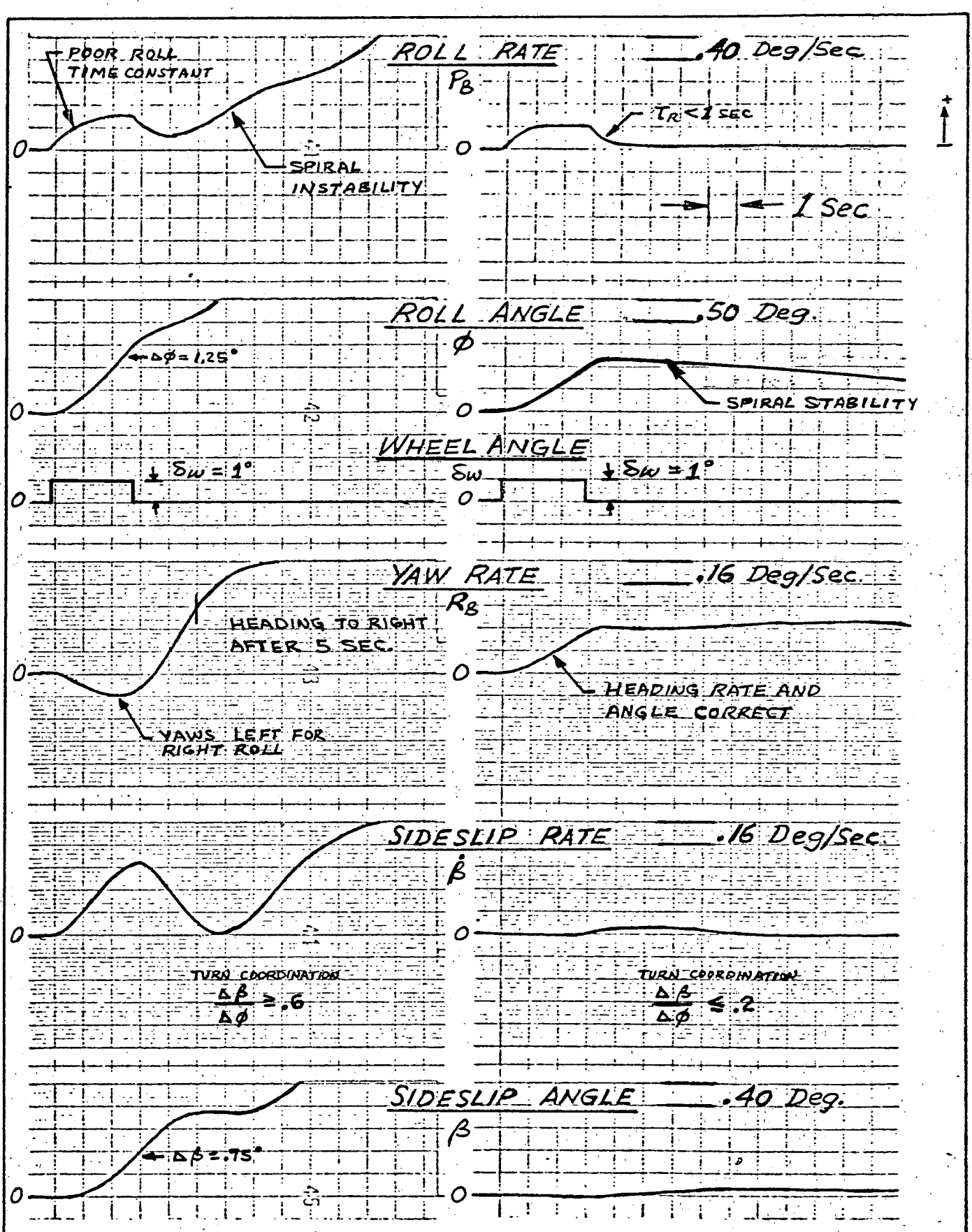

MOD. C-8A RESPONSE TO A 1° WHEEL PULSE (V_e=60 KTS., C_{ℓ_β}=.0)

SPITZER 2-16-72

FIG 4-31

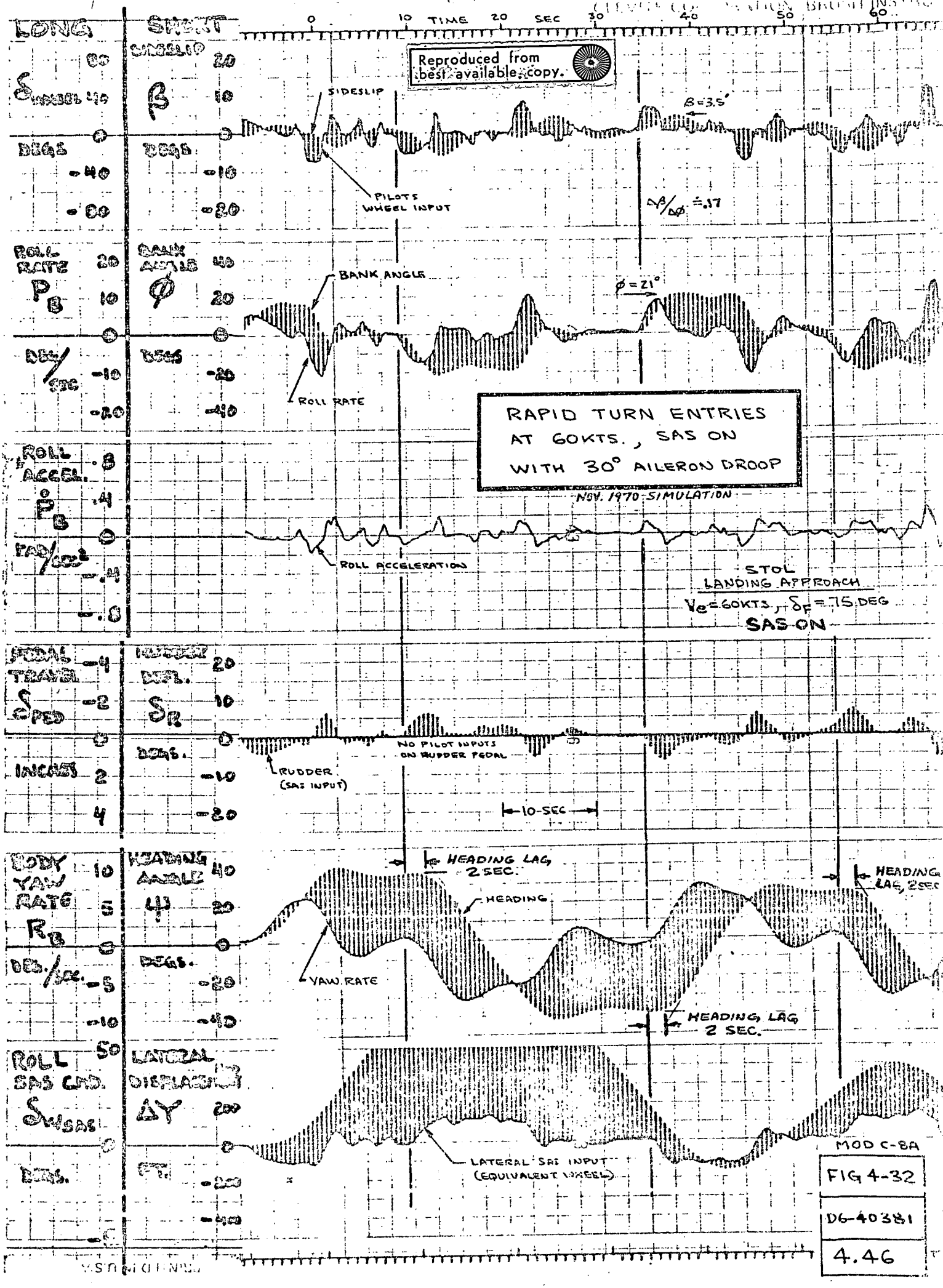
LONG
LAT
0
10 TIME 20 SEC 30 40 50 60
Reproduced from best available copy.
SIDESLIP
PILOTS WHEEL INPUT
B=3.5°
Δβ/Δφ =.17
BANK ANGLE
ROLL RATE
φ=21°
RAPID TURN ENTRIES AT 60KTS., SAS ON WITH 30° AILERON DROOP
NOV. 1970 SIMULATION
ROLL ACCELERATION
STOL LANDING APPROACH
Ve=60KTS, δF=75 DEG
SAS ON
NO PILOT INPUTS ON RUDDER PEDAL
RUDDER (SAS INPUT)
10-SEC
HEADING LAG 2 SEC.
HEADING
YAW RATE
HEADING LAG 2 SEC.
LATERAL SAS INPUT (EQUIVALENT WHEEL)
MOD C-8A
FIG 4-32
D6-40381
4.46

MODE	FEEDBACK LOOP	GAIN RANGE	PRIMARY CONTROLLED PARAMETER	RANGE (@V_e=60 KTS)
Dihedral Effect	$\beta \rightarrow \delta_W$	-2.7 → +2.7,.3	$C_{\ell\beta}$	-.38 → +.38 1/rad --- (a) -.63 → +.13 1/rad --- (b)
Roll Mode	$p \rightarrow \delta_W$	-2.7 → +2.7,.3	Roll Mode Time Constant τ_R	0.65 → 3.3 sec 0.68 → 2.6 sec
Spiral Mode	$R \rightarrow \delta_W$	-2.7 → +2.7,.3	Time to Half/ Double Amplitude T_2 OR $T_{1/2}$	1.7 sec Convergent → 2.0 sec divergent 2.1 sec Convergent → 3.3 sec divergent
Turn Coordination (c)	$\phi \rightarrow \delta_R$	-.54 → .54,.06	(β/ϕ) Steady State	-.42 → +.91
	$p \rightarrow \delta_R$	-2.7 → +2.7,.3	$\Delta(\beta/\phi)$ Transient	-.73 → +1.6
	$\delta_W \rightarrow \delta_R$	-.54 → +.54,.06	$C_{n\delta_W}$	+.17 → -.17 1/rad
Dutch Roll Damping	$R \rightarrow \delta_R$	-2.7 → +2.7;.3	ζ_{DR}	+.85 → -.50 +.44 → -.51 8sec < PERIOD < 15sec

NOTES: (a) Free airplane C_{ℓ_β} = .0 1/rad
(b) Free airplane C_{ℓ_β} = -.25 1/rad
(c) Free airplane with roll and spiral mode augmentation

MOD. C-8A "VARIABLE STABILITY MODE"
PARAMETER VARIATION RANGE

FIG 4-33

5.0 ENGINE-OUT CHARACTERISTICS

Engine-out characteristics are given special attention in this section. The Modified C-8A has many of the general engine-out features found on STOL transports plus a few unique problems of its own. Production of an augmentor wing research aircraft started with two fixed constraints: the airframe and the engine. Increased wing loading requirements caused the wing span (aspect ratio) reduction. Being a twin, the airplane has a 50% loss in thrust at engine failure. Engine-out climb performance with all of the above factors becomes a fine balance between thrust and drag.

Low-speed, STOL operation calls for relatively high flap deflection for takeoff (drag levels on the order of conventional airplanes at landing flaps). Early in the program the takeoff flap setting was raised from $\delta_F = 50°$ to $\delta_F = 30°$ primarily to provide engine-out climb capability.

Low-speed, steep approach at landing dictates very large flap deflection (δ_F=65°) with even higher drag level. STOL operation, particularly landing, requires "powered lift" where engine power is needed to stay in the air. On approach, hot thrust is vectored downward to provide lifting force. Hence, engine failure results in lift loss, both direct hot and jet flap cold flow, as well as loss in forward thrust. The airplane sinks, which is "unconventional", and flap retraction is required to climb away.

Hot thrust comprises over two-thirds of the total producing relatively large engine-out thrust asymmetries. With vectorable nozzles hot thrust moment

may roll the airplane as well as produce conventional yawing. Engine-out control becomes a significant problem, particularly at 60 kt approach. Generally, the Modified C-8A operates at speeds closer to V_{MC} than usually found in conventional transports.

5.1 Engine-Out Steady-State Performance

Engine-out climb performance at maximum landing weight is presented in Figure 5-1 for standard-day operation at emergency power. (Pilot action is required to advance throttle to emergency setting after engine failure.) Performance improves at reduced gross weight and deteriorates with increased weight, altitude or temperature. At flaps 30° (takeoff or go-around) climb gradient at $V_2 \approx 75$ kts meets FAR Part XX criteria (Reference 9). Better takeoff engine-out climb performance is possible by further reduction in flap setting (longer field lengths). Engine-out climb at cruise conditions is satisfactory at $V_e \geq 100$ kts.

Design landing approach ($\delta_F = 65°$, $\nu = 90°$, $V_{APP} = 60$ kts) is made at "approach power setting", approximately 92% RPM. At this setting each engine is producing 46% of its hot thrust capability and 69% of its cold thrust. After an engine failure, if the remaining engine is left at 92% RPM, the resulting descent angle is greater than $\gamma = -11°$ (Figure 5-1). Stall speed at 62 kts exceeds the original approach trim condition. The following action must be taken immediately:

- Advance power on the remaining engine to emergency setting.

If desired, the landing approach may then be continued at emergency power setting with some reduction in vector angle position. Approach speed should be increased to nearly 70 kts and the glide slope reduced to keep rate of descent at 800 fpm. Stall margins are then adequate for continued approach.

At landing flaps the drag level is too high to permit go-around to a conventional landing approach. A steady positive climb angle with acceptable stall margin can only be achieved at emergency power setting by:

- Vectoring the hot thrust vector full aft, and
- Retracting the flaps to the 30° position, and
- Increasing speed above the 60 kt approach speed at which the engine failed to best climb speed of 75 kts.

A finite amount of time is required to accomplish these steps during which the workload on the pilot is very heavy.

ENGINE-OUT APPROACH PERFORMANCE

GR. WT. = 43000 LB.
STD. DAY, SEA LEVEL

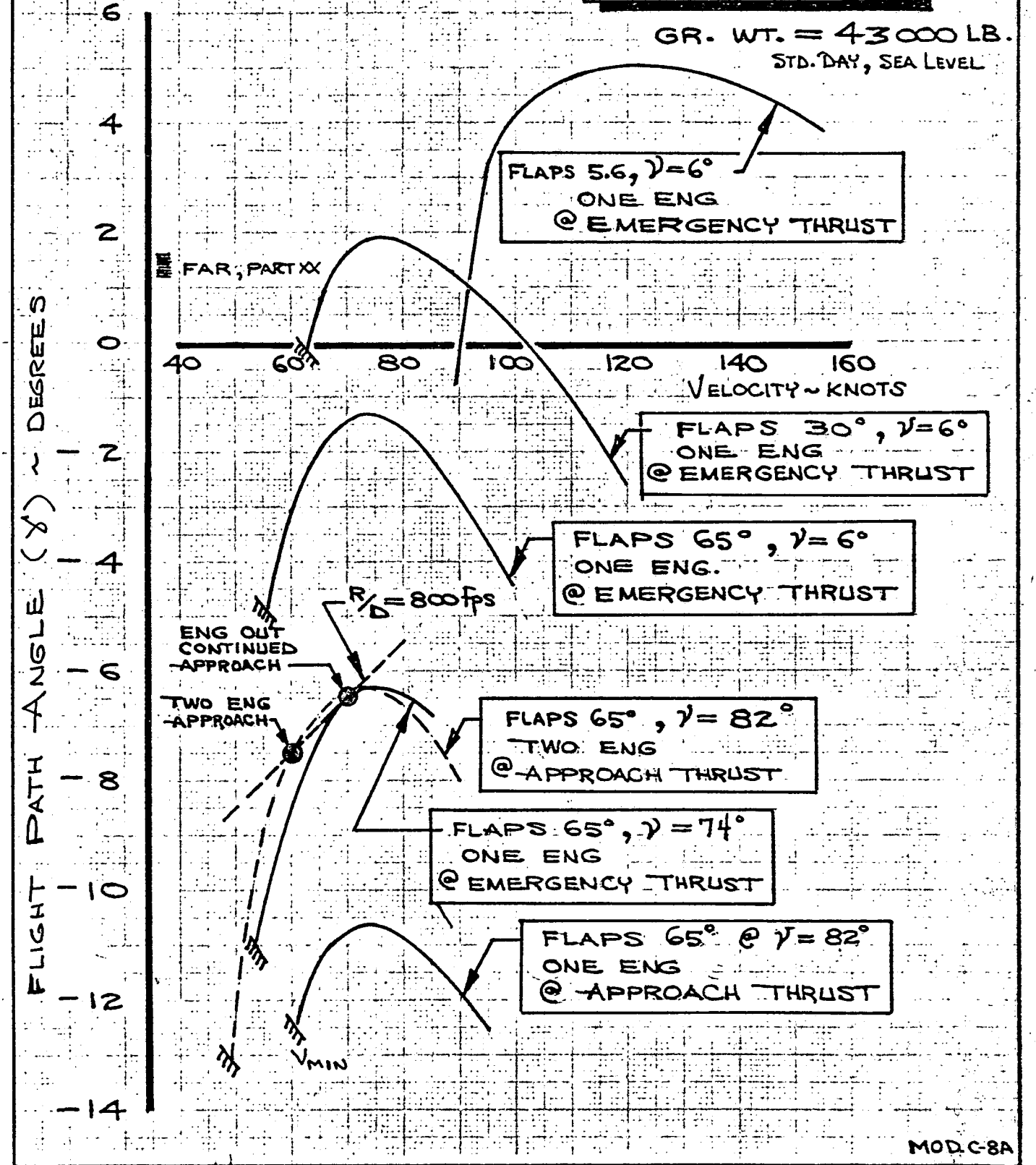

MOD C-8A

CALC	V. PAGE	2 3 72	REVISED	DATE	ENGINE-OUT CLIMB CAPABILITY	FIG 5-1
CHECK						D6-40381
APR					THE BOEING COMPANY	PAGE 5.4
APR						

5.2 Engine-out Steady-state Control

Sufficient control must exist to counteract an engine failure and continue the flight to a safe landing. Engine fan air is ducted across the fuselage to maintain flap blowing over the entire wing via the duct-within-a-duct system. With symmetrical cold thrust blowing, early NASA simulator studies revealed that direct hot thrust rolling moment was too large. To partially compensate for some of the hot thrust rolling moment, the duct system has been designed to deliver a greater proportionality of cold flow to the opposite wing. Most of this asymmetric blowing is delivered to the aileron, which receives air from only one engine (opposite side of the airplane). Figure 5-2 illustrates the blowing distribution from one engine. Asymmetric lift distribution, primarily due to blown-and-unblown drooped aileron lift, generates aerodynamic rolling moment which partially cancels the direct hot thrust moment. The remainder of the hot thrust must be handled by the pilot using lateral control and rudder.

Engine-out control at cruise poses no problem. Full emergency thrust, vectors aft, can be handled by the rudder on only one hydraulic system. In fact, engine-out is controllable by sideslip using no rudder down to V_e = 100 kts without exceeding β = 10° (steady state). Engine-out control at takeoff with vectors rotated full aft is essentially a "conventional" rudder problem. Rolling moment is relatively small and easily controllable.

The asymmetric blowing feature is most needed at landing approach, where thrust is vectored at ν = 90°. (Airplane flap and power setting were specifically chosen for the 60 kt, γ = -7.5° approach condition so that ample margins exist with hot thrust perpendicular to the flight path). Engine failure at approach power produces the rolling characteristic shown in Figure 5-3. Two things happen:

Loss of blowing causes available lateral control power to degenerate by about 40% while asymmetric blowing reduces the net engine-out rolling moment to a small level - much less than direct hot thrust. Very little wheel is required to keep the wings level.

As shown in Figure 5-1, the airplane has a very high rate of descent unless the remaining engine is advanced in power. Increasing power on the remaining engine before rotating the nozzles aft almost doubles the direct hot thrust rolling moment. Engine thrust characteristics are such that there is much less increase in compensating cold thrust. Figure 5-4 presents the net, compensated engine-out rolling moment and the maximum available lateral control power at emergency power setting. (Note: Even though emergency thrust can be achieved with vectors down, test stand engine running structurally deformed the Pegasus nozzle "trousers piece" at full power. Therefore, the pilot is cautioned not to select power settings above takeoff rating with vectors down.) At 60 kts the pilot needs about 50% of the available roll control to balance the engine-out condition. Continued approach with vectors down (see Figure 5-1) means that significant lateral trim is required to maintain wings level and that remaining lateral control capability for maneuvering is just adequate for emergency operation.

If the pilot elects to rotate the nozzles aft for a more conventional landing (or go-around) the engine-out rolling moment becomes yawing moment. Figure 5-5 shows that at constant speed engine-out rolling moment is reduced, but changes sign, as thrust vector reaches ν=6°. Yawing moment becomes quite large, nearly exceeding rudder capability at 60 kts (ϕ = 0°, β = 0°). Thus, the pilot must change control input from almost no rudder to full pedal and half wheel to nearly half wheel in the opposite direction. Such control transients, when coupled with zero dihedral effect, are very difficult to cope with.

The reversal in lateral control input with vector angle could be reduced by changing the amount of asymmetric blowing. Reduced blowing asymmetry was evaluated in the simulator. The characteristic shown in Figure 5-5 implies the need for nearly full lateral control if full power is reached with vectors down. Pilots rated this as unacceptable. With no option for valving in the duct system to regulate blowing, the current asymmetric blowing design is rated as the best compromise for engine-out control.

5.3 Engine-out Minimum Control Speed

There is no single "minimum control speed" for the Modified C-8A. Control requirements change with flap angle and vector angle as well as airspeed. For vectors aft conditions such as takeoff, cruise and go-around minimum control speed, V_{MC_A}, has been defined as the lowest speed at which engine-out yawing moment can be countered by rudder using ϕ=5° bank angle (dead engine high) on a straight-ahead flight path. With thrust vectored downward minimum control speed occurs when lateral control available after trimming the rolling moment is just adequate for emergency maneuvering control. One definition of this level is sufficient lateral control power to generate $\dot{p}$=.15 to .30 RAD/SEC^2 roll acceleration on landing approach (see Ref. 15 and 16). A value of $\dot{p}$=.2 RAD/SEC^2 has been used for design because it corresponds to Boeing experience with manual reversion landings on commercial transports, and the level was deemed adequate for the Modified C-8A on the simulator.

V_{MC_A} has been determined at the lightest airplane gross weight deemed practical and at sea level, standard day, emergency thrust level. Reduced weight permits the airplane to fly slower which is most critical for engine-out control, as opposed to engine-out climb performance. Figure 5-6 shows the fraction of available control required to trim engine-out moments at takeoff flap setting. Characteristics at three bank angles are shown. Minimum control speed at ϕ=5°

is declared at V_e = 47 kts, which is below single-engine stall speed. The speed at which full rudder is reached is strongly dependent on bank angle used to balance rudder sideforce and maintain straight flight path. Lateral control requirement and sideslip indication (left slip for left engine failure) should aid the pilot in holding correct bank angle. Takeoff rotation and climb speeds are noted on Figure 5-6. Both are well above V_{MC_A}.

Engine failure during the takeoff ground roll must be counteracted directly by the rudder without the benefit of bank angle. Conventional transport airworthiness policy defines ground minimum control speed, V_{MC_g}, as the engine failure speed on takeoff at which controllability by primary aerodynamic controls alone (no steering) can be demonstrated without exceeding 25 ft. lateral deviation from the runway centerline. V_{MC_g} is generally slightly below actual static balance speed (rudder moment equals engine moment) because the airplane continues to accelerate after engine failure. V_{MC_g} has been estimated for the Modified C-8A at takeoff flaps (δ_F = 30°)and 40,000 lb at V_e = 53 kts. Since many assumptions were made in the calculations, pilots should add a few knots when testing the airplane. Even so, V_{MC_g} is well below the takeoff rotation speed.

At landing flaps, V_{MC_A} is declared at V_e = 53 kts with vectors aft and $\emptyset$ = 5°. Figure 5-7 shows the same strong effect of bank angle as seen at takeoff. At landing flaps the lack of dihedral effect results in left wheel for right rudder (left engine failed), which is opposite to conventional airplane characteristics. At the light gross weight of 35,000 lb, V_{MC_A} is above stall speed. One should also note that landing flaps V_{MC_A} is somewhat higher than takeoff flaps. This can be attributed to "adverse yaw" due to greater blowing on the opposite drooped aileron and flap. Since actual wind tunnel data do not exist for engine-out conditions, it is possible that this effect may not be so great.

With nozzles vectored downward, engine-out is a lateral control problem. Figure 5-8 shows the control required to trim the engine-out at landing flaps and 35,000 lbs. Very little rudder is needed. The speed for full lateral control is almost the same as one-engine stall speed. However, if sufficient control power is held back for maneuvering at $\ddot{\phi}$ = .2 RAD/SEC^2, then V_{MC_A} occurs near 60 kts. Recommended speed for continued approach is about 70 kts for this condition. For engine-out with vectors down the pilot should keep both bank angle and sideslip small.

It should be noted that engine-out control is more difficult with thrust vectored downward at reduced flap settings. Less aileron droop and flap angle reduces the amount of aerodynamic rolling moment produced by asymmetric blowing (see Figure 5-2). Also there is less lateral control power available. By holding back lateral control power for maneuvering at $\ddot{\phi}$ = .2 RAD/SEC^2, the V_{MC_A} occurs at nearly 80 knots for vectors down at δ_F = 30°.

Figure 5-9 summarizes the minimum control speed situation. With nozzles aft at ν = 6°, V_{MC_A} occurs at speeds below one-engine stall speeds except for light-weight, landing flap conditions. With vectors down at ν = 90° the speed for adequate roll control (emergency basis) is greater than 60 kts, although full lateral control is not required until reaching stall speed. It is recommended that, if possible, the nozzles be rotated aft after engine failure for better performance, control margins and more-or-less conventional flight characteristics.

LATERAL CONTROL INFLUENCE ON BLOWING DISTRIBUTION

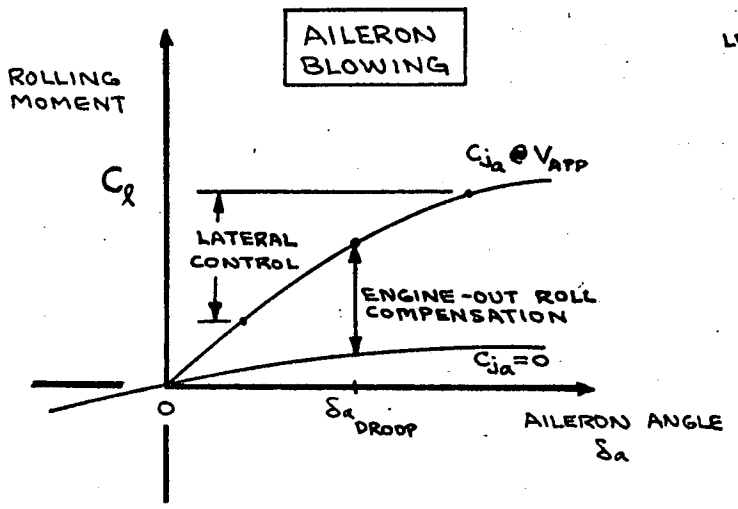

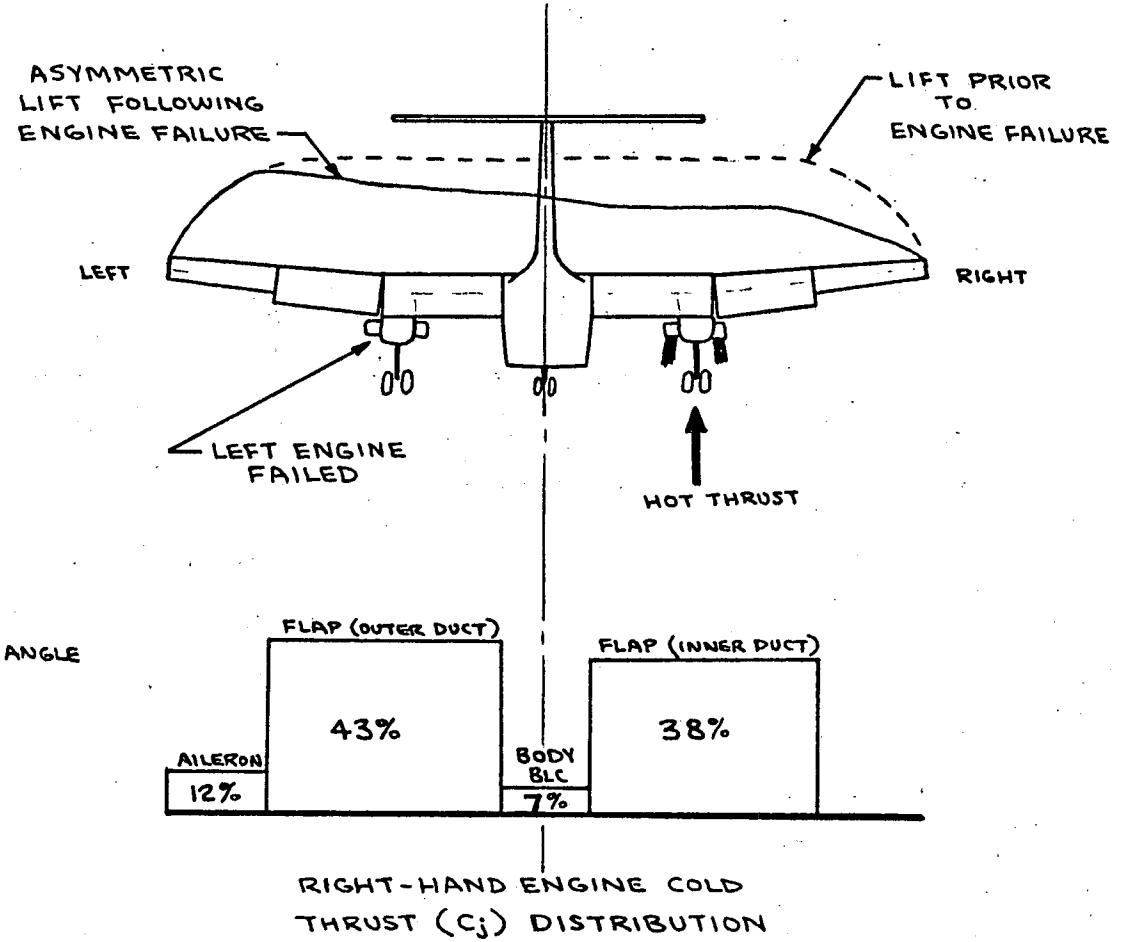

MODIFIED C-8A

FIG 5-2

ENGINE-OUT LATERAL CONTROL
- LANDING CONFIGURATION
- APPROACH POWER SETTING

- FLAPS 65°
- NOZZLE ANGLE @ $\nu = 90°$
- $0° \leq \alpha_F \leq 10°$
- POWER SETTING AT 92% RPM

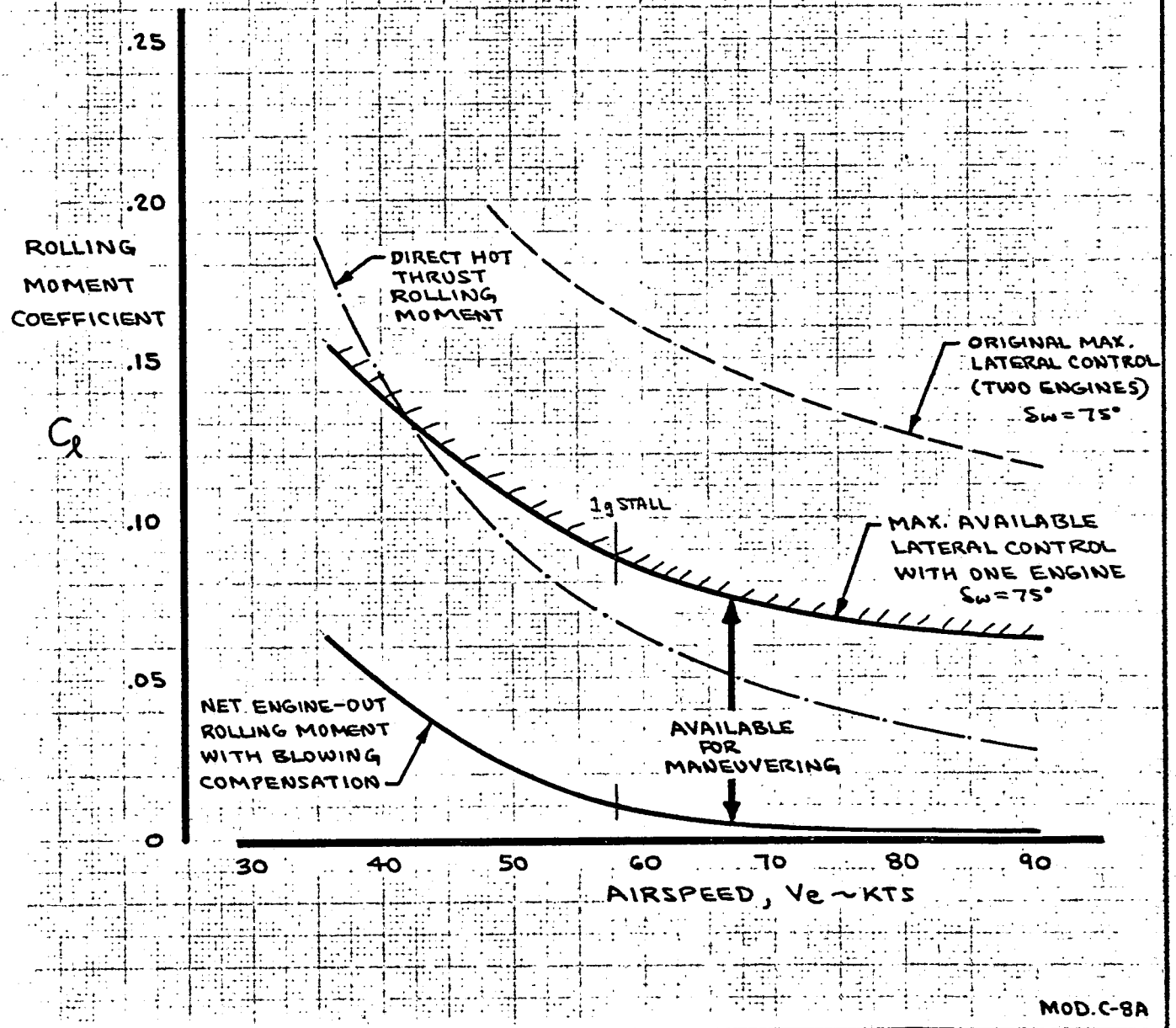

MOD. C-8A

CALC	SPITZER	9-28-70	REVISED	DATE	ENGINE-OUT LATERAL CONTROL WITH STOL LANDING CONFIGURATION AT "APPROACH" POWER SETTING
CHECK			SPITZER	2-10-72	
APR					
APR					
					THE BOEING COMPANY

FIG 5-3

D6-40381

PAGE 5.11

ENGINE-OUT LATERAL CONTROL
- LANDING CONFIGURATION
- EMERGENCY POWER SETTING

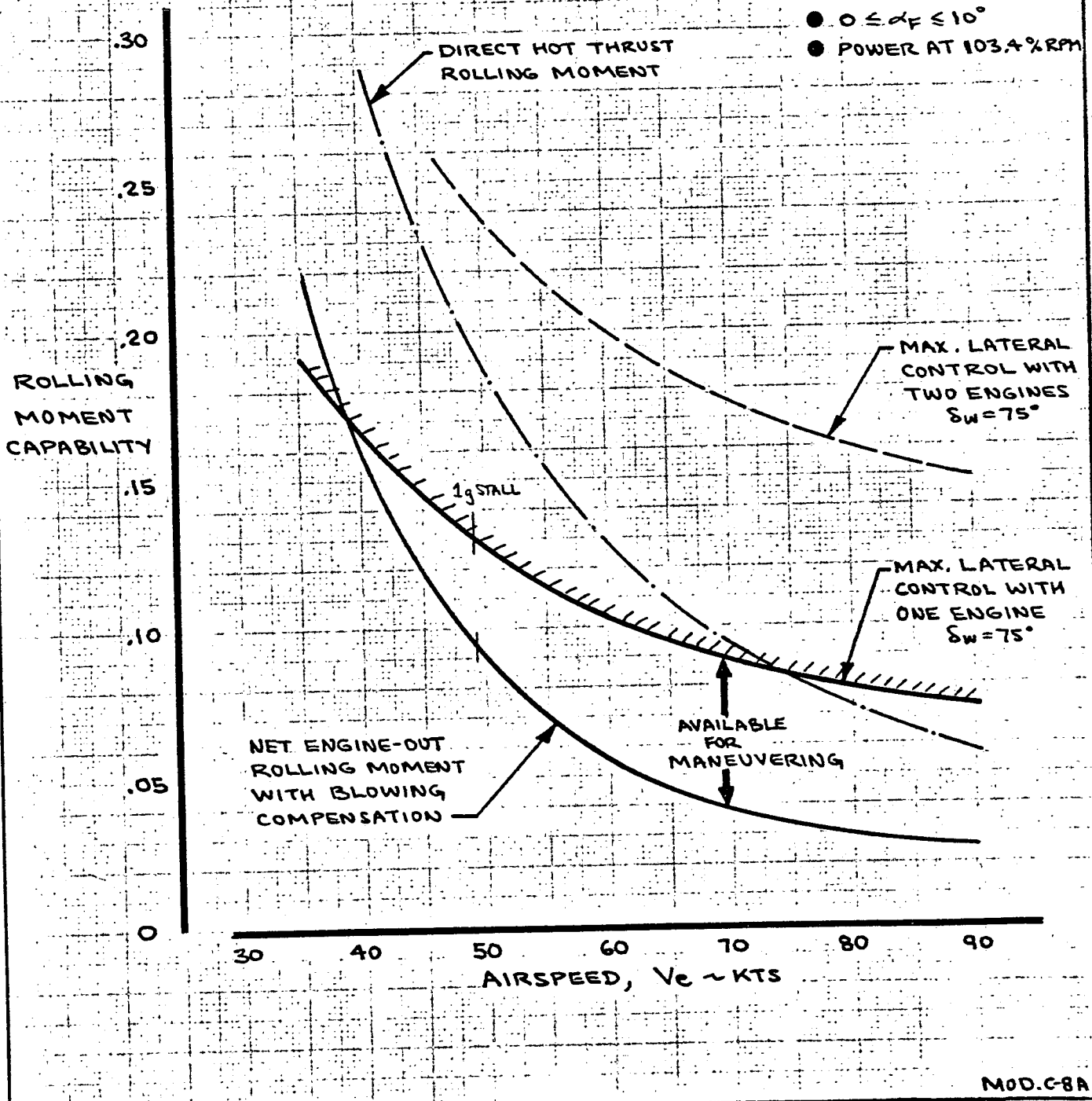

MOD.C-8A

CALC	SPITZER	9-28-70	REVISED	DATE	ENGINE-OUT LATERAL CONTROL WITH STOL LANDING CONFIGURATION AT "EMERGENCY" POWER SETTING	FIG 5-4
CHECK			SPITZER	2-10-72		D6-40381
APR						
APR					THE BOEING COMPANY	PAGE 5.12

EFFECT OF THRUST VECTOR ON ENGINE-OUT CONTROL AT LANDING FLAPS

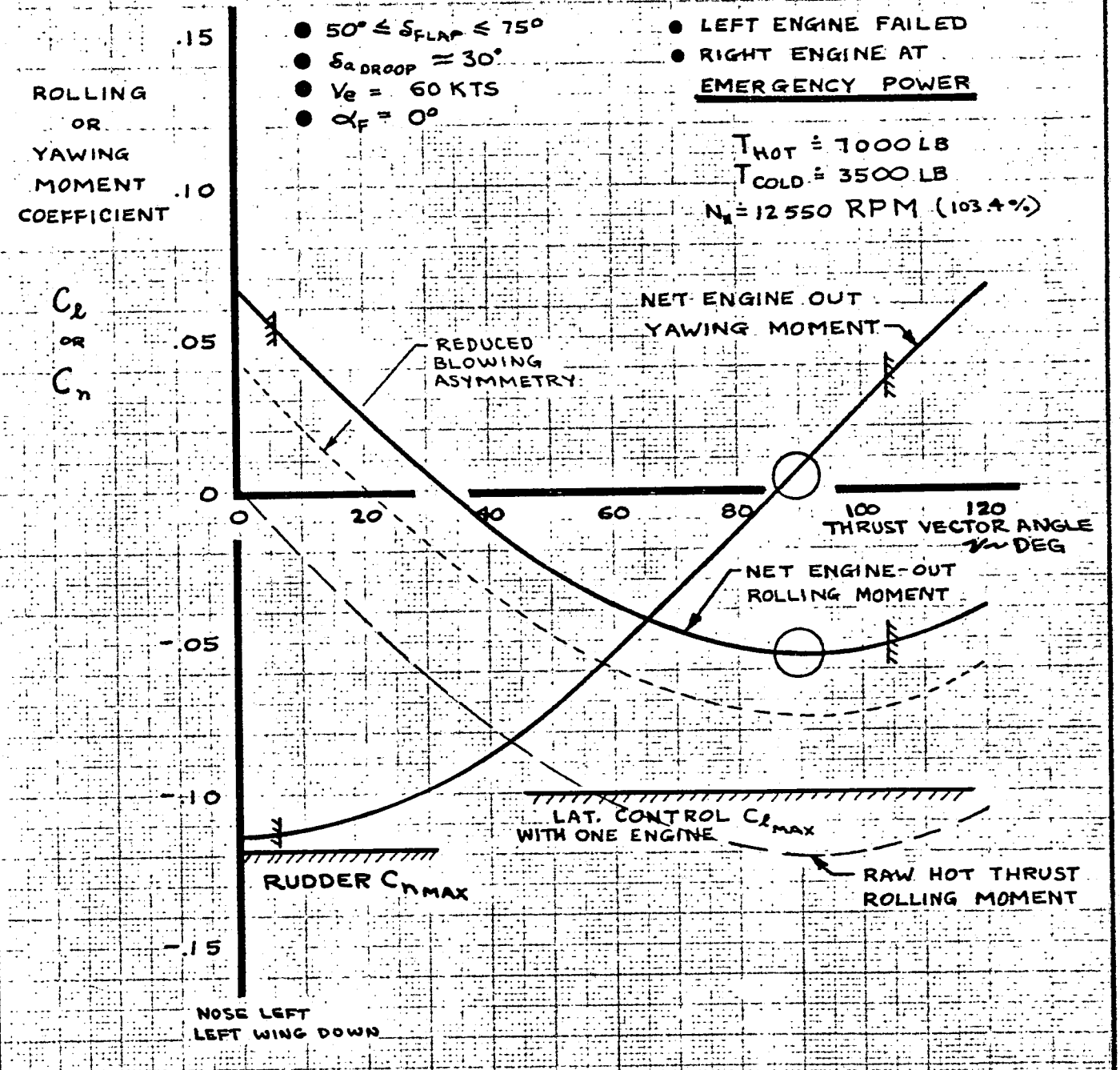

NOTE:
CONVENTIONAL AIRPLANES (ENGINES EXHAUSTING AFT, NO POWERED-LIFT BLOWING) WOULD YAW NOSE LEFT AND ROLL LEFT WING DOWN WITH LEFT ENGINE FAILED.

MOD C-8A

CALC	SPITZER	12-11-70	REVISED	DATE	EFFECT OF THRUST VECTOR ON ENGINE-OUT ROLLING AND YAWING MOMENT AT 60 KTS	FIG. 5-5
CHECK			SPITZER	2-10-72		D6-40381
APR					THE BOEING COMPANY	PAGE 5.13
APR						

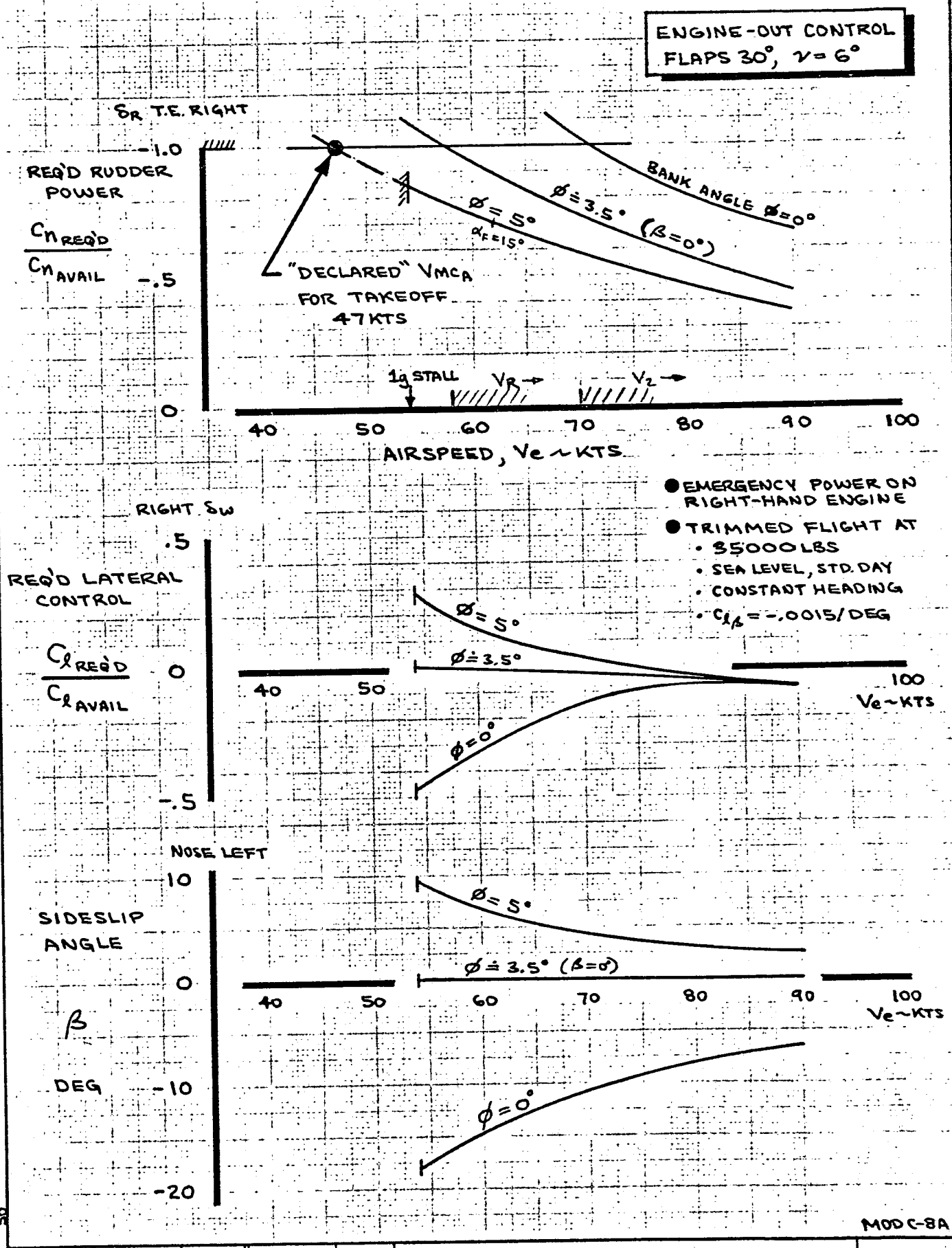

CALC	SPITZER	10-19-71	REVISED	DATE	ENGINE-OUT CONTROL AT TAKEOFF FLAPS 30°, ν = 6°	FIG 5-6
CHECK						D6-40381
APR					THE BOEING COMPANY	PAGE 5.14
APR						

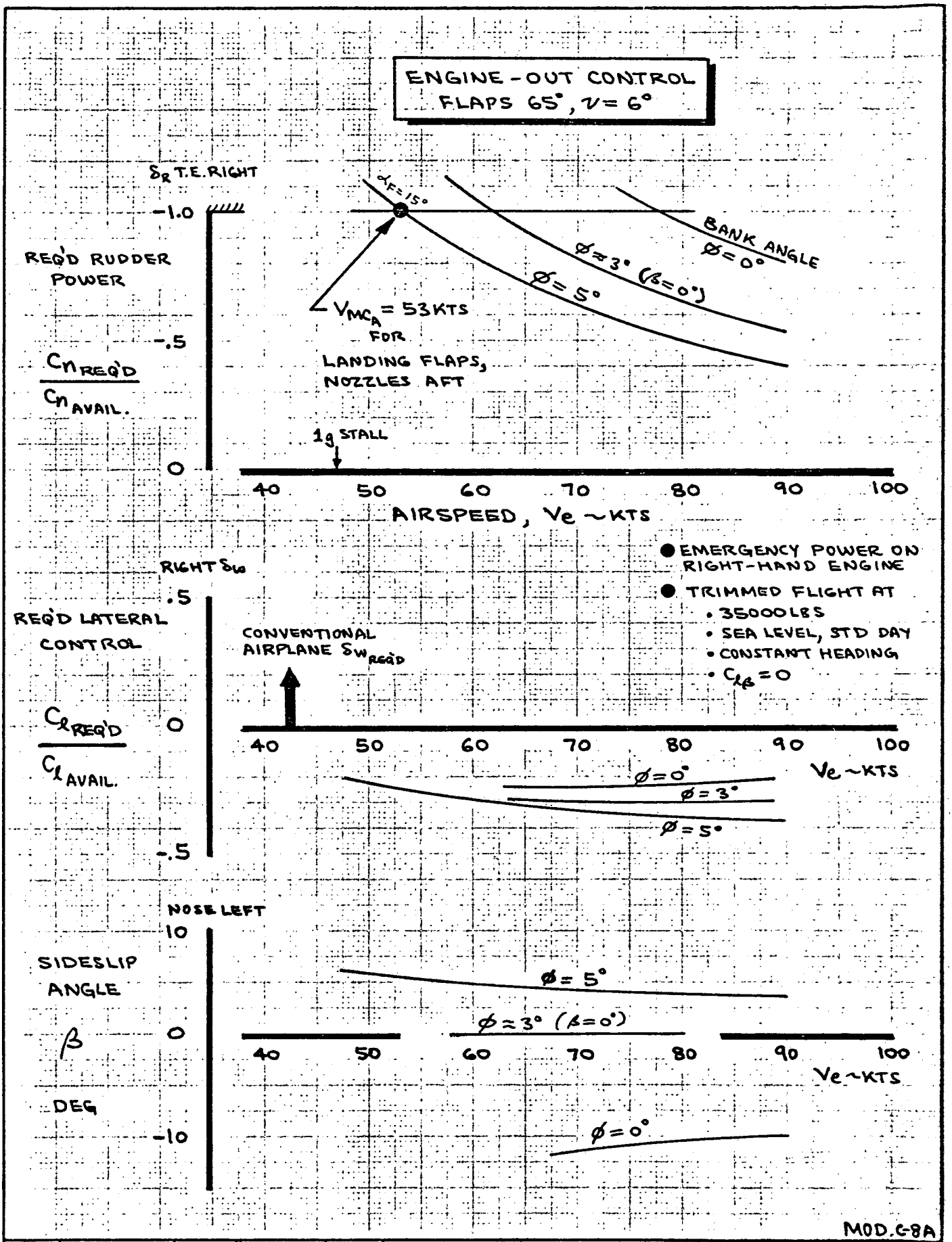

MOD. C-8A

CALC	SPITZER	10-21-72	REVISED	DATE	ENGINE-OUT CONTROL AT FLAPS 65°, ν = 6°	FIG 5-7
CHECK						D6-40381
APR						
APR					THE BOEING COMPANY	PAGE 5.15

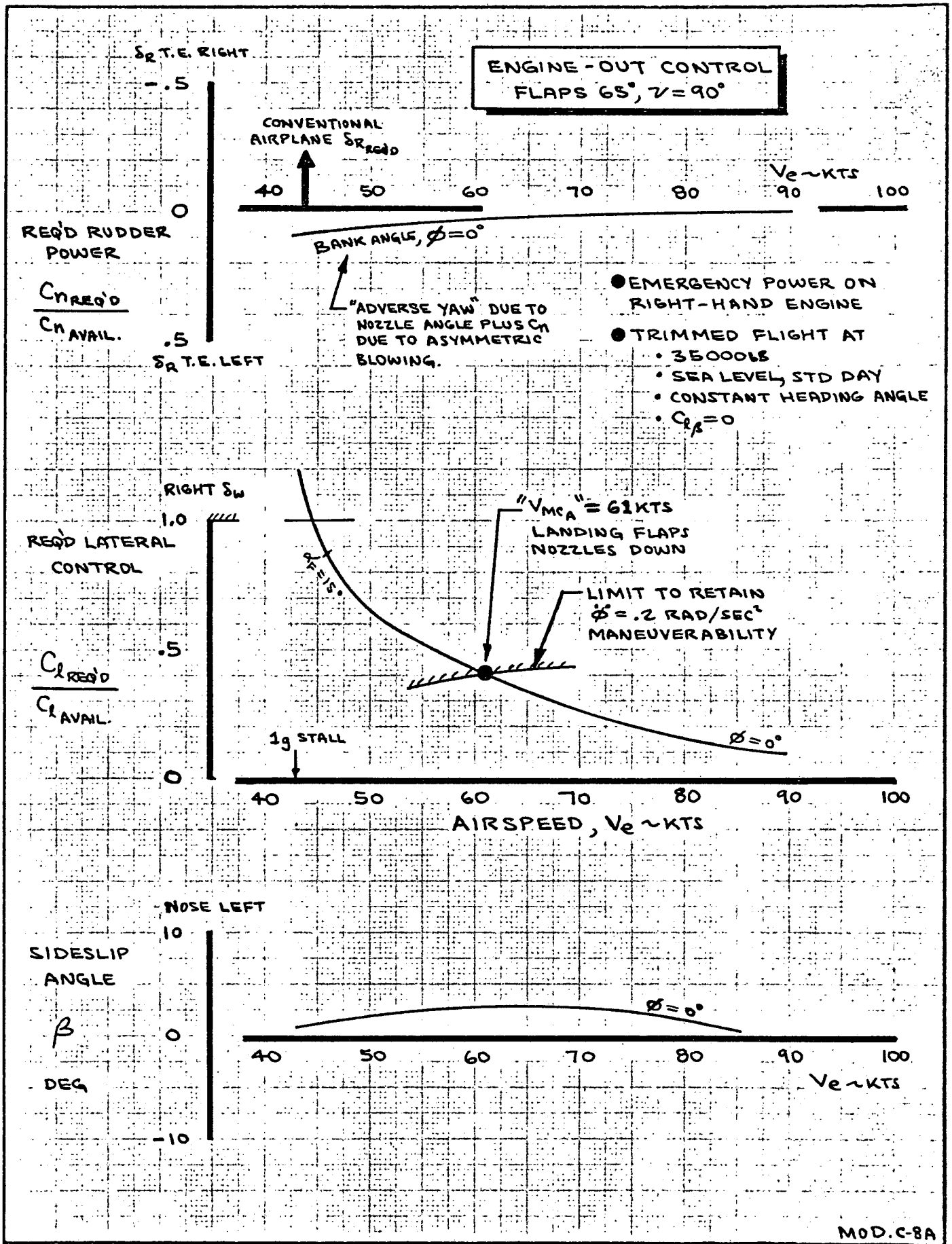

MOD. C-8A

CALC	SPITZER	10-27-72	REVISED	DATE	ENGINE-OUT CONTROL AT FLAPS 65°, ν = 90°	FIG 5-8
CHECK						D6-40381
APR					THE BOEING COMPANY	PAGE 5.16
APR						

#57

16

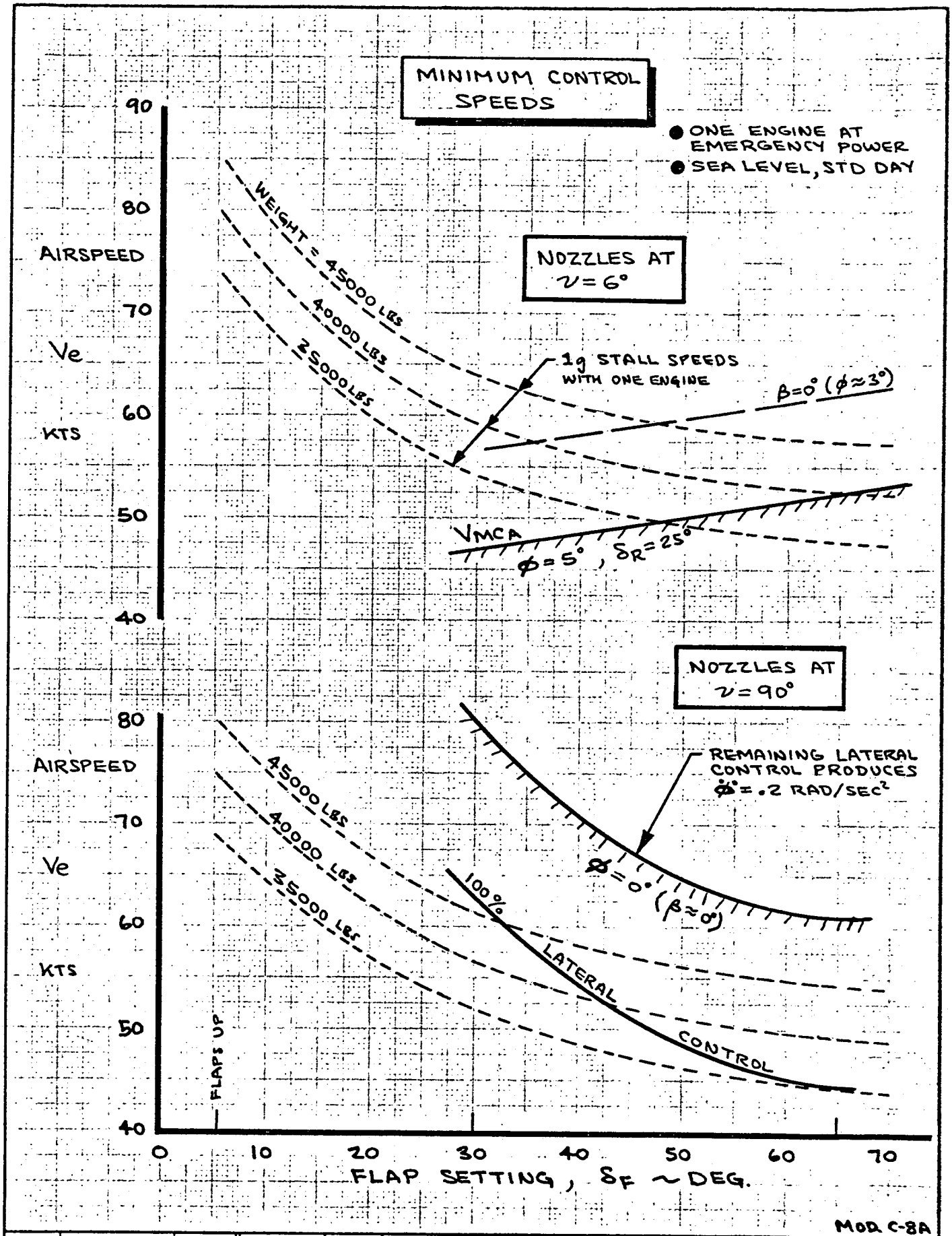

MOD C-8A

CALC	PATTERSON	12-14-71	REVISED	DATE	MINIMUM CONTROL SPEED SUMMARY
CHECK			SPITZER	12-20-71	FIG 5-9
APR					D6-40381
APR					THE BOEING COMPANY
					PAGE 5.17

5.4 Engine-Out on the Simulator

The performance and control problems associated with engine failure dictated a real time, pilot-in-the-loop simulation. Dynamic characteristics and pilot time delays and workload can only be appreciated on the simulator. Two piloted simulation periods (Oct. 1970 and May 1971) were used on the NASA-Ames FSAA system (Reference 7). In addition, an appreciation of the physics of the problem was gained in simulator studies conducted at Boeing using an "electronic" pilot.

Engine-out handling qualities at takeoff were judged to be adequate. Pilots were able to maintain control using more or less conventional techniques. The low engine-out climb gradient was appreciated but considered tolerable.

Engine failure on STOL landing approach* presented a more difficult situation. The pilots were subjected to numerous engine failures; the choice of which engine to fail and at what altitude being randomly selected by test engineers. After each failure the pilots were allowed to choose whether to continue the approach to a landing or initiate an engine-out go-around to set up a conventional landing.

The first indication of engine failure was loss in lift and rapid build-up in sink rate. Airspeed and angle of attack inherently increased due to airplane settling. Initial rolling and yawing moments were low (see Section 5.2) posing no initial control problem. Pilots almost immediately increased power on the remaining engine. Control response varied depending on subsequent action taken with the thrust nozzles and flap setting.

---

* Engine failure on approach is much less of a problem at higher speeds and reduced glide slope.

Out of a sampling of 70 engine failures by three pilots, about 60% of the conditions were go-arounds. If possible, a new approach at conventional conditions (δ_F = 30°, V_{APP} = 90 kts, γ = 6°) was deemed prudent. The pilots had adequate control to counter the engine failure, particularly since speed increased naturally. Initial control was gained using $\delta_w \approx 35°-45°$ ($\delta_{w_{max}}$ = 75°) and $\delta_R \approx 5°$ ($\delta_{R_{max}}$ = 25°). With nozzles aft rudder requirement increased to $\delta_R \approx 10°-15°$. Bank angle upset was $\phi \approx 7°$ and recovery maneuvering was made using $\phi \approx 12°$ to return to runway centerline. Even though adequate control was available, the engine-out condition was rated as a very demanding task. The change in sign in rolling moment with nozzle angle coupled with lack of dihedral effect was very confusing. Yawing and pitching moment changes further complicated the problem. Confusing and unconventional control characteristics plus marginal single-engine climb performance makes an engine failure on approach a very serious matter. Two control techniques were worked out for dealing with an engine failure and making a go-around.

Technique A

The first technique was to immediately increase thrust on the remaining engine. Nozzle and flap position were changed subsequently depending on the decision to land or go-around. If go-around were made, the nozzles were raised and flaps selected at δ_F = 30° as the speed built up. Figure 5-10 illustrates this technique. While restoring lost lift, increasing power with no change in vector angle generates large rolling moment. Wheel input is necessary when the nozzles are rotated. Wheel direction must be reversed, although the amount required falls off with continued go-around. Rudder input is seen with aft vector angle. Rotating the nozzles in this condition also produced a large nose-up pitching moment. Considerable control coordination was required to keep the wings level and airplane on a straight course.

AD 1546D

Technique B

In technique "B" the nozzles were rotated aft before power was increased on the remaining engine. This technique minimizes the control problems and reduces the confusing change in control direction. Figure 5-11 illustrates this technique. Very little wheel motion is required. For the most part rudder becomes the dominant control input as in a conventional airplane. (The large sideslip angle shown in the figure resulted from failure to use enough rudder initially, then too much later in the go-around).

Current engine-out control philosophy leans toward the more conventional technique "B" . Throttle and nozzle control levers have been modified so that both may be advanced simultaneously using one hand. This results in full power and vectors aft conditions occurring at the same time thereby speeding the recovery. Low wheel and stick forces now permit easy control of the airplane using only one hand. Engine-out control is well within the capability of the airplane.

The most pressing consideration lies in minimizing altitude loss in making the go-around. Steep approach, loss of lift, high drag flaps, etc. all add to the high sink rate encountered following engine failure. Figure 5-12 presents a selected example of a one-engine go-around. The rapid increase in sink rate (22 ft/sec) and loss in load factor must be dealt with at the same time that roll, yaw and pitch control is being maintained. Downward acceleration, increase in thrust and thrust vectoring aft produce an increase in airspeed which helps to regain margin from stall and accelerate the airplane towards a positive climb gradient. Approximately constant pitch attitude is flown while flaps are retracted for go-around.

Fast reactions are needed to effect a go-around with minimum altitude loss. Early trials in the simulator saw altitude loss from point of engine failure in excess of 350 feet. Mean levels from early piloted simulator work tended toward 250 feet altitude loss. Techniques for taking corrective action in minimum time were practiced in the second simulation period. Prior work using an "electronic" pilot showed the merits of moving quickly (Reference 5). The analysis showed that pull up to moderate angle of attack ($\alpha_F \approx 12°$) followed by tracking on flaps 30° climb speed ($V_e \approx 75$ kts) results in minimum altitude loss in the go-around. This technique was followed by the pilots. Piloted recovery results are compared with the analysis in Figure 5-13.

Although go-arounds were accomplished from as low as 90 ft altitude in calm air, the minimum go-around altitude had to be increased in turbulent conditions. It would appear that minimum go-around altitude should be on the order of 150 ft.

It should be recalled that the pilots elected to continue the approach to a landing in about 40% of the trials. Figure 5-14 shows a successful one engine landing after engine failure at 150 feet altitude. In this case immediate reaction to an engine failure is to increase power, vector the thrust aft and leave the flaps down for maximum lift capability. Again note the reduction in load factor at engine failure and the large increase in sink rate at 23 ft/sec. Speed is allowed to build up only as necessary to retain stall margin and produce reasonable body attitude at an allowable rate of descent. As can be seen from this condition, there is plenty of flare capability; touchdown sink rate was held to only 3.5 ft/sec. (Engine-out landing occurs up to 500 ft short of the original touchdown aiming point. Pilots are encouraged to aim to land over 1000 feet beyond the actual end of the runway when making STOL approaches.)

The actual vector angle chosen for a continued landing after engine failure varied between different pilots and depended to some extent on the techniques used to control rate of descent. Using nozzle vectoring inevitably introduces pitching, rolling and yawing moments from the operative engine's hot thrust jet. Power changes introduced mainly rolling moments. Two pilots stated a preference for thrust modulation, but when faced with the problem in subsequent cases, all pilots used combined techniques.

Touchdowns will occur at increasingly higher angles of attack, up to a stalling flare, as the engine failure altitude comes nearer the ground. At very low altitude engine failures will result in hard touchdowns. If immediate flaring is attempted, the pilot may be able to reduce sink rate to the landing gear structural limits (12 ft/sec). Full elevator flare immediately after engine failure (with increase in power) was found to arrest sink rate to gear limits in the "electronic" pilot simulation. Engine failures above about 50 ft altitude can probably be corrected to the point that little, if any, damage will be done to the airplane.

There does exist a region near the ground where an engine failure would cause a very hard landing, beyond landing gear structural capability. This failure altitude roughly corresponds to that for flare initiation. Exposure to this critical condition lasts for about the last 4 to 5 seconds prior to touchdown. Special seats have been installed on the airplane to take high sink rate landings without injuring the pilot. New emergency egress doors have been added in the cockpit to facilitate getting out of the airplane. Since the exposure time is short, the risk of critical engine failure near the ground has been considered reasonable for a research airplane.

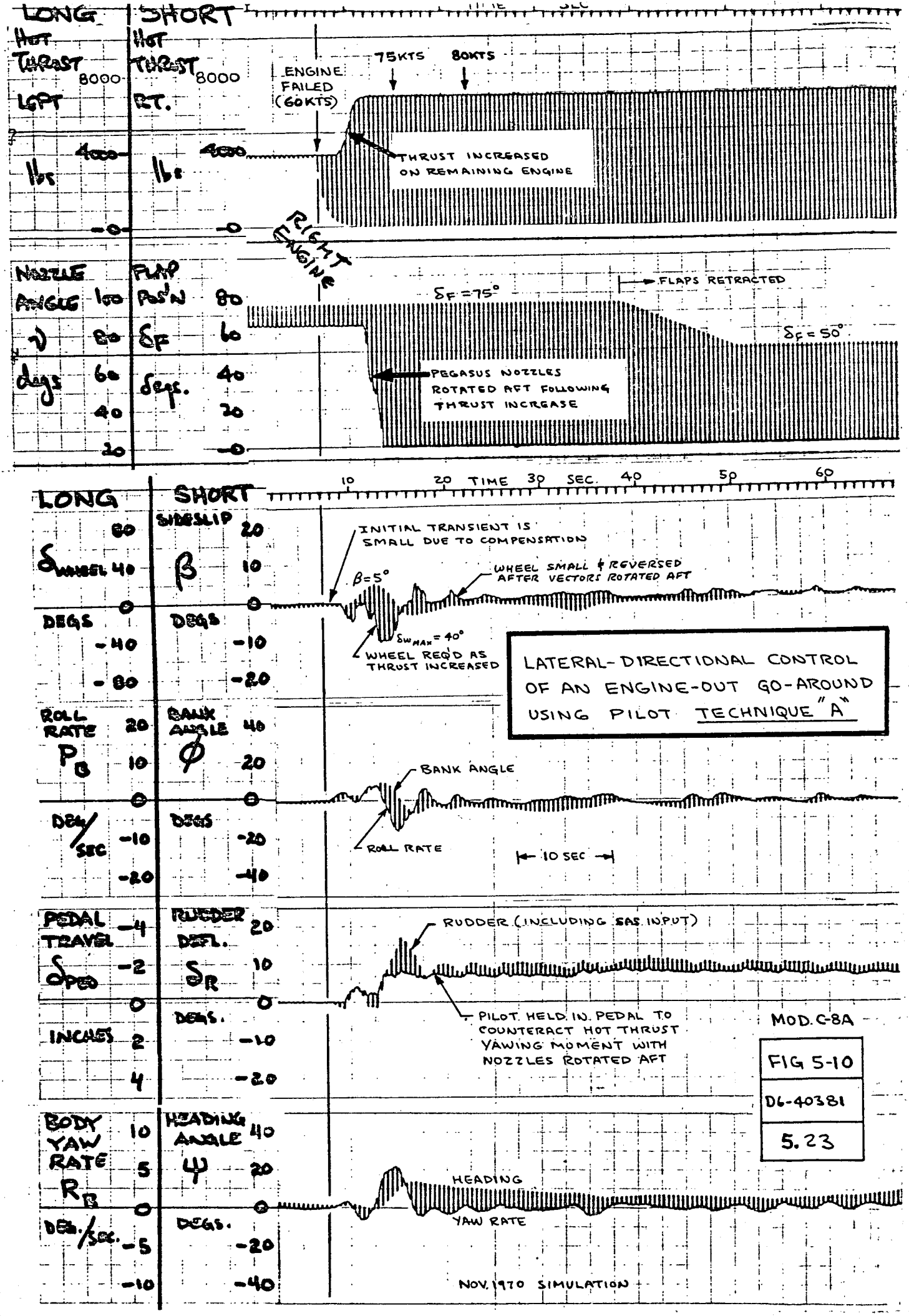

LATERAL-DIRECTIONAL CONTROL OF AN ENGINE-OUT GO-AROUND USING PILOT TECHNIQUE "A"

MOD. C-8A

FIG 5-10

D6-40381

5.23

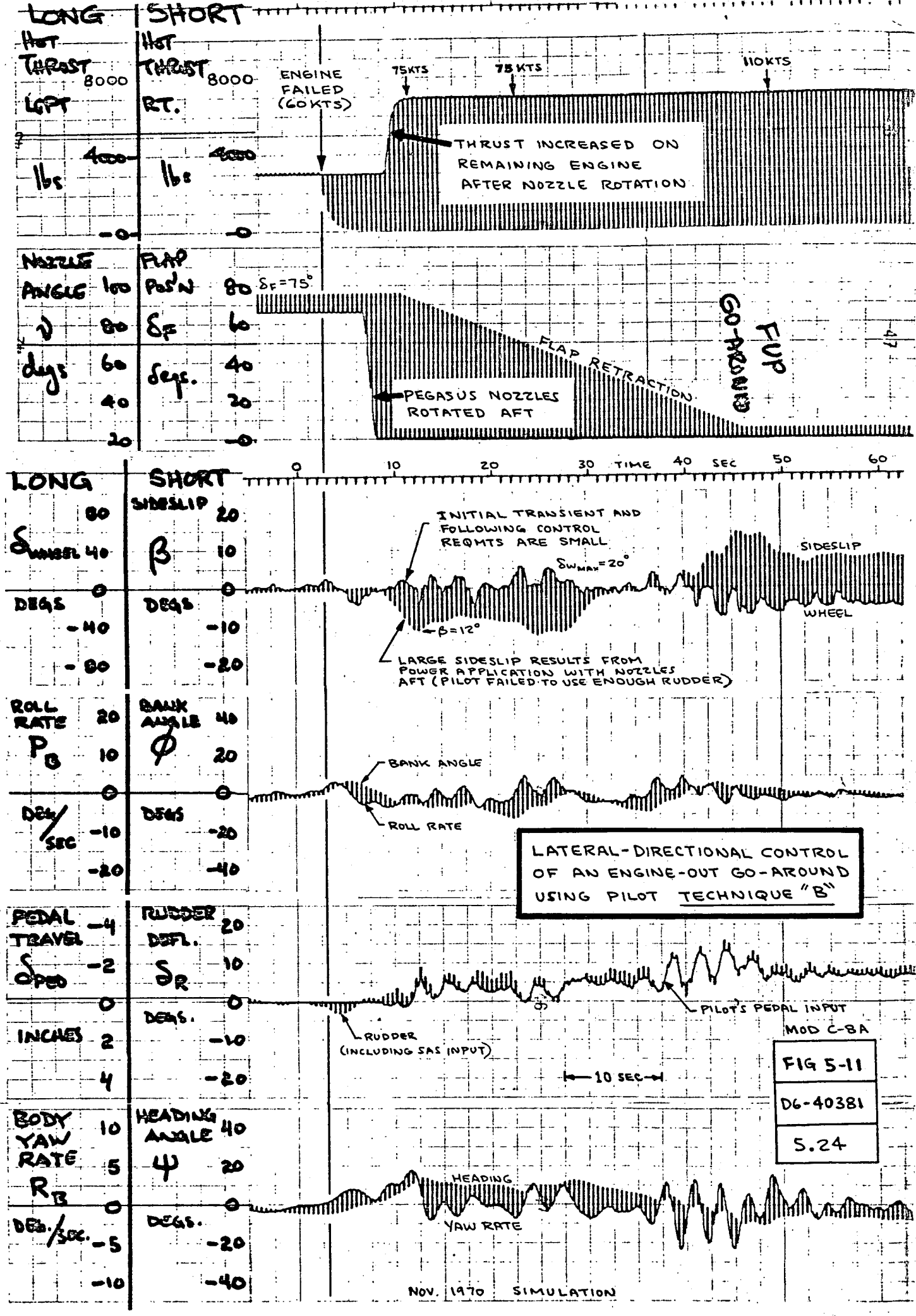
LONG
SHORT
HOT THRUST LEFT
HOT THRUST RT.
8000
4000
0
lbs
ENGINE FAILED (60KTS)
75KTS
78 KTS
110KTS
THRUST INCREASED ON REMAINING ENGINE AFTER NOZZLE ROTATION
NOZZLE ANGLE
100
80
60
40
20
degs
FLAP POS'N
80
60
40
20
0
degs.
δ_F=75°
FLAP RETRACTION
PEGASUS NOZZLES ROTATED AFT
FUP GO-AROUND
0
10
20
30 TIME 40 SEC
50
60
LONG
SHORT
SIDESLIP
80
40
0
-40
-80
δ_{WHEEL}
20
10
0
-10
-20
β
DEGS
INITIAL TRANSIENT AND FOLLOWING CONTROL REQMTS ARE SMALL
$\delta_{W_{MAX}}$=20°
SIDESLIP
WHEEL
β=12°
LARGE SIDESLIP RESULTS FROM POWER APPLICATION WITH NOZZLES AFT (PILOT FAILED TO USE ENOUGH RUDDER)
ROLL RATE
20
10
0
-10
-20
P_B
DEG/SEC
BANK ANGLE
40
20
0
-20
-40
ϕ
DEGS
BANK ANGLE
ROLL RATE
LATERAL-DIRECTIONAL CONTROL OF AN ENGINE-OUT GO-AROUND USING PILOT TECHNIQUE "B"
PEDAL TRAVEL
-4
-2
0
2
4
INCHES
δ_{PED}
RUDDER DEFL.
20
10
0
-10
-20
DEGS.
δ_R
PILOT'S PEDAL INPUT
RUDDER (INCLUDING SAS INPUT)
10 SEC
MOD C-8A
FIG 5-11
D6-40381
5.24
BODY YAW RATE
10
5
0
-5
-10
DEG./SEC.
R_B
HEADING ANGLE
40
20
0
-20
-40
DEGS.
ψ
HEADING
YAW RATE
NOV. 1970 SIMULATION

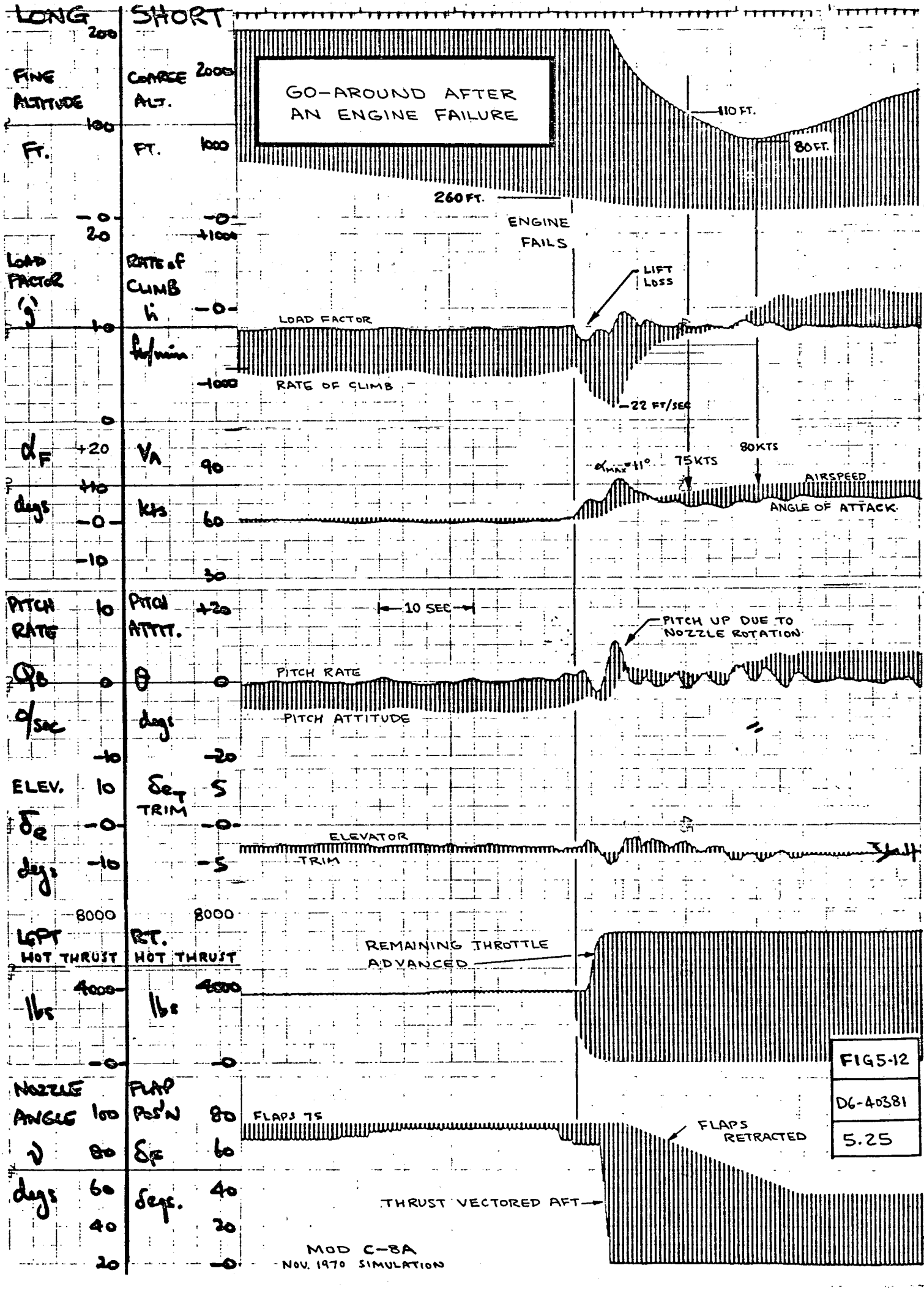
LONG
SHORT
GO-AROUND AFTER AN ENGINE FAILURE
FINE ALTITUDE
COARSE ALT.
FT.
110 FT.
80 FT.
260 FT.
ENGINE FAILS
LOAD FACTOR (g)
RATE of CLIMB
LIFT LOSS
LOAD FACTOR
RATE OF CLIMB
-22 FT/SEC
α_F
V_A
α_{MAX}=11°
75KTS
80KTS
AIRSPEED
ANGLE OF ATTACK
PITCH RATE
PITCH ATTITT.
10 SEC
PITCH UP DUE TO NOZZLE ROTATION
q_B
θ
PITCH RATE
PITCH ATTITUDE
ELEV.
δ_e
δ_{e_T} TRIM
ELEVATOR TRIM
LEFT HOT THRUST
RT. HOT THRUST
REMAINING THROTTLE ADVANCED
NOZZLE ANGLE
δ
FLAP POS'N
δ_F
FLAPS 75
FLAPS RETRACTED
THRUST VECTORED AFT
MOD C-8A
NOV. 1970 SIMULATION
FIG 5-12
D6-40381
5.25

ALTITUDE LOSS
ENGINE-OUT GO-AROUND
40000 LBS

	INITIAL CONDITION	FINAL CONDITION
FLAP ANGLE	65 DEG	30 DEG
AIRSPEED	60 KNOTS	VARIABLE
GLIDE SLOPE	-7.5 DEG	≥ 0 DEG
THRUST SETTING	92% RPM	103.4% RPM (EMERGENCY)
NOZZLE POSITION	≈ 90 DEG	6→18 DEG

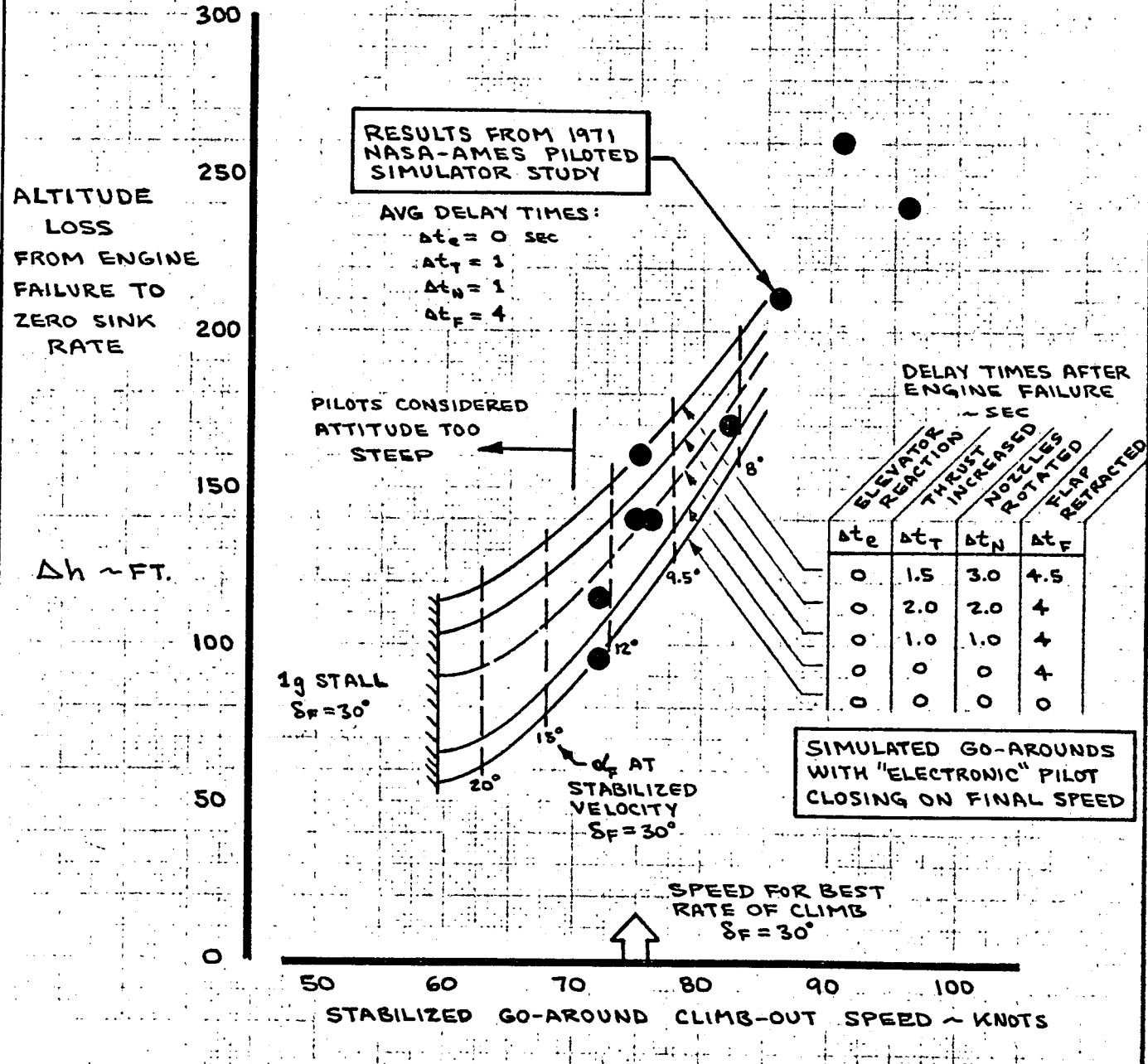

DELAY TIMES AFTER ENGINE FAILURE ~ SEC

ELEVATOR REACTION Δt_e	THRUST INCREASED Δt_T	NOZZLES ROTATED Δt_N	FLAP RETRACTED Δt_F
0	1.5	3.0	4.5
0	2.0	2.0	4
0	1.0	1.0	4
0	0	0	4
0	0	0	0

SIMULATED GO-AROUNDS WITH "ELECTRONIC" PILOT CLOSING ON FINAL SPEED

MOD. C-8A

CALC	ELBEL	3-15-71	REVISED	DATE
CHECK			SPITZER	2-10-72
APR				
APR				

COMPARISON OF ENGINE-OUT GO-AROUND PERFORMANCE BETWEEN PILOTED & UNPILOTED SIMULATION

FIG 5-13

D6-40381

THE BOEING COMPANY

PAGE 5.26

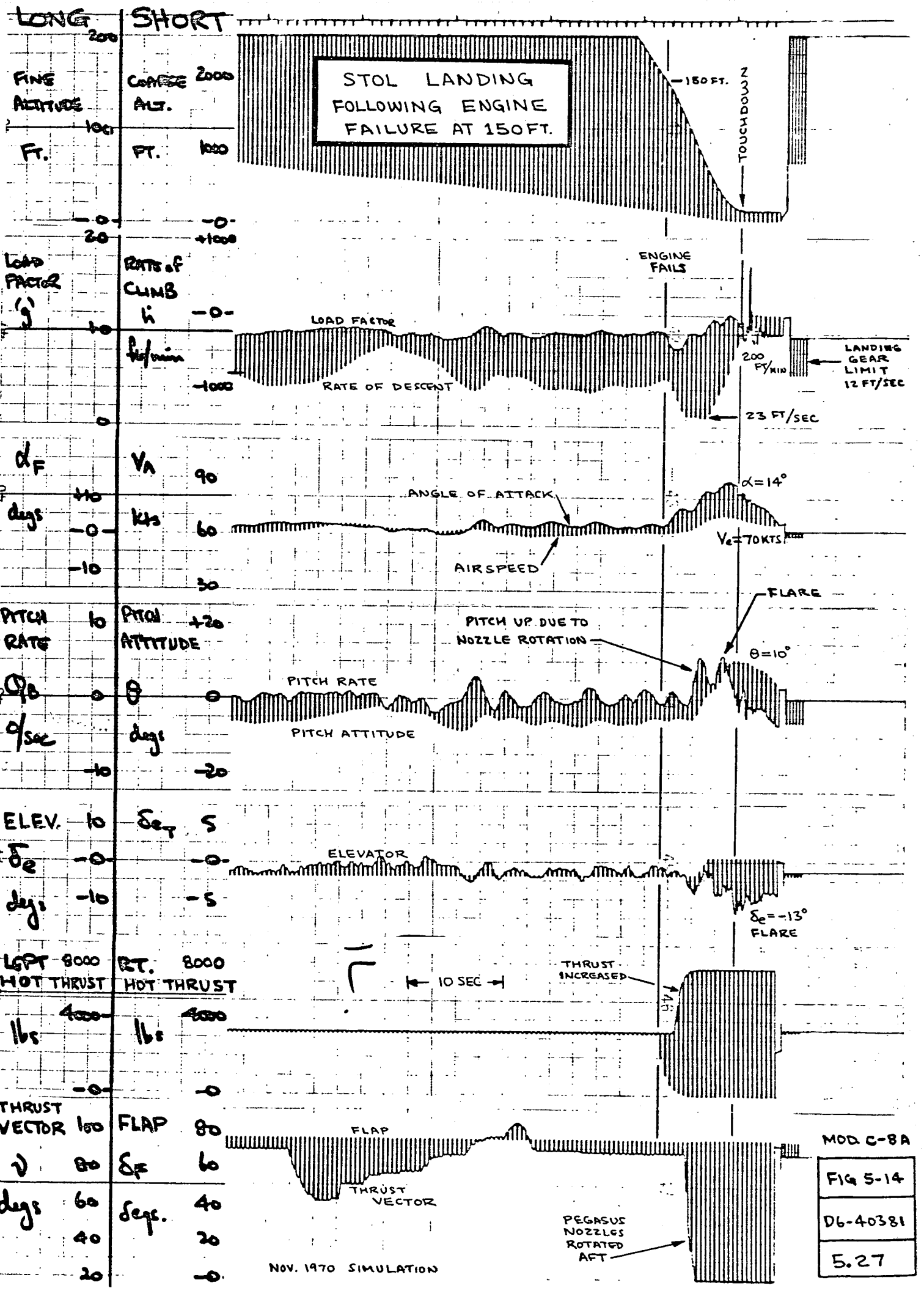
LONG
SHORT
STOL LANDING FOLLOWING ENGINE FAILURE AT 150FT.
150 FT.
TOUCHDOWN
FINE ALTITUDE Ft.
COARSE ALT. FT.
ENGINE FAILS
LOAD FACTOR (g)
RATE of CLIMB ft/min
LOAD FACTOR
RATE OF DESCENT
200 FT/MIN
LANDING GEAR LIMIT 12 FT/SEC
23 FT/SEC
α_F degs
V_A kts
ANGLE OF ATTACK
α=14°
V_e=70KTS
AIRSPEED
FLARE
PITCH RATE Q_B °/sec
PITCH ATTITUDE θ degs
PITCH UP DUE TO NOZZLE ROTATION
θ=10°
PITCH RATE
PITCH ATTITUDE
ELEV. δ_e degs
δ_{e_T}
ELEVATOR
δ_e=-13° FLARE
LEFT HOT THRUST lbs
RT. HOT THRUST lbs
10 SEC
THRUST INCREASED
THRUST VECTOR ν degs
FLAP δ_F degs
FLAP
THRUST VECTOR
PEGASUS NOZZLES ROTATED AFT
NOV. 1970 SIMULATION
MOD C-8A
FIG 5-14
D6-40381
5.27

NOMENCLATURE

AR	Aspect ratio = b^2/S
b	Span
$\bar{c}$, MAC	Mean Aerodynamic Chord
CG	Center of Gravity
C_j	Isentropic Thrust Coefficient - T_{cold}/qS
C_L	Lift Coefficient = LIFT/qs (positive up)
C_D	Drag Coefficient = DRAG/qs (positive aft)
C_m	Pitch moment coefficient = P.M./$q_f S\bar{c}$ (positive nose up)
C_n	Yawing moment coefficient = N/$q_f Sb$ (positive nose right)
C_Y	Sideforce coefficient = Y/qS (positive right)
C_ℓ	Rolling moment coefficient = $\mathcal{L}/q_f Sb$ (positive right wing down)
F_P	Pedal Force (positive for positive rudder)
F_S	Stick Force (positive for pull)
F_W	Wheel Force (positive for right wheel)
i_T	Horizontal tail incidence (positive L.E. up)
N_H	Engine RPM
n_z	Load factor (g's)
q_f	Dynamic pressure
S	Wing Area
t_{30}	Time required to reach 30° bank angle
t_{15}	Time required to reach 15° heading angle
V_e	Equivalent airspeed
X_S	Column position (positive aft)
α_F	Angle of attack (positive L.E. up, relative to fuselage datum)

β	Sideslip (positive nose left)
γ	Flight path angle (positive up)
δ_a	Aileron deflection (positive T.E. down)
δ_{CH}	Augmentor choke deflection (positive up)
δ_e	Elevator deflection (positive T.E. down)
δ_F	Flap deflection (positive T.E. down)
δ_P	Pedal deflection (positive for positive δ_R)
δ_{SP}	Spoiler deflection (positive T.E. up)
δ_R	Rudder deflection (positive T.E. left)
δ_t	Tab deflection (poisitive T.E. down)
δ_W	Wheel deflection (positive right)
ϵ	Downwash angle (positive down)
ζ	Damping ratio
θ	Pitch attitude
$\ddot{\theta}$	Pitch acceleration
Λ	Sweep angle
λ	Taper ratio
ν	Hot thrust nozzle angle (positive down)
τ	Time constant
ϕ	Bank angle
ϕ_1	Bank angle in first second
$\dot{\phi}, P_B$	Roll rate
$\ddot{\phi}$	Roll acceleration
ψ	Yaw angle
$\ddot{\psi}$	Yaw acceleration
ω	Frequency

REFERENCES

1. "Turbofan STOL Research at NASA", B. H. Wick, and R. E. Kuhn, Astronautics and Aeronautics (AIAA), Vol. 9, No. 5, May 1971.

2. NASA TMX-62017, "Low-Speed Aerodynamic Characteristics of a Large-Scale STOL Transport Model with an Augmented Jet Flap", A. M. Cook and T. N. Aiken, 1971.

3. NASA TND-4610, "Aerodynamic Characteristics of a Large-Scale Model with an Unswept Wing and Augmented Jet Flap", D. G. Koenig and V. R. Corsiglia, June 1968.

4. RAE TR 68111, "Low-Speed Wind-Tunnel Tests of an Aircraft Wing-Fuselage Model of Aspect Ratio 9.8, with Tangential Blowing over Trailing Edge Flaps and Ailerons, Including the Effect of Slipstream", Royal Aircraft Establishment, J. A. Lawford, May 1968.

5. NASA CR114434, "Simulator Model Specification for the Augmentor Wing Jet STOL Research Aircraft", P. C. Rumsey and R. E. Spitzer, December 1971.

6. NASA TMX 62,149, "Augmentor Wing Jet STOL Research Aircraft Digital Simulation," W. B. Cleveland. March 1972.

7. NASA CR 114435, "A Design Support Simulation of the Augmentor Wing Jet STOL Research Aircraft", P. C. Rumsey, R. E. Spitzer and W. L. B. Glende, 1972.

8. FAR Part 25, "Airworthiness Standards: Transport Category Airplane", Federal Aviation Administration, May 1970.

9. FAR Part XX, "Tentative Airworthiness Standards for Powered Lift Transport Category Aircraft", Federal Aviation Administrations, August 1970.

10. NASA TMX 62,144, "Longitudinal Handling Qualities During Approach and Landing of a Powered Lift STOL Aircraft", J. A. Franklin and R. C. Innis, March 1972.

11. AFFDL-TR-69-72, "Background Information and User Guide for MIL-F-8785B (ASG) Military Specification - Flying Qualities of Piloted Airplanes", C. R. Chalk, T. P. Neal, T. M. Harris, F. E. Pritchard, R. J. Woodcock, Air Force Flight Dynamics Laboratory, August 1969.

12. R.A.E. Report AERO 2646, "The Aerodynamics of Jet Flaps", J. Williams, S. F. J. Butler, and M. N. Wood, Royal Aircraft Establishment, January 1961.

13. Report C.D. No. 869, "Low-Speed Wind-Tunnel Measurements of Damping in Yaw on an R9 Jet Flap Complete Model", A. P. Cox and S. F. J. Butler, Aeronautical Research Council, 1967.

14. USAAVNTA Project No. 65-10 Final Report, "Stability and Control and Performance Test (Phase D) of the CV-7A Transport Airplane", J. T. Blaha, N. A. Mattmuller and D. R. Wilson, U. S. Army Aviation Test Activity, March 1966.

15. NASA TN D-5594, "Airworthiness Considerations for STOL Aircraft", R. C. Innis, C. A. Holzhauser and H. C. Quigley, January 1970.

16. FAA-RD-70-61, "A Flight Simulator Study of STOL Transport Lateral Control Characteristics", Federal Aviation Administration, D. E. Drake, et al (Douglas Aircraft Co.), September 1970.